UNIVERSITY OF OKLAHOMA

GRADUATE COLLEGE

PHYLOGENETICS, SYSTEMATICS, AND BIOGEOGRAPHY OF *LYGOSOMA* GROUP SKINKS (SQUAMATA: SCINCIDAE: LYGOSOMINAE) AND LOCOMOTOR CAPACITIES OF THREE LYGOSOMINE SKINKS FROM THAILAND

A DISSERTATION

SUBMITTED TO THE GRADUATE FACULTY

in partial fulfillment of the requirements for the

Degree of

DOCTOR OF PHILOSOPHY

By

ELYSE SUSANNE FREITAS
Norman, Oklahoma
2020

PHYLOGENETICS, SYSTEMATICS, AND BIOGEOGRAPHY OF *LYGOSOMA* GROUP SKINKS (SQUAMATA: SCINCIDAE: LYGOSOMINAE) AND LOCOMOTOR CAPACITIES OF THREE LYGOSOMINE SKINKS FROM THAILAND

A DISSERTATION APPROVED FOR THE
DEPARTMENT OF BIOLOGY

BY THE COMMITTEE CONSISTING OF

Dr. Cameron D. Siler, Chair

Dr. Richard E. Broughton

Dr. John P. Masly

Dr. Michael A. Patten

Dr. Jennifer Koch

This dissertation is dedicated to my family and friends who supported me throughout this endeavor. Thank you for being patient with my absence at important events and my lack of telecommunication, and please know that I was always there in spirit! Your support means the world to me.

Acknowledgements

None of this research was done in a vacuum: science as a field is highly collaborative and depends on the ideas and hard work of previous researchers and current colleagues. My dissertation research could not have occurred without the previous research of herpetologists, evolutionary biologists, ecologists, geologists, and paleontologists, and I depend on those scientists who developed laboratory methods, phylogenetic analyses, and bioinformatics software. I thank you for your work!

I also want to thank my coauthors for their collaboration on the following chapters. This work could not have occurred without your advice, comments, and critiques.

A number of people have helped me with ideas and analyses throughout the years. I am extremely grateful for your time and willingness to help. Tamaki Yuri trained me in lab work at the Sam Noble Museum and was always willing to help when I had a question or problem. Jamie Oaks has been my main source for BEAST analyses questions. Michael Patten, Claire Curry, and Rachel Hartnett answered my questions about multivariate statistical analyses. Aaron Bauer double checked the taxonomic revision section of chapter one, and George Shea, one of the reviewers for my chapter one manuscript, gave detailed feedback that improved historical and taxonomic content of the manuscript. Dahiana Arcila met with me on multiple occasions to discuss FBD divergence dating methods in MrBayes for chapter three. Aintzane Santaquiteria walked me through her R code for the BioGeoBEARS analysis for chapter three. Gen Morinaga taught me data collection and digitization for chapter four.

I want to give a special acknowledgement to Jessa Watters, who helped me import specimens, request loans, manage data, and provided me with tons of help while I was the TA for herpetology. She also edited my grants and manuscripts. Jessa's office was on the way to the

graduate student office, and I spent many mornings, lunch breaks, and afternoons asking questions and conversing about herp-related and non-herp-related topics.

Behind every successful graduate student is the administration and staff. To the staff: your behind-the-scenes organization and work was instrumental in my success, and I can't thank you enough for your help and support. Thank you so much to the graduate student liaisons Rosemary Knapp and JP Masly who kept me on track with paperwork and other deadlines and were always available to answer questions. I want to thank former and current members of the OU Department of Biology staff including Carol Baylor, Kyle Baker, Ashley Benson, Kaye Carter, Liz Cooley, George Martin, and Diana Wilson for everything you do in support of graduate students and research. At the Sam Noble Museum, I would like to thank the current and former members of the maintenance staff, janitorial staff, and security for their dedication and friendship, including Deanna Ashbaker, Ricky Birdwell, Adam Burnett, Marlin Butcher, Sue Day, Warren Dressler, Quinn Floch, Jimmy Gerner, Graham Horsey, Coral McCallister, Ross McClish, Darin Moser, Wes Wilson, and Ben Wood.

Having a support network of friends and family has been extremely important throughout this process. Thank you so much to everyone who has been there for me over the last six years. A few specific shout outs: Thank you to my partner, Brent Tweedy, for being, well, my partner, as I navigated these last six years. Thank you to my sister, Nina Freitas, who was always encouraging and also provided me with tough love when needed, especially in the field in Thailand. Thank you to Eira Whitty, whose nightly calls and words of support helped me through some tough times in 2016. Thank you to the Siler lab members: Jessa Watters, Greg Jongsma, Nick Huron, Kai Wang, Joey Brown, Sam Eliades, Elyse Ellsworth, Miranda Vesy, Sierra Smith, Marie Labonte, Michelle Penrod, Brendan Heitz, and Stephanie Maguire, who

provided discussions on methods and results, support during long hours in the office, tons of fun during work hours, field work, and social events, and who always re-inspired me when I was feeling uninspired. Thank you to the Anchalee Aowphol and her lab members: Atapol Rujirawan, Natee Ampai, Piyawan Panprapai, Siriporn Yodthong, Korkhwan Termprayoon, and Akrachai Aksornneam for hosting me in Thailand. Thank you to the museum community, including Tamaki Yuri, Katrina Menard, and Sara Cartwright for being wonderful workmates. Thank you to the OU Department of Biology graduate student community for your friendship and encouragement.

I'd like to give a special acknowledgement to the Museum of Vertebrate Zoology, who got me started on this journey, especially Monica Albe, Carla Cicero, and Josh Peñalba.

Thank you to the Affordable Care Act (aka Obamacare), which made this all possible for me.

Finally, a huge thank you to my committee members, Rich Broughton, JP Masly, Michael Patten, and Jennifer Koch, and my advisor, Cameron Siler, who gave me advice and guidance as I worked through these chapters, and whose help greatly improved the quality of my work.

Table of Contents

Table of Tables

Table of Figures

Abstract

The lizard family Scincidae is the most species-rich family of squamate reptiles, comprising more than 1,600 species. Skinks are ecologically and morphologically diverse, occurring in tropical and temperate zones on all continents excluding Antarctica, as well as on many oceanic islands. Although skinks are a ubiquitous part of most of the world's herpetofauna, we still lack a basic understanding of the evolutionary history and biodiversity of many clades within the family. Using molecular data, concatenated- and coalescent-based phylogenetic analyses, morphological datasets, and multivariate statistics, I reconstruct the evolutionary history of a clade of skinks called the *Lygosoma* group skinks, a group of elongate-bodied semifossorial species distributed across the Old World tropics in Africa, South Asia, Southeast Asia, and Sundaland. My dissertation focuses on the phylogenetics, systematics, taxonomy, species-level diversity, and biogeography of this group, and I address questions including: *How are species related*? *What macroevolutionary factors have influenced species diversification across evolutionary time*? And, *how have historical processes shaped the modern biodiversity of* Lygosoma *group skinks*? Additionally, I use high speed videos of locomotion and multivariate statistics to investigate the locomotor kinematics and performance of three species of co-distributed skinks in Thailand to address the following question: *Does diversity in morphology result in diversity in locomotor performance and kinematics*? The results of my dissertation provide insight into the evolutionary history and biodiversity of skinks in the Old World tropics.

In my first chapter, I delve into the taxonomic history of *Lygosoma* group skinks and propose a new classification based on phylogeny generated with the most robust genetic and taxonomic sampling of the group to date. The genera Lepidothyris, Lygosoma and Mochlus comprise the writhing or supple skinks (*Lygosoma s.l.*), a group of semi-fossorial, elongate-bodied skinks

distributed across the Old World Tropics. Due to their generalized morphology and lack of diagnostic characters, species- and clade-level relationships have long been debated. Recent molecular phylogenetic studies of the group have provided some clarification of species-level relationships, but a number of issues regarding higher level relationships among genera still remain. In this study, I present a phylogenetic estimate of relationships among species in *Lygosoma*, *Mochlus* and *Lepidothyris* generated by concatenated and species tree analyses of multilocus data using the most extensive taxonomic sampling of the group to date. I also use multivariate statistics to examine species and clade distributions in morphospace. The results reject the monophyly of *Lygosoma s.l.*, *Lygosoma s.s.*, and *Mochlus*, which highlights the instability of the current taxonomic classification of the radiation. Based on these findings, I revise the taxonomy of the writhing skinks to better reflect the evolutionary history of *Lygosoma s.l.* by restricting the genus *Lygosoma* to Southeast Asia, resurrecting the genus *Riopa* for a clade of Indian and Southeast Asian species, expanding the genus *Mochlus* to include all African species of writhing skinks, and describing a new genus in Southeast Asia. By providing a new classification for *Lygosoma* group skinks and the most robust species-level molecular phylogeny to date, this chapter establishes a new set of names for the group that are important in communicating about clades and species and facilitating future studies on evolution and diversification within this radiation of lizards.

In my second chapter, I transition from a broad-scale study on biodiversity and systematics of *Lygosoma* group skinks and focus on fine-scale species-level diversity within the group. Specifically, I investigate the biodiversity of a species complex of skinks in the genus *Riopa* in Myanmar and show that the current species-level diversity of the group is highly underestimated. Recognizing species-level diversity is important for studying evolutionary patterns across

biological disciplines and is critical for conservation efforts. However, challenges remain in delimiting species-level diversity, especially in cryptic radiations where species are genetically divergent but show little morphological differentiation. Using multilocus molecular data, phylogenetic analyses, species delimitation analyses, and morphological data, I examine lineage diversification in a cryptic radiation of *Riopa* skinks in Myanmar. Four species of *Riopa* skinks are currently recognized from Myanmar based on morphological traits, but the boundaries between three of these species, *R. anguina*, *R. lineolata*, and *R. popae* are not well-defined. I find high levels of genetic diversity within these three species, and analyses suggest that they may comprise as many as 12 independently evolving lineages, which highlights the extent to which species diversity in the region is underestimated. However, quantitative trait data suggest that these lineages have not differentiated morphologically, possibly indicating that this cryptic radiation represents a non-adaptive evolution, although additional data is needed to corroborate this. The results of this chapter provide essential data on the biodiversity of a clade of skinks in Myanmar, an understudied region, and are therefore important in conservation and management. Additionally, this study corroborates a previously recognized hypothesis that species-level diversification is high within the country's Central Dry Zone. Finally, this study provides important information on the true species-level diversity of Myanmar *Riopa*, which is critical for future studies of diversification in *Lygosoma* group skinks.

In my third chapter, I increase taxonomic and genetic sampling of my molecular dataset, including the additional lineages discovered in chapter two, to investigate the historical biogeography of *Lygosoma* group skinks across the Old World tropics. Through this research, I gain an understanding of how large-scale geological and climatic processes affected diversification of the group since the late Paleocene approximately 60 million years ago. Using

Bayesian fossilized birth-death divergence dating for 40 ingroup lineages and species of *Lygosoma* group skinks, I reconstruct ancestral ranges and estimate shifts in evolutionary rates and species through time for all genera. Additionally, while logic suggests that geographic sampling has a large impact on biogeographic reconstructions of a clade, this result has never been demonstrated empirically. Therefore, I investigate the impact geographic sampling has on biogeographic analyses and the resulting ancestral range reconstructions by randomly sub-sampling the species in my analysis and rerunning biogeographic analyses to generate null distributions for the probabilities of ancestral ranges. The results of this study support early diversification of *Lygosoma* group skinks just over 50 mya from an ancestral range that included India, with subsequent dispersal throughout the Old World tropics. Diversification continued throughout the Eocene and Miocene and was not accompanied by shifts in evolutionary rates. Resampling analyses indicate that biogeographic reconstruction is strongly influenced by the geographic sampling of taxa. The biogeographic scenario I present in this chapter provides a testable hypothesis for future studies on paleontology, diversification, and trait evolution in *Lygosoma* group skinks. Additionally, the results emphasize the importance of taxonomic and geographic sampling in understanding the evolutionary history of clades, indicating that biodiversity surveys remain an essential part of phylogenetic and evolutionary research.

In my fourth chapter, I take a different approach to understanding the biodiversity of skinks by investigating how differences in body morphology affect the performance and kinematics of three species of skinks in Thailand. The goal of this study is to if species with different morphologies maintain locomotor performance and the process by which this happens. Locomotion is an essential function in the life of vertebrates and higher locomotor performance is correlated with increased survival. Although studies over the past three decades have made

substantial progress in understanding the locomotion and locomotor kinematics in squamate reptiles, we still lack an understanding of how locomotion occurs across the diversity of body forms in squamate reptiles. In this study, I investigate the locomotion and kinematics of three co-distributed skink species from Southeast Asia: *Eutropis macularia*, *Sphenomorphus maculatus*, and *Subdoluseps bowringii-frontoparietale*. I find that the more elongate species, *Subdoluseps bowringii-frontoparietale*, has greater axial bending, whereas *Sphenomorphus maculatus*, the species with the relatively longest hind limb length, has a higher maximum velocity. Additionally, the results show correlations between stride mechanics (stride duration, stride length, and duty factor) and maximum velocity across all three species and correlations between stride mechanics and morphology in *Eutropis macularia* and *Sphenomorphus maculatus*. Finally, statistical analyses suggest that the two robust-limbed species, *Eutropis macularia* and *Sphenomorphus maculatus*, have higher reliance on limbed propulsion during locomotion than *Subdoluseps bowringii-frontoparietale*. This study is the first to investigate locomotor performance and kinematics in these three species and corroborates most previous hypotheses of locomotion in squamate reptiles.

Chapter 1: Multilocus phylogeny and a new classification for African, Asian, and Indian Supple and Writhing Skinks (Scincidae: Lygosominae)

Elyse S. Freitas, Aniruddha Datta-Roy, Praveen Karanth, L. Lee Grismer, and Cameron D. Siler

Published in Zoological Journal of the Linnean Society 2019, 186: 1067–1096.

ABSTRACT

The genera Lepidothyris, Lygosoma and Mochlus comprise the writhing or supple skinks (*Lygosoma s.l.*), a group of semi-fossorial, elongate-bodied skinks distributed across the Old World Tropics. Due to their generalized morphology and lack of diagnostic characters, species- and clade-level relationships have long been debated. Recent molecular phylogenetic studies of the group have provided some clarification of species-level relationships, but a number of issues regarding higher level relationships among genera still remain. Here we present a phylogenetic estimate of relationships among species in *Lygosoma*, *Mochlus* and *Lepidothyris* generated by concatenated and species tree analyses of multilocus data using the most extensive taxonomic sampling of the group to date. We also use multivariate statistics to examine species and clade distributions in morpho space. Our results reject the monophyly of *Lygosoma s.l.*, *Lygosoma s.s.* and *Mochlus*, which highlights the instability of the current taxonomic classification of the group. We, therefore, revise the taxonomy of the writhing skinks to better reflect the evolutionary history of *Lygosoma s.l.* by restricting *Lygosoma* for Southeast Asia, resurrecting the genus *Riopa* for a clade of Indian and Southeast Asian species, expanding the genus *Mochlus* to include all African species of writhing skinks and describing a new genus in Southeast Asia.

KEYWORDS: Africa – India – *Lamprolepis – Lepidothyris – Lygosoma – Mochlus – Riopa –* Southeast Asia – taxonomy.

INTRODUCTION

The lizard family Scincidae is the most species-rich family of squamate reptiles. Skinks are ecologically and morphologically diverse, with more than 1,600 taxa recognized currently (Uetz et al., 2018) throughout tropical and temperate zones on all continents excluding Antarctica, as well as on many oceanic islands (Greer, 1970a; Vitt & Caldwell, 2013). Despite this high diversity, inter- and intra-generic phylogenetic relationships across many clades within the family remain poorly resolved (Pyron et al., 2013; Skinner et al., 2013; Barley et al., 2015a; Lambert et al., 2015; Zheng & Wiens, 2016), However, with the continued growth in available genetic data and increased taxonomic sampling in molecular systematic studies of various clades, research over the last decade has contributed greatly to an improved understanding of the diversity of scincid lizards (e.g. Linkem et al., 2011; Siler et al., 2011; Brandley et al., 2012; Datta-Roy et al., 2012; Sindaco et al., 2012; Skinner et al., 2013; Datta-Roy et al., 2014; Barley et al., 2015a; Pinto-Sánchez et al., 2015; Karin et al., 2016; Klein et al., 2016; Erens et al., 2017). Additionally, this nascent body of work has resulted in a dramatic increase in the rate of discovery of morphologically cryptic lineages (e.g. Daniels et al., 2009; Linkem et al., 2010; Chapple et al., 2011; Heideman et al., 2011; Siler et al., 2011, 2012, 2014, 2016, 2018; Kay & Keogh, 2012; Barley et al., 2013; Davis et al., 2014, 2016; Geheber et al., 2016; Heitz et al., 2016; Medina et al., 2016; Busschau et al, 2017; Conradie et al., 2018; Karin et al., 2018; Pietersen et al., 2018). However, there remain many lingering taxonomic and phylogenetic

challenges within the family, possibly none more so than within the large and diverse subfamily Lygosominae.

One of three subfamilies recognized widely within the lizard family Scincidae (Greer, 1970a; Pyron et al., 2013; Skinner et al., 2013; Lambert et al., 2015; Karin et al., 2016; Linkem et al., 2016; Zheng & Wiens, 2016; but see an alternative not widely-accepted classification in Hedges & Conn, 2012; Hedges, 2014; Uetz et al., 2018), the Lygosominae contains approximately 1,320 species (estimated from Uetz et al., 2018), and represents currently the most speciose radiation of scincid lizards, with a broad, global distribution (Greer, 1970a; Honda et al., 2000; Skinner, et al., 2011). The radiation likely began diversifying 100.6–63.6 Myr, during the late Cretaceous to early Paleocene (Skinner et al., 2011). Extant genera exhibit a rich biogeographic history, with evidence for historical transoceanic dispersal in some lineages (Carranza & Arnold, 2003; Honda et al., 2003; Rocha et al., 2006; Linkem et al., 2013; Skinner et al., 2013; Karin et al., 2016). Many genera have been the subject of recent phylogenetic studies, including *Afroablepharus* and *Panaspis* (Medina et al., 2016), *Eutropis* (Datta-Roy et al., 2012; Barley et al., 2013, 2015a), *Lygosoma* (Datta-Roy et al., 2014), *Mabuya* (Hedges & Conn, 2012; Pinto-Sánchez et al., 2015), *Sphenomorphus* (Linkem et al., 2011), *Trachylepis* (Sindaco et al., 2012), and *Tytthoscincus* (Grismer et al., 2018a). Although these studies have increased the understanding of diversity and relationships among these focal clades, they also have highlighted a number of phylogenetic and taxonomic issues that remain unresolved. As taxonomy reflects our knowledge of organisms in the tree of life (Vences et al., 2013), resolving these conflicts is important for investigating a myriad of higher-level questions, including studies of ecology, diversification, morphological evolution, and conservation of imperiled species.

One prime example of unresolved taxonomic issues among lygosomine skinks is the genus *Lygosoma*, which has a long and controversial history of uncertainty regarding species- and generic-level relationships. *Lygosoma* Hardwicke & Gray 1827, the type genus of the subfamily Lygosominae, comprises 31 recognized species distributed across Africa, India, Southeast Asia, the western and southern Philippines, and Christmas Island (Australia) (Geissler et al., 2011; Cogger, 2014; Datta-Roy et al., 2014; Heitz et al., 2016; Grismer et al., 2018b; Siler et al., 2018; Uetz et al., 2018). Genera closely allied to *Lygosoma* include *Mochlus*, consisting of 15 species found in semi-arid regions across central and subtropical southern Africa, and *Lepidothyris*, consisting of three species found in forested regions of central Africa (Greer, 1977; Wagner et al., 2009). Historically, the taxonomic status of these three genera has been debated extensively, with species in *Mochlus* and *Lepidothyris* often included within *Lygosoma* (e.g. Boulenger, 1887; Greer, 1977; see taxonomic history of the group below), but recent phylogenetic analyses suggest that *Lygosoma* is paraphyletic with respect to both genera (Pyron et al., 2013; Datta-Roy et al., 2014). Therefore, from here on out, we refer to the 49 species represented by these three genera collectively, as *Lygosoma sensu lato* (*s.l.*), whereas, we refer to the 31 species in the genus *Lygosoma* (as currently recognized) as *Lygosoma sensu stricto* (*s.s.*).

Although Greer (1977) found all members of *Lygosoma s.l.* to be united by osteological characteristics of the secondary palate, morphology has offered few clues to the phylogenetic relationships of species and clades within the group, which has resulted in considerable taxonomic confusion regarding the status of species and genera (e.g. Broadley, 1966; Greer, 1977). Known as Supple or Writhing Skinks, species have been allocated to *Lygosoma s.l.* generally on the basis of their semi-fossorial ecology, head scale patterns and the presence of well-developed eyelids, elongate bodies and short fore- and hind limbs that do not meet when

adpressed (Smith, 1935; Mittleman, 1952; Greer, 1977; Geissler et al., 2011; Geissler, Hartmann & Neang, 2012). All species are pentadactyl with the exception of *Lygosoma lineata*, which has tetradactyl fore-limbs (Greer, 1977), and color and pigmentation patterns vary within and between species (Wagner et al., 2009). However, beyond these generalizations, species exhibit diverse body forms that range from moderately large (e.g. *L. kinabatanganense*: snout–vent length (SVL)=141 mm; *L. haroldyoungi*: SVL=148 mm; *M. sundevallii*: SVL=140 mm) to small (e.g. *L. frontoparietale*: SVL=41 mm; *L. veunsaiense*: SVL=34 mm), and more robust with short limbs (e.g. *M. brevicaudis*), to elongate and more gracile with small, slender limbs and shorter digits (e.g. *L. quadrupes*) (Broadley, 1966; Greer, 1977; Geissler et al., 2011). As a result of this considerable diversity in body form, researchers have struggled to define morphological boundaries between groups (Boulenger, 1887; Smith, 1937a; Greer, 1977).

More recently, molecular phylogenetic techniques have been employed to examine species-level relationships within *Lygosoma s.l.*, resulting in increased taxonomic resolution (Ziegler et al., 2007; Wagner et al., 2009; Pyron et al., 2013; Datta-Roy et al., 2014). Nevertheless, not only have the results of this body of work revealed significant genetic lineage diversity, but also failed to support the monophyly of several recognized clades, including *Lygosoma s.s.* with respect to *Mochlus* and *Lepidothyris*, and *Lygosoma s.l.* with respect to the species *Lamprolepis smaragdina* (Honda et al., 2000, 2003; Pyron et al., 2013; Datta-Roy et al., 2014). Unfortunately, to date, the paucity of available genetic samples for many species has limited the degree to which studies have been able to resolve the intra- and intergeneric relationships in *Lygosoma s.l.* Additionally, several new species have been described recently based on genetic and/or morphological data (*Lygosoma boehmei* [Ziegler et al., 2007]; *L. kinabatanganense* [Grismer et al., 2018b]; *L. peninsulare* [Grismer et al., 2018b]; *L. samajaya* [Karin et al., 2018]; *L. siamense*

[Siler et al., 2018]; *L. tabonorum* [Heitz et al., 2016]; *L. veunsaiense* [Geissler et al., 2012]; and *Lepidothyris hinkeli* [Wagner et al., 2009]), but how these species relate to others within *Lygosoma s.l.* remains unresolved. In this manuscript, we employ phylogenetic approaches and analyses of external morphology to investigate species- and generic-level relationships and taxonomic conflicts within *Lygosoma s.l.*

TAXONOMIC HISTORY OF *LYGOSOMA S.L.*

Early classifications based on morphology

The taxonomy of *Lygosoma s.l.* has a long and complex history. Within *Lygosoma s.l.*, the traditionally used phenotypic characters in skink classifications are non-diagnostic and have overlapping numerical values, making it difficult to assign species to identifiable groups. Historically, taxonomic hypotheses for skinks employed a variety of morphological characters in genus-level classifications, such as the degree of body elongation, limb size and digit number, size of the ear opening, lower eyelid characteristics (*i.e.* scaly vs. with a transparent disc), head scalation patterns and pigmentation patterns (e.g. Duméril & Bibron, 1839; Gray, 1839). However, many of these characters have been shown to be convergent among skinks, calling into question the breadth of their diagnostic utility, especially in *Lygosoma s.l.*, in which species exhibit varying body sizes and degrees of elongation (Smith, 1937a; Greer, 1977). Further complicating clear morphological definitions for members of this radiation is the anomalous morphology of the type species of *Lygosoma s.s.*, *L. quadrupes*, which has a thin, snake-like body, tiny limbs, short digits and an atypical head scale pattern (single frontoparietal scale, nasals fused with supranasals; Greer, 1977). Whereas other species in the radiation also possess some of these characters (e.g. *L. lineatum* and *L. vosmaerii* have bodies nearly as elongate as *L.*

quadrupes; *L. isodactylum* has nasals fused anteriorly with supranasals [Greer, 1977; Geissler et al. 2011, 2012]), the combination of morphological traits in *L. quadrupes* is different from other species in *Lygosoma s.l.* (although the recently described species *L. siamense* and *L. tabonorum*, both part of the *L. quadrupes* species complex also have these morphological characters [Heitz et al., 2016; Siler et al., 2018]). Therefore, historically it has been difficult to classify *L. quadrupes* within a broader taxonomic context, as evidenced by multiple taxonomists classifying the species not with other members of *Lygosoma s.l.* but with superficially similar elongate-bodied species (e.g. Boulenger, 1887; Smith, 1935, 1937a; Mittleman, 1952) that have been shown subsequently not to be closely related. As a result, for the previous 150 years species within *Lygosoma s.l.* have alternated between being lumped within the same genus to being separated into multiple genera (Boulenger, 1887; Smith, 1935, 1937a; Mittleman, 1952; Broadley, 1966; Greer, 1977; Wagner et al., 2009), leading to taxonomic instability within the group.

Currently, three genera are recognized within *Lygosoma s.l.*: *Lygosoma s.s.*, *Lepidothyris* and *Mochlus* (Datta-Roy et al., 2014). However, less than a decade ago a fourth genus, *Riopa*, also was considered valid (Wagner et al., 2009). Of these four genera, the genus *Lygosoma* has undergone the most revisionary changes through the years, with species and species group compositions (*i.e.* sections and subgenera) a subject of continued confusion and debate (e.g. Smith, 1935, 1937a; Mittleman, 1952; Glauert, 1960; Laurent & Gans, 1965). The genus *Lygosoma* was first described in 1827 (Hardwicke & Gray) for the species *Lacerta serpens* Bloch 1776. In their description, the authors note that *Lacerta serpens* is a distinct species from *Anguis quadrupes* Linnaeus 1766, failing to realize that Bloch's description of *Lacerta serpens* was a redescription of Linnaeus' (1766) *Anguis quadrupes*. Bloch (1776) had redescribed *Anguis quadrupes* because the Linnaeus' original description of the species had classified it as a four-

legged snake (reviewed in Bauer & Günther, 2006). Hardwicke's and Gray's (1827) oversight, which may have resulted from the assignment of additional specimens to *Lacerta serpens* that were not truly *quadrupes* specimens (G. Shea, pers. comm.), was not resolved until Smith (1935) synonymized *Lacerta serpens* with *Anguis quadrupes*, thus making *Lygosoma quadrupes* the type species of *Lygosoma*. Over the next two centuries, in addition to *Lygosoma* Hardwicke & Gray, 1827, species currently in *Lygosoma s.l.* have been described as members of 12 disparate genera: *Campsodactylus* Duméril & Bibron 1839; *Chiamela* Gray 1839; *Eumeces* Wiegmann 1834; *Hagria* Gray 1839; *Lepidothyris* Cope 1892 (*nomen nudum* until Cope 1900); *Mochlus* Günther 1864a; *Podophis* Wiegmann 1834; *Riopa* Gray 1839; *Sphenosoma* Fitzinger 1843; *Sepacontias* Günther 1880; *Squamicilia* Mittleman 1952; and *Tiliqua* Gray 1825. These genera were revised and reorganized in major works throughout the 19th century (Schneider, 1801; Daudin, 1802; Fitzinger, 1826, 1843; Wiegmann, 1834; Cocteau, 1836; Duméril & Bibron, 1839; Gray, 1839, 1845; Günther, 1864b; Theobald, 1876), culminating in Boulenger's (1887) monograph cataloguing the lizards in the British Museum. Faced with the difficulty of classifying 2,340 specimens of scincid lizards representing 369 recognized species and having remarked on the difficulty of classifying skink genera, Boulenger (1887) synonymized most of these genera with *Lygosoma*, which resulted in the genus comprising 159 species (43% of all skink species recognized at the time). Additionally, Boulenger (1887) subdivided *Lygosoma* into 11 sections (*Emoa* [sic] Gray 1845, *Hemiergis* Wagler 1830, *Hinulia* Gray 1845, *Homolepida* [sic] Gray 1845, *Keneuxia* Gray 1845, *Liolepisma* [sic] Duméril & Bibron, 1839, *Lygosoma*, *Otosaurus* Gray 1845, *Rhodona* Gray 1839, *Riopa*, and *Siaphos* [sic] Gray 1831) based on limb proportions and head scalation characters. For a half-century, his revision was the only large-scale treatment of skink taxonomy.

By the early 1900s, there was growing concern about taxonomic confusion resulting from piecemeal adoption of a subset of Boulenger's (1887) *Lygosoma* sections as genera. For example, his section *Emoa* [sic] was recognized as the genus *Emoia* by Barbour (1912), his section *Otosaurus* as the genus *Otosaurus* by Taylor (1923), his section *Rhodona* as the genus *Rhodona* by Loveridge (1933) and his section *Liolepisma* [sic] as the genus *Leiolopisma* by Smith (1935). Consequently, in 1937, Smith undertook a large-scale revision of *Lygosoma*, reevaluating and reclassifying Boulenger's (1887) 11 sections. In doing so, Smith (1937a) elevated five sections to genera, believing each to be distinct enough morphologically from the rest of *Lygosoma* to warrant generic status: *Emoia*, *Keneuxia* as the genus *Dasia*, *Otosaurus*, *Rhodona* and *Riopa*. Four subgenera were recognized within *Riopa*—*Eugongylus* Fitzinger 1843, *Eumecia* Barboza du Bocage 1870, *Panaspis* Cope 1868 and *Riopa* (Smith, 1937a). Additionally, Smith (1937a) synonymized the section *Homolepida* [sic] with the genus *Tiliqua* and considered the sections *Hemiergis* and *Siaphos* [sic] invalid due to a lack of diagnostic characters, placing their species into the section *Leiolopisma*. Despite these many changes, the genus *Lygosoma*, as defined by Smith (1937a), remained species-rich, comprising more than 166 taxa separated into three sections—*Leiolopisma*, *Lygosoma*, and *Sphenomorphus* Fitzinger 1843 and one subgenus—*Ictiscincus* Smith 1937a. In his revision, Smith (1937a:219) lamented the lack of diagnostic characters separating species and sections within this large genus, writing, "I am unable to find any character by which to separate the well-developed forms of *Lygosoma*…from the degenerate ones. Between the extremes in each section, the difference is enormous, but the gap can be bridged by connecting forms showing every stage of development."

The next major revision of *Lygosoma* was conducted by Mittleman (1952), who felt that a taxonomic system in which genera are defined narrowly was preferable to the approach of

Boulenger (1887) and Smith (1937a), both of whom, in struggling to find diagnostic characters, treated *Lygosoma* as a catch-all genus. Therefore, in his revision Mittleman (1952) avoided using subgenera and sections and instead defined multiple genera for species formerly included in Boulenger's (1887) and Smith's (1937a) definitions of *Lygosoma.* Although he worked primarily from the literature instead of examining specimens (G. Shea, pers. comm.), Mittleman described three new genera and resurrected and redefined 30 genera based on body proportions, limb size, size of the ear opening and head scalation patterns (Mittleman, 1952). Consequently, the number of species in *Lygosoma* was reduced considerably to eight elongate, small-limbed species from Southeast Asia and Australia. Of the new genera described, the genus *Squamicilia* Mittleman 1952 contained a species of *Lygosoma s.l.* (*isodactylum*) included previously in *Riopa* subgenus *Riopa* by Smith (1937a) and was defined on the basis of a scaly lower eyelid and absence of contact between supranasals (Mittleman, 1952). Additionally, the genera *Mochlus* and *Riopa* were redefined to comprise 14 and nine species, respectively (Mittleman, 1952). Prior to this work, *Mochlus* had long been treated as a synonym of *Riopa*, regardless of whether *Riopa* was considered a genus or a section at the time (Boulenger, 1887; Schmidt, 1919; Barbour & Loveridge, 1928; Loveridge, 1933; Smith, 1937a; FitzSimons, 1943). Mittleman (1952), in an effort to define genera that more accurately reflected perceived evolutionary relationships, considered *Mochlus* as a genus distinct from *Riopa* based on its scaly (vs. transparent) lower eyelid and more robust (vs. small) limbs. Even so, many authors have questioned the diagnostic value of the lower eyelid state and relative limb proportions for genera, noting considerable variation in states for both characters among many genera of skinks (Smith 1937a; Broadley, 1966; Greer, 1974, 1977; Datta-Roy et al., 2015). As a result of this uncertainty, as well as concerns with over-splitting of genera by Mittleman (1952), many subsequent studies rejected

Mittleman's (1952) separation of *Mochlus* and *Riopa* and continued to treat *Mochlus*, along with *Squamicilia*, as synonyms of *Riopa* (Loveridge, 1957; Broadley, 1962, 1966; Taylor, 1963; Greer, 1977).

Despite disagreements regarding the taxonomic rank of *Riopa*, *Mochlus* and *Squamicilia*, the species composition of these genera remained stable over time, with all 24 species included in these genera recognized historically as being closely allied, representing part of *Lygosoma* section *Riopa* by Boulenger (1887) and *Riopa* subgenus *Riopa* by Smith (1937a). The genus *Lepidothyris*, mentioned by Cope (1892) (as a *nomen nudum*) and attributed formally to the species *Lepidothyris fernandi* by Cope (1900), also has continued to be allied with *Riopa* + *Mochlus* (synonymized with *Riopa* subgenus *Riopa* by Smith [1937] and *Mochlus* Mittleman [1952]). In contrast, since Boulenger (1887), the species composition of *Lygosoma* has changed considerably, with Smith (1937a) and Mittleman (1952) both offering different morphological definitions and species compositions for the genus—Smith treating the genus as a default group comprising otherwise unclassifiable species, and Mittleman treating it as a narrowly defined unit. After Mittleman (1952), authors continued to reclassify the species in *Lygosoma* placing them in different genera (e.g. Storr, 1964, 1967; Greer, 1970a; Cogger, 1975), so that by 1977, the only species that remained in the genus *Lygosoma* was the type species, *Lygosoma quadrupes*.

The taxonomy of the genus *Lygosoma* was not revisited until Greer (1977) reexamined the morphology of *Lygosoma quadrupes*, looking at internal osteological characters of the skull in addition to the more traditional external morphological characters. In a paper that established the foundation of our current understanding of *Lygosoma s.l.* phylogenetic relationships, Greer (1977) proposed that *L. quadrupes* was closely related to species in the genus *Riopa* (which included Mittleman's [1952] *Mochlus* and *Squamicilia*) based on the morphology of the

secondary palate. He further suggested that the characteristic elongate body plan of *L. quadrupes* was part of a gradient in gross body form morphology that encompassed the less elongate body morphologies of species of *Riopa* and concluded that the amount of overlap in characters between *Riopa* and *Lygosoma quadrupes* was insufficient to warrant the recognition of two separate genera (Greer, 1977). The genus *Riopa* was therefore synonymized with *Lygosoma*, resulting in a genus of 32 recognized species (Greer, 1977). Since Greer's (1977) work, more recent phylogenetic studies of the genus have corroborated the close relationship between *Lygosoma quadrupes* + *Riopa* (Ziegler et al., 2007; Wagner et al., 2009; Pyron et al., 2013; Datta-Roy et al., 2014; see below), and this work remains a major influence on our current understanding of evolutionary patterns within *Lygosoma s.l.*

Recent classifications based on molecular sequence data

Over the last two decades, molecular phylogenetic studies focusing on lygosomine skinks have helped to resolve some of the long-standing taxonomic issues regarding genera within the Lygosominae (Honda et al., 2000, 2003; Skinner et al., 2011). Although molecular studies have increased our understanding of relationships among certain taxa within *Lygosoma s.l.*, these studies exposed additional taxonomic challenges regarding the taxonomic rank and allocation to clusters of species, variably ascribed to the genera *Lepidothyris*, *Lygosoma*, *Mochlus* and *Riopa*. Ziegler et al. (2007) conducted the first molecular phylogenetic study of *Lygosoma s.l.*, collecting sequence data for six Southeast Asian and Indian species from the mitochondrial gene *16S*. Not only did this study confirm Greer's (1977) hypothesis of a close relationship between *Lygosoma quadrupes* and *Riopa*, but it also recovered *L. quadrupes* as nested within a clade of

species recognized previously by Mittleman (1952) as part of the genus *Mochlus* (Ziegler et al., 2007).

Wagner et al. (2009) conducted a molecular study focused on African species of *Lygosoma* to infer the phylogenetic position and biogeographic history of the *Lygosoma fernandi* species group from west-central Africa. Adding a second mitochondrial gene (*12S*) and additional African, Indian, and Southeast Asian taxa to the dataset of Ziegler et al. (2007) for a total of 11 ingroup species, analyses recovered three, well-supported clades: two African clades (one comprising the *L. fernandi* species group [*L. fernandi* + *L. hinkeli* + *L. striatus*] and one comprising *Lygosoma afer* + *L. sundevalli* [*afer* subsequently has been synonymized into *sundevallii*, by Freitas et al., 2018]), and one Southeast Asian clade comprising *L. koratense* + *L. quadrupes*. However, inter-clade relationships, the placement of several Southeast Asian (*L. bowringii*, *L. lineolatum*) and Indian (*L. albopunctata*) taxa remained poorly supported, and the monophyly of the genus *Lygosoma* was not resolved with strong support (Wagner et al., 2009). Despite this lack of resolution across major portions of the phylogeny, Wagner et al. (2009) recommended a major revision to Greer's (1977) taxonomy by splitting *Lygosoma* again into four genera: *Lygosoma* for Southeast Asian species, *Lepidothyris* for the *Lygosoma fernandi* species group, *Mochlus* for *Lygosoma sundevallii*, and *Riopa* for Indian species, referencing Mittleman (1952) for the morphological definition of these genera. Yet, this classification contradicted that of Mittleman (1952) in several ways that were not addressed. First, the species *lineolatum* and *bowringii* were placed in the genus *Lygosoma* instead of *Riopa* and *Mochlus*, respectively, as they were in Mittleman (1952), and second, the species *albopunctatus* was moved to the genus *Riopa* instead of *Mochlus* as it was in Mittleman [1952] (Wagner et al., 2009). In fact, it appears that although Wagner et al. (2009) refer to Mittleman (1952) for the

definition of *Lygosoma*, *Mochlus* and *Riopa*, the authors did not follow Mittleman's (1952) definition of the genera and instead implicitly define them geographically (*Lygosoma* for species from Southeast Asia*, Mochlus* for species from Africa excluding the *Lepidothyris fernandi* species group and *Riopa* for species from India). This lack of morphological definitions and the implicit reliance on geography as a diagnostic feature for these genera resulted in an unstable taxonomy in which generic boundaries were not well-defined. Whereas *Mochlus* was widely adopted as the generic name for African species (e.g. Kennedy et al., 2012; Trape, et al., 2012; Pyron et al., 2013; Hedges, 2014; Masterson, 2014; Uetz et al., 2018), most subsequent studies continued to treat *Riopa* as part of *Lygosoma* (Geissler et al., 2011, 2012; Pyron et al., 2013).

Poor support along the backbone of their tree meant that Wagner et al. (2009) could not assess the reciprocal monophyly of genera, nor were they able to estimate the relationships of the genera to each other. Additionally, the lack of tissue samples for a majority of species meant that most of the species in *Lygosoma* could not be ascribed to Wagner et al.'s (2009) genera. Pyron et al.'s (2013) squamate phylogeny, in which *Lygosoma s.l.* was included as part of a much larger investigation into the evolutionary relationships of squamate reptiles, had better support at basal nodes. Although Pyron et al.'s (2013) study did not employ additional molecular or taxonomic sampling for *Lygosoma s.l.*, the authors' use of a supermatrix in an analysis that included thousands of other species resulted in a phylogeny that better resolved relationships among major clades in the group. *Lygosoma s.l.* was inferred to be monophyletic within Lygosominae; however, the genus *Lygosoma* was polyphyletic with respect to *Lepidothyris* and *Mochlus* (*Riopa* was treated as a synonym of *Lygosoma*), and *Mochlus* was not supported as monophyletic.

A paraphyletic *Lygosoma* was corroborated through a molecular phylogenetic analysis of *Lygosoma s.l.* by Datta-Roy et al. (2014), which represents the most recent study conducted to

date on the genera. The 17-species dataset included additional Indian and Southeast Asian species of *Lygosoma s.l.* (Datta-Roy *et al.*, 2014). Like Pyron et al.'s (2013) study, the results suggested that *Lygosoma* was polyphyletic with respect to *Riopa* and to both African genera. Based on these results, Datta-Roy et al. (2014) synonymized *Riopa* with *Lygosoma*, but they retained *Mochlus* and *Lepidothyris* as separate genera due to low support for the placement of the genera within the larger *Lygosoma s.l.* group. However, unlike Pyron et al. (2013), Datta-Roy et al. (2014) did not recover *Lygosoma s.l.* as monophyletic, instead observing the morphologically and ecologically distinct, arboreal species *Lamprolepis smaragdina* as nested within the clade with high support, although the species' exact position was not resolved.

Taken together, these molecular phylogenetic studies reflect the long-standing problems in arriving at a stable taxonomy for this Old World radiation of skinks. Despite considerable efforts to revise the taxonomy based on morphological characters and molecular data, the current taxonomic status of *Lepidothyris*, *Lygosoma s.s.*, *Mochlus* and *Riopa*, remain unresolved, with recent phylogenetic studies suggesting that relationships within *Lygosoma s.l.* are more complex than previously recognized (Datta-Roy et al., 2014). In this study, we employ increased taxonomic and genetic sampling of *Lygosoma s.l.*, combining concatenated and coalescent-based molecular phylogenetic analyses with multivariate statistical analyses of morphological data to address the following issues: (1) the monophyly of *Lygosoma s.l.* with respect to *Lamprolepis*; (2) the status and relationships of *Lepidothyris*, *Lygosoma s.s.*, *Mochlus* and *Riopa*; (3) the ability to determine diagnostic morphological characters for clades; and (4) the taxonomic stability of *Lygosoma s.l.*

MATERIALS AND METHODS

TAXON SAMPLING

We sampled species from across the geographic distribution of *Lygosoma s.l.*, including lineages from Africa, India, Southeast Asia and the Philippines, using one to two individuals per species (when available) for phylogenetic analyses. Our ingroup sampling consisted of 34 individuals representing 22 species of *Lygosoma s.l.* This sampling comprised 17 species of *Lygosoma s.s.*, one species of *Lepidothyris* and four species of *Mochlus* (Table S1). Tissue samples for the remaining 27 species in *Lygosoma s.l.* are not available in museum collections. Outgroup sampling was chosen based on Pyron et al. (2013) to assess the monophyly of *Lygosoma s.l.* and comprised nine individuals from species from closely and distantly related scincid genera, the lygosomine species *Eutropis multifasciata*, *Lamprolepis smaragdina*, *Larutia* sp., *Lipinia pulchella*, *Otosaurus cumingi*, *Pinoyscincus jagori* and *Sphenomorphus fasciatus*, and the scincine species *Plestiodon fasciata* (Table S1).

GENETIC SAMPLING AND MOLECULAR METHODS

Most of the sequences used in our analyses were novel; however, we were able to obtain data for several ingroup and outgroup samples from GenBank (Table S1). To generate our sequence data, we extracted genomic DNA from liver or muscle tissue using a high salt precipitation method (Aljanabi & Martinez, 1997) and amplified seven nuclear loci (nuDNA; oocyte maturation factor [*cmos*, 374 base pairs (bp)], follistatin-like protein 5 [*FSTL5*, 622 bp], prolactin receptor [*PRLR*, 566 bp], prostaglandin E receptor 4 [*PTGER4*, 470 bp], RNA fingerprint protein 35 [*R35*, 665 bp], recombination activating gene 1 [*RAG-1*, 828 bp], synuclein alpha interacting protein [*SNCAIP*, 484 bp]) and two mitochondrial markers (mtDNA; NADH dehydrogenase

subunit 1 [*ND1*, 969 bp], 16S ribosomal RNA [*16S*, 559 bp]) using standard PCR protocols (Siler et al., 2011). All loci were chosen based on their ability to resolve relationships at different tree depths as shown in previous species-level phylogenetic studies of skinks (Whiting, Bauer & Sites Jr., 2003; Siler et al., 2011; Brandley et al., 2012), and several ingroup had available sequence data for these loci on GenBank (Table S1). Primers and annealing temperatures are listed in Table 1. PCR products were purified by ExoSAP-IT (Thermo Fisher Scientific), sequenced with BigDye® Terminator v3.1 sequencing kit (Thermo Fisher Scientific) and cleaned using ethanol precipitation. We sent sequencing product to Eurofins Genomics for visualization. All novel sequences are deposited in GenBank (Table S1).

SEQUENCE ALIGNMENT AND CONCATENATED PHYLOGENETIC ANALYSES

Raw sequence data were examined for heterozygous sites and erroneous base calls and were trimmed in Geneious v9.0.4 (Biomatters, Ltd.). We aligned each locus with MUSCLE (Edgar, 2004) using default settings as implemented in Geneious and examined the resulting alignments by eye. For protein coding loci (all nuDNA and *ND1*), we used Geneious to translate and place alignments in the correct reading frame to check for errors in the location of insertions-deletions and to detect mismatched codons and erroneous internal stop codons. We retained ambiguous sites in the*16S* alignment after running preliminary maximum likelihood analyses on an alignment with the ambiguous sites included and an alignment with the ambiguous sites removed using RAxML v8.0.0 (Stamatakis, 2014). The resulting topologies did not show any highly supported incongruencies, and we therefore used the longer alignment in our subsequent concatenated analyses to maximize the size of our dataset.

Table 1. The primers and annealing temperatures for the seven nuclear genes and two mitochondrial genes used in this study.

Gene	Sequence Length (bp)	Primer	Primer Sequence (5'–3')	Annealing Temp (ºC)	Reference
cmos	374	cmosG73.1	GGCTRTAAARCARGTGAAGAAA	52.5	Whiting et al., 2003
		cmosG74.1	GARCWTCCAAAGTCTCCAATC		
FSTL5	622	FSTL5.F1	TTGGRTTTATTCTTCAYAAAGA	55	Townsend et al., 2008
		FSTL5.R2	YTCTSAACYTCAGTGATYTCACA		
PRLR	566	PRLR.F1	GACARYGARGACCAGCAACTRATGCC	55	Townsend et al., 2008
		PRLR.R3	GACYTTGTGRACTTCYACRTAATCCAT		
PTGER4	470	PTGER4.F1	GACCATCCCGGCCGTMATGTTCATCTT	55	Townsend et al., 2008
		PTGER4.R5	AGGAAGGARCTGAAGCCCGCATACA		
R35	665	R35.F	GACTGTGGAYGAYCTGATCAGTGTGG	55	Fry et al., 2006
		R35.R	GCCAAAATGAGSGAGAARCGCTTCTG		
RAG-1	828	RAG-1.R13	TCTGCTGTTAATGGAAATTCAAG	52.5	Groth & Barrowclough 1999
		RAG-1.R13.rev	AAAGCAAGGATAGCGACAAGAG		
SNCAIP	484	SNCAIP.F10	CGCCAGYTGYTGGGRAARGAWAT	55	Townsend et al., 2008
		SNCAIP.R13	GGWGAYTTGAGDGCACTCTTRGGRC		
ND1	969	16dR	CTACGTGATCTGAGTTCAGACCGGAG	53	Leaché & Reeder, 2002
		tMet	ACCAACATTTTCGGGGTATGGG		
16S	559	16Sar-L	CGCCTGTTTATCAAAAACAT	46	Palumbi, 1991
		16Sbr-H	CCGGTCTGAACTCAGATCACGT		

Although many studies have suggested that partitioning a concatenated dataset by gene and codon position results in improved topologies (Brandley, Schmitz & Reeder, 2005; Brown & Lemmon, 2007; Linkem et al., 2011, 2013), empirical and simulated phylogenetic data have shown that when partitions have few variable sites, over-parameterization leads to estimation of values for unidentifiable parameters and the resulting topology can have incorrect long branch lengths due to poor estimation of substitution rate parameters (Marshall, 2010). Therefore, to determine the best partitioning strategy for each protein-coding gene, we calculated Bayes Factors to compare the unpartitioned to partitioned-by-codon topologies for each gene. First, weselected the best substitution model for each protein coding gene and codon position using the Akaike Information Criteria (AIC; Akaike, 1974) implemented in the program JMODELTEST v2.1.10 (Darriba et al., 2012; Table 2). We then generated trees for each partitioning strategy using Bayesian Inference (BI) with MRBAYES v3.2.6 (Ronquist et al., 2012). Each BI analysis consisted of two independent runs of four chains, run for 5,000,000 generations sampling every 1,000 generations. Stationarity and convergence were assessed in Tracer v1.6 (Rambaut et al., 2014). Convergence for all runs occurred within the first 3,000,000 generations and we conservatively discarded the first 10% of each run as burn-in. To estimate the marginal likelihoods of each topology, we used the stepping stone analysis (Fan et al., 2011; Xie et al., 2011) implemented in MRBAYES, run for 50 steps and 2,958,000 generations with the first 58,000 generations discarded as burn-in and an additional 5,000 generations removed from the beginning of each step as additional burn-in. We diagnosed the analysis every 1,000 generations, resulting in 58 trees in each step. We compared the marginal likelihoods of the topologies for each gene generated by the two partitioning strategies and calculated the Bayes Factor using the equation $2\ln(BF_{10}) = 2[\ln(MarL_1)-\ln(MarL_0)]$ (Kass & Raftery, 1995; Brandley et al., 2005;

Brown & Lemmon, 2007), where $MarL_1$ is the marginal likelihood of the topology where the gene was partitioned by codon and $MarL_0$ is the marginal likelihood of the topology where the gene was not partitioned. Results of the stepping stone analysis supported partitioning by codon

Table 2. The results of JModelTest v2.1.10 showing inferred substitution models for the loci partitioned by gene and codon position. Partitions used in concatenated and coalescent-based analyses are shown in bold.

Gene	Partition	Length (bp)	Substitution model
cmos	**Gene**	**374**	**HKY + Γ**
	1st Codon Position	125	HKY + Γ
	2nd Codon Position	125	GTR + Γ
	3rd Codon Position	124	HKY + Γ
FSTL5	Gene	622	GTR + Γ
	1st Codon Position	**207**	**GTR + Γ**
	2nd Codon Position	**207**	**F81 + Γ**
	3rd Codon Position	**208**	**HKY + Γ**
PRLR	**Gene**	**566**	**GTR + Γ**
	1st Codon Position	188	HKY + Γ
	2nd Codon Position	189	GTR + Γ
	3rd Codon Position	189	GTR + Γ
PTGER4	Gene	470	HKY + Γ
	1st Codon Position	**157**	**GTR + Γ**
	2nd Codon Position	**156**	**F81 + Γ**
	3rd Codon Position	**157**	**GTR + Γ**
R35	Gene	665	GTR + Γ
	1st Codon Position	**221**	**K80 + Γ**
	2nd Codon Position	**222**	**GTR + Γ**
	3rd Codon Position	**222**	**GTR + Γ**
RAG-1	**Gene**	**828**	**GTR + Γ**
	1st Codon Position	276	GTR + Γ
	2nd Codon Position	276	HKY + Γ
	3rd Codon Position	276	HKY + Γ
SNCAIP	Gene	484	GTR + Γ
	1st Codon Position	**161**	**HKY + Γ**
	2nd Codon Position	**161**	**HKY + Γ**
	3rd Codon Position	**162**	**GTR + Γ**
ND1	Gene	969	GTR + Γ
	1st Codon Position	**323**	**GTR + Γ**
	2nd Codon Position	**323**	**GTR + Γ**
	3rd Codon Position	**323**	**GTR + Γ**
16S	**Gene**	**558**	**GTR + Γ**

position for *FSTL5*, *PTGER4*, *R35*, *SNCAIP* and *ND1*, and partitioning by gene for *cmos*, *PRLR* and *RAG-1* (Table 3). The non-protein-coding gene *16S* was partitioned by gene. We ran three additional stepping stone analyses on the concatenated dataset, partitioning all loci by gene, codon position (except *16S*), and by the partitioning scheme determined for each gene above. The results of these analysis supported the partitioning scheme determined above.

Examining relationships recovered among gene trees revealed highly supported discordance for the relationship of *Lamprolepis smaragdina* and *Lygosoma s.l.* and for the relative placement of the major clades, with six of the nine genes—*cmos*, *PTGER4*, *R35*, *RAG-1* and *SNCAIP* (nuDNA) and *ND1* (mtDNA) having discordant nodes along the backbone of their respective trees compared with other gene trees. However, the species composition of major clades was congruent across all loci. Therefore, we used both concatenated phylogenetic methods and coalescent-based species tree methods to analyze higher-level evolutionary relationships within *Lygosoma s.l.*

Table 3. The results of the stepping stone analysis implemented in MRBAYES v3.2.6. Positive values for 2*ln*(BF) were considered support for the partitioned model (partitioned by codon position) and negative values were considered support for the non-partitioned model (Brown & Lemmon, 2007).

Gene	*ln*(MarL0)	*ln*(MarL1)	2*ln*(BF)	Supported Model
cmos	-1393.50	-1398.15	-9.3	unpartitioned
FSTL5	-1633.78	-1570.91	125.74	partitioned
PRLR	-3081.56	-3090.07	-17.02	unpartitioned
PTGER4	-1577.97	-1481.96	192.02	partitioned
R35	-3369.47	-3291.48	155.98	partitioned
RAG-1	-3057.01	-3057.20	-0.38	unpartitioned
SNCAIP	-2095.3	-2048.92	92.76	partitioned
ND1	-14400.31	-13853.07	1094.48	partitioned

We performed concatenated partitioned Bayesian phylogenetic analyses with MRBAYES, partitioning the genes as determined above (Tables 2, 3). We ran two independent metropolis-coupled Monte Carlo Markov Chain runs each with four chains for 30,000,000 generations

sampling every 5,000 generations. Stationarity of parameters was assessed in Tracer v1.6 and convergence of topologies in tree space analyzed using the commands topological.approx.ess and analyze.rwty in the package RWTY v1.0.1 (Warren, Geneva & Lanfear, 2017) in R v3.3.2 (R Core Team, 2016). The effective sample sizes (ESS) for all parameters were above 200 (Drummond et al., 2006). The samples exhibited convergence by 2,500,000 generations and we conservatively discarded the first 10% of samples as burnin, leaving 10,800 trees in the combined MCMC posterior distribution. Nodes with posterior probability support of at least 0.95 were considered highly supported (Huelsenbeck & Rannala, 2004), and nodes with posterior probability support of 0.75–0.94 were considered moderately supported.

SPECIES TREE ANALYSIS

In light of our observed gene tree discordance, we conducted a coalescent-based species tree analysis in addition to concatenated phylogenetic analyses using the program *BEAST (Heled & Drummond, 2010) implemented in BEAST v2.4.6 (Bouckaert et al., 2014). When incomplete lineage sorting occurs, concatenated analyses can result in highly supported incorrect topologies (Degnan & Rosenberg, 2009; Heled & Drummond, 2010), especially if species had large ancestral populations sizes and speciation was rapid (Maddison, 1997). Coalescent-based analyses use the multi-species coalescent originally developed for population genetics (Kingman, 1982; Tajima, 1983) to assess the probability that a gene tree evolved within the framework of a particular species tree (Rosenberg, 2002; Degnan & Rosenberg, 2009). To run our species tree analysis, we pared down our concatenated dataset to include only the nuclear genes *cmos*, *PRLR*, *R35*, *RAG-1* and *SNCAIP* and the mitochondrial gene *ND1*. We excluded the nuclear genes *FSTL5* and *PTGER4* from our species tree analyses because these two loci had the most missing

data non-randomly distributed across ingroup taxa (*i.e.* these genes did not amplify across all clades), and we excluded the non-coding mtDNA gene *16S* because while it was successful at resolving very shallow nodes, it was uncertain regarding relationships at deeper nodes in the tree where most of the problems with discordance occurred. Additionally, BEAST2 estimates the root of the tree during MCMC analyses making the inclusion of any outgroup taxa unnecessary, except to give additional information to the position of the ingroup root position (Drummond & Bouckaert, 2015). Therefore, we decreased the number of outgroup species used in our analysis to the two species with the lowest amount of missing data (*Eutropis multifasciata* and *Lamprolepis smaragdina*) to reduce computation effort and errors in prior estimation associated with the inclusion of less well-sampled taxa with long branches in BEAST time tree estimation (Drummond & Bouckaert, 2015). The data were partitioned according to the same partitioning scheme in our concatenated analysis (Tables 2–3) and each partition was assigned the same substitution model. Analyses were run using an estimated strict clock prior, a Yule process species tree prior and a piecewise linear and constant population size prior for all analyses. We changed the default Birthrate.t:Species and popMean priors from an inverse 1/X distribution to a lognormal distribution and the default clockRate prior for all loci from a uniform [-∞,∞] distribution to an exponential distribution. These default priors are inappropriate because they do not integrate to one (Drummond & Bouckaert, 2015). Three initial runs were conducted for 20,000,000 generations each to tune the operators to values suggested by the BEAST2 operator outputs. Following the adjustment of operators, three additional runs were conducted for 200,000,000 generations each to check the performance of priors; several substitution rate priors were adjusted based on the results of these runs from a default gamma distribution to an exponential distribution with a mean of 1.0 to place higher probability on values closer to 0. We

ran four final runs for 1,000,000,000 generations each sampling every 100,000 generations, using the CIPRES Science Gateway portal (Miller, Pfeiffer & Schwartz, 2010). These runs were examined separately and together in Tracer and RWTY (see above) to assess stationarity and convergence. We combined the species tree analyses in LogCombiner v2.4.6 (Bouckaert et al., 2014), discarding the first 20% of trees in each posterior distribution as burnin, keeping a total of 32,004 trees in the combined posterior distribution. We used TreeAnnotator v2.4.6 (Bouckaert et al., 2014) to select the maximum clade credibility tree and calculate the posterior probability of each bifurcation.

MORPHOLOGICAL DATA AND MULTIVARIATE ANALYSES

Specimens were examined for a total of 27 quantitative and qualitative characters, including mensural body measurements, meristic scale counts and head scale patterns. Characters were chosen based on their utility in previous taxonomic studies of skinks (e.g. Siler, et al., 2010; Linkem et al., 2011; Davis et al., 2014; Geissler et al., 2012; Grismer et al., 2014) and include: snout–vent length (SVL)—distance from the tip of the snout to the anterior edge of the vent, measured on the ventral surface of the specimen; axilla–groin distance (AGD)—distance between the posterior fore-limb insertion and the anterior hind limb insertion, measured on the ventral surface of the specimen; midbody width (MBW)—width of the body approximately midway between fore-limbs and hind limbs; tail length (TL)—distance from the posterior end of the vent to the tip of the tail, measured on the ventral surface of the specimen; tail width (TW)—width of the tail at the widest part just posterior to the vent excluding the hemipene bulge in males; head length (HL)—distance from the tip of the snout to the widest portion of the head generally at the jaw articulation, which is anterior to the auricular opening; head width (HW)—

width of the head at the widest part, generally at the jaw articulation; head depth (HD)—depth of the head from the occiput to the underside of the jaws at the widest part, generally at the jaw articulation; eye–nares distance (END)—distance from the anterior edge of the eye opening to the posterior edge of the naris along a line parallel to the mouth; snout length (SNL)—distance from the anterior edge of the eye opening to the tip of the snout along a line parallel to the mouth; internarial distance (IND)—distance between the nares; midbody scale row count (MBSRC)—number of scales around the midbody approximately midway between fore-limbs and hind limbs; axilla–groin scale row count (AGSRC)—number of dorsal scales along a line from the posterior fore-limb insertion and the anterior hind limb insertion; paravertebral scale row count (PVSRC)—number of mid-dorsal scales along a line from the parietals to a point opposite the vent, excluding enlarged nuchals; Finger-III lamellae count (FinIIILam)—number of enlarged scales under Finger-III; Toe-IV lamellae count (ToeIVLam)—number of enlarged scales under Toe-IV; supralabial scale count (SuprL)—number of enlarged scales in a line directly dorsal and parallel to the mouth opening; infralabial scale count (InfrL)—number of enlarged scales in a line directly ventral and parallel to the mouth opening; supraocular scale count (SO)—number of enlarged scales above the eye, the ventral edges of which are in contact with the dorsal edges of the superciliary scales and dorsal edges of which are in contact with the lateral edges of the frontal and/or frontoparietal scales; superciliary scale count (SC)—number of small scales directly above the eyelid and below the supraocculars, the first of which is in contact with the preocculars, and the last of which begins above the eye and terminates beyond the posterior edge of the orbital opening, not including superciliary #7 of Taylor (1935: 71 Fig. IV); supranasal scale contact (SN)—contact of supranasals along the midline; prefrontal scale contact (PF)—contact of prefrontals along the midline; frontoparietal contact (FP)—contact of

frontoparietal scales along the midline; parietal contact (P)—contact of parietal scales along the midline posterior to the interparietal scale; presence of enlarged nuchals (NU); first chin shield scale contact (1stChin)—contact of first chin shields along the midline; and presence of enlarged third chin shields (3rdChin). All specimens were measured by ESF, ADR, CDS, B. Karin, E. Ellsworth, and S. Pal. Because older specimens were often fixed with curved bodies, the three major body length measurements, SVL, AGD and TL, were measured with a measuring tape and rounded to the nearest mm. The remaining mensural characters were measured using digital calipers accurate to 0.01 mm. When measurements were obviously distorted due to specimen preparation (e.g. specimens flattened during preparation could lead to inaccuracies in midbody depth), the measurement was flagged and excluded from statistical analyses. When possible, characters were measured or counted on the right side of the body.

Our morphological dataset included 254 specimens representing 25 species: 20/22 ingroup species from our phylogenetic analyses were included in our morphological dataset along with five additional species (*L. kinabatanganense*, *L. koratense*, *L. pembanum*, *L. siamense*, *L. tanae*) for which we were unable to obtain genetic samples (Table S2). One of these species, *L. siamense* is a new species described as part of the *Lygosoma quadrupes* species complex (Siler et al., 2018), and so we consider that species as part of the same clade as *L. quadrupes*, even though we lack DNA sequence data for it. Species in our phylogeny that we did not have morphological data for are *M. guineensis* and *Lepidothyris fernandi*. We ran principal components analysis (PCA) and discriminant analysis of principal components (DAPC) on the mensural and meristic characters, excluding the head scale patterns (SN, PF, FP, P, NU, 1stChin, 3rdChin) because of problems using discrete categorical characters in PCA when they do not exhibit strong taxonomic structure (Hill & Smith, 1976). We excluded juveniles (juveniles considered to be

individuals whose SVL fell outside of the lower range of previously published adult SVL for the species [Broadley, 1966, 1994; Das, 2010; Geissler et al., 2011, 2012; Heitz et al., 2016]) and outliers, which may have been individuals that were misidentified, so that our final dataset comprised a total of 199 individuals representing 25 species. Additionally, we excluded one mensural character (TL) due to missing data as a number of species in our morphological dataset only contained TL measurements from individuals with autotomized or regenerated tails, and four meristic characters (SuprL, InfrL, SO and SC) because these counts did not vary meaningfully between species and were introducing "noise" into preliminary analyses Therefore, differences in the variance of these characters seen by in the PCA results were artifacts of sampling, not statistically significant taxonomic differences. These excluded measurements and coded head scale patterns are used in our taxonomic descriptions below and in Table S3. Three species in our morphological dataset (*L. albopunctatum*, *L. herberti* and *L. tanae*) had a majority of individuals that were missing MBSRC data, and we filled in these missing values with average values from the literature (Tabachnick & Fidell, 2013). For the mensural characters, we converted characters to ratiometric data by dividing all measurements by SVL to lessen the disproportionate effect of body size variance on the analysis and then prior to performing multivariate analyses, we log-transformed (natural log) all mensural and meristic values to normalize the data (Tabachnick & Fidell, 2013). Therefore, we included the following 14 characters in the PCA/DAPC morphological dataset: AGD, MBW, TW, HL, HW, HD, END, SNL, IND, MBSRC, AGSRC, PVSRC, FinIIILam and ToeIVLam.

We ran PCA on the data using the command prcomp in the package stats in R v3.5.0 (R Core Team, 2018), setting scale=True so that the analysis was performed on the correlation matrix of the data. PCA analyzes the variance of all measurements for all samples and determines which

measurements contribute the majority of the variance to the entire dataset. Each successive principal component describes the majority of the variance that was not captured by the preceding principal component. We used the resulting principal components from the PCA as input variables for DAPC. Whereas PCA seeks to maximize the total variance captured across the dataset, DAPC compares within-group variance to between-group variance and seeks to minimize the amount of within group variance while maximizing between group variance (Jombart, Devillard & Balloux, 2010). Therefore, PCA illustrates the distribution of the entire dataset in morphospace whereas DAPC shows how groups differ in morphospace. We ran DAPC on the data grouping by phylogenetic clades using the first four principal components from the PCA as the variables, which accounted for 90% of the variance. The analysis was run in R using the command dapc in the package adegenet (Jombart, 2008).

RESULTS

CONCATENATED BAYESIAN PHYLOGENETIC ANALYSIS

Our concatenated alignment comprised 43 individuals (34 ingroup samples, nine outgroup samples) sequenced for seven nuclear loci and two mitochondrial markers, for up to of 5,537 base pairs (bp) per individual (average [$\bar{x}$] = 4,237 bp per individual). Ingroup taxa contained an average of 21.1% missing data for each individual (standard deviation = 18.6%) resulting from difficulty in obtaining complete sequence data for several loci for all species and species groups; for example, *PRLR* was not amplified successfully for *L. quadrupes* and *L. tabonorum* (Table S1).

Bayesian concatenated phylogenetic analyses showed strong support for four divergent clades represented by the sampled taxa (Fig. 1), with no analysis supporting the monophyly of

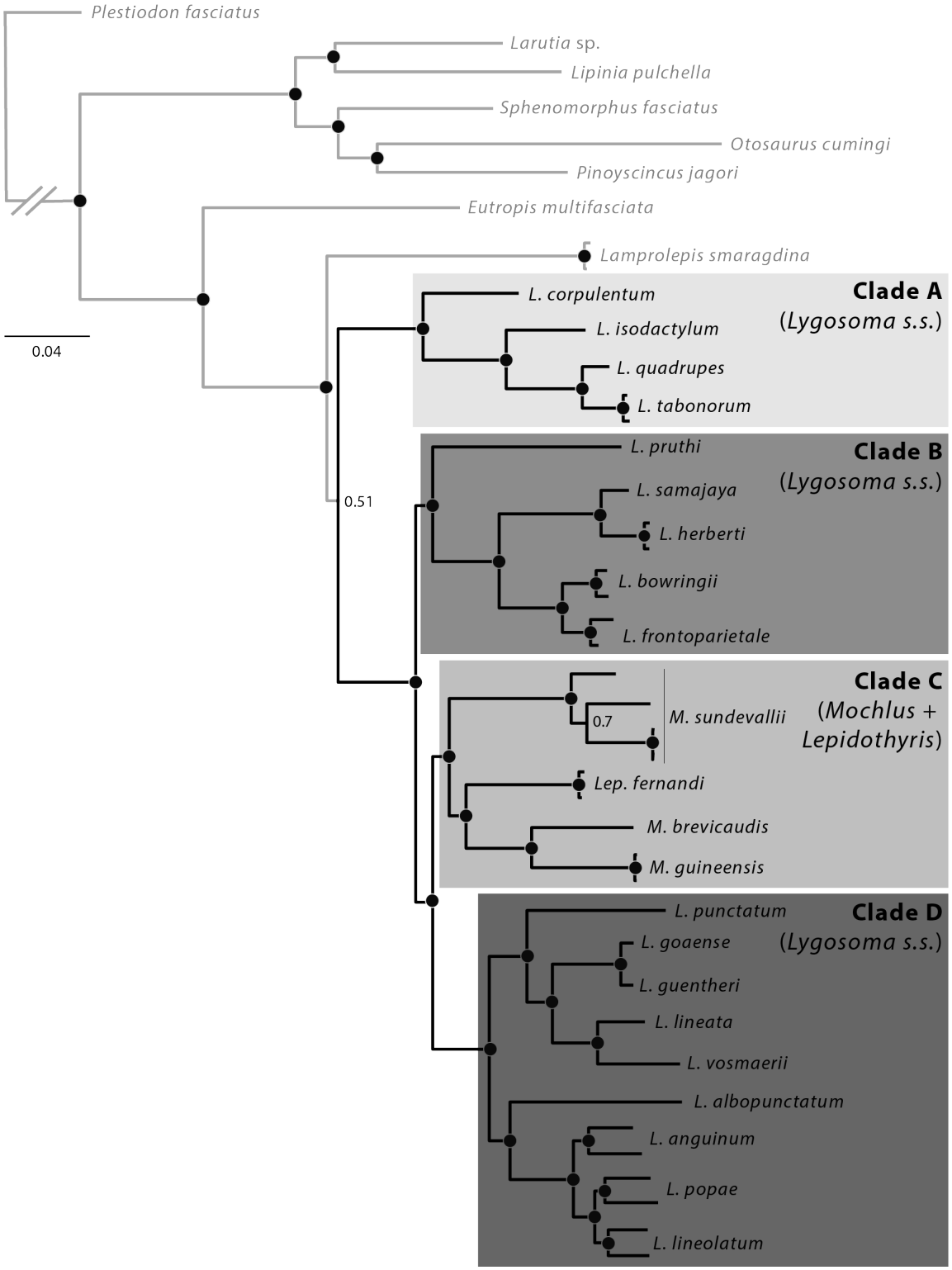

Figure 1. The concatenated Bayesian consensus topology. Black circles denote highly supported nodes (pp≥0.95). Clades outlined in grayscale boxes refer to those listed in results and discussion.

Lygosoma s.l. (clade containing *Lygosoma s.s.*, *Mochlus* and *Lepidothyris*, Bayesian posterior probability [pp]=0.51). Instead, we recover *Lygosoma s.l.* as part of a clade also comprising *Lamprolepis smaragdina* (Fig. 1, pp=1.0). Within *Lygosoma s.l.*, we find four well-supported clades (Fig. 1, Clades A–D, pp=1.0;). The genus *Lygosoma s.s* is not recovered as monophyletic, with the African genera *Mochlus* and *Lepidothyris* nested within *Lygosoma s.s.* (Fig. 1, pp=1.0), breaking up *Lygosoma s.s.* into three separate clades: (1) Clade A contains the Southeast Asian species *L. corpulentum*, *L. isodactylum*, *L. quadrupes* and *L. tabonorum*; (2) Clade B contains the Southeast Asian species *L. bowringii*, *L. frontoparietale*, *L. herberti* and *L. samajaya*, and the Indian species *L. pruthi*; and (3) Clade D contains the Southeast Asian species *L. anguinum*, *L. lineolatum* and *L. popae* and the Indian species *L. albopunctatum*, *L. goaense*, *L. guentheri*, *L. lineatum*, *L. punctatum* and *L. vosmaerii*. Additionally, analyses did not support the monophyly of the genus *Mochlus*, with results instead showing *Lepidothyris* as nested within *Mochlus* (Fig. 1, Clade C, pp=1.0), sister to Clade D (pp=1.0). The type species of *Lygosoma s.s.*, *L. quadrupes*, is recovered as part of Clade A, which is supported as sister to the remaining *Lygosoma s.l.* clades (Fig. 1, pp=1.0).

SPECIES TREE ANALYSIS

Similar to the results of the concatenated Bayesian phylogenetic analysis, species tree analyses recover four clades within *Lygosoma s.l.* (Fig. 2; Clades A–D, pp=1.0, 0.85, 0.84, and 1.0, respectively), with *Lygosoma s.s.* supported as paraphyletic. The genera *Mochlus* and *Lepidothyris* are both nested within *Lygosoma s.s.*, separating the genus into three clades (Clades A, B, D, see concatenated results above for definition). Once again, *Mochlus* is found to be paraphyletic with respect to *Lepidothyris*, instead forming a *Mochlus* + *Lepidothyris* clade with

moderate support (Fig. 2, Clade C, pp=0.84). Clades B–D together are supported as a monophyletic group of taxa (pp=1.0) to the exclusion of Clade A (Fig. 2).

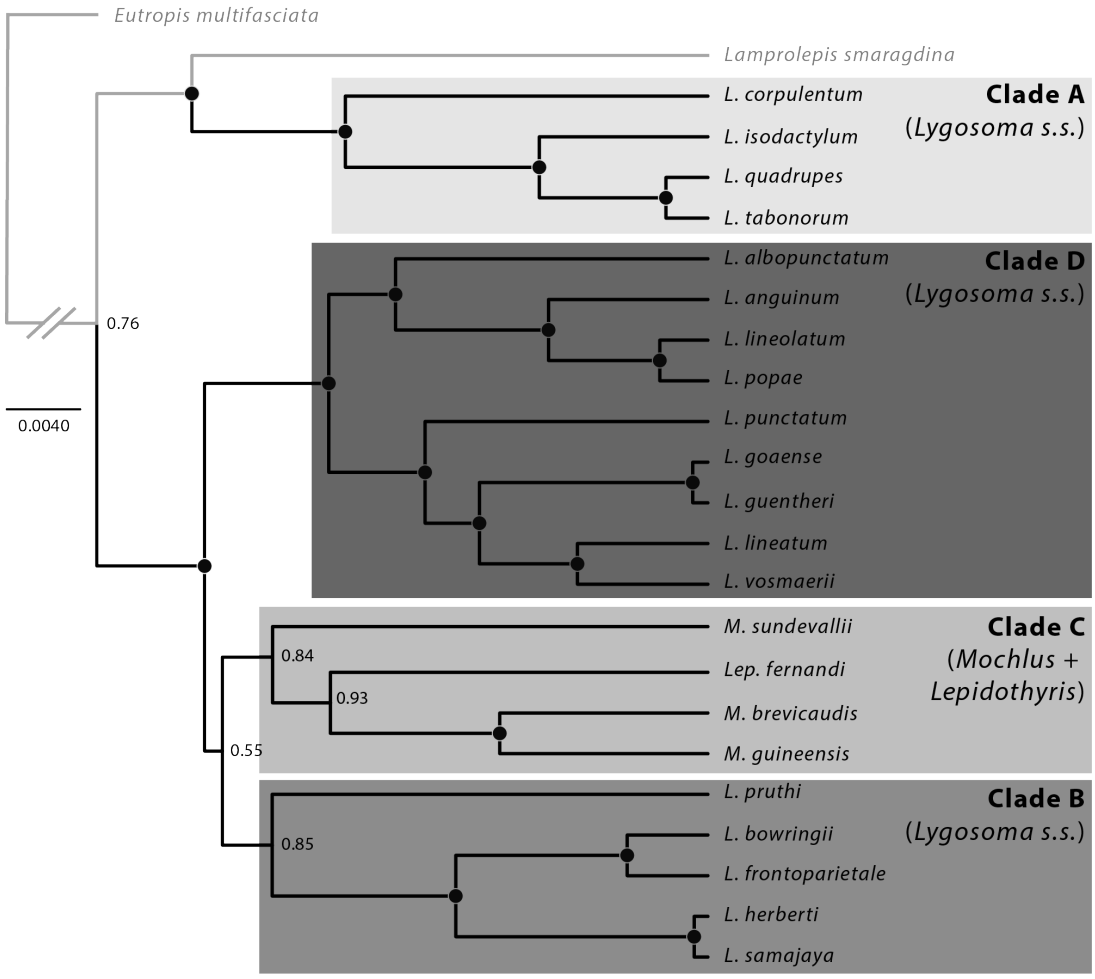

Figure 2. The coalescent-based species tree maximum clade credibility topology. Black circles denote highly supported nodes (pp≥0.95). Clades outlined in grayscale boxes refer to those listed in results and discussion.

The inferred species tree topology (Fig. 2) is broadly consistent with the Bayesian topology in regard to intraclade species-level relationships, with a few notable exceptions. First, the placement of *M. sundevalli* as part of Clade C, and *L. pruthi* as part of Clade B, received moderate support (pp=0.84 and 0.85, respectively). Second, although there is high support for superclade comprising Clades B, C, and D and excluding Clade A, there is no support for

interclade sister relationships between Clades B, C, and D (Fig. 2, pp=0.55). Finally, unlike the Bayesian topology, the species tree topology supports *Lamprolepis smaragdina* as the sister taxon to Clade A (Fig. 2, pp=0.97).

MULTIVARIATE ANALYSES

The principal components analysis shows that species in *Lygosoma s.l.* vary in degree of body elongation; however, the results show considerable overlap among species in morphospace (Fig. 3). The first two principal components (PCs) account for 82.8% of the total variance, with PC1 representing body size and accounting for 76.7% of the total variance and PC2 representing body robustness and accounting for 6.1% of the variance. For PC1, all characters have roughly equal loadings with the exception of MBSRC, which has a lower loading than the other characters. Three characters (AGD, AGSRC, and PVSRC) are negatively correlated with the remaining characters, confirming that as body elongation increases, body width decreases. For PC2, AGD, PVSRC, MBSRC, and ToeIVLam have the highest loadings, with AGD and ToeIVLam negatively correlated with PVSRC and MBSRC, suggesting that at a larger body size, relative elongation and digit lengths decrease (Table 4). The PCA reveals that clades (see Figures 1 and 2 for the phylogenetic definition of each clade) overlap highly in morphospace (Fig. 4A), with Clades B and C, and Clades C and D, showing the most overlap. Four species were not represented in our phylogenetic analyses and are therefore denoted as *incertae sedis* (*L. kinabatanganense*, *L. koratense*, *L. pembanum*, *L. tanae*; Fig. 4A), as their phylogenetic position remains unknown. As a result, we were not able to associate them definitively with any of the four *Lygosoma s.l.* clades.

Discriminant function analyses of principal components corroborates the PCA in showing that clades overlap highly in morphospace (Fig. 4B). Although the clades have distinct, non-overlapping centroids (averages) and 95% inertia ellipses in morphospace, several individual species overlap with centroids of different clades. This suggests that no clade is morphologically distinct from the other clades in *Lygosoma s.l.* Clades B and C exhibit the highest amount of overlap, whereas Clades A and B do not overlap at all. Interestingly, Clades B and C occupy smaller areas of morphospace than Clades A and D.

Table 4. The results of the PCA showing the variance, cumulative variance and character loadings for the first four principal components. These components were used as the input variables for the DAPC

	PC1	PC2	PC3	PC4
% variance	76.7	6.1	3.9	3.1
Cumulative variance	76.7	82.8	86.7	89.8
AGD	0.2205	0.2752	0.7428	-0.4484
MBW	-0.2861	-0.4484	0.2181	-0.0299
TW	-0.2712	0.0450	0.2999	0.2188
HL	-0.2811	0.0715	0.0047	-0.0911
HW	-0.2920	0.0026	0.1331	0.0222
HD	-0.2865	-0.0056	0.2126	0.0194
END	-0.2664	0.0782	-0.1287	-0.1761
SNL	-0.2601	0.0145	0.2820	0.3981
IND	-0.2829	0.0293	0.0611	0.2398
PVSRC	0.2918	-0.1149	0.1260	-0.0264
MBSRC	-0.1440	-0.9264	0.1966	-0.2266
AGSRC	0.2933	-0.0503	0.1537	-0.0144
FinIIILam	-0.2586	0.0596	-0.2559	-0.5660
ToeIVLam	-0.2686	0.1622	-0.0659	-0.3483

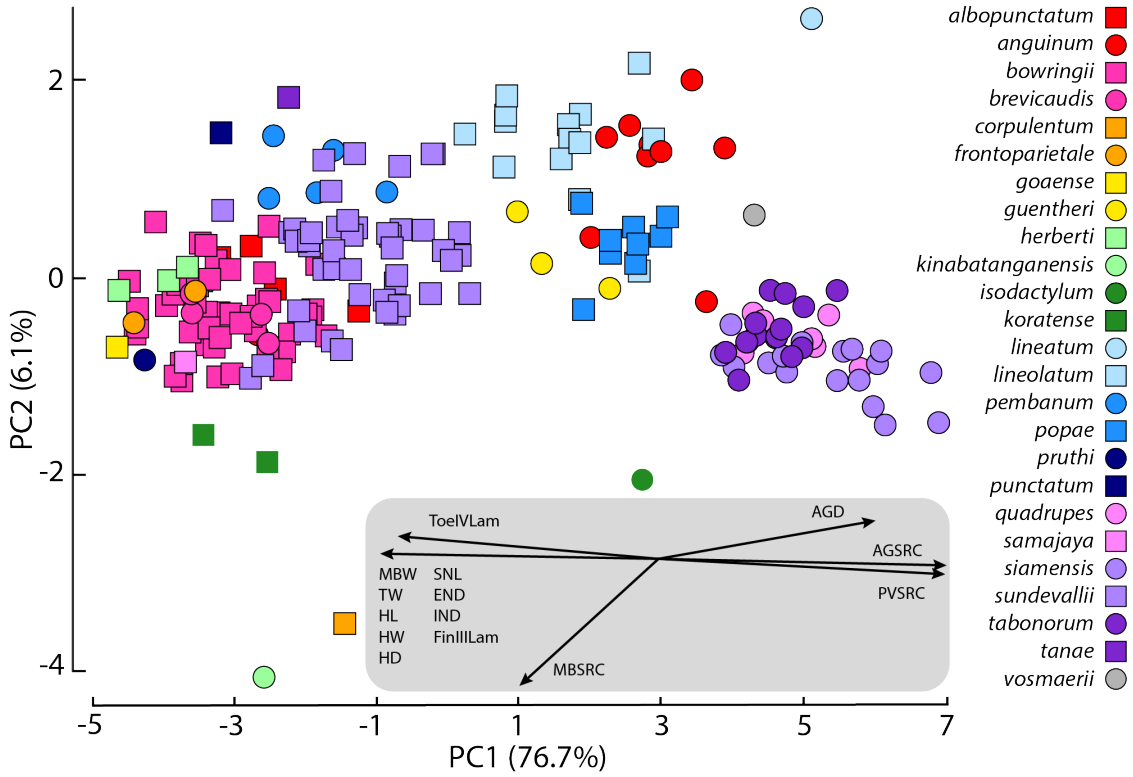

Figure 3. Principal components analysis of 14 characters for 25 species of *Lygosoma s.l.* with points given a different color and shape combination for each species.

DISCUSSION

NON-MONOPHYLY OF *LYGOSOMA S.L.* AND PARAPHYLY OF *LYGOSOMA S.S.* AND *MOCHLUS*

A stable taxonomy reflects evolutionary relationships of species and clades and thus continues to be of paramount importance for studies in biological science. Diverse fields, from ecology to development, rely on accurate species- and supra-specific-level identifications for their research (Mayr, 1976; Felsenstein, 1985; Winston, 1999; Wheeler, Raven & Wilson, 2004). Furthermore, taxonomy plays a critical role in biodiversity conservation and management, with agencies using recognized nomenclature for identification and classification of regional fauna, including rare and threatened species (e.g. CITES and IUCN; Kaiser et al., 2013; Groves et al., 2017; IUCN-SSC Species Conservation Planning Sub-Committee, 2017).

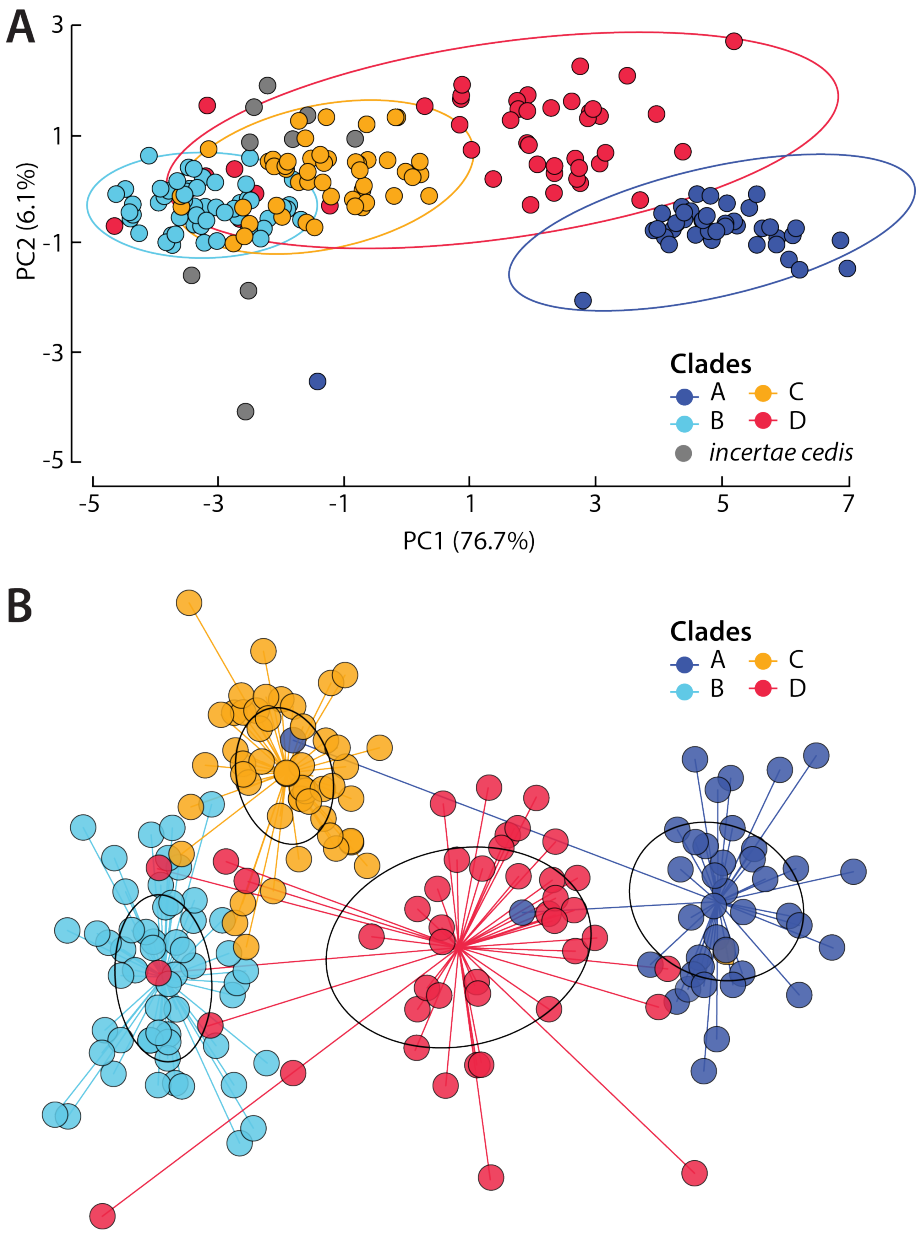

Figure 4. A. Principal components analysis of 14 characters for 25 species of *Lygosoma s.l.* with points colored by phylogenetic clade. Ellipses around clusters are colored by clade and show the 95% boundary for each clade. **B.** Discriminant analysis of principal components based on the first four principal components obtained in our PCA analysis. Points and 95% inertia ellipses are colored by clade.

Within supra-specific taxonomy, the genus category is included within the binomial name of a species, so while the genus category is not based inherently on biological criteria, it is an important communication tool in the name of a species, depicting relatedness between species

grouped within the same genus to the exclusion of other species that may be also closely related (Cain, 1956; Winston, 1999). Therefore, the genus reflects information about the evolutionary history of the species it composes. Inger (1958) proposed a definition of genera that uses ecological criteria to determine the species that fall within a genus, with "mode of life" (*i.e.* adaptive zone; Vences et al., 2013) as a major diagnostic character of the genus. However, this approach is problematic, especially for little-known clades, because it requires ecological knowledge of all species included within a genus and of closely related species excluded from the genus. Furthermore, congeners that live in sympatry may have undergone niche displacement (e.g. genus *Brachymeles*; Huron & Siler, unpubl. data), making the adaptive zone difficult to define empirically (Vences et al., 2013). Accordingly, the only current defining characteristic of a genus is that it represents a clade nested within a broader family-level clade.

Among scincid lizards, a growing number of studies have shown that many taxonomic groupings are not supported as monophyletic (e.g. *Amphiglossus* [Whiting, Sites & Bauer, 2004]; *Sphenomorphus* [Linkem et al., 2011]; *Anomalopus* and *Eulamprus* [Skinner et al., 2013]; *Trachylepis* [Karin et al., 2016]; *Afroablepharus* [Medina et al., 2016]). These inconsistencies between historical nomenclature and hypothesized evolutionary relationships recovered through molecular datasets, necessitate revised genus-level classifications for taxonomic stability and for discussions of evolutionary patterns and processes within and among clades (Kaiser et al., 2013; Vences et al., 2013).

Our concatenated, Bayesian Inference phylogenetic and coalescent-based species tree analyses reveal that *Lygosoma s.l.* is not monophyletic. Additionally, *Lygosoma s.s.* is paraphyletic, with both *Mochlus* and *Lepidothyris* nested within the genus, and the genus *Mochlus* is paraphyletic with *Lepidothyris* nested within the genus (Figs. 1–3). These results are

consistent across all analyses and unsurprisingly corroborate the findings of previous studies—Datta-Roy et al. (2014) observed similar relationships between *Lamprolepis* and *Lygosoma s.l.*, and *Lygosoma s.s.* and *Mochlus* in their study using the mtDNA genes *16S* and *12S*, albeit with low support at some of their deeper nodes. In our concatenated and coalescent-based analyses, *Lygosoma s.s.* Clade A, containing *Lygosoma quadrupes*, the type species of the genus, is supported as divergent from the other two major clades within *Lygosoma s.s.* (Figs. 1–3), again corroborating the results of Datta-Roy et al. (2014).

Some differences between our concatenated and coalescent-based topologies are seen regarding the relationship between *Lamprolepis smaragdina* and *Lygosoma s.l.* In concatenated analyses, *Lamprolepis smaragdina* is recovered as part of *Lygosoma s.l.* with strong support (Fig. 1), although its position within *Lygosoma s.l.* is unresolved, which suggests that *Lygosoma s.l.* is paraphyletic with respect to *Lamprolepis smaragdina*. In contrast, the relationship between *Lamprolepis smaragdina* and *Lygosoma s.l.* is resolved fully in our coalescent-based species tree analyses, which recovered *Lamprolepis smaragdina* as the sister taxon to Clade A with strong support (Fig. 2). Although the finding of a paraphyletic *Lygosoma s.l.* with respect to *Lamprolepis smaragdina* is consistent with previous studies (Honda et al., 2000, 2003; Datta-Roy et al., 2014), it is surprising nevertheless given the highly divergent life histories of the species in question: *Lamprolepis smaragdina* is a larger, more robust, bright-colored, arboreal skink, whereas most of the species in the genus *Lygosoma* are small, colored inconspicuously, and semi-fossorial (Greer, 1977; Das, 2010). In fact, Greer (1977) cited this ecological difference as clear evidence that the genera *Lygosoma* and *Lamprolepis* were not each other's closest relatives. The differences in the relationship between *Lamprolepis smaragdina* and *Lygosoma s.l.* seen in our concatenated and coalescent-based analyses may be attributed to issues concerning

concatenated phylogenetic analyses, where the analysis of a concatenated dataset may result in misleading topologies in the presence of gene tree discordance (Degnan & Rosenberg, 2009; Linkem et al., 2016). We believe this may have contributed to the discrepancies between the two types of analyses, given the presence of some discordance between loci in our nuDNA dataset.

The relationships of Clades B, C and D are resolved fully in our concatenated analyses but not in our coalescent-based analyses (Figs. 1, 2). In our concatenated analyses, Clades C and D are supported highly as sister, and together are recovered sister to Clade B. However, in coalescent-based analyses, the relationship between the three clades are not resolved, although they are still recovered together as distinct from Clade A with high support (Fig. 2). We suspect that incomplete taxonomic sampling across the radiation and low sample sizes for some rare or secretive species contributed to these results. To estimate the multispecies coalescent process for each gene, sequences from at least two individuals per lineage need to be included within the dataset (Heled & Drummond, 2010), which implies that increasing the taxonomic sampling per lineage will increase resolution of the species tree. Additionally, studies have shown that increased taxonomic sampling improves species tree accuracy (Hovmöller, Knowles & Kubatko, 2013; Lambert et al., 2015). Unfortunately, these two issues could not be addressed fully at this time given the rarity or absence of tissues in collections for some focal taxa. However, as next-generation sequencing techniques are quickly revolutionizing approaches to phylogenetic studies by providing datasets of thousands of loci at increasingly lower costs (Ekblom & Galindo, 2011), these datasets are becoming more common in skink population and phylogenetic research (Barley et al., 2015b; Brandley et al., 2015; Rittmeyer & Austin, 2015; Linkem et al., 2016; Bryson et al., 2017). These techniques have the power to resolve difficult intra- and interclade

relationships (e.g. Crawford et al., 2012; McCormack et al., 2012; Streicher & Wiens, 2017) and may be a promising tool for resolving the relationships among Clades B, C and D.

CLADES ARE NOT DIFFERENTIATED BY MORPHOLOGY

Researchers have struggled to find diagnostic characters for *Lygosoma s.l.*, which has resulted in challenges to understanding the systematics of the group (Boulenger, 1887; Smith, 1937a; Mittleman, 1952). As a result, species relationships have been in flux for almost two centuries, with species sometimes lumped together within a single genus (Boulenger, 1887), or split into multiple genera (Smith, 1937a; Mittleman, 1952). In performing multivariate analyses, we investigated whether combinations of characters commonly used in delimitating species and genera could differentiate *Lygosoma s.l.* species and clades in morphospace; however the results of our principal components analysis (PCA) and discriminant analysis of principal components (DAPC) underscore the historical difficulties in using morphology to classify *Lygosoma s.l.* skinks (Fig. 4), illustrating how traditional morphological approaches have largely failed in diagnosing clades with *Lygosoma s.l.* because of the large amount of morphological overlap between species in the group. Among species examined, our PCA results reveal transitions within *Lygosoma s.l.* between robust and elongated body forms, with species overlapping along a morphological gradient (Fig. 3). As a result, among the major clades, we find that none form distinct clusters in morphospace (Fig. 4A), although it appears that Clade A contains the most elongated species, followed by Clade D, and then by Clades B and C, with the highest amount of morphological overlap between Clades B, C, and D. Given our phylogenetic results which indicate that Clades B, C, and D together form a clade to the exclusion of Clade A, our observations of these clades having the highest amount of morphological overlap makes sense.

Our DAPC, which used the principal components from the PCA as descriptor variables, was conducted to compare within-clade variance to between-clade variance and revealed Clades B and C to have the highest amount of overlap and occupy more restricted areas of morphospace when compared with Clades A and D (Fig. 4B). Interestingly, Clade A seems the most distinct morphologically in the DAPC, with only two samples falling within the inertia ellipses of other clades, and only a single individual from another clade (Clade D) recovered within the Clade A inertia ellipse (Fig. 4B), which suggests that clade A comprises the most morphologically diagnosable species within *Lygosoma s.l.* However, this pattern may be driven by the large number of individuals of the *Lygosoma quadrupes* species complex in our morphological dataset, which have a highly derived body form in comparison to other species in Clade A and in *Lygosoma s.l.* (Greer, 1977), and it is likely that the inclusion of additional samples of other species in this clade (e.g. *L. corpulentum*, *L. isodactylum*) and from other clades, as well as the inclusion of additional species not currently included in our morphological dataset at all would temper this pattern.

Four species are labeled as *incertae sedis* in our PCA analysis because they were not represented in our phylogenetic analyses. Among these, *Lygosoma koratense* from Southeast Asia appears to be morphologically most similar to species in Clade B and *L. pembanum* and *L. tanae* from Africa appear to be morphologically most similar to Clade C (Figs. 4, 5A). The remaining species, *L. kinabatanganense*, a large and robust species from Malaysia (Sabah, Borneo), does not fall within the morphological boundaries of any of the clades in our PCA. (Figs. 4, 5A). Interestingly, a previous phylogenetic study of *Lygosoma s.l.* suggested a close relationship between *Lygosoma quadrupes* and *L. koratense* (Honda et al., 2000), which was corroborated in subsequent studies using the same sequence data (Ziegler et al., 2007; Wagner et

al., 2009; Skinner et al., 2011 Pyron et al., 2013; Datta-Roy et al., 2014). Unfortunately, vouchered tissue samples of *L. koratense* were not available for this study. If the relationship of *L. quadrupes* and *L. koratense* holds true in future phylogenetic analyses, this would expand the extent of the occupied morphospace of Clade A, which currently includes only species that are more elongate, and thus would have interesting implications for the evolution of body form within the clade.

The results of our PCA and DAPC analyses show that, like traditional morphological approaches based on external characters, multivariate approaches have largely failed to differentiate clades within *Lygosoma s.l.* While there exists variation in body form among species in the group, this appears to change along a morphological gradient that only partially conforms to phylogeny (Fig. 4A). However, there are two characters not included in our PCA and DAPC analyses that have been employed historically in *Lygosoma s.l.* systematics, which are worth discussing further because they may be of use to differentiating phylogenetic clades within *Lygosoma s.l.* These characters are the morphology of the secondary palate and the character state of the lower eyelid. Of these characters, the morphology of the secondary palate is the least controversial. Greer (1977) used the morphology of the secondary palate to unite *L. quadrupes* with *Riopa*, and he described all species of *Riopa* recognized at the time (31 species) as having processes that project from the posteromedial edge of the palatine bones which separate the two pterygoid bones. Interestingly, two character states of the secondary palate were noted within *Lygosoma*—an open state (pterygoids emarginated along their posterior edge) and a closed state (pterygoids not emarginated along their posterior edge), each of which correspond consistently with clades in our phylogenetic analyses (Figs. 1, 2; Greer, 1977). Greer (1977) listed all species found in our Clade B (with the exception of the recently described *L. samajaya*,

which he did not examine) and our Clade C (*Mochlus* + *Lepidothyris*) as having a closed palate, and listed all species found in our Clade A (with the exception of *L. corpulentum*, which he did not examine) and our Clade D (with the exception of *L. vosmaerii*, which he did not examine and *L. punctatum* which was variable) as having an open palate. The palate of *L. koratense* was listed as closed, again morphologically linking this species more closely with Clade B than Clade A. The morphology of the secondary palate has also been used to diagnose the genus *Lamprolepis* from *Lygosoma s.l*. (Greer, 1977). However, examination of written descriptions and drawings of the palate of *Lamprolepis* indicates that *Lamprolepis smaragdina* has posteromedial projecting processes separating the pterygoid bones (Greer, 1970b:fig. 1, 1977:Fig. 5), similar to although not as pronounced as the processes in *Lygosoma s.l.* Therefore, the morphology of the secondary palate is useful in diagnosing the larger *Lygosoma s.l.* group of clades, and may also be a useful descriptor variable for clades within *Lyogosoma s.l.*

In contrast to the morphology of the secondary palate, the taxonomic utility of the lower eyelid character has been more controversial. Mittleman (1952) proposed the state of the lower eyelid, which has been defined broadly as either scaly or with a transparent window, as a diagnostic character separating groups, and he relied exclusively on eyelid state to split *Mochlus* from *Riopa*. Subsequent authors have disagreed with the taxonomic value of this character (Broadley, 1966; Greer, 1974, 1977), arguing that the character is highly variable within clades. Nevertheless, several recent skink taxonomic studies have mentioned the state of the lower eyelid as part of the combinations of diagnostic characters for some skink genera descriptions (*Euprepis* and *Eutropis* [Mausfeld & Schmitz, 2003]; *Brachymeles* [Siler et al., 2011]; *Heremites* and *Toenayar* [Karin et al., 2016]), although the presence of both states within the genus *Scincella* was noted by Linkem et al. (2011). In our study, the state of the lower eyelid does not

appear to be consistent within our clades, with the exception of Clade A in which all our sampled members have a scaly lower eyelid. Instead, the lower eyelid character state appears to be highly variable between species and may also exhibit intraspecific variation. Within Clade B, four of the five sampled species have a scaly lower eyelid; the exception being *L. pruthi*, which has a transparent disc on its lower eyelid (Sharma, 1977). In Clade C, all sampled species have a scaly lower eyelid, with the possible exception of *M. guineensis*. In the original description, *M. guineensis* was recorded as having a lower eyelid with a transparent disc (Peters, 1879); however, the eyelid state was revised subsequently as scaly by Greer (1977). Additionally, four species from Africa that we lack genetic data for but include provisionally in Clade C (*M. laeviceps*, *M. mabuiiformis*, *M. simonettai*, and *M. tanae*; see justification in our taxonomic revision section), also were described originally as having a lower eyelid with a transparent disc (Peters, 1874; Loveridge, 1935; Lanza 1979). One of these lineages, *M. laeviceps*, later was reclassified as having a scaly lower eyelid (Greer, 1977). In Clade D, all of our sampled species have a transparent lower eyelid; however, there is a record of one specimen of *L. albopunctatum* from Sarbhog, Assam, India in the Indian Museum, Kolkata that possesses a lower eyelid with a transparent window on its right side and a scaly lower eyelid on its left side (Hora, 1927). Additionally, *L. lineolatum* was described originally as having a scaly lower eyelid (Stoliczka, 1870), but Smith (1935) reclassified the species as having a transparent disc in its lower eyelid. Nevertheless, several *Lygosoma* sp. individuals from Myanmar appear to have a scaly lower eyelid (ESF, unpubl. data), suggesting that the lower eyelid state is variable in Clade D. Therefore, unlike the morphology of the secondary palate, the lower eyelid character state seems to be inconsistent across most clades of *Lygosoma s.l.* and not useful for clade-level diagnosis.

A REVISED CLASSIFICATION OF *LYGOSOMA S.L.*

OVERVIEW

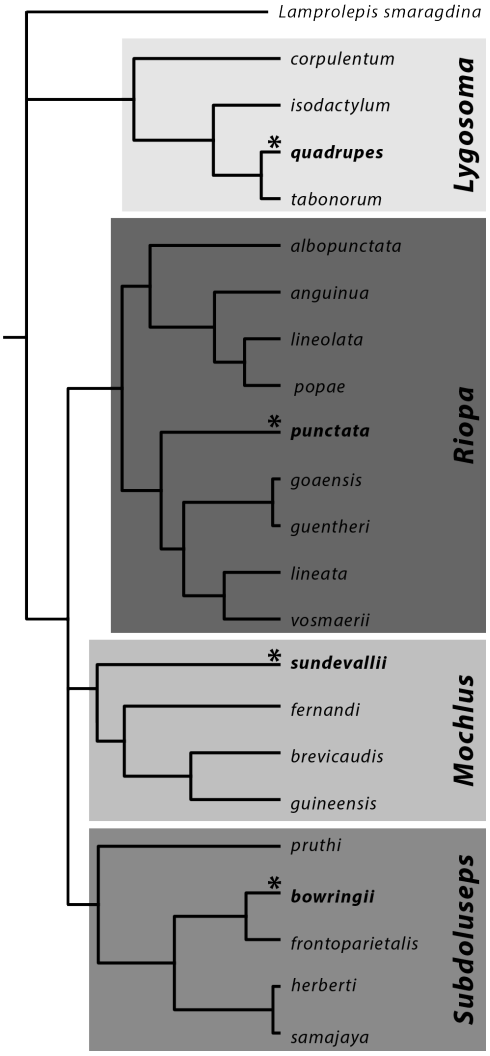

Figure 5. Phylogenetic tree showing the revised taxonomy of *Lygosoma s.l.* The topology is based on the species-tree topology (see Figure 2). Support values are not shown. Species' names shown in bold with asterisks above branches represent the type species for that genus.

Currently, *Lygosoma s.l.* comprises 49 nominal species: 33 species in the genus *Lygosoma s.s.*, 13 species in the genus *Mochlus*, and three species in the genus *Lepidothyris*. Of these 49 species, we were able to include 22 in our phylogenetic analyses, representing all three genera, for the most complete assessment of the radiation to date. The results of our phylogenetic analyses suggest that *Lygosoma s.s.* does not form a monophyletic group with respect to the other genera in *Lygosoma s.l.*—*Lepidothyris* Cope 1892 and *Mochlus* Günther 1864a, and the genus *Lamprolepis* Fitzinger 1842. Instead, *Lygosoma s.s.*is separated into three clades, one comprising elongate-bodied species from Southeast Asia, Indonesia and the Philippines (Clade A), one comprising the widespread species *L. bowringii* and other small, stouter-bodied species from India and Southeast Asia, Indonesia, the Philippines, and Christmas Island (Clade B), and one comprising species from India and Southeast Asia (Clade D). Additionally, we do not recover *Mochlus* as monophyletic, with our results suggesting it is paraphyletic with respect to *Lepidothyris*. Given these results, we propose several taxonomic changes to this group (Fig. 5). First, we redefine the genus *Lygosoma* to include only

Clade A, comprising the type species *Lygosoma quadrupes*, and other elongate-bodied taxa. Second, we resurrect the genus *Riopa* for Clade D, comprising the type species *Riopa punctata* and other species from India and Southeast Asia. Third, we synonymize the genus *Lepidothyris* with *Mochlus*. Last, we describe a new genus, *Subdoluseps* **gen. nov.** for Clade B, comprising the type species *S. bowringii* and additional species distributed across India, Southeast Asia, Indonesia, the Philippines and Christmas Island. We recognize that our taxonomic sampling is incomplete considering the large diversity of species that are recognized currently in the genus *Lygosoma*, and we therefore advocate for continued efforts to voucher and include more recognized diversity in future studies to better understand the diversity, distribution and boundaries of this unique radiation of Old World scincid lizards.

GENUS *LYGOSOMA* HARDWICKE & GRAY 1827:228

Type species

Lacerta serpens Bloch 1776 = *Anguis quadrupes* Linnaeus 1766 (Smith, 1935) by monotypy.

Podophis Wiegmann 1834:11. Type species *Anguis quadrupes* Linnaeus 1766 by monotypy.

Eumeces: Günther 1864b:84. Part, not *Eumeces* Wiegmann 1834.

Riopa: Smith 1935:312. Part, not *Riopa* Gray 1839.

Mochlus: Mittleman 1952:9. Part, not *Mochlus* Günther 1864a.

Squamicilia Mittleman 1952:9. Type species *Eumeces isodactylus* Günther 1864b by original designation.

Diagnosis

Lygosoma can be identified by the following combination of characters: (1) Body size small to large (SVL 49–168 mm); (2) trunk moderately elongate to elongate (AGD 58–93% SVL); (3) digits short (FinIIILam 4–9, ToeIVLam 5–13); (4) MBSRC 25–38; (5) PVSRC 84–123; (6) lower eyelid scaly; (7) supranasal scales in contact medially or not in contact medially, usually fully- or partially fused with nasals; (8) prefrontals not in contact medially; (9) frontoparietal single or paired; (10) parietals in contact medially posterior to interparietal; (11) enlarged nuchal scales present or absent; and (12) palatine bones with posteriomedially projecting processes, pterygoids emarginated along posterior edge.

Phylogenetic definition

This genus comprises species that share a more recent common ancestor with *L. quadrupes* than with *Subdoluseps bowringii, Lamprolepis smaragdina*, *Mochlus sundevallii*, or *Riopa punctata*.

Content

L. quadrupes, *L. corpulentum* Smith 1921, *L. isodactylum* (Günther 1864b) *L. siamense* Siler, Heitz, Davis, Freitas, Aowphol, Termprrayoon & Grismer 2018 and *L. tabonorum* Heitz, Diesmos, Freitas, Ellsworth, Grismer, Aowphol, Brown & Siler 2016.

Comments

The suggested common name for this genus is Southeast Asian Writhing Skinks. *Lygosoma* means “writhing body” in Greek (lygos=writhe, soma=body). Linnaeus (1766) provided the earliest description of the type species of the genus, *Anguis quadrupes* and, due to its extremely elongate body and diminutive legs, mistook it for a member of the order Serpentes (snakes). Ten

years later, Bloch (1776) re-described the species as the lizard *Lacerta serpens* from two specimens, one of which (ZMB 1276) is a syntype of the species and the oldest herpetological specimen in the Zoological Museum of Berlin (Bauer & Günther, 2006). Later, Hardwicke & Gray (1827) described the genus *Lygosoma* for *Lacerta serpens*, mistakenly mentioning that the species was not the same as *Anguis quadrupes*, and consequently, the epithet *quadrupes* was not associated with the genus until *serpens* was synonymized with *quadrupes* by Smith (1935).

Species included within *Lygosoma* display considerable variation in gross body size and shape. The smallest species included currently in the genus is *L. siamense*, which has an adult SVL of 49–79 mm, compared to the largest species, *L. corpulentum*, with an adult SVL of up to 168 mm (although this measurement is only based on a single specimen). Additionally, species differ in the degree of trunk elongation, with species in the *L. quadrupes* species complex (*L quadrupes*, *L. siamense*, and *L. tabonorum*) being more elongate (AGD/SVL = 62.0–93.3%) when compared with other species such as *L. corpulentum* (AGD/SVL = 57.7%). Additional phylogenetic studies of morphological diversity and body form evolution are warranted for this group.

Due to the lack of tissues samples in museum collections, we were not able to sample a large number of species from Southeast Asia recognized currently in the genus *Lygosoma*, including: *L. angeli* (Smith 1937b), *L. bampfyldei* Bartlett 1894, *L. boehmei* Ziegler, Schmitz, Heidrich, Vu & Nguyen 2007, *L. haroldyoungi* (Taylor 1962), *L. kinabatanganense* Grismer, Quah, Duzulkafly & Yambun 2018, *L. koratense* Smith 1917, *L. opisthorhodum* Werner 1910, *L. peninsulare* Grismer, Quah, Duzulkafly & Yambun 2018, *L. schneideri* Werner 1900, *L. singha* (Taylor 1950) and *L. veunsaiense* Geissler, Hartmann & Neang 2012. To avoid introducing additional taxonomic instability from speculating on their phylogenetic affinities, we treat these

species as *incertae sedis* and hope that future studies on the phylogenetics of this group will include samples of these taxa to elucidate their relationships to other species in *Lygosoma s.l.* We also did not include the species *L. siamense* in our phylogeny because the only available sequence was a portion of the 16S gene on GenBank; however, this species has been shown to be the sister taxon to the clade comprising *L. quadrupes* + *L. siamense* (Siler et al., 2018), and so we consider it to be definitively a member of *Lygosoma.*

GENUS *MOCHLUS* GÜNTHER 1864a:308

Type species

Mochlus punctulatus = *Eumeces afer* Peters 1854 (Barboza du Bocage 1867) = *Eumeces sundevallii* (*Eumices* [sic] *sunderallii* [sic]) Smith 1849 (Freitas et al., 2018) by monotypy.

Tiliqua: Burton 1836:62. Not *Tiliqua* Gray 1825.

Sepacontias Günther 1880:235. Type species *Sepacontias modestus* Günther 1880 = *Mochlus sundevallii* (Freitas et al., 2018) by monotypy.

Euprepes [sic]: Vaillant 1884:169. Part, not *Euprepis* Wagler 1830.

Lygosoma: Boulenger 1887:209. Part, not *Lygosoma* Hardwick & Gray 1827.

Lepidothyris Cope 1892:233. Type species *Tiliqua fernandi* Burton 1836 by subsequent designation (Cope, 1900).

Riopa: Smith 1935:312. Part, not *Riopa* Gray 1839.

Diagnosis

Mochlus can be identified by the following combination of characters: (1) Body size medium to large (SVL 55–166 mm); (2) trunk moderately elongate to elongate (AGD 44–83% SVL); (3)

digits short to long (FinIIILam 6–10, ToeIVLam 9–17); (4) MBSRC 24–38; (5) PVSRC 60–78; (6) lower eyelid scaly or with a transparent disc; (7) supranasal scales in contact medially, occasionally fused or partially fused with nasals; (8) prefrontals not in contact medially, occasionally fused with frontonasal; (9) frontoparietal paired; (10) parietals in contact medially posterior to interparietal; (11) enlarged nuchal scales present or absent; and (12) palatine bones with posteriomedially projecting processes, pterygoids rounded along posterior edge.

Phylogenetic definition

This genus comprises species that share a more recent common ancestor with *M. sundevallii* than with *Riopa punctata*, *Subdoluseps bowringii*, *Lygosoma quadrupes* and *Lamprolepis smaragdina*.

Content

M. sundevallii, *M. brevicaudis* (Greer, Grandison & Barbault 1985), *M. fernandi* (Burton 1836), *M. guineensis* (Peters 1879), *M. hinkeli* (Wagner, Böhme, Pauwels & Schmitz 2009) and *M. striatus* (Hallowell 1854).

Comments

The suggested common name for this genus is African Supple Skinks. Studies of other African—Southeast Asian radiations have suggested that African species comprise a single radiation within the continent (Mausfeld et al., 2000; Fabre et al., 2012; Oliver et al., 2015; Karin et al., 2016). However, without greater taxonomic sampling of African species, we cannot corroborate this hypothesis for African species in *Lygosoma s.l.* The majority of *Lygosoma s.l.*

species in Africa lack tissues samples in museum collections and have never been included in phylogenetic studies. Therefore, we were unable to include them definitively in the genus *Mochlus* at this time. These species are: *M. grandisonianus* Lanza & Carfi, 1966, *M. laeviceps* (Peters 1874), *M. lanceolatus* (Broadley 1994), *M. mabuiiformis* (Loveridge 1935), *M. mafianus* (Broadley 1994), *M. mocquardi* (Chabanaud 1917), *M. paedocarinatus* Lanza & Carfi 1968, *M. pembanus* (Boettger 1913), *M. productus* (Boulenger 1909), *M. simonettai* (Lanza 1979), *M. somalicus* (Parker 1942), *M. tanae* (Loveridge 1935) and *M. vinciguerrae* (Parker 1932). Two of these species, *M. pembanus* and *M. tanae* were included in our morphological dataset and appeared to occupy a similar area of morphospace as species in *Mochlus*; however, given the large amount of overlap of clades in morphospace, their morphological affinities are not strong evidence alone for their placement in *Mochlus*. Alternatively, Greer (1977:527) suggested that *M. tanae* and another African species, *M. mabuiiformis*, were more closely related to Southeast Asian species than to other African species based on a combination of discrete character traits: open secondary palate, lower eyelid with a transparent disc, presence of pterygoid teeth, paired frontoparietal scales, distinct supranasal scales, and prentadactly digits. However, combinations of these states are shared across all *Lygosoma s.l.* and are not unique to a single clade, and some of these characters may represent convergence instead of phylogenetic relatedness. Additionally, Perret and Wuest (1983) examined the scale microstructure of *M. guineensis*, *M. mabuiiformis*, and *M. fernandi*, and found that they were all very similar, which may suggest that *M. mabuiiformis* is more closely related to African species than Asian species in *Lygosoma s.l.* Therefore, biogeography and morphology do not help us resolve the placement of these 13 African species, and so we treat them as *incertae sedis* and hope that future studies will elucidate their phylogenetic position. Two African species, *M. hinkeli* and *M. striatus* have been included

in a recent phylogenetic study (Wagner et al., 2009) and were shown to form a clade with *M. fernandi*. Therefore, we treat these species definitively as members of *Mochlus*.

GENUS *RIOPA* GRAY 1839:332

Type species

Riopa punctata = *Lacerta punctata* Linnaeus 1758 (Gray, 1845) by subsequent designation (Smith, 1935).

Chiamela Gray 1839:332. Type species *Chiamela lineata* Gray 1839 by subsequent designation (Gray, 1845).

Hagria Gray 1839:333.Type species *Hagria vosmaerii* Gray 1839 by monotypy.

Campsodactylus Dumeríl & Bibron 1839:761.Type species *Campsodactylus lamarrei* Dumeríl & Bibron 1839 = *Hagria vosmaerii* Gray 1839 by monotypy.

Sphenosoma Fitzinger 1843:23. Type species *Eumeces punctatus* Weigmann 1834 = *Lacerta punctata* Linnaeus 1758 by original designation.

Eumeces: Günther 1864b:84. Part, not *Eumeces* Wiegmann 1834.

Lygosoma: Boulenger 1887:209. Part, not *Lygosoma* Hardwicke & Gray 1827.

Diagnosis

Riopa can be identified by the following combination of characters: (1) body size small to medium (SVL 35–96 mm); (2) trunk moderately elongate (AGD 55–75% SVL); (3) digits short to long (FinIIILam 5–11, ToeIVLam 6–16); (4) MBSRC 19–30; (5) PVSRC 70–115; (6) lower eyelid scaly or with a transparent disc; (7) supranasal scales in contact medially, occasionally barely touching; (8) prefrontals not in contact medially; (9) frontoparietal single or paired; (10)

parietals in contact behind interparietal; (11) enlarged nuchal scales usually present, occasionally absent; and (12) palatine bones with posteriomedially projecting processes, pterygoids emarginated along posterior edge or occasionally rounded.

Phylogenetic definition

This genus comprises the species that share a more recent common ancestor with *Riopa punctata* than with *Mochlus sundevallii*, *Subdoluseps bowringii*, *Lygosoma quadrupes* and *Lamprolepis smaragdina*.

Content

R. punctata, *R. albopunctata* Gray 1846, *R. anguina* Theobald 1867, *R. goaensis* Sharma 1976, *R. guentheri* (Peters 1879), *R. lineata* (Gray 1839), *R. lineolata* Stoliczka 1870, *R. popae* Shreve 1940, and *R. vosmaerii* (Gray 1839).

Comments

Our suggested common name for this clade is Asian Gracile Skinks. The species *Lacerta punctata*, described by Linnaeus (1758), referred to an illustration by Seba (1735: pl. II, fig. IX,) and two specimens housed in the Swedish Museum of Natural History (NRM 135). However, it was later discovered that the illustration and the specimens represented two different species. Although the majority of publications used *Lacerta punctata* to refer to the elongate Indian species now recognized as *Riopa punctata*, several publications used it to refer to the species now recognized as *Trachylepis homalocephala*. This led to confusion with the identity of *Lacerta punctata*, as the name was applied to the type species of two separate genera—*Riopa*

and *Euprepis* Wagler 1830 (reviewed in Bauer, 2003). Bauer (2003) fixed the name *Lacerta punctata* to Seba's drawings, choosing the illustration of the male as the lectotype.

GENUS *SUBDOLUSEPS* GEN. NOV.

Type species

Eumeces bowringii Günther 1864b.

Eumeces: Günther 1864b:84. Part, not *Eumeces* Wiegmann 1834.

Lygosoma: Boulenger 1887:209. Part, not *Lygosoma* Hardwicke & Gray 1827.

Riopa: Smith 1935:312. Part, not *Riopa* Gray 1839.

Mochlus: Mittleman 1952:9. Part, not *Mochlus* Günther 1864a.

Diagnosis

Subdoluseps can be identified by the following combination of characters: (1) body size small (SVL 35–70 mm); (2) trunk moderately elongate (AGD 42–69% SVL); (3) digits medium to long (FinIIILam 7–12, ToeIVLam 11–16); (4) MBSRC 26–34; (5) PVSRC 50–69; (6) lower eyelid scaly or with a transparent disc; (7) supranasal scales in contact medially or not in contact medially; (8) prefrontals not in contact medially; (9) frontoparietal single or paired; (10) parietals in contact behind interparietal; (11) enlarged nuchal scales present or absent; and (12) palatine bones with posteriomedially projecting processes, pterygoids rounded along posterior edge.

Phylogenetic definition

This genus comprises the species that share a more recent common ancestor with *S. bowringii* than with *Riopa punctata*, *Mochlus sundevallii*, *Lygosoma quadrupes* and *Lamprolepis smaragdina*.

Content

S. bowringii, *S. frontoparietalis* (Taylor 1962), *S. herberti* (Smith 1916), *S. pruthi* (Sharma 1977), and *S. samajaya* (Karin, Freitas, Shonleben, Bauer & Das 2018).

Etymology

From the Latin word "Subdolus" which means crafty or slippery and the Greek word "Seps" which means a snake-like animal and has been used previously as a genus name for skinks. This name describes the quickness of these skinks in the wild. The name is masculine. The suggested common name for this genus is Asian Agile Skinks.

CONCLUSIONS

Having a stable taxonomy to communicate about biodiversity is crucial for both scientific study and conservation management (Mayr, 1976; Felsenstein, 1985; Winston, 1999; Wheeler et al., 2004; Kaiser et al., 2013; Groves et al., 2017; IUCN-SSC Species Conservation Planning Sub-Committee, 2017). As molecular methods and phylogenetic analyses have improved, phylogenetic studies have contributed greatly to our growing understanding of global skink biodiversity. Over the last decade alone, five new scincid genera have been described (*Pinoyscincus* and *Tythoscincus* [Linkem et al., 2011], *Toenayar* [Karin et al. 2016], *Brachyseps* and *Flexiseps* [Erens et al., 2017]) to better reflect the evolutionary history of the family. Given

that species in *Lygosoma s.l.* are distributed across six of the 25 global biodiversity hotspots (Myers et al., 2000), classifying the biodiversity in this group is critical to discussions of skink diversity in these imperiled regions. Here, using the most comprehensive taxonomic sampling available, we have employed concatenated, coalescent-based and multivariate morphological analyses to illustrate the need for a revised classification of *Lygosoma s.l.* Therefore, we modify the taxonomy of *Lygosoma s.l.* to reflect our phylogenetic results, splitting the group into four genera—*Lygosoma*, *Mochlus*, *Riopa*, and *Subdoluseps*. Our revised classification can be used to more accurately assess lygosomine skink biodiversity including diversification rates and biogeographic and trait evolution patterns within and between clades in *Lygosoma s.l.*

ACKNOWLEDGEMENTS

For tissue and specimen loans (Tables S1 and S2), we thank the following people and institutions: A. Aowphol (ZMKU), A. Bauer and B. Karin (Villanova University), R. Brown and L. Welton (KU), D. Cannatella and T. Laduc (TNHC), A. Diesmos (PNM), E. Greenbaum (UTEP), A. Resetar (FMNH) and L. Scheinberg and J. Vindem (CAS). We are grateful to T. Yuri, M. Labonte and M. Penrod at SNOMNH for help with molecular data collection and B. Karin at MVZ, E. Ellsworth at SNOMNH and S. Pal at BNHS for help with specimen measurements. We thank J. Oaks for discussion of methods and help with *BEAST analyses and A. Bauer for reviewing our taxonomic history section and genus synonymies. This research was supported by a National Science Foundation (NSF) grant (DEB 074391) to Rafe M. Brown, travel awards from the Department of Biology and the Graduate Student Senate at the University of Oklahoma, the California Academy of Sciences Charles Stearns Memorial travel grant and a Fulbright Fellowship to ESF, the a Science and Engineering Research Board (SERB) National

Postdoctoral fellowship (PDF/2017/000476 entry number 15225; http://dx.doi.org/10.13039/501100001843) to ADR and NSF grants (IOS 1353683 and DEB 1657648) to CDS.

REFERENCES

Akaike H. 1974. A new look at the statistical model identification. *IEEE Transactions on Automatic Control* **19:** 716–723.

Aljanabi SM, Martinez I. 1997. Universal and rapid salt-extraction of high quality genomic DNA for PCR-based techniques. *Nucleic Acids Research* **25:** 4692–4693.

Barbour T. 1912. A contribution to the zoogeography of the East Indian islands. *Memoirs of the Museum of Comparative Zoology at Harvard College* **44:** 5–203, pl. 1–8.

Barbour T, Loveridge A. 1928. A comparative study of the herpetological faunae of the Uluguru and Usambara mountains, Tanganyika Territory with descriptions of new species. *Memoirs of the Museum of Comparative Zoology at Harvard College* **50:** 87–265, pl. 1–4.

Barley AJ, White J, Diesmos AC, Brown RM. 2013. The challenge of species delimitation at the extremes: diversification without morphological change in Philippine sun skinks. *Evolution* **67:** 3556–3572.

Barley AJ, Datta-Roy A, Karanth KP, Brown RM. 2015a. Sun skink diversification across the Indian-Southeast Asian biogeographical interface. *Journal of Biogeography* **42**: 292–304.

Barley AJ, Monnahan PJ, Thomson RC, Grismer LL, Brown RM. 2015b. Sun skink landscape genomics: assessing the roles of micro-evolutionary processes in shaping genetic and phenotypic diversity across a heterogenous and fragmented landscape. *Molecular Ecology* **24:** 1696–1712.

Bartlett E. 1894. The crocodiles and lizards of Borneo in the Sarawak Museum with descriptions of supposed new species, and the variation of colours in the several species during life. *Journal of the Straits Branch of the Royal Asiatic Society* **28:** 73–97.

Bauer AM. 2003. On the identity of *Lacerta punctata* Linnaeus 1758, the type species of the genus *Euprepis* Wagler 1830, and the generic assignment of Afro-Malagasy skinks. *African Journal of Herpetology* **52:** 1–7.

Bauer AM, Günther R. 2006. A syntype of *Lacerta serpens* Bloch 1776 (Reptilia: Squamata: Scincidae): the oldest type specimen in the founding collection of the Zoological Museum of Berlin. *Bibliotheca Herpetologica* **6:** 17–25.

Barboza du Bocage JV. 1867. Segunda lista dos reptis das possesões Portuguezas d'Africa Occidental que existem no Museu de Lisboa. *Jornal de Sciencias Mathematicas Physicas e Naturaes* **1:** 217–228.

Barboza du Bocage JV. 1870. Description d'un Saurien nouveau de l'Afrique occidentale. *Jornal de Sciencias Mathematicas Physicas e Naturaes* **3:** 66–68, 1pl.

Bloch ME. 1776. Beschreibung der schleicheidexe, *Lacerta serpens*. *Beschäftigungen der Berlinischen Gesellschaft Naturforschender Freunde* **2:** 28–34, pl. II.

Boettger O. 1913. Reptilien und amphibian von Madagascar, den Inseln und dem Festland Ostafrikas. (Sammlung Voeltzkow 1889–1885 und 1903–1905). In: Voeltzkow A. *Reise in Ostafrika in den Jahren 1903–1905 mit Mitteln der Hermann und Elise geb. Heckmann Wentzel-Stiftung Ausgeführt*. Stuttgart: E. Schweizerbart'sche Verlagsbuchhandlung Nägele & Dr. Sproesser, 269–375, pl. 23–30.

Bouckaert R, Heled J, Kühnert D, Vaughan T, Wu CH, Xie D, Suchard MA, Rambaut A, Drummond AJ. 2014. BEAST 2: a software platform for Bayesian evolutionary analysis. *PLOS Computational Biology* **10:** e1003537.

Boulenger GA. 1887. *Catalogue of the Lizards in the British Museum (Natural History). Volume III: Lacertidae, Gerrhosauridae, Scincidae, Anelytropidae, Dibamidae. Chamaelontidae. Second edition.* London: Taylor and Francis.

Boulenger GA. 1909. List of reptiles collected by Capt. G. Ferrari at Jumbo, Lower Juba. *Annali del Museo Civico di Storia Naturale di Genova* **4:** 308–315.

Brandley MC, Schmitz A, Reeder TW. 2005. Partitioned Bayesian analyses, partition choice, and the phylogenetic relationships of scincid lizards. *Systematic Biology* **54:** 373–390.

Brandley MC, Ota H, Hikida T, Montes de Oca AN, Fería-Ortíz M, Guo X, Wang Y. 2012. The phylogenetic systematics of blue-tailed skinks (*Plestiodon*) and the family Scincidae. *Zoological Journal of the Linnean Society* **165:** 163–189.

Brandley MC, Bragg JC, Singhal S, Chaple DG, Jennings CK, Lemmon AR, Lemmon EM, Thompson MB, Moritz C. 2015. Evaluating the performance of anchored hybrid enrichment at the tips of the tree of life: a phylogenetic analysis of Australian *Eugongylus* group scincid lizards. *BMC Evolutionary Biology* **15:** 1–14.

Broadley DG. 1962. A tangled group of writhing-skinks (*Riopa*). *Journal of the Herpetological Association of Rhodesia* **17:** 3–4.

Broadley DG. 1966. A review of the *Riopa sundevalli* group (Sauria: Scincidae) in southern Africa. *Arnoldia (Rhodesia) Series of Miscellaneous Publications National Museums of Southern Rhodesia* **2:** 1–7.

Broadley DG. 1994. A review of *Lygosoma* Hardwicke & Gray 1827 (Reptilia Scincidae) on the East African coast, with the description of a new species. *Tropical Zoology* **7**: 217–222.

Brown JM, Lemmon AR. 2007. The importance of data partitioning and the utility of Bayes Factors in Bayesian phylogenetics. *Systematic Biology* **56**: 643–655.

Bryson Jr. RW, Linkem CW, Pavón-Vásquez CJ, Nieto-Montes de Oca A, Klicka J, McCormack JE. 2017. A phylogenomic perspective on the biogeography of skinks in the *Plestiodon brevistrostris* group inferred from target enrichment of ultraconserved elements. *Journal of Biogeography* **44:** 2033–2044.

Burton E. 1836. A saurian reptile of the family Scincidae and the genus *Tiliqua*, Gray. *Proceedings of the Zoological Society of London* **4:** 62.

Busschau T, Conradie W, Jordaan A, Daniels SR. 2017. Unmasking evolutionary diversity among two closely related South African legless skink species (Acontinae: *Acontias*) using molecular data. *Zoology* **121:** 72–82.

Cain AJ. 1956. The genus in evolutionary taxonomy. *Systematic Zoology* **5:** 97–109.

Carranza S, Arnold EN. 2003. Investigating the origins of transoceanic distributions: mtDNA shows *Mabuya* lizards (Reptilia, Scincidae) crossed the Atlantic twice. *Systematics and Biodiversity* **2:** 275–282.

Chabanaud MP. 1917. Revision de quelques reptiles d'Afrique et description de trois espéces nouvelles. *Bulletin du Meséum National d'Histoire Naturelle* **23:** 442–453.

Chapple DG, Bell TB, Chapple SNJ, Miller KA, Daugherty CH, Patterson GB. 2011. Phylogeography and taxonomic revision of the New Zealand cryptic skink (*Oligosoma insconspicuum*; Reptilia: Scincidae) species complex. *Zootaxa* **2782:** 1–33.

Cocteau JT. 1836. *Études sur les scincoïdes*. Paris: Terzuolo.

Cogger HG. 1975. *Reptiles and Amphibians of Australia*. Sydney: Reed.

Cogger HG. 2014. *Reptiles and Amphibians of Australia, 7th edition*. Collingwood: CSIRO.

Conradie W, Busschau T, Edwards S. 2018. Two new species of *Acontias* (Acontinae, Scincidae) from the Mpumalanga Highveld escarpment of South Africa. *Zootaxa* **4429:** 89–106.

Cope ED. 1868. Observations on reptiles of the Old World. Art. II. *Proceedings of the Academy of Natural Scienes of Philadelphia* **20:** 316–323.

Cope ED. 1892. On degenerate types of scapular and pelvic arches in the Lacertilia. *Journal of Morphology* **7:** 223–244, pl. XIII.

Cope ED. 1900. The crocodilians, lizards, and snakes of North America. *Annual Report of the United States National Museum* **1898:** 155–1270.

Crawford NG, Faircloth BC, McCormack JE, Brumfield RT, Winker K, Glenn TC. 2012. More than 1000 ultraconserved elements provide evidence that turtles are the sister group of archosaurs. *Biology Letters* **8:** 783–786.

Daniels SR, Heideman NJL, Hendricks MGJ. 2009. Examination of evolutionary relationships in the Cape fossorial skink species complex (Acontinae: *Acontias meleagris meleagris*) reveals the presence of five cryptic lineages. *Zoologica Scripta* **38:** 449–463.

Das, I. 2010. *A Fieldguide to the Reptiles of Southeast Asia*. London: New Holland.

Darriba D, Taboada GL, Doallo R, Posada D. 2012. JModelTest2: more models, new heuristics and parallel computing. *Nature Methods* **9:** 772.

Datta-Roy A, Singh M, Srinivasulu C, Karanth KP. 2012. Phylogeny of the Asian *Eutropis* (Squamata: Scincidae) reveals an into India endemic Indian radiation. *Molecular Phylogenetics and Evolution* **63:** 817–824.

Datta-Roy A, Singh M, Karanth KP. 2014. Phylogeny of endemic skinks of the genus *Lygosoma* (Squamata: Scincidae) from India suggests an *in situ* radiation. *Journal of Genetics* **93:** 163–167.

Datta-Roy A, Deepak V, Sidharthan C, Barley AJ, Karanth KP. 2015. An addition to the endemic Indian radiation of *Eustropis dissimilis* Halowell (Squamata: Scincidae). *Zootaxa* **4027:** 145–150.

Daudin FM. 1802. *Histoire Naturelle, Générale et Particulière, des Reptiles: Ouvrage Faisant suite à l'Histoire Naturelle générale et Particulière, Composée par Leclerc de Buffon, et Rédigée par C.S. Sonnini, Member de Plusieurs Sociétés Savantes. Tome quatriéme.* Paris: F Dufart.

Davis DR, Feller KD, Brown RM, Siler CD. 2014. Evaluating the diversity of Philippine slender skinks of the *Brachymeles bonitae* complex (Reptilia: Squamata: Scincidae): redescription of *B. tridactylus* and description of two new species. *Journal of Herpetology* **48:** 480–494.

Davis DR, Geheber AD, Watters JL, Penrod ML, Feller KD, Ashford A, Kouri J, Nguyen D, Shauberger K, Sheatsley K, Winfrey C, Wong R, Sanguila MB, Brown RM, Siler CD. 2016. Additions to Philippine slender skinks of the *Brachymeles bonitae* complex (Reptilia: Squamata: Scincidae) III: a new species from Tablas Island. *Zootaxa* **4132:** 30–43.

Degnan JH, Rosenberg NA. 2009. Gene tree discordance, phylogenetic inference and the multispecies coalescent. *Trends in Ecology and Evolution* **24:** 332–340.

Drummond AJ, Ho SYW, Phillips MJ, Rambaut A. 2006. Relaxed phylogenetics and dating with confidence. *PLoS Biology* **4:** e88.

Drummond AJ, Bouckaert RR. 2015. *Bayesian evolutionary analysis with BEAST.* Cambridge: Cambridge University Press.

Duméril AMC, Bibron G. 1839. *Erpétologie générale ou histoire naturelle compléte des reptiles*. *Tome cinquiéme*. Paris: Roret.

Edgar RC. 2004. MUSCLE: multiple sequence alignment with high accuracy and high throughput. *Nucleic Acids Research* **32:** 1792–1797.

Ekblom R, Galindo J. 2011. Applications of next generation sequencing in molecular ecology of non-model organisms. *Heredity* **107:** 1–15.

Erens J, Miralles A, Glaw F, Chatrou LW, Vences M. 2017. Extended molecular phylogenetics and revised systematics of Malagasay scincine lizards. *Molecular Phylogenetics and Evolution* **107:** 466–472.

Fabre PH, Irestedt M, Fjeldså J, Bristol R, Groombridge JJ, Irham M, Jønsson KA. 2012. Dynamic colonization exchanges between continents and islands drive diversification in paradise-flycatchers (*Terpsiphone*, Monarchidae). *Journal of Biogeography* **39:** 1900–1918.

Fan W, Wu R, Chen MH, Lewis PO. 2011. Choosing among partition models in Bayesian phylogenetics. *Molecular Biology and Evolution* **28:** 523–532.

Felsenstein J. 1985. Phylogenies and the comparative method. *American Naturalist* **125:** 1–15.

FitzSimons VF. 1943. *The lizards of South Africa*. Johannesburg: Voortrekerpers.

Fitzinger LJ. 1826. *Neue classification der reptilien nach ihren natürlichen verwandtschaften. Nebst einer verwantschafts—tafel und einem verzeichnisse der Reptilien— sammlung des K.K. Zoologischen Museum's zu Wien*. Wien [Vienna]: JG Heubner.

Fitzinger LJ. 1842. Der smaragdgrüne Glanzscink. In: Trietschke F. *Naturhistorischer Bildersaal des Thierreiches Dritter Band.* Pesth [Budapest]: CA Hartleben, 139, pl. ccxlvii.

Fitzinger LJ. 1843. *Systema reptilium. Fasciculus primus Amblyglossae*. Vindobonae [Vienna]: Braumüller et Seidel.

Freitas ES, Bauer AM, Siler CD, Broadley DG, Jackman TR. **2018.** Phylogenetic and morphological investigation of the *Mochlus afer-sundevallii* species complex (Squamata: Scincidae) across the arid corridor of sub-Saharan Africa. *Molecular Phylogenetics and Evolution* **127:** 280–287.

Fry BG, Vidal N, Norman JA, Vonk FJ, Scheib H, Ramjan, SFR, Kuruppu S, Fung K, Hedges SB, Richardson MK, Hodgson WC, Ignjatovic V, Summerhayes R, Kochva E. 2006. Early evolution of the venom system in lizards and snakes. *Nature (London)* **439**: 584–588.

Geheber AD, Davis DR, Watters JL, Penrod ML, Feller KD, Davey CS, Ellsworth ED, Flanagan RL, Heitz BB, Moore T, Nguyen MDC, Roberts A, Sutton J, Sanguila MB, Linkem CW, Brown RM, Siler CD. 2016. Additions to Philippine slender skinks of the *Brachymeles bonitae* complex (Reptilia: Squamata: Scincidae) I: a new species from Lubang Island. *Zootaxa* **4132:** 1–14.

Geissler P, Nguyen TQ, Phung TM, van Devender RW, Hartmann T, Farkas B, Ziegler T, Böhme W. 2011. A review of Indochinese skinks of the genus *Lygosoma* Hardwicke & Gray, 1827 (Squamata: Scincidae), with natural history notes and an identification key. *Biologia* **66:** 1159–1176.

Geissler P, Hartmann T, Neang T. 2012. A new species of the genus *Lygosoma* Hardwicke & Gray, 1827 (Squamata: Scincidae) from northeastern Cambodia, with an updated identification key to the genus *Lygosoma* in mainland Southeast Asia. *Zootaxa* **3190:** 56–68.

Glauert L. 1960. The family Scincidae in Western Australia. Part 2: the genus *Lygosoma*. *Western Australian Naturalist* **7:** 81–99.

Gray JE. 1825. A synopsis of the genera of reptiles and Amphibia, with a description of some new species. *Annals of Philosophy* **10:** 193–217.

Gray JE. 1831. A synopsis of the species of the class Reptilia. In: Cuvier G, Griffith E., eds. *The Animal Kingdom Arranged in Conformity with its Organization with Additional Descriptions of all the Species Hitherto Named, and of Many not before Noticed. Volume the Ninth.* London: Whittaker, Treacher and Co.

Gray JE. 1839. Catalogue of the slender-tongued saurians with descriptions of many new genera and species. *Annals of Natural History or, Magazine of Zoology, Botany and Geology* **2:** 331–337.

Gray JE. 1845. *Catalogue of the Specimens of Lizards in the Collection of the British museum.* London: Edward Newman.

Gray JE. 1846. Descriptions of some new species of Indian lizards. *Annals and Magazine of Natural History including Zoology, Botany, and Geology* **18:** 429–430.

Greer AE. 1970a. A subfamilial classification of scincid lizards. *Bulletin of the Museum of Comparative Zoology at Harvard College* **139:** 151–183.

Greer AE. 1970b. The relationships of the skinks referred to the genus *Dasia*. *Breviora* **348:** 1–30.

Greer AE. 1974. The generic relationships of the scincid lizard genus *Leiolopisma* and its relatives. *Australian Journal of Zoology, Supplementary Series* **31:** 1–67.

Greer AE. 1977. The systematics and evolutionary relationships of the scincid lizard genus *Lygosoma*. *Journal of Natural History* **11:** 515–540.

Greer AE, Grandison AGC, Barbault R. 1985. A new species of *Lygosoma* (Lacertilia: Scincidae) from West Africa, with comments on its biology. *Journal of Herpetology* **19:** 365–372.

Grismer LL, Ismail LB, Awang MT, Rizal SA, Ahmad AB. 2014. A new species of lowland skink (genus *Lipinia* Gray, 1845) from northeastern peninsular Malaysia. *Zootaxa* **3821:** 457–464.

Grismer LL, Wood Jr. PL, Quah ESH, Anuar S, Ngadi EB, Izam NAM, Ahmad N. 2018a. Systematics, ecomorphology, cryptic speciation and biogeography of the lizard genus *Tytthoscincus* Linkem, Diesmos & Brown (Squamata: Scincindae) from the sky-island archipelago of Peninsular Malaysia. *Zoological Journal of the Linnean Society* **183:** 635–671.

Grismer LL, Quah ESH, Duzulkafly Z, Yambun P. 2018b. On the taxonomy of *Lygosoma bampfyldei* Bartlett, 1895 (Squamata: Scincidae) with descriptions of new species from Borneo and Peninsular Malaysia and the resurrection of *Lygosoma schneideri* Werner 1900.

Groth JG, Barrowclough GF. 1999. Basal divergences in birds and the utility of the nuclear RAG-1 gene. *Molecular Phylogenetics and Evolution* **12:** 115–123.

Groves CP, Cotterill FPD, Gippoliti S, Rabovsky J, Roos C, Taylor PJ, Zinner D. 2017. Species definitions and conservation: a review and case studies from African mammals. *Conservation Genetics* **18:** 1247–1256.

Günther AG. 1864a. Report on a collection of reptiles and fishes made by Dr. Kirk in the Zambesi and Nyassa regions. *Proceedings of the Zoological Society of London* **1864:** 305–314.

Günther AG. 1864b. *The reptiles of British India*. London: Robert Hardwicke for the Ray Society.

Günther AG. 1880. Description of new species of reptiles from Eastern Africa. *Annals and Magazine of Natural History including Zoology, Botany, and Geology*. *Fifth series* **6:** 234–238.

Hallowell E. 1854. Remarks on the geographical distribution of reptiles, with descriptions of several species supposed to be new, and corrections of former papers. *Proceedings of the Academy of Natural Sciences of Philadelphia* **7:** 98–105.

Hardwicke T, Gray JE. 1827. A synopsis of the species of saurian reptiles, collected in India by Major-General Hardwicke. *Zoological Journal* **3:** 213–229.

Hedges SB, Conn CE. 2012. A new skink fauna from Caribbean islands (Squamata, Mabuyidae, Mabuyinae). *Zootaxa* **3288:** 1–244.

Hedges SB. 2014. The high-level classification of skinks (Reptilia, Squamata, Scincomorpha). *Zootaxa* **3765:** 317–338.

Heideman NJL, Maulcahy DG, Sites Jr. JW, Hendricks MGJ, Daniels SR. 2011. Cryptic diversity and morphological convergence in threatened species of fossorial skinks in the genus *Scelotes* (Squamata: Scincidae) from the Western Cape Coast of South Africa: implications for species boundaries, digit reduction and conservation. *Molecular Phylogenetics and Evolution* **61:** 823–833.

Heitz BB, Diesmos AC, Freitas ES, Ellsworth ED, Grismer LL, Aowphol A, Brown RM, Siler CD. 2016. A new supple skink, genus *Lygosoma* (Reptilia: Squamata: Scincidae), from the western Philippines. *Herpetologica* **72:** 352–361.

Heled J, Drummond AJ. 2010. Bayesian inference of species trees from multilocus data. *Molecular Biology and Evolution* **27:** 570–580.

Hill MO, Smith AJE. 1976. Principal component analysis of taxonomic data with multi-state discrete characters. *Taxon* **25:** 249–255.

Hora SL. **1927.** Notes on lizards in the Indian museum. III. On the unnamed collection of lizards of the family Scincidae. *Records of the Indian Museum* **29:** 1–6.

Honda M, Ota H, Kobayashi M, Nabhitabhata J, Yong HS, Hikida T. 2000. Phylogenetic relationships, character evolution and biogeography of the subfamily Lygosominae (Reptilia: Scincidae) inferred from mitochondrial DNA sequences. *Molecular Phylogenetics and Evolution* **15:** 452–461.

Honda M, Ota H, Köhler G, Ineich I, Chirio L, Chen SL, Hikida T. 2003. Phylogeny of the lizard subfamily Lygosominae (Reptilia: Scincidae), with special reference to the origin of New World taxa. *Genes and Genetic Systems* **78:** 71–80.

Hovmöller R, Knowles LL, Kubatko LS. 2013. Effects of missing data on species tree estimation under the coalescent. *Molecular Phylogenetics and Evolution* **69:** 1057–1062.

Huelsenbeck JP, Rannala B. 2004. Frequentist properties of Bayesian posterior probabilities of phylogenetic trees under simple and complex substitution models. *Systematic Biology* **53:** 904–913.

Inger RF. 1958. Comments on the definition of genera. *Evolution* **12:** 370–384.

IUCN-SSC Species Conservation Planning Sub-Committee. 2017. *Guidelines for Species Conservation Planning*. *Version 1.0*. Gland: International Union for Conservation of Nature.

Jombart T. **2008.** Adegenet: a R package for the multivariate analysis of genetic markers. *Bioinformatics* **24:** 1403–1405.

Jombart T, Devillard S, Balloux F. **2010.** Discriminant analysis of principal components. *BMC Genetics* **11:** 1–15.

Kaiser H, Crother BI, Kelly CMR, Luiselli L, O'Shea M, Ota H, Passos P, Schleip WD, Wüster W. 2013. Best practices: in the 21st century, taxonomic decisions in herpetology are acceptable only when supported by a body of evidence and published via peer-review. *Herpetological Review* **44:** 8–23.

Karin BR, Metallinou M, Weinell JL, Jackman TR, Bauer AM. 2016. Resolving the higher order phylogenetic relationships of the circumtropical *Mabuya* group (Squamata: Scincidae): an out-of-Asia diversification. *Molecular Phylogenetics and Evolution* **102:** 220–232.

Karin BR, Freitas ES, Shonlebin S, Grismer LL, Bauer AM, Das I. 2018. Unrealized diversity in an urban rainforest: a new species of *Lygosoma* (Squamata: Scincidae) from western Sarawak, Malaysia (Borneo). *Zootaxa* **4370:** 345–362.

Kass RE, Raftery AE. 1995. Bayes Factors. *Journal of the American Statistical Association* **90:** 773–795.

Kay GM, Keogh JS. 2012. Molecular phylogeny and morphological revision of the *Ctenotus labillardieri* (Reptilia: Squamata: Scincidae) species group and a new species of immediate conservation concern in the southwestern Australian biodiversity hotspot. *Zootaxa* **3390:** 1–18.

Kennedy AM, Marias J, Bauer AM, Lewis PJ, Thies ML. 2012. Effect of fire on the herpetofauna of the Koanaka Hills, Ngamiland, Botswana. *Check List* **8:** 666–674.

Kingman JFC. 1982. On the genealogy of large populations. *Journal of Applied Probability* **19:** 27–43.

Klein ER, Harris RB, Fisher RN, Reeder TW. 2016. Biogeographical history and coalescent species delimitation of Pacific Island skinks (Squamata: Scincidae: *Emoia cyanura* species group). *Journal of Biogeography* **43:** 1917–1929.

Lambert SM, Reeder TW, Wiens JJ. 2015. When do species-tree and concatenated estimates disagree? An empirical analysis with higher-level scincid lizard phylogeny. *Molecular Phylogenetics and Evolution* **82:** 146–155.

Lanza B, Carfí S. 1966. Note su alcuni Scincidae della Somalia e descrizione di una nuova specie di *Mochlus* (Reptilia Squamata). *Monitore Zoologico Italiano. Supplemento* **1:** 34–43.

Lanza B, Carfí S. 1968. Gli scincidi della Somalia (Reptilia, Squamata). *Monitore Zoologico Italiano. Supplemento* **2:** 207–260.

Lanza B. 1979. *Lygosoma simonettai*, a new black-headed skink from Somalia (Reptilia Scincidae). *Monitore Zoologico Italiano*. *Supplemento* **12:** 25–32.

Laurent RF, Gans C. 1965. Lizards. In: Gans C, Laurent RF, Pandit H. Notes on a herpetological collection from the Somali Republic. *Musée Royal de l'Afrique Centrale, Tervuren, Belgique: Annales — Serie in 8° — Sciences Zoologiques* **134:** 25–46.

Leaché AD, Reeder TW. 2002. Molecular systematics of the Eastern Fence Lizard (*Sceloporus undulatus*): a comparison of parsimony, likelihood, and Bayesian approaches. *Systematic Biology* **51:** 44–68.

Linkem CW, Hesed KM, Diesmos AC, Brown RM. 2010. Species boundaries and cryptic lineage diversity in a Philippine forest skink complex (Reptilia; Squamata; Scincidae: Lygosominae). *Molecular Phylogenetics and Evolution* **56:** 572–585.

Linkem CW, Diesmos AC, Brown RM. 2011. Molecular systematics of the Philippine forest skinks: testing morphological hypotheses of interspecific relationships. *Zoological Journal of the Linnean Society* **163:** 1217–1243.

Linkem CW, Brown RM, Siler CD, Evans BJ, Austin CC, Iskandar DT, Diesmos AC, Supriatna J, Andayani N, McGuire JA. 2013. Stochastic faunal exchanges drive diversification in widespread Wallacean and Pacific island lizards (Squamata: Scincidae: *Lamprolepis smaragdina*). *Journal of Biogeography* **40:** 507–520.

Linkem CW, Minin VN, Leaché AD. 2016. Detecting the anomaly zone in species trees and evidence for a misleading signal in higher-level skink phylogeny (Squamata: Scincidae). *Systematic Biology* **65:** 465–477.

Linnaeus C. 1758. *Systema naturæ per regna tria naturæ, secundum classes, ordines, genera, species, cum characteribus, differentiis, synonymis, locis. Tomus I. Edito decima, reformata*. Holmiae [Stockholm]: Laurentii Salvii.

Linnaeus C. 1766. *Systema naturæ per regna tria naturæ, secundum classes, ordines, genera, species, cum characteribus, differentiis, synonymis, locis. Tomus I. Edito duodecima, reformata*. Holmiae [Stockholm]: Laurentii Salvii.

Loveridge A. 1933. New scincid lizards of the genera *Sphenomorphus*, *Rhodona*, and *Lygosoma* from Australia. *Occasional Papers of the Boston Society of Natural History* **8:** 95–100.

Loveridge A. 1935. Scientific results of an expedition to rain forest regions in Eastern Africa. I. New reptiles and amphibians from East Africa. *Bulletin of the Museum of Comparative Zoology at Harvard College* **79:** 3–19.

Loveridge A. 1957. Checklist of the reptiles and amphibians of east Africa (Uganda; Kenya; Tanganyika; Zanzibar). *Bulletin of the Museum of Comparative Zoology at Harvard College* **117:** 153–360.

Maddison WP. 1997. Gene trees in species trees. *Systematic Biology* **46:** 523–536.

Marshall DC. 2010. Cryptic failure of partitioned Bayesian phylogenetic analyses: lost in the land of long trees. *Systematic Biology* **59:** 108–117.

Masterson G. 2014. *Mochlus sundevallii sundevallii* (A. Smith, 1849): Sundevall's writhing skink. In: Bates MF, Branch WR, Bauer AM, Burger M, Marias J, Alexander GJ, de Villiers MS, eds. *Atlas and Red List of the Reptiles of South Africa, Lesotho and Swaziland*. Pretoria: South African National Biodiversity Institute.

Mausfeld P, Vences M, Schmitz A, Veith M. 2000. First data on the molecular phylogeography of scincid lizards of the genus *Mabuya*. *Molecular Phylogenetics and Evolution* **17:** 11–14.

Mausfeld P, Schmitz A. 2003. Molecular phylogeography, intraspecific variation and speciation of the Asian scincid lizard genus *Eutropis* Fitzinger, 1843 (Squamata: Reptilia: Scincidae): taxonomic and biogeographic implications. *Organisms, Diversity and Evolution* **3:** 161–171.

Mayr E. 1976. The role of systematics in biology. In Mayr E. *Evolution and the diversity of life: selected essays*. Cambridge: Belknap Press. 416–424.

McCormack JE, Faircloth BC, Crawford NG, Gowaty PA, Brumfield RT, Glenn TC. 2012. Ultraconserved elements are novel phylogenomic markers that resolve placental mammal phylogeny when combined with species-tree analysis. *Genome Research* **22:** 746–754.

Medina MF, Bauer AM, Branch WR, Schmitz A, Conradie W, Nagy ZT, Hibbits TJ, Ernst R, Portik DM, Nielsen SV, Colston TJ, Kusamba C, Behandana M, Rödel MO, Greenbaum E. 2016. Molecular phylogeny of *Panaspis* and *Afroablepharus* skinks

(Squamata: Scincidae) in the savannas of sub-Saharan Africa. *Molecular Phylogenetics and Evolution* **100:** 409–423.

Miller MA, Pfeiffer W, Schwartz T. 2010. Creating the CIPRES Science Gateway for inference of large phylogenetic trees. In *Gateway Computing Environments Workshop 2010.* New Orleans: IEEE.

Mittleman MB. 1952. Generic synopsis of the lizards of the subfamily Lygosominae. *Smithsonian Miscellaneous Collections* **117:** 1–35.

Myers N, Mittermeier RA, Mittermeier CG, da Fonseca GAB, Kent J. 2000. Biodiversity hotspots for conservation priorities. *Nature (London)* **403:** 853–848.

Oliver LA, Prendini E, Kraus F, Raxworthy CJ. 2015. Systematics and biogeography of the *Hylarana* frog (Anura: Ranidae) radiation across tropical Australasia, Southeast Asia, and Africa. *Molecular Phylogenetics and Evolution* **90:** 176–192.

Palumbi S. **1991.** *The simple fool's guide to PCR*. Honolulu: Department of Zoology and Kewalo Marine Laboratory.

Parker HW. 1932. Two collections of reptiles and amphibians from British Somaliland. *Proceedings of the Zoological Society of London* **102:** 335–367.

Parker HW. 1942. The lizards of British Somaliland. *Bulletin of the Museum of Comparative Zoology at Harvard College* **91:** 3–101.

Perret JL, Wuest J. 1983. La microstructure des écailles de quelques scincidés Africains et paléarctiques (Lacerilia), observée au microscope électronique á balayage, II. *Revue Suisse de Zoologie* **90:** 913–928.

Peters W. 1854. Diagnosen neuer batrachier, welche zusammen mit der früher (24. Juli und 17. August) gegebenen übersicht der schlangen und eidechsen mitgetheilt werden.

Monatsberichte der Königlichen Preussische Akademie des Wissenschaften zu Berlin **1854:** 614–628.

Peters W. 1874. Über einige neue reptilien (*Lacerta*, *Eremias*, *Diploglossus*, *Euprepes*, *Lygosoma*, *Sepsina*, *Ablepharus*, *Simotes*, *Onychocephalus*). *Monatsberichte der Königlichen Preussische Akademie des Wissenschaften zu Berlin* **1874:** 368–377.

Peters W. 1879. Über neue amphibien des Kgl. Zoologischen Museums (*Euprepes*, *Acontias*, *Typhlops*, *Zamenensis*, *Spilotes*, *Oedipus*). *Monatsberichte der Königlichen Preussische Akademie des Wissenschaften zu Berlin* **1879:** 773–779.

Pietersen DW, Scholtz CH, Bastos ADS. 2018. Multi-locus phylogeny of southern African *Acontias aurantiacus* (Peters) subspecies (Scincidae: Acontinae) confirms the presence of three genetically, geographically and morphologically discrete taxa. *Zootaxa* **4442:** 427–440.

Pinto-Sánchez NR, Calderón-Espinosa ML, Miralles A, Crawford AJ, Ramírez-Pinilla MP. 2015. Molecular phylogenetics and biogeography of the neotropical skink genus *Mabuya* Fitzinger (Squamata: Scincidae) with emphasis on Columbian populations. *Molecular Phylogenetics and Evolution* **93:** 188–211.

Pyron RA, Burbrink FT, Wiens JJ. 2013. A phylogeny and revised classification of Squamata, including 4161 species of lizards and snakes. *BMC Evolutionary Biology* **93:** 1–53.

R Core Team. 2016. R: a language and environment for statistical computing. R Foundation for Statistical Computing. Available at: https://www.R-project.org/.

R Core Team. 2018. R: a language and environment for statistical computing. R Foundation for Statistical Computing. Available at: https://www.R-project.org/.

Rambaut A, Suchard MA, Xie D, Drummond AJ. 2014. Tracer v1.6. Available at: http://tree.bio.ed.ac.uk/software/tracer/.

Rittmeyer EN, Austin CC. 2015. Combined next-generation sequencing and morphology reveal fine-scale speciation in Crocodile Skinks (Squamata: Scincidae: *Tribolonotus*). *Molecular Ecology* **24:** 466–483.

Rocha S, Carretero MA, Vences M, Glaw F, Harris DJ. 2006. Deciphering patterns of transoceanic dispersal: the evolutionary origin and biogeography of coastal lizards (*Cryptoblepharus*) in the western Indian Ocean region. *Journal of Biogeography* **33:** 13–22.

Ronquist F, Telsenko M, van der Mark P, Ayres DL, Darling A, Höhna S, Larget B, Liu L, Suchard MA, Huelsenbeck JP. 2012. MrBayes 3.2: efficient Bayesian phylogenetic inference and model choice across a large model space. *Systematic Biology* **61**: 539–542.

Rosenberg NA. 2002. The probability of topological concordance of gene trees and species trees. *Theoretical Population Biology* **61:** 225–247.

Schmidt KP. 1919. Contributions to the herpetology of the Belgian Congo based on the collections of the American Museum Congo Expedition, 1909–1915. Part I. Turtles, crocodiles, lizards, and chameleons. With field notes by Herbert Land and James P. Chapin. *Bulletin of the American Museum of Natural History* **39:** 385–624.

Schneider JG. 1801. *Historiae amphibiorum naturalis et literariae. Fasciculus secundus*. *Continens Crocodilos, Scincus, Chamaesaurus, Boas, Ppseudoboas, Elapes, Angues, Amphisbaenas et Caecilias.* Jenae [Jena]: Friederich Frommann.

Sharma RC. **1976** Records of the reptiles of Goa. *Records of the Zoological Survey of India* **71:** 149–167.

Sharma RC. **1977**. A new lizard of the genus *Riopa* Gray (Scincidae) from Tamil Nadu, India. *Records of the Zoological Survey of India* **73:** 41–42.

Shreve B. **1940.** Reptiles and amphibians from Burma with descriptions of three new skincs [sic]. *Proceedings of the New England Zoological Club* **18:** 17–26.

Siler CD, Diesmos AC, Brown RM. 2010. New loam-swimming skink, genus *Brachymeles* (Reptilia: Squamata: Scincidae) from Luzon and Catanduanes Islands, Philippines. *Journal of Herpetology* **44:** 49–60.

Siler CD, Diesmos AC, Alcala AC, Brown RM. 2011. Phylogeny of the Philippine slender skinks (Scincidae: *Brachymeles*) reveals underestimated species diversity, complex biogeographical relationships, and cryptic patterns of lineage diversification. *Molecular Phylogenetics and Evolution* **59:** 53–65.

Siler CD, Jones RM, Diesmos AC, Diesmos ML, Brown RM. 2012. Phylogeny-based species delimitation in Philippine slender skinks (Reptilia: Squamata: Scincidae) III: taxonomic revision of the *Brachymeles gracilis* complex, with descriptions of three new species. *Herpetological Monographs* **26:** 135–172.

Siler CD, Linkem CW, Cobb K, Watters JL, Cummings ST, Diesmos AC, Brown RM. 2014. Taxonomic revision of the semi-aquatic skink *Parvoscincus leucospilos* (Reptilia: Squamata: Scincidae), with description of three new species. *Zootaxa* **3847:** 388–412.

Siler CD, Davis DR, Freitas ES, Huron NA, Geheber AD, Watters JL, Penrod ML, Papes M, Amrein A, Anwar A, Cooper D, Hein T, Manning A, Patel N, Pinaroc L, Diesmos AC, Diesmos ML, Oliveros CH, Brown RM. 2016. Additions to Philippine slender skinks of the *Brachymeles bonitae* complex (Reptilia: Squamata: Scincidae) II: a new species from the northern Philippines. *Zootaxa* **4132:** 15–29.

Siler CD, Heitz BB, Davis DR, Freitas ES, Aowphol A, Termprayoon K, Grismer LL. 2018. New supple skink genus *Lygosoma* (Reptilia: Squamata: Scincidae) from Thailand and redescription of *Lygosoma quadrupes* (Linnaeus, 1766). *Journal of Herpetology* **52:** 332–347.

Sindaco R, Metallinou M, Pupin F, Fasola M, Carranza S. 2012. Forgotten in the ocean: systematics, biogeography and evolution of the *Trachylepis* skinks of the Socotra Archipelago. *Zoologica Scripta* **41:** 346–362.

Skinner A, Hugall AF, Hutchinson MN. 2011. Lygosomine phylogeny and the origins of Australian scincid lizards. *Journal of Biogeography* **38:** 1044–1058.

Skinner A, Hutchinson MN, Lee MSY. 2013. Phylogeny and divergence times of Australian *Sphenomorphus* group skinks (Scincidae, Squamata). *Molecular Phylogenetics and Evolution* **69:** 906–918.

Smith A. **1849.** *Illustrations of the zoology of South Africa consisting chiefly of figures and descriptions of the objects of natural history collected during an expedition into the interior of South Africa in the years 1834, 1835, and 1836; Fitted out by "The Cape of Good Hope Association for Exploring Central Africa." Reptilia.* London: Smith, Elder and Co.

Smith MA. **1916.** Descriptions of three new lizards and a new snake from Siam. *Journal of the Natural History of Siam* **2:** 44–47.

Smith MA. 1917. Descriptions of new reptiles and a new batrachian from Siam. *Journal of the Natural History Society of Siam* **2:** 221–225.

Smith MA. 1921. New or little-known reptiles and batrachians from southern Annam (Indo-China). *Proceedings of the Zoological Society of London* **1921:** 423–440.

Smith MA. 1935. *The fauna of British India, including Ceylon and Burma*. *Reptilia and Amphibia. Volume II—Sauria*. London: Taylor and Francis.

Smith MA. 1937a. A review of the genus *Lygosoma* (Scincidae: Reptilia) and its allies. *Records of the Indian Museum* **39:** 213–234.

Smith MA. 1937b. Un nouveau lézard de Cochinchine. *Bulletin du Muséum National d'Histoire Naturelle* **9:** 366.

Stamatakis A. 2014. RAxML version 8: a tool for phylogenetic analysis and post-analysis of large phylogenies. *Bioinformatics* **30:** 1312–1313.

Stoliczka F. 1870. Observations on some Indian and Malayan amphibia and reptilia. *Journal of the Asiatic Society of Bengal* **39:** 134–228, pl. x–xii.

Storr GM. 1964. *Ctenotus*, a new generic name for a group of Australian skinks. *Western Australian Naturalist* **9:** 84–85.

Storr GM. 1967. The genus *Sphenomorphus* (Lacertilia, Scincidae) in western Australia and the Northern Territory. *Journal of the Royal Society of Western Australia* **50:** 10–20.

Streicher JW, Wiens JJ. 2017. Phylogenomic analyses of more than 4000 nuclear loci resolve the origin of snakes among lizard families. *Biology Letters* **13:** 20170393.

Tabachnick BG, Fidell LS. 2013. *Using Multivariate Statistics*. *Sixth edition*. Essex: Pearson.

Tajima F. 1983. Evolutionary relationship of DNA sequences in finite populations. *Genetics* **105:** 437–460.

Taylor EH. 1923. Additions to the herpetological fauna of the Philippine Islands, III. *Philippine Journal of Science* **22:** 515–557, pl. 1–3.

Taylor EH. 1935. A taxonomic study of the cosmopolitan scincoid lizards of the genus *Eumeces* with an account of the distribution ond relationsips of its species. *University of Kansas Science Bulletin* **23:** 19–643.

Taylor EH. 1950. Ceylonese lizards of the family Scincidae. *University of Kansas Science Bulletin* **33:** 481–518.

Taylor EH. 1962 New Oriental reptiles. *University of Kansas Science Bulletin* **43:** 209–263.

Taylor EH. 1963. The lizards of Thailand. *University of Kansas Science Bulletin* **44:** 687–1077.

Theobald W. 1867. Catalogue of the reptiles of British Burma, embracing the provinces of Pegu, Martaban, and Tenasserim; with descriptions of new or little-known species. *Journal of the Linnean Society. Zoology* **10:** 4–67.

Theobald W. 1876. *Descriptive Catalogue of the Reptiles of British India*. Calcutta: Thacker, Spink and Co.

Townsend TM, Alagre RE, Kelley ST, Wiens JJ, Reeder TW. 2008. Rapid development of multiple nuclear loci for phylogenetic analysis using genomic resources: an example from squamate reptiles. *Molecular Phylogenetics and Evolution* **47:** 129–142.

Trape JF, Trape S, Chirio L. 2012. *Lézards, crocodiles et tortues d'Afrique occidentale et du Sahara*. Marseille: Institut de Recherché pour le Dévelopement.

Uetz P, Freed P, Hošek J, eds. 2018. *The reptile database*. Available at: http://www.reptile-database.org. Accessed: December 2018.

Vaillant ML. 1884. Note sur une collection de reptiles rapportée d'Assinie par M. Chaper. *Bulletin de la Société Philomathique de Paris* **70:** 168–171.

Vences M, Guayasamin JM, Miralles A, de la Riva I. 2013. To name or not to name: criteria to promote economy of change in Linnaean classification schemes. *Zootaxa* **3636:** 201–244.

Vitt L, Caldwell J. 2013. *Herpetology*: *an introductory biology of amphibians and reptiles.* London: Academic Press.

Wagler JG. 1830. *Natürliches System der Amphibien, mit vorangehender Classification der Säugthiere und Vögel*. München [Munich]: J.G. Cotta.

Wagner P, Böhme W, Pauwels OS, Schmitz A. 2009. A review of the African red-flanked skinks of the *Lygosoma fernandi* (Burton, 1836) species group (Squamata: Scincidae) and the role of climate change in their speciation. *Zootaxa* **2050:** 1–30.

Warren D, Geneva A, Lanfear R. 2017. RWTY (R We There Yet): an R package for examining convergence of Bayesian phylogenetic analyses. *Molecular Biology and Evolution* **34:** 1016–1020.

Werner F. 1900. Reptilien und batrachier aus Sumatra, gesammelt von Herrn Gustav Schneider jr. im jahre 1897–98. *Zoologische Jahrbücher abtheilung für Systematik, Geographie und Biologie der Thiere* **13:** 479–508.

Werner F. 1910. Über neue oder seltene Reptilien des Naturhistorischen Museums in Hamburg. II. Eidechsen. *Jahrbuch der Hamburgischen Wissenschaftlichen Anstalten.* **27:** 1–46.

Wheeler QD, Raven PH, Wilson EO. 2004. Taxonomy: impediment or expedient? *Science (Washington)* **303:** 285.

Whiting AS, Bauer AM, Sites Jr. JW. 2003. Phylogenetic relationships and limb loss in sub-Saharan African scincine lizards (Squamata: Scincidae). *Molecular Phylogenetics and Evolution* **29:** 582–598.

Whiting AS, Sites Jr. JW, Bauer AM. 2004. Molecular phylogenetics of Malagasy skinks (Squamata: Scincidae). *African Journal of Herpetology* **53:** 135–146.

Wiegmann AFA. 1834. *Herpetologia Mexicana, seu descriptio amphibiorum Novae Hispaniae: quae itineribus comitis de Sack, Ferdinandi Deppe et Chr. Guil. Schiede in Museum Zoologicum Berolinense pervenerunt*. Berolini [Berlin]: CG Lüderitz.

Winston JE. 1999. *Describing species: practical taxonomic procedure for biologists.* New York: Columbia University Press.

Xie W, Lewis PO, Fan Y, Kuo L, Chen MH. 2011. Improving marginal likelihood estimation for Bayesian phylogenetic model selection. *Systematic Biology* **60:** 150–160.

Zheng Y, Wiens JJ. 2016. Combining phylogenomic and supermatrix approaches, and a time-calibrated phylogeny for squamate reptiles (lizards and snakes) based on 52 genes and 4162 species. *Molecular Phylogenetics and Evolution* **94:** 537–547.

Ziegler T, Schmitz A, Heidrich A, Vu NT, Nguyen QT. 2007. A new species of *Lygosoma* (Squamata: Sauria: Scincidae) from the central Truong Son, Vietnam, with notes on its molecular phylogenetic position. *Revue Suisse de Zoologie* **114:** 397–415.

SUPPLEMENTARY MATERIAL

Table S1. Table showing the taxonomic and genetic sampling for this study. Museum voucher numbers and country of origin for each sample and GenBank numbers for each gene are listed in the columns.

Species	Museum No.	Country	*CMOS*	*FSTL5*	*PRLR*	*PTGER4*	*R35*	*RAG1*	*SNCAIP*	*ND1*	*16S*
Lygosoma corpulentum	LSUHC 9321	Cambodia	---	MK409433	MK409453	HQ907531	HQ907638	MK409538	MK409565	HQ907329	---
Lygosoma isodactylum	FMNH 262154	Vietnam	MK409390	MK409422	MK409444	---	MK409500	---	MK409554	MK409589	MK414547
Lygosoma quadrupes	ENS 13639	Indonesia	MK409409	MK409438	---	MK409489	KX774339	MK409543	MK409572	KX774344	MG367368
Lygosoma tabonorum	PNM 9820	Philippines	MK409400	MK409432	---	MK409484	KX774338	MK409537	MK409564	KX774343	MK414557
Lygosoma tabonorum	PNM 9821	Philippines	MK409399	MK409431	---	MK409483	PNM 9821	MK409536	MK409563	KX774340	MG367367
Mochlus brevicaudis	MVZ 249721	Ghana	MK409389	MK409421	HM160878	MK409474	HM161064	HM161159	HM161256	HM160781	MK414546
Mochlus fernandi	PEM R5370	Gabon	MK409403	---	---	---	MK409512	MH129994	---	MK409601	---
Mochlus fernandi	PEM R5444	Gabon	MK409404	---	MK409455	MK409487	MK409513	MH129995	MK409568	MK409602	MK414560
Mochlus guineensis	MVZ 252551	Ghana	MK409391	MK409423	MK409445	MK409475	MK409501	MK409528	MK409555	MK409590	MK414548
Mochlus guineensis	MVZ 252556	Ghana	MK409392	MK409424	MK409446	MK409476	MK409502	MK409529	MK409556	MK409591	MK414549
Mochlus sundevallii	CAS 209609	South Africa	MK409407	---	---	---	MK409515	MH130003	---	MK409604	MK414561
Mochlus sundevallii	UTEP 21777	Democratic Republic of Congo	MK409386	MK409418	MK409441	---	MK409497	MH130034	MK409551	MK409586	MK414543
Mochlus sundevallii	UTEP 21778	Democratic Republic of Congo	MK409398	---	---	---	MK409507	MH130033	---	MK409596	MK414555
Mochlus sundevallii	WCDNA 1077: no voucher	Mozambique	MK409408	---	MK409458	---	MK409516	MH130041	MK409571	MK409605	MK414562
Riopa albopunctata	CES 14/823	India	---	---	MK409466	---	---	MK409544	MK409580	MK409620	MK414540

Riopa anguina	CAS 223228	Myanmar	MK409393	MK409425	MK409447	MK409477	MK409503	MK409530	MK409557	MK409592	MK414550
Riopa anguina	CAS 230414	Myanmar	MK409395	MK409427	MK409449	MK409479	MK409505	MK409532	MK409559	MK409594	MK414552
Riopa goaensis	BNHS 1966	India	---	---	MK409467	---	---	MK409545	MK409581	MK409619	KF577802
Riopa guentheri	CES 13/802	India	---	---	MK409468	---	---	MK409546	MK409582	MK409621	MK414541
Riopa lineata	CES 13/805	India	---	---	MK409469	---	---	MK409547	MK409583	MK409615	MK414542
Riopa lineolata	CAS 213615	Myanmar	MK409396	MK409428	MK409450	MK409480	MK409506	MK409533	MK409560	MK409595	MK414553
Riopa lineolata	CAS 240673	Myanmar	---	MK409430	MK409452	MK409482	MK409508	MK409535	MK409562	MK409597	MK414556
Riopa popae	CAS 231327	Myanmar	MK409397	MK409429	MK409451	MK409481	MF981875	MK409534	MK409561	MF981878	MK414554
Riopa popae	CAS 239204	Myanmar	MK409394	MK409426	MK409448	MK409478	MK409504	MK409531	MK409558	MK409593	MK414551
Riopa punctata	CES 14/811	India	---	---	MK409471	---	---	MK409549	---	MK409616	MK414573
Riopa vosmaerii	BNHS 1975	India	---	---	MK409472	---	---	MK409550	MK409585	MK409618	KF577803
Subdoluseps bowringii	FMNH 261839	Cambodia	MK409387	MK409419	MK409442	MK409473	MK409498	MK409526	MK409552	MK409587	MK414544
Subdoluseps bowringii	LSUHC 7993	Malaysia	MK409388	MK409420	MK409443	---	MK409499	MK409527	MK409553	MK409588	MK414545
Subdoluseps frontoparietalis	ZMKU R705	Thailand	MK409401	MK409434	---	MK409485	MK409509	MK409539	MK409566	MK409598	MK414558
Subdoluseps frontoparietalis	ZMKU R707	Thailand	MK409402	MK409435	MK409454	MK409486	MK409510	---	MK409567	MK409599	MK414559
Subdoluseps herberti	LSUHC 10995	Malaysia	---	---	---	---	MK409511	MK409540	---	MK409600	MG020472
Subdoluseps herberti	LSUHC 12098	Malaysia	MK409405	MK409436	MK409456	---	MK409514	MK409541	MK409569	MK409603	MG020473
Subdoluseps pruthi	CES 09/905	India	---	---	MK409470	---	---	MK409548	MK409584	MK409617	MK414572
Subdoluseps samajaya	CAS 259777	Malaysia	MK409406	MK409437	MK409457	MK409488	MF981876	MK409542	MK409570	MF981879	MG020475
Eutropis multifasciata	KU 337427	Philippines	MK409412	MK409439	MK409460	MK409491	MK409520	---	MK409574	MK409609	MK414566
Lamprolepis smaragdina	KU 337729	Philippines	MK409415	---	MK409463	MK409494	MK409523	---	MK409577	MK409612	MK414569
Lamprolepis smaragdina	KU 337740	Philippines	MK409416	MK409440	MK409464	MK409495	MK409524	---	MK409578	MK409613	MK414570
Larutia sp.	ENS 16755	Indonesia	MK409410	---	MK409459	MK409490	MK409517	---	MK409573	MK409606	MK414563

Lipinia pulchella	THNC 56379	Philippines	---	---	---	---	MK409518	---	---	MK409607	MK414564
Otosaurus cumingi	KU 338082	Philippines	MK409413	---	MK409461	MK409492	MK409521	---	MK409575	MK409610	MK414567
Pinoyscincus jagori	KU 338232	Philippines	MK409417	---	MK409465	MK409496	MK409525	---	MK409579	MK409614	MK414571
Plestiodon fasciatus	KU 289463	United States	MK409411	---	---	---	MK409519	---	---	MK409608	MK414565
Sphenomorphus fasciatus	KU 338668	Philippines	MK409414	---	MK409462	MK409493	MK409522	---	MK409576	MK409611	MK414568

Table S2. Table showing the museum number (or collector number when the museum number was not available) and country of origin for each specimen in our morphological dataset.

Species	Museum No.	Country: Island
Lygosoma corpulentum	FMNH 213927	Thailand
Lygosoma isodactylum	FMNH 177678	Thailand
Lygosoma kinabatanganense	FMNH 76226	Malaysia: Borneo
Lygosoma koratense	FMNH 177656	Thailand
Lygosoma koratense	USNM 81879	Thailand
Lygosoma quadrupes	FMNH 122264	Indonesia: Java
Lygosoma quadrupes	FMNH 261866	Cambodia
Lygosoma quadrupes	MCZ 25209	Vietnam
Lygosoma quadrupes	MCZ 39278	Cambodia
Lygosoma quadrupes	MCZ 7667	Indonesia: Java
Lygosoma quadrupes	USNM 29414	Indonesia: Java
Lygosoma quadrupes	USNM 43257	Indonesia: Java

	USNM	Indonesia:
Lygosoma quadrupes	43578	Java
	USNM	Indonesia:
Lygosoma quadrupes	43677	Java
	USNM	Indonesia:
Lygosoma quadrupes	43780	Java
	FMNH	
Lygosoma siamense	152332	Thailand
	FMNH	
Lygosoma siamense	171438	Thailand
	FMNH	
Lygosoma siamense	176979	Thailand
	FMNH	
Lygosoma siamense	176980	Thailand
	FMNH	
Lygosoma siamense	177491	Thailand
	FMNH	
Lygosoma siamense	177492	Thailand
	FMNH	
Lygosoma siamense	177495	Thailand
	FMNH	
Lygosoma siamense	177496	Thailand
	FMNH	
Lygosoma siamense	177497	Thailand
	FMNH	
Lygosoma siamense	177502	Thailand
	FMNH	
Lygosoma siamense	177503	Thailand
	FMNH	
Lygosoma siamense	177505	Thailand
	FMNH	
Lygosoma siamense	177506	Thailand
	FMNH	
Lygosoma siamense	177508	Thailand
	FMNH	
Lygosoma siamense	177509	Thailand
	FMNH	
Lygosoma siamense	181084	Thailand
	MCZ	
Lygosoma siamense	39279	Thailand
	MCZ	
Lygosoma siamense	39280	Thailand
	MCZ	
Lygosoma siamense	39281	Thailand
		Philippines:
Lygosoma tabonorum	ACD 7365	Palawan
		Philippines:
Lygosoma tabonorum	ACD 7366	Palawan
	CAS	Philippines:
Lygosoma tabonorum	152030	Cuyo

	CAS	Philippines:
Lygosoma tabonorum	152032	Cuyo
	CAS	Philippines:
Lygosoma tabonorum	157345	Palawan
	CAS	Philippines:
Lygosoma tabonorum	28465	Palawan
	MCZ	Philippines:
Lygosoma tabonorum	183651	Palawan
	MCZ	Philippines:
Lygosoma tabonorum	26514	Palawan
	MCZ	Philippines:
Lygosoma tabonorum	26515	Palawan
	MCZ	Philippines:
Lygosoma tabonorum	26521	Palawan
	MCZ	Philippines:
Lygosoma tabonorum	26523	Palawan
	MCZ	Philippines:
Lygosoma tabonorum	26524	Palawan
	MCZ	Philippines:
Lygosoma tabonorum	26525	Palawan
		Philippines:
Lygosoma tabonorum	PNM 9820	Palawan
		Philippines:
Lygosoma tabonorum	PNM 9821	Palawan
	CAS	
Mochlus brevicaudis	136150	Ghana
	CAS	
Mochlus brevicaudis	97523	Ghana
	CAS	
Mochlus brevicaudis	97524	Ghana
	MVZ	
Mochlus brevicaudis	249721	Ghana
	CAS	
Mochlus pembanus	154565	Kenya
	CAS	
Mochlus pembanus	154566	Kenya
	CAS	
Mochlus pembanus	160957	Kenya
	CAS	
Mochlus pembanus	160958	Kenya
	CAS	
Mochlus pembanus	160959	Kenya
	CAS	
Mochlus sundevallii	111823	Kenya
	CAS	
Mochlus sundevallii	129752	Kenya
	CAS	
Mochlus sundevallii	140243	Kenya
	CAS	
Mochlus sundevallii	141515	Kenya

	CAS	
Mochlus sundevallii	147900	Kenya
	CAS	
Mochlus sundevallii	148254	Somalia
	CAS	
Mochlus sundevallii	148262	Somalia
	CAS	
Mochlus sundevallii	148265	Somalia
	CAS	
Mochlus sundevallii	148280	Somalia
	CAS	
Mochlus sundevallii	148282	Somalia
	CAS	
Mochlus sundevallii	153215	Kenya
	CAS	
Mochlus sundevallii	154773	Kenya
	CAS	
Mochlus sundevallii	161353	Tanzania
	CAS	
Mochlus sundevallii	164458	Tanzania
	CAS	
Mochlus sundevallii	165559	Kenya
	CAS	
Mochlus sundevallii	173808	Tanzania
	CAS	
Mochlus sundevallii	175604	Namibia
	CAS	
Mochlus sundevallii	225113	Tanzania
	CAS	
Mochlus sundevallii	227754	Tanzania
	CAS	
Mochlus sundevallii	234120	South Africa
	CAS	
Mochlus sundevallii	85750	Kenya
	FMNH	
Mochlus sundevallii	12308	Tanzania
	FMNH	
Mochlus sundevallii	142802	Zambia
	FMNH	
Mochlus sundevallii	142803	Zambia
		Democratic
	FMNH	Republic of
Mochlus sundevallii	168835	Congo
	FMNH	
Mochlus sundevallii	17248	Zimbabwe
	FMNH	
Mochlus sundevallii	17260	Botswana
	FMNH	
Mochlus sundevallii	17261	Botswana

	FMNH	
Mochlus sundevallii	190713	Mozambique
	FMNH	
Mochlus sundevallii	190716	Mozambique
	FMNH	
Mochlus sundevallii	195938	Mozambique
	FMNH	
Mochlus sundevallii	255925	Tanzania
	FMNH	
Mochlus sundevallii	64526	Namibia
	FMNH	
Mochlus sundevallii	6565	Kenya
	FMNH	
Mochlus sundevallii	65845	Namibia
	FMNH	
Mochlus sundevallii	78159	Tanzania
	MCZ	
Mochlus sundevallii	144868	Botswana
	MCZ	
Mochlus sundevallii	144869	Botswana
	MCZ	
Mochlus sundevallii	144870	Botswana
	MCZ	
Mochlus sundevallii	18336	Mozambique
	MCZ	
Mochlus sundevallii	18337	Mozambique
	MCZ	
Mochlus sundevallii	24200	Tanzania
	MCZ	
Mochlus sundevallii	31008	Kenya
	MCZ	
Mochlus sundevallii	31011	Tanzania
	MCZ	
Mochlus sundevallii	31013	Tanzania
	MCZ	
Mochlus sundevallii	31014	Tanzania
	MCZ	
Mochlus sundevallii	31020	Tanzania
	MCZ	
Mochlus sundevallii	31022	Tanzania
	MCZ	
Mochlus sundevallii	31031	Tanzania
	MCZ	
Mochlus sundevallii	65156	South Africa
	FMNH	
Mochlus tanae	255923	Tanzania
	FMNH	
Mochlus tanae	255924	Tanzania
	CES	
Riopa albopunctata	14/823	India

	FMNH	
Riopa albopunctata	152402	India
	FMNH	
Riopa albopunctata	60662	India
	FMNH	
Riopa albopunctata	74942	India
	FMNH	
Riopa albopunctata	82911	Bangladesh
	CAS	
Riopa anguina	206645	Myanmar
	CAS	
Riopa anguina	206646	Myanmar
	CAS	
Riopa anguina	206647	Myanmar
	CAS	
Riopa anguina	215589	Myanmar
	CAS	
Riopa anguina	215732	Myanmar
	CAS	
Riopa anguina	221110	Myanmar
	CAS	
Riopa anguina	222127	Myanmar
	CAS	
Riopa anguina	223228	Myanmar
	CAS	
Riopa anguina	234962	Myanmar
	FMNH	
Riopa anguina	42673	Myanmar
	BNHM	
Riopa goaensis	1966	India
	CAS	
Riopa guentheri	11007	India
	CAS	
Riopa guentheri	11008	India
	CES	
Riopa guentheri	13/802	India
	CES	
Riopa lineata	13/805	India
	CAS	
Riopa lineolata	206533	Myanmar
	CAS	
Riopa lineolata	210669	Myanmar
	CAS	
Riopa lineolata	213615	Myanmar
	CAS	
Riopa lineolata	215536	Myanmar
	CAS	
Riopa lineolata	215537	Myanmar
	CAS	
Riopa lineolata	215717	Myanmar

	CAS	
Riopa lineolata	231273	Myanmar
	CAS	
Riopa lineolata	231325	Myanmar
	CAS	
Riopa lineolata	232549	Myanmar
	USNM	
Riopa lineolata	520566	Myanmar
	USNM	
Riopa lineolata	520567	Myanmar
	USNM	
Riopa lineolata	520570	Myanmar
	USNM	
Riopa lineolata	520581	Myanmar
	USNM	
Riopa lineolata	520586	Myanmar
	USNM	
Riopa lineolata	520587	Myanmar
	USNM	
Riopa lineolata	520598	Myanmar
	CAS	
Riopa popae	210503	Myanmar
	CAS	
Riopa popae	210503	Myanmar
	CAS	
Riopa popae	216328	Myanmar
	CAS	
Riopa popae	216329	Myanmar
	CAS	
Riopa popae	231327	Myanmar
	CAS	
Riopa popae	231329	Myanmar
	CAS	
Riopa popae	232289	Myanmar
	CAS	
Riopa popae	232550	Myanmar
	CAS	
Riopa popae	233106	Myanmar
	CES	
Riopa punctata	14/811	India
	BNHM	
Riopa vosmaerii	1975	India
Subdoluseps	CAS	
bowringii	123960	Thailand
Subdoluseps	CAS	Philippines:
bowringii	157408	Palawan
Subdoluseps	CAS	Philippines:
bowringii	157411	Palawan
Subdoluseps	CAS	Philippines:
bowringii	157412	Palawan

Subdoluseps	CAS	Philippines:
bowringii	157415	Palawan
Subdoluseps	CAS	
bowringii	172730	Thailand
Subdoluseps	CAS	
bowringii	172731	Thailand
Subdoluseps	CAS	
bowringii	23577	Thailand
Subdoluseps	CAS	
bowringii	23579	Thailand
Subdoluseps	CAS	
bowringii	23580	Thailand
Subdoluseps	CAS	Philippines: Sulu
bowringii	60741	Archipelago
Subdoluseps	CAS	Philippines: Sulu
bowringii	60742	Archipelago
Subdoluseps	CAS	Philippines: Sulu
bowringii	60744	Archipelago
Subdoluseps	CAS	Philippines: Sulu
bowringii	60861	Archipelago
Subdoluseps	CAS	Philippines: Sulu
bowringii	60862	Archipelago
Subdoluseps	CAS	Philippines: Sulu
bowringii	62495	Archipelago
Subdoluseps	FMNH (no	
bowringii	number)	---
Subdoluseps	FMNH	
bowringii	119684	Indonesia
Subdoluseps	FMNH	Philippines:
bowringii	125640	Palawan
Subdoluseps	FMNH	Philippines:
bowringii	125641	Palawan
Subdoluseps	FMNH	Philippines:
bowringii	125642	Palawan
Subdoluseps	FMNH	
bowringii	125889	Malaysia
Subdoluseps	FMNH	
bowringii	125893	Malaysia
Subdoluseps	FMNH	
bowringii	125896	Malaysia
Subdoluseps	FMNH	
bowringii	125899	Malaysia
Subdoluseps	FMNH	Malaysia:
bowringii	134715	Borneo

Subdoluseps	FMNH	Malaysia:
bowringii	134716	Borneo
Subdoluseps	FMNH	Malaysia:
bowringii	158736	Borneo
Subdoluseps	FMNH	Malaysia:
bowringii	158737	Borneo
Subdoluseps	FMNH	
bowringii	171461	Thailand
Subdoluseps	FMNH	
bowringii	177494	Thailand
Subdoluseps	FMNH	
bowringii	178327	Thailand
Subdoluseps	FMNH	
bowringii	179449	Thailand
Subdoluseps	FMNH	
bowringii	179456	Thailand
Subdoluseps	FMNH	
bowringii	181847	Thailand
Subdoluseps	FMNH	
bowringii	181880	Thailand
Subdoluseps	FMNH	
bowringii	182044	Thailand
Subdoluseps	FMNH	
bowringii	182054	Thailand
Subdoluseps	FMNH	
bowringii	182059	Thailand
Subdoluseps	FMNH	
bowringii	182234	Thailand
Subdoluseps	FMNH	
bowringii	188764	Thailand
Subdoluseps	FMNH	
bowringii	188828	Thailand
Subdoluseps	FMNH	
bowringii	188829	Thailand
Subdoluseps	FMNH	
bowringii	188833	Thailand
Subdoluseps	FMNH	
bowringii	188836	Thailand
Subdoluseps	FMNH	
bowringii	188837	Thailand
Subdoluseps	FMNH	
bowringii	188843	Thailand
Subdoluseps	FMNH	
bowringii	188856	Thailand
Subdoluseps	FMNH	
bowringii	188859	Thailand
Subdoluseps	FMNH	
bowringii	188868	Thailand
Subdoluseps	FMNH	
bowringii	188869	Thailand

Subdoluseps	FMNH	
bowringii	188885	Thailand
Subdoluseps	FMNH	
bowringii	611?	Thailand
Subdoluseps	FMNH	
bowringii	611?	Thailand
Subdoluseps	FMNH	Philippines:
bowringii	83488	Mindanao
Subdoluseps	KU	
bowringii	328482	Thailand
Subdoluseps	KU	
bowringii	328483	Thailand
Subdoluseps	KU	
bowringii	328484	Thailand
Subdoluseps	KU	
bowringii	328485	Thailand
Subdoluseps	KU	
bowringii	328486	Thailand
Subdoluseps	MCZ	
bowringii	16666	Thailand
Subdoluseps	MCZ	
bowringii	16667	Thailand
Subdoluseps	MCZ	
bowringii	222214	Vietnam
Subdoluseps	MCZ	
bowringii	222215	Vietnam
Subdoluseps	MCZ	
bowringii	258372	Cambodia
Subdoluseps	MCZ	
bowringii	258373	Cambodia
Subdoluseps	MCZ	Indonesia:
bowringii	268478	Sulawesi
Subdoluseps	MCZ	Indonesia:
bowringii	268480	Sulawesi
Subdoluseps	MCZ	Indonesia:
bowringii	268482	Sulawesi
Subdoluseps	MCZ	Indonesia:
bowringii	268484	Sulawesi
Subdoluseps		Philippines:
bowringii	PNM 9827	Palawan
Subdoluseps		Philippines:
bowringii	PNM 9828	Palawan
Subdoluseps		Philippines:
bowringii	PNM 9829	Palawan
Subdoluseps		Philippines:
bowringii	PNM 9830	Palawan
Subdoluseps	USNM	
bowringii	163808	Vietnam
Subdoluseps	USNM	
bowringii	164381	Vietnam

Subdoluseps bowringii	USNM 43575	Indonesia: Java
Subdoluseps bowringii	USNM 53496	Thailand
Subdoluseps bowringii	USNM 72279	Thailand
Subdoluseps bowringii	USNM 84858	Thailand
Subdoluseps bowringii	ZMKU 612	Thailand
Subdoluseps bowringii	ZMKU 712	Thailand
Subdoluseps bowringii	ZMKU 713	Thailand
Subdoluseps bowringii	ZMKU 714	Thailand
Subdoluseps bowringii	ZMKU 715	Thailand
Subdoluseps frontoparietale	AA 1908	Thailand
Subdoluseps frontoparietale	AA 1911	Thailand
Subdoluseps frontoparietale	ZMKU 705	Thailand
Subdoluseps frontoparietale	ZMKU 706	Thailand
Subdoluseps herberti	FMNH 176974	Thailand
Subdoluseps herberti	FMNH 176975	Thailand
Subdoluseps herberti	FMNH 176976	Thailand
Subdoluseps herberti	USNM 76076	Thailand
Subdoluseps herberti	USNM 76148	Thailand
Subdoluseps pruthi	CES 09/905	India
Subdoluseps samajaya	CAS 259777	Malaysia: Borneo
Subdoluseps samajaya	UNIMAS 9503	Malaysia: Borneo

Table S3: Table with values (minimum–maximum) for mensural, meristic and qualitative characters for each species in *Lygosoma*, *Mochlus*, *Riopa*, and *Subdoluseps* **gen. nov** included in our morphological dataset. Means and standard deviations for mensural characters are shown in parentheses when the number of samples included is three or higher. Measurements and counts for juveniles and individuals suspected of being misidentified are excluded from this table. SVL=snout–vent length, AGD=axilla–groin distance, MBW=mid-body width, TL=tail length, TW=tail width, HL=head length, HW=head width, HD=head depth, END=eye–nares distance, SNL=snout length, IND=internarial distance, MBSRC=mid-body scale row count, PVSRC=paravertebral scale row count, FinIIILam=Finger-III lamellae, ToeIVLam=Toe-IV lamellae, SuprL=supralabials, InfrL=infralabials, SO=supraocculars, SC=supercilliaries. Definitions of each character are found in the text.

LYGOSOMA	*kinabatanganense* (n=1)	*corpulentum* (n=1)	*isodactylum* (n=1)	*koratense* (n=2)	*quadrupes* (n=8)
SVL (mm)	166.0	168.0	107.0	112.0–129.0	51.0–78.0 (65.1 ± 10.3)
AGD/SVL (%)	53.0	57.7	72.0	49.0–60.5	70.6–82.4 (75.8 ± 3.8)
MBW (mm)	23.5	21.5	9.0	18.4–18.5	3.1–5.7 (4.5 ± 0.9)
MBW/SVL (%)	14.2	12.8	8.4	14.2–16.6	5.1–8.3 (6.9 ± 1.0)
TL (mm)	NA	NA	NA	90–109	36.0–72.0 (54.0 ± 12.7)
TL/SVL (%)	NA	NA	NA	80.4–84.5	66.7–105.9 (73.0 ± 32.6)
TW (mm)	18.2	15.8	5.5	13.3–14.6	2.2–4.1 (3.4 ± 0.7)
TW/MBW (%)	77.3	73.5	61.6	71.6–79.5	54.1–95.5 (75.6 ± 11.9)
HL (mm)	17.7	18.0	8.3	12.8–15.7	3.9–5.6 (4.6 ± 0.6)
HL/SVL (%)	10.7	10.7	7.7	11.4–12.1	6.4–8.4 (7.1 ± 0.7)
HW (mm)	18.1	17.5	7.7	12.9–14.5	3.3–5.2 (4.4 ± 0.6)
HW/MBW (%)	77.0	81.4	86.3	69.3–79.1	83.2–116.0 (99.6 ± 10.5)
HD (mm)	16.7	14.3	5.2	9.0–11.7	2.9–4.1 (3.5 ± 0.5)
END (mm)	5.9	5.1	2.5	4.6–4.7	1.2–1.8 (1.6 ± 0.2)
SNL (mm)	8.7	7.5	4.3	6.6–7.2	1.9–2.9 (2.4 ± 0.4)
IND (mm)	5.2	4.3	1.9	3.6–3.8	0.9–1.5 (1.2 ± 0.2)
MBSRC	40	38	32	31–33	25–26
AGSRC	57	55	77	39–46	90–101
PVSRC	113	84	102	64–70	114–121
Fin3Lam	11	9	9	9	4–7
Toe4Lam	15	13	12	13	6–7
SuprL	7	6	7	6–7	6–7
InfrL	7	5	6	6	5–6
SO	4	4	4	4	4
SC	7	7	7	6–7	7
contact of supranasal scales	+	+	–	+	+/–
contact of prefrontal scales	–	–	–	–	–
frontoparietal scales	paired	paired	single	paired	single
contact of parietal scales	+	+	+	+	+
enlarged nuchal scales	–	–	–	–	+/–
contact of 1st chin shields	+	+	+	+	+
enlarged 3rd chin shields	–	–	–	–	–
lower eyelid	scaly	scaly	scaly	scaly	scaly

LYGOSOMA	*siamense* (n=19)	*tabonorum* (n=15)
SVL (mm)	49.0–79.0 (61.1 ± 7.7)	58–79 (67.7 ± 5.9)
AGD/SVL (%)	62.0–79.0 (73.1 ± 6.5)	63.3–93.3 (75.3 ± 7.1)
MBW (mm)	3.0–4.8 (4.0 ± 0.5)	3.8–6.1 (4.7 ± 0.6)
MBW/SVL (%)	5.0–7.8 (6.5 ± 0.7)	5.7–8.7 (7.0 ± 0.9)
TL (mm)	34–74 (57.8 ± 12.3)	47–72 (63.9 ± 7.7)
TL/SVL (%)	54.8 –124.5 (99.3 ± 22.7)	80.9–117.2 (99.3 ± 10.9)
TW (mm)	2.3–4.3 (2.0 ± 0.5)	3.1–4.3 (3.6 ± 0.3)
TW/MBW (%)	63.7–94.7 (75.6 ± 7.7)	62.2–92.8 (76.8 ± 8.8)
HL (mm)	3.4–5.1 (4.2 ± 0.5)	4.1–5.6 (5.0 ± 0.5)
HL/SVL (%)	5.4–8.2 (6.9 ± 0.8)	6.0–8.3 (7.4 ± 0.8)
HW (mm)	3.2–5.3 (3.9 ± 0.5)	3.9–4.9 (4.5 ± 0.3)
HW/MBW (%)	75.7–116.4 (97.5 ± 8.6)	74.2–118.8 (97.5 ± 13.6)
HD (mm)	2.3–3.6 (3.0 ± 0.4)	3.1–3.8 (3.4 ± 0.2)
END (mm)	1.1–1.6 (1.4 ± 0.1)	1.3–2.0 (1.6 ± 0.2)
SNL (mm)	1.5–2.4 (2.0 ± 0.2)	2.1–3.0 (2.4 ± 0.3)
IND (mm)	0.9–1.3 (1.1 ± 0.1)	1.1–1.5 (1.4 ± 0.1)
MBSRC	26–28	25–26
AGSRC	88–98	83–90
PVSRC	114–123	106–111
Fin3Lam	4–7	5–6
Toe4Lam	5–7	6–7
SuprL	6–7	6–7
InfrL	5–6	6
SO	4	4
SC	6–8	5–6
contact of supranasal scales	–	–
contact of prefrontal scales	–	–
frontoparietal scales	single	single
contact of parietal scales	+	+
enlarged nuchal scales	+/–	+/–
contact of 1st chin shields	+	+/–
enlarged 3rd chin shields	–	–
lower eyelid	scaly	scaly

MOCHLUS	*brevicaudis* (n=4)	*sundevallii* (n=49)	*pembanus* (n=5)	*tanae* (n=2)
SVL (mm)	55.064.0 (61.5 ± 4.5)	56.0–126.0 (89.6 ± 20.2)	40.0–64.0 (50.0 ± 11.0)	89.0–90.0
AGD/SVL (%)	43.8–64.5 (58.2 ± 4.6)	47.4–82.5 (64.7 ± 6.5)	55.0–72.5 (65.2 ± 7.2)	60.7–70.4
MBW (mm)	7.8–10.5 (8.9 ± 1.2)	7.6–16.3 (11.8 ± 2.4)	5.5–8.0 (6.7 ± 1.0)	11.6–15.2
MBW/SVL (%)	12.7–16.9 (14.5 ± 1.7)	10.9–18.0 (13.4 ± 1.3)	11.5–16.5 (13.6 ± 2.1)	13.0–16.9
TL (mm)	NA	39.097.0 (64.8 ± 14.9)	35–56 (43.8 ± 9.4)	NA
TL/SVL (%)	NA	51.3–110.8 (73.2 ± 15.2)	87.5–97.9 (93.8 ± 4.4)	NA
TW (mm)	6.4–7.2 (6.8 ± 0.4)	4.9–12.3 (8.6 ± 2.0)	4.0–6.5 (4.8 ± 0.7)	8.4–10.2
TW/MBW (%)	68.5–82.8 (76.3 ± 5.9)	61.2–86.2 (72.2 ± 6.6)	60.7–99.5 (77.6 ± 15.8)	67.3–72.8
HL (mm)	7.4–7.7 (7.6 ± 0.2)	6.1–13.9 (9.3 ± 2.0)	5.1–7.0 (6.1 ± 0.8)	10.4–10.9
HL/SVL (%)	11.8–13.4 (12.4 ± 0.8)	8.2–13.2 (10.5 ± 1.2)	10.9–13.9 (12.4 ± 1.1)	11.7–12.1
HW (mm)	7.1–8.9 (8.04 ± 0.8)	6.0–12.1 (8.9 ± 1.7)	4.5–6.6 (5.4 ± 0.9)	10.5–12.3
HW/MBW (%)	85.2–95.3 (90.4 ± 0.4)	59.8–92.4 (75.9 ± 6.6)	68.7–92.9 (81.2 ± 8.9)	81.2–90.8
HD (mm)	5.6–7.0 (6.3 ± 0.6)	4.7–11.0 (7.3 ± 1.6)	3.8–5.6 (4.7 ± 0.8)	7.7–10.0
END (mm)	1.6–2.9 (2.4 ± 0.6)	2.0–4.5 (3.1 ± 0.6)	1.4–2.4 (1.8 ± 0.4)	3.3–3.6
SNL (mm)	3.7–4.5 (4.0 ± 0.4)	2.9–7.1 (4.9 ± 1.0)	2.6–3.4 (3.0 ± 0.3)	5.3
IND (mm)	2.1–2.3 (2.2 ± 0.1)	1.7–3.1 (2.4 ± 0.4)	1.4–1.9 (1.7 ± 0.2)	2.9
MBSRC	27–28	24–30	24	23
AGSRC	36–42	43–60	41–44	52–56
PVSRC	61–64	65–78	59–65	70–73
Fin3Lam	8–9	7–10	6–7	9
Toe4Lam	10–11	10–15	9–12	12
SuprL	6–7	5–7	6	6
InfrL	6	6–7	6	7
SO	4	4	4	4
SC	6–8	6–8	6–7	NA
contact of supranasal scales	+	+	+	+
contact of prefrontal scales	–	+//fused with frontonasal	fused with frontonasal	–
frontoparietal scales	paired	paired	paired	paired
contact of parietal scales	+	+/–	+	–
enlarged nuchal scales	–	+/–	–	–
contact of 1st chin shields	+	+/–	+	+
enlarged 3rd chin shields	–	–	–	–
lower eyelid	scaly	scaly	scaly	scaly

RIOPA	*albopunctata* (n=5)	*anguina* (n=9)	*goaensis* (n=1)	*guentheri* (n=3)	*lineata* (n=1)
SVL (mm)	35.0–48.0 (41.2 ± 6.3)	50–58 (54.0 ± 2.8)	49.0	77–96 (87.0 ± 9.5)	57.0
AGD/SVL (%)	57.1–71.4 (62.0 ± 5.8)	63.2–73.7 (69.8 ± 3.1)	54.6	70.8–76.3 (73.7 ± 2.7)	82.1
MBW (mm)	3.4–6.4 (4.8 ± 1.3)	3.7–5.0 (4.5 ± 0.5)	7.5	8.5–9.6 (9.1 ± 0.6)	3.9
MBW/SVL (%)	7.2–14.0 (11.7 ± 2.7)	7.2–9.3 (8.3 ± 0.8)	15.4	10.0–11.0 (10.4 ± 0.5)	6.8
TL (mm)	33–37 (35.0 ± 2.9)	46–65 (53.3 ± 7.9)	48.0	107	NA
TL/SVL (%)	80.5–105.7 *=(93.1 ± 17.8)	82.5–120.4 (101.2 ± 16.2)	98.7	111.5	NA
TW (mm)	2.6–4.4 (3.6 ± 0.7)	2.5–3.9 (3.2 ± 0.5)	3.9	5.3–7.0 (6.2 ± 0.8)	2.9
TW/MBW (%)	65.8–106.2 (78.8 ± 17.6)	57.5–76.4 (71.2 ± 6.8)	52.1	62.4–76.6 (68.3 ± 7.3)	75.0
HL (mm)	4.2–6.6 (5.1 ± 1.0)	3.7–5.6 (4.6 ± 0.7)	9.7	7.2–9.1 (8.1 ± 0.9)	4.6
HL/SVL (%)	11.4–13.8 (12.3 ± 0.9)	7.0–9.9 (8.5 ± 1.1)	20.0	8.2–11.7 (9.4 ± 2.0)	8.1
HW (mm)	3.9–6.2 (4.8 ± 0.9)	3.6–4.7 (4.1 ± 0.3)	6.2	7.0–7.5 (7.3 ± 0.3)	3.8
HW/MBW (%)	85.8–138.5 (104.6 ± 20.0)	79.4–97.6 (91.0 ± 7.6)	83.2	78.3–82.1 (80.1 ± 1.9)	95.9
HD (mm)	3.1–4.4 (3.9 ± 0.5)	2.7–3.7 (3.1 ± 0.4)	4.3	4.9–5.6	2.1
END (mm)	1.4–2.0 (1.7 ± 0.2)	1.4–1.7 (1.6 ± 0.1)	3.3	2.5–2.9 (2.7 ± 0.2)	1.5
SNL (mm)	2.0–3.5 (2.7 ± 0.5)	1.9–2.8 (2.3 ± 0.3)	3.9	3.6–4.4 (3.9 ± 0.4)	2.1
IND (mm)	1.2–1.7 (1.3 ± 0.2)	1.0–1.4 (1.2 ± 0.2)	2.0	1.9–2.0 (1.9± 0.1)	0.9
MBSRC	27–29	20–25	30	25–26	19
AGSRC	37–55	64–77	46	72–76	89
PVSRC	59–71	86–99	58	93–98	107
Fin3Lam	7–10	5–8	10	7–8	7
Toe4Lam	13–16	7–9	15	12	8
SuprL	6–7	7	7	6–7	5
InfrL	5–6	5–6	7	6	5
SO	4–5	4	4	4	4
SC	7	6–7	NA	6–7	6
contact of supranasal scales	+	+/	NA	+	+
contact of prefrontal scales	–		–	–	–
frontoparietal scales	paired	single or paired	paired	paired	single
contact of parietal scales	+	+	+	+	+
enlarged nuchal scales	+/–	+/–	+	–	–
contact of 1st chin shields	+/–	+	+	+	+
enlarged 3rd chin shields	–	–	–	–	
lower eyelid	transp. disc	transp. disc	transp. disc	transp. disc	transp. disc

RIOPA	*lineolata* (n=16)	*popae* (n=9)	*punctata* (n=1)	*vosmaerii* (n=1)
SVL (mm)	39.0–57.0 (48.8 ± 4.8)	46.0–57.0 (51.6 ± 4.3)	45.0	50
AGD/SVL (%)	56.8–76.1 (67.5 ± 5.1)	63.5–76.1 (69.3 ± 4.4)	68.8	75.9
MBW (mm)	3.3–5.7 (4.6 ± 0.6)	3.8–6.1 (4.8 ± 0.7)	6.6	3.2
MBW/SVL (%)	8.4–10.2 (9.4 ± 0.5)	8.0–10.8 (9.2 ± 1.0)	14.8	6.4
TL (mm)	37.0–60.0 (52.7 ± 8.6)	NA	NA	NA
TL/SVL (%)	70.4–128.3 (110.9 ± 21.9)	NA	NA	NA
TW (mm)	2.4–4.0 (3.1 ± 0.4)	2.8–4.0 (3.3 ± 0.4)	4.1	2.0
TW/MBW (%)	46.7–83.9 (68.8 ± 10.1)	58.9–80.4 (70.0 ± 8.0)	62.7	63.5
HL (mm)	4.0–5.5 (4.7 ± 0.5)	3.4–4.9 (4.4 ± 0.5)	8.0	4.1
HL/SVL (%)	8.2–12.1 (9.7 ± 1.2)	7.3–10.2 (8.5 ± 0.9)	18.0	8.4
HW (mm)	3.4–4.4 (3.9 ± 0.3)	3.6–4.6 (4.1 ± 0.3)	6.6	3.6
HW/MBW (%)	62.3–103.4 (87.5 ± 10.2)	73.4–96.6 (86.4 ± 7.0)	100.5	114.5
HD (mm)	2.6–3.3 (3.0 ± 0.2)	2.8–3.5 (3.1 ± 0.3)	5.1	2.1
END (mm)	1.2–1.9 (1.6 ± 0.2)	1.3–1.6 (1.5 ± 0.1)	2.0	1.5
SNL (mm)	1.6–2.4 (2.1 ± 0.2)	1.3–2.3 (2.1 ± 0.1)	2.8	2.2
IND (mm)	0.9–1.3 (1.2 ± 0.1)	1.0–1.3 (1.1 ± 0.1)	1.5	1.3
MBSRC	20–24	24–26	24	23
AGSRC	55–71	68–72	52	93
PVSRC	78–93	90–96	70	114
Fin3Lam	6–9	5–7	11	6
Toe4Lam	9–14	8–9	13	7
SuprL	6–7	7	7	6
InfrL	6–7	6	5	6
SO	4	4	4	5
SC	6–8	6–7	7	7
contact of supranasal scales	+/–	+	+	+
contact of prefrontal scales	–	+/–	–	–
frontoparietal scales	single or paired	single or paired	paired	single
contact of parietal scales	+	+	+	+
enlarged nuchal scales	+/–	+/–	–	–
contact of 1st chin shields	+	+	+	–
enlarged 3rd chin shields	–	–	–	–
lower eyelid	transp. disc	transp. disc	transp. disc	transp. disc

SUBDOLUSEPS	*bowringii* (n=74)	*frontoparietalis* (n=2)	*herberti* (n=4)	*pruthi* (n=1)	*samajaya* (n=2)
SVL (mm)	40.0–64.0 (47.7 ± 5.3)	36.0–43.0	59–64 (61.3 ± 2.2)	46.0	70.0
AGD/SVL (%)	41.7–68.9 (58.8 ± 5.1)	55.6–60.5	55.0–61.0 (58.0 ± 2.5)	68.5	40.0–43.0
MBW (mm)	4.6–10.0 (6.8 ± 1.2)	5.6–7.0	8.2–9.4 (8.9 ± 0.6)	8.7	9.6
MBW/SVL (%)	10.0–17.7 (14.2 ±1.8)–	15.5–16.3	13.3–15.8 (14.5 ± 1.4)	18.8	13.7
TL (mm)	27.0–89.0 (46.0 ± 12.6)	47.0–54.0	NA	NA	67.0
TL/SVL (%)	59.6–100.2 (98.6 ± 25.5)	125.6–130.6	NA	NA	96.4
TW (mm)	3.0–6.2 (4.3 ± 0.6)	3.4–3.7	5.4–6.8 (5.9 ± 0.5)	4.4	6.7–7.2
TW/MBW (%)	41.2–85.0 (63.9 ± 9.1)	52.5–60.8	57.8–72.3 (66.5 ± 6.3)	49.9	69.8
HL (mm)	5.0–7.8 (6.3 ± 0.6)	5.5–6.1	6.8–8.8 (7.7 ± 0.9)	7.9	10.8–11.0
HL/SVL (%)	10.8–16.1 (13.2 ± 1.2)	14.2–15.3	11.2–14.7 (12.6 ± 1.6)	17.0	15.5–15.7
HW (mm)	4.5–7.3 (5.7 ± 0.6)	4.5–6.0	7.5–8.4 (8.0 ± 0.4)	5.9	7.9–9.0
HW/MBW (%)	64.8–111.3 (85.5 ± 10.4)	80.6–85.2	85.5–99.0 (90.2 ± 6.0)	67.5	93.8
HD (mm)	3.2–5.9 (4.3 ± 0.6)	3.5–3.7	5.1–6.2 (5.7 ± 0.4)	4.8	4.5–4.8
END (mm)	1.6–3.2 (2.2 ± 0.3)	NA	2.7–2.8 (2.7 ± 0.1)	2.4	2.9–3.1
SNL (mm)	1.8–3.9 (3.0 ± 0.4)	NA	3.5–4.4 (4.0 ± 0.4)	3.4	4.2–4.7
IND (mm)	1.2–1.9 (1.5 ± 0.2)	1.3–1.5	2.1–2.3 (2.2 ± 0.1)	1.6	2.4–2.8
MBSRC	26–31	28–29	27	32	28–30
AGSRC	33–46	40–41	35–37	47	36
PVSRC	51–69	60	54–58	60	60–61
Fin3Lam	7–12	9–10	9–12	10	10
Toe4Lam	11–16	13–15	14–15	16	13–14
SuprL	5–8	7	6–7	7	7
InfrL	6–7	6	6	6	6
SO	4	4	4	4–5	4
SC	6–8	5	NA	6	7
contact of supranasal scales	+/–	+	+	–	+
contact of prefrontal scales	–	–	–	–	–
frontoparietal scales	single or paired	single	paired	paired	paired
contact of parietal scales	+/–	+	+	+	+
enlarged nuchal scales	+/–	+	–	+	–
contact of 1st chin shields	+/–	–	+/–	+	+
enlarged 3rd chin shields	+/–	+	–	+	–
lower eyelid	scaly	scaly	scaly	transp. disc	scaly

Chapter 2: A taxonomic conundrum: Characterizing a cryptic radiation of Asian gracile skinks (Squamata: Scincidae: *Riopa*) in Myanmar

Elyse S. Freitas, Aryeh H. Miller, R. Graham Reynolds, Cameron D. Siler

Published in Molecular Phylogenetics and Evolution 2020, 146: 106754

ABSTRACT

Recognizing species-level diversity is important for studying evolutionary patterns across biological disciplines and is critical for conservation efforts. However, challenges remain in delimiting species-level diversity, especially in cryptic radiations where species are genetically divergent but show little morphological differentiation. Using multilocus molecular data, phylogenetic analyses, species delimitation analyses, and morphological data, we examine lineage diversification in a cryptic radiation of *Riopa* skinks in Myanmar. Four species of *Riopa* skinks are currently recognized from Myanmar based on morphological traits, but the boundaries between three of these species, *R. anguina*, *R. lineolata*, and *R. popae* are not well-defined. We find high levels of genetic diversity within these three species, and analyses suggest that they may comprise as many as 12 independently evolving lineages, which highlights the extent to which species diversity in the region is underestimated. However, quantitative trait data suggest that these lineages have not differentiated morphologically, possibly indicating that this cryptic radiation represents non-adaptive evolution, although additional data is needed to corroborate this.

Keywords: bModelTest; Bayesian Phylogenetics and Phylogeography (BPP); cryptic species; principal components analysis; non-ecological diversification; species delimitation

1. Introduction

The species is the fundamental taxonomic unit in characterizing biodiversity (de Queiroz, 2005). Diverse biological research fields, including ecology, developmental biology, genetics, and physiology rely on the accurate identification of species-level lineages to analyze and interpret results (Knowlton and Jackson, 1994; Bickford et al., 2007; Bortolus, 2008). Additionally, accurate species identification is crucial for conservation efforts (e.g. Dubois, 2003; Frankham et al., 2012; Seifan et al., 2016; Garnett and Christidis, 2017; Tantipisanuh and Gale, 2018), with organizations such as the IUCN using data on the distribution, ecology, and demography of recognized species for conservation assessments (IUCN-SSC, 2017).

Nevertheless, despite the fundamental nature of the species-level unit in research and conservation, challenges remain in recognizing entities that constitute species. Historically, species were defined based on morphological characteristics (e.g. Linnaeus, 1758); however, with the advent of molecular phylogenetics and phylogenomics, it has become possible to recognize distinct lineages from genetic data alone. Use of molecular data in species identification over the last three decades has indicated that many widespread species actually comprise multiple genetically divergent morphologically similar cryptic species. Complexes of cryptic species often result from non-ecological speciation, in which diversification is not accompanied by apparent ecological or morphological separation in traditional quantitative traits (Czekanski-Moir and Rundell, 2019). Despite the advance of techniques in molecular-based species identifications, morphology remains a critical component of taxonomy and systematics (Ceríaco et al., 2016); therefore, cryptic radiations present particular challenges for

taxonomists because of the lack of criteria for describing species that do not exhibit clear diagnostic phenotypic characters (Barley et al., 2013). As the number of recognized cases of cryptic speciation increases, many people suggest taking an integrative approach towards describing these new species that incorporates morphological, ecological, demographic, and geographic datasets with phylogenetic evidence (e.g. Bauer et al., 2011; Barley et al., 2013; Sukumaran and Knowles, 2017; Singhal et al., 2018; Denham et al., 2019; Duran et al., 2019; Hillis, 2019). However, these integrative approaches, although ideal, are challenging when there is a paucity of genetic samples for lineages or observational data on a group's habits—a situation particularly manifest in tropical scincid lizards.

Lizards in the Family Scincidae (skinks) are a remarkably successful group of vertebrates, comprising more than 1,600 species (Uetz et al., 2019). Found in tropical and temperate regions on all continents except Antarctica, and on most oceanic islands, skinks have evolved a diverse array of ecologies, including terrestrial, fossorial, arboreal, rupicolous, and aquatic and are a major part of the global herpetofauna (Vitt and Caldwell, 2013). Therefore, recognizing species-level diversity is critical to understanding the evolutionary history of these lizards and the role they play in regional ecosystems. However, there has been historical taxonomic confusion and instability for a number of groups (e.g. Linkem et al., 2011; Brandley et al., 2012; Skinner et al., 2013; Erens et al., 2017; Freitas et al., 2019), driven in part by lack of diagnostic morphological characters for genera. Furthermore, within genera, cryptic and non-adaptive diversification appears common, which complicates efforts to quantify species-level diversity of the family—44 of the 94 new scincid species described between 2014–2019 (Uetz et al., 2019) were considered members of formerly recognized widespread species that subsequently were found to be distinct species based on genetic data (Table S1). These taxonomic revisions highlight broadly generalized and highly conserved external morphologies and body plans across species as contributing to difficulties in recognizing taxonomic boundaries.

Despite this high number of taxonomic revisions over the years, it is likely that underestimated levels of cryptic diversity still exist across the family Scincidae, particularly within poorly studied regions of the globe. Previous phylogenetic explorations of Asian Gracile Skinks (genus *Riopa*) from South and Southeast Asia have suggested that the genus harbors substantial genetic diversity beyond what has been formally recognized taxonomically (Freitas et al., 2019), and we report on this unrecognized diversity here. The genus *Riopa* comprises nine recognized species from Bangladesh, India, Maldives, Myanmar, Nepal, Pakistan, and Sri Lanka (Uetz et al., 2019). Members of the genus are semifossorial with small, gracile, and elongate bodies, found in or among rotting logs, loose soil, leaf litter and rocks in dry–semi-dry forest, grassland, and urban habitats across their range (Das, 2010; Vyas, 2014; Bhattarai et al., 2018; Prasad et al., 2018), although little is known about their natural history in Myanmar (Das, 2010). Long a source of taxonomic confusion due to their lack of diagnostic characters (reviewed in Freitas et al., 2019), *Riopa* recently has been the subject of several revisionary studies which have attempted to elucidate species-level relationships within the genus (Datta-Roy et al., 2014; Freitas et al., 2019). Currently, there are four species of *Riopa* recognized from Myanmar: *R. albopunctata* Gray 1846, *R. anguina* Theobald 1868, *R. lineolata* Stoliczka 1870, and *R. popae* Shreve 1940. Of these, *R. lineolata* and *R. popae* are endemic; *R. albopunctata* was described originally from India but is widespread across southern Asia and is recognized to occur in both countries (Manthey and Grossman, 1997**)**, and *R. anguina*, described originally from Myanmar, also occurs in localities in southwestern Thailand in Prachuap Khiri Khan and Chumphon Provinces (Nabhitabhata et al., 2000; Chan-ard et al., 2015). Historically, the four species from Myanmar have been diagnosed by variation in mensural and meristic characters, including relative limb lengths, midbody scale row count, and coloration (Theobald, 1868; Stoliczka 1870; Shreve 1940; Das, 2010; Geissler et al., 2012; Freitas et al., 2019). However, the considerable overlap in these characters between taxa have made recognizing species

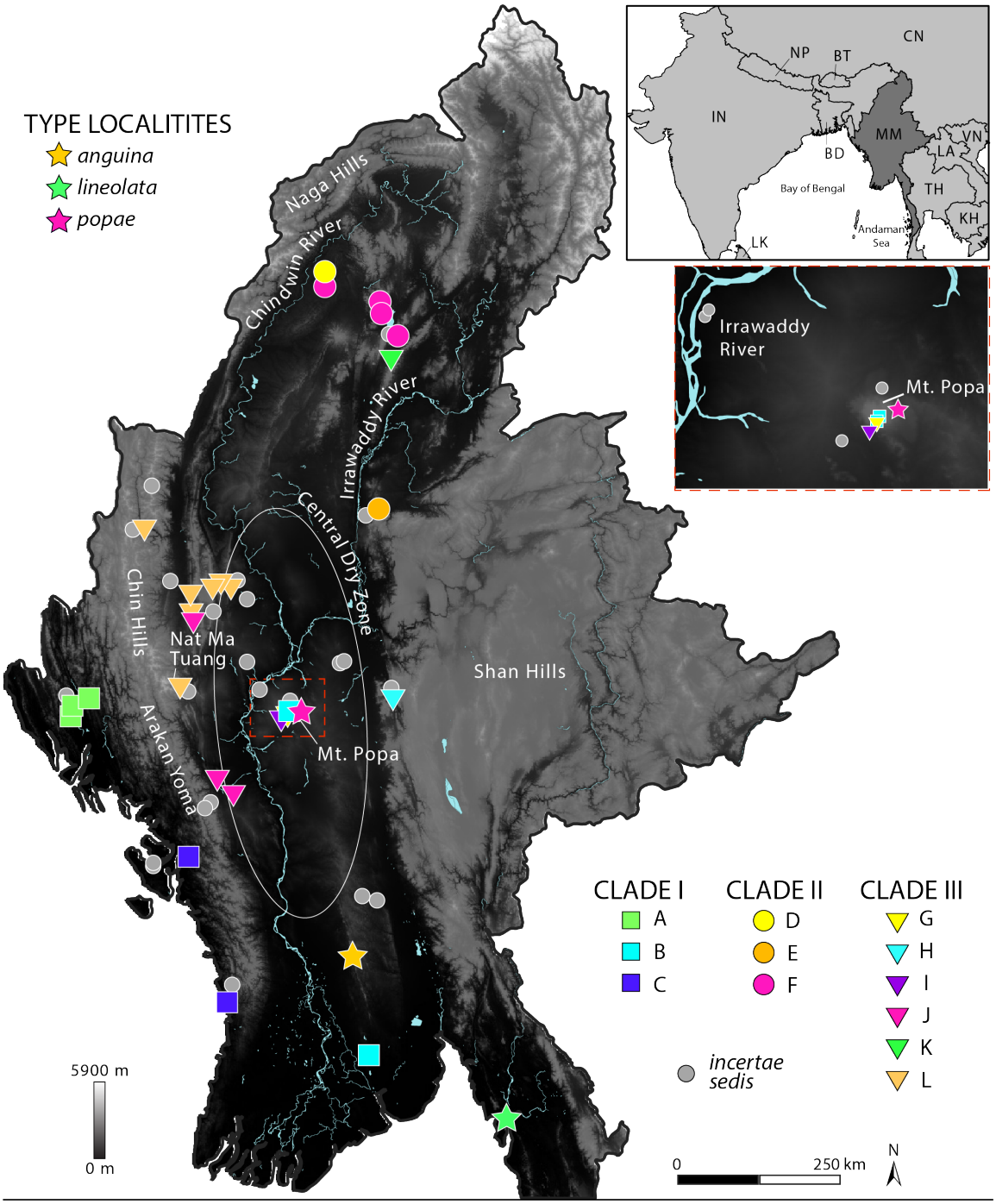

Fig. 1. Map of Myanmar showing localities of specimens and tissues used in this study and the type localities for the three species described from Myanmar. Myanmar is shaded according to elevation, with lighter colors indicating higher elevations. Geographic features mentioned in text are labeled on the map, with the exception of the Central Myanmar Basin, which comprises the low elevation region between the Indo-Myanmar Range in the west (Naga Hills, Chin Hills, Arakan Yoma) and Shan Hills in the east. The lower right inset shows the closeup of sampling around Mount Popa, the type locality of *Riopa popae*. The upper right inset shows the location of Myanmar in South and Southeast Asia, with the countries labeled according to their two letter ISO 3166-1 alpha-2 country codes: BD = Bangladesh, BT = Bhutan, CN = China, IN = India, KH = Cambodia, LA = Laos, LK = Sri Lanka, MM = Myanmar, NP = Nepal, TH = Thailand, VN = Vietnam.

boundaries difficult (Jayaram, 1949; Vyas 2001, 2010; Seetharamaraju et al., 2009; Srinivasulu and Seetharamaraju, 2010).

Myanmar is located in Southeast Asia, bordered by India and Bangladesh in the northwest, the Bay of Bengal and the Andaman Sea in the southwest, China and Laos in the northeast, and Thailand in the southeast (Fig. 1). The country is diverse ecologically, varying in habitat type and abiotic factors such as elevation, temperature and precipitation (Fig. 2). Although Myanmar and the surrounding region were not initially identified as a biodiversity hotspot (Myers, 1988, 1990), over the past three decades there has been an increase in recognized species-level biodiversity in the region, prompting its classification as the Indo-Burma Biodiversity Hotspot (Mittermeier et al., 1999; Myers et al., 2000). During the last five years alone, expeditions across Myanmar have discovered large amounts of population- and species-level diversity among major vertebrate groups and has resulted in the description of 65 new species: ten species of amphibian,17 species of fish, two species of mammal, and 36 species of reptile (Table S2). However, the level of unrecognized and cryptic diversity within scincid lizards in Myanmar remains poorly understood. In this paper, we use multilocus coalescent-based species delimitation methods and multivariate analyses of morphological data to illustrate that species diversity within the genus *Riopa* in Myanmar is greatly underestimated. The results of our study suggest that the genus has undergone significant lineage diversification with little discernable divergence in external morphology. These levels of potential cryptic species diversity affect our understanding of the evolutionary, biogeographic, and ecological patterns of vertebrate diversification within the country.

2. Materials and methods

2.1. Taxon sampling and molecular methods

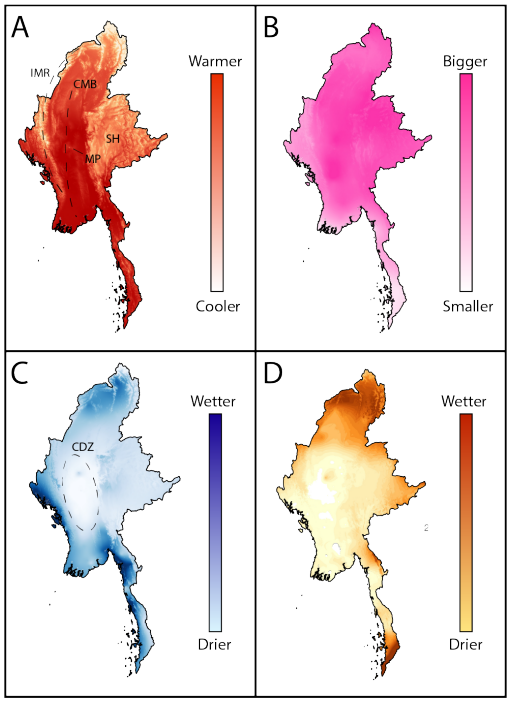

Fig. 2. Maps of Myanmar showing different abiotic gradients: A) Mean annual temperature; B) Difference between the mean annual high temperature and the mean annual low temperature; C) Mean annual precipitation; and D) Precipitation of the driest month. Abbreviations for geographic features mentioned in text: CMB = Central Myanmar Basin, CDZ = Central Dry Zone, IMR = Indo-Myanmar Range, MP = Mount Popa, SH = Shan Hills.

Ingroup sampling comprised 41 individuals of *Riopa* from central and northern Myanmar (Fig. 1) identified in museum collections as *R. anguina* (18 individuals), *R. bowringii* (three individuals), *R. lineolata* (nine individuals), *R. popae* (five individuals), and *R.* sp. (six individuals) (Table S3). Several samples were obtained from Mount Popa, the type locality of *R. popae*, and Bago and Yangoon provinces, the approximate type locality of *R. anguina*; however, we did not obtain samples from the type locality of *R. lineolata*, which is farther south in Mon State (Fig. 1). Outgroup sampling included sequences from seven members of three closely related genera obtained from GenBank: *Lygosoma quadrupes*, *Mochlus brevicaudis*, *M. guineensis*, *M. sundevallii*, *Subdoluseps bowringii*, *S. herberti*, and *S. samajaya*, and one additional species from the genus *Riopa*, *R. albopunctata*, shown previously to be the sister species to Myanmar *Riopa* (Freitas et al., 2019; Table S3). Tissue samples were provided by the following institutions (museum acronyms follow Sabaj [2016]): California Academy of Science (CAS), La Sierra University Herpetology Collection (LSUHC), Museum of Vertebrate Zoology (MVZ), and Villanova University. Genomic DNA was extracted from ethanol-preserved liver, muscle, or tail tissue using a high-salt extraction method (Aljanabi and Martinez, 1997) or the Wizard SV© Genomic DNA Purification System (Promega). Extracts were amplified via PCR in 10 μL reactions following

standard protocols (Siler et al., 2011; Freitas et al., 2019) for three nuclear DNA (nuDNA) loci and three mitochondrial DNA (mtDNA) genes. Nuclear loci comprised brain-derived neurotrophic factor (*BDNF*; 690 base pairs [bp]), RNA fingerprint protein 35 (*R35*; 662 bp), and recombination activating gene 1 (*RAG1*; 891 bp); mtDNA genes comprised NADH dehydrogenase subunit 1 (*ND1*; 966 bp) and subunit 2 (*ND2*; 1032 bp), and 16S ribosomal RNA (*16S*; 535 bp; Table 1). PCR products were purified by ExoSAP-IT (ThermoFisher Scientific), sequenced with BigDye® Terminator v3.1 sequencing kit (ThermoFisher Scientific) and cleaned using ethanol precipitation. We sent sequencing products to Eurofins Genomics in Louisville, Kentucky or the Genomic Sciences Laboratory at North Carolina State University for visualization. All novel sequences were deposited in GenBank (Table S3).

2.2. Sequence alignment and phylogenetic analyses

Raw sequences were imported into Geneious v10.2.4 (Biomatters, Ltd.), assembled into contigs, and checked for quality. All nuDNA contigs were examined for miscalled heterozygous sites. Once we were satisfied with data quality, we trimmed the primer binding sites from both ends of each contig and aligned contigs using MUSCLE (Edgar, 2004) in Geneious with default settings. Alignments were checked by eye for misplaced indels and, for all coding genes (all genes except *16S*), erroneous internal stop codons.

We ran preliminary Maximum Likelihood (ML) analyses in RAxML v8.2.12 (Stamatakis, 2014) on each nuDNA gene separately and on the concatenated mtDNA dataset to check for discordance between loci. For ML analyses, *16S* was analyzed as a single partition and nuDNA and mtDNA protein coding genes were partitioned by codon position, and the substitution model GTR+Γ was applied to each partition. Topological support was assessed by 100 bootstrap

Table 1
The primers, primer sequences, and annealing temperatures used in this study.

Gene	Primer	Sequence (5'–3')	Annealing Temp (ºC)	Reference
BDNF	BDNF.F	GACCATCCTTTTCCTKACTATGGTTATTTCATACTT	61	Leaché &McGuire, 2006
	BDNF.R	CTATCTTCCCCTTTTAATGGTCAGTGTACAAAC		
R35	R35.F	GACTGTGGAYGAYCTGATCAGTGTGG	55	Fry et al., 2006
	R35.R	GCCAAAATGAGSGAGAARCGCTTCTG		
RAG1	RAG1.R13	TCTGCTGTTAATGGAAATTCAAG	53	Adapted from Groth & Barrowclough, 1999 by unknown
	RAG1.R13.rev	AAAGCAAGGATAGCGACAAGAG		
ND1	16dR	CTACGTGATCTGAGTTCAGACCGGAG	53	Leaché & Reeder, 2002
	tMet	TCGGGGTATGGGCCCRARAGCTT		
ND2	ND2_L4437	AAGCTTTCGGGCCCATACC	53	Macey et al., 1997
	ND2_H5730	AGCGAATRGAAGCCCGCTGG		
16S	16Sar-L	CGCCTGTTTATCAAAAACAT	46	Palumbi et al., 1991
	16Sbr-H	CCGGTCTGAACTCAGATCACGT		

pseudoreplicates. Results of these analyses showed no incongruence between the mtDNA and nuDNA topologies; therefore, we conducted additional partitioned, phylogenetic analyses on a concatenated nuDNA + mtDNA dataset.

We used BEAST v2.5.1 (Bouckaert et al., 2014) to conduct a Bayesian phylogenetic analysis on our concatenated dataset, employing the package bModelTest v1.1.2 (Bouckaert and Drummond, 2017) to calculate the best substitution model for each partition. This approach estimates the phylogeny and the substitution models jointly using a reversible jump Monte Carlo Markov Chain (rjMCMC) algorithm, which allows the chain to analyze substitution models with different numbers of parameters (Bouckaert and Drummond, 2017). We limited our rjMCMC search to models containing different transition-transversion rates for computational efficiency, which includes the Jukes-Cantor model where all rates are equal, the GTR model where all rates are different, and all models where the rate of transitions is different from the rate of transversions—a total of 31 models (Bouckaert and Drummond, 2017). Although bModeltTest can search for the best substitution model for each partition, it requires *a priori* selection of the partitioning scheme. Therefore, like the ML single gene analyses, we partitioned our data by codon position, with the exception of *16S*, which was treated as a single partition. The analysis was run using a relaxed lognormal molecular clock with default priors and a Yule Speciation model with default priors. We applied separate molecular clocks and tree models for the mtDNA and nuDNA. We conducted two runs of 100,000,000 generations each sampling every 10,000 generations using the CIPRES Science Gateway (Miller et al., 2010). The results of these two analyses were examined separately and together in Tracer v1.7.1 (Rambaut et al., 2018) and RWTY v1.0.1 (Warren et al., 2017) in R v3.5.0 (R Core Team, 2018) to assess stationarity and convergence, determined by ESS values above 200 for parameters and runs sampling the same

regions of tree space in RWTY. The RWTY analyses were run using the command analyze.rwty. Convergence of most parameters occurred after 10,000,000 generations, and so we discarded the first 10% of each run as burnin. We combined the BEAST2 bModelTest analyses in LogCombiner v2.5.1 (Bouckaert et al., 2014), discarding the first 10% of trees in each posterior distribution as burnin (observed as appropriate for cutoff, see above). The output had 18,002 trees in the combined posterior distribution of the final two runs. We used TreeAnnotator v2.5.1 (Bouckaert et al., 2014) to select the maximum clade credibility tree and calculated the posterior probability of each bifurcation.

2.3. Putative lineage identification

The coalescent-based species delimitation program Bayesian Phylogenetics and Phylogeography (BPP), used to delimit species within Myanmar *Riopa* (see below), requires input of putative species-level lineages *a priori* to the analysis. BPP then tests these lineages and determines whether they warrant species-level recognition. Because specimen morphology gives few clues to the species-level identity of each individual, we used barcoding distance thresholds and the Bayesian species delimitation program bGMYC (Reid and Carstens, 2012) to determine lineages objectively within Myanmar *Riopa*. These methods determine groups of samples that can then be used as hypotheses for species assignment in BPP. We implemented barcoding distance thresholds and bGMYC on our *ND2* ingroup data. As a mtDNA gene, *ND2* has a higher mutation rate than nuDNA loci (Vawter and Brown, 1986), making it useful for detecting structure at shallow nodes in our topology. Additionally, we chose to use *ND2* for species discovery because this gene had the most complete dataset of all our mtDNA markers (Table S3).

The barcoding distance threshold method clusters sequences based on a genetic threshold value determined by the barcoding gap, which is the numerical value not represented in a dataset of pairwise genetic distances, and thus a value that represents the gap between intra- and interspecific genetic diversity (Meyer and Paulay, 2005). Although this approach to lineage identification is purely distance-based and does not account for evolutionary processes, it is useful for identifying monophyletic genetic clusters that serve as *a priori* hypotheses of conspecificity within a set of samples. To implement the barcoding distance threshold method, we first calculated the uncorrected pairwise distance for ND2 (Table 2; S4) using the command dist.dna in the R package ape v5.2 (Paradis and Schliep, 2018), and then used these distances to identify the barcoding gap with the command localMinima in the R package Spider v1.5.0 (Brown et al., 2012) with the barcoding gap corresponding to the lowest local minimum as determined by plotting the distances using the command plot. We then determined the number of genetic clusters by setting the barcoding gap as the maximum intraspecific genetic diversity threshold with the command tclust in Spider.

In addition to the barcoding distance threshold method, we used the species delimitation program bGMYC to determine species-level lineages. BGMYC is the Bayesian implementation of GMYC (Pons et al., 2006), which uses the general mixed Yule coalescent model to estimate divergence events on a topology. The program bGMYC goes a step farther, in that it uses the general mixed Yule coalescent model to estimate divergent events on a posterior distribution of topologies, allowing it to incorporate phylogenetic uncertainty into its lineage assignment hypotheses and generate probabilities of conspecificity. Although the program has been used previously in species delimitation studies to identify species-level lineages, it was shown in

Table 2
The uncorrected pairwise distance for the mitochondrial gene *ND2* for all lineages recovered in barcoding distance thresholds lineage discovery method. The intra-lineage distances are bolded. Distances between lineages within each of the three major clades are highlighted in gray: Clade I=light gray; Clade II=medium gray; Clade III =dark gray.

	Lineage A n=3	**Lineage B n=3**	**Lineage C n=6**	**Lineage D n=1**	**Lineage E n=1**	**Lineage F n=6**
Lineage A	**0.0–0.3**					
Lineage B	10.4–11.1	**0.0–4.7**				
Lineage C	9.0–9.6	7.8–9.2	**0.5–6.1**			
Lineage D	11.1–11.4	12.4–13.4	10.8–12.7	**NA**		
Lineage E	11.8	12.8–13.6	11.6–12.4	8.7	**NA**	
Lineage F	11.3–11.7	11.7–13.1	9.6–12.4	8.5–8.7	9.0–9.2	**0.0–0.5**
Lineage G	12.5–12.8	11.1–13.1	10.4–12.8	13.7	13.4	12.5–12.8
Lineage H	12.7	12.4–13.4	11.1–12.2	12.8	13.1	12.2–12.5
Lineage I	12.2–12.5	13.3–14.0	11.3–12.5	13.4	12.5	12.5–13.0
Lineage J	10.5–12.0	10.4–12.5	10.4–13.0	11.6–13.6	10.8–12.5	10.8–12.5
Lineage K	11.4–12.8	15.4–15.7	13.3–14.5	14.2	14.2	14.3–14.5
Lineage L	11.1–12.8	12.2–14.8	12.0–14.2	11.9–13.6	12.0–13.1	12.7–13.9

	Lineage G n=1	**Lineage H n=1**	**Lineage I n=1**	**Lineage J n=2**	**Lineage K n=1**	**Lineage L n=14**
Lineage G	**NA**					
Lineage H	11.6	**NA**				
Lineage I	12.2	12.7	**NA**			
Lineage J	11.6–12.5	10.7–13.0	9.5–9.6	**5.6**		
Lineage K	13.3	14.5	12.5	11.4–11.7	**NA**	
Lineage L	11.7–12.8	11.4–12.2	8.7–10.4	7.2–9.3	8.2–10.7	**0.0–5.8**

simulation studies that it overestimates the number of species more often than BPP (Luo et al., 2018); therefore, we used bGMYC instead to identify putative lineages within our *ND2* dataset. BGMYC requires ultrametric topologies as input and so we generated *ND2* phylogenies with ingroup samples only using bModelTest in BEAST2, partitioning *ND2* by codon position and using a random local clock. This phylogenetic analysis was run once for 5,000,000 generations sampling every 500 generations and the output was viewed in Tracer to check for convergence, as described above. We used LogCombiner to remove the first 10% of trees as burnin andresample the posterior distribution every 5,000 generations, so that there were 181 trees in our posterior distribution to use as input for bGMYC. We implemented bGMYC in the R package bGMYC v1.0.2 (Reid, 2014) using the command bgmyc.multiphylo. We ran the MCMC chain for 50,000 generations with a burnin of 25,000 and a thinning interval of 500, which resulted in a total of 9,050 samples in the posterior distribution of the analysis. We used the command plot to visualize the MCMC output and determine if the analysis had converged. Finally, the MCMC samples were analyzed using the command bgmyc.point and a threshold value of 0.05, so that individuals or groups of individuals needed a more than 95% chance that they were distinct from other samples to be considered an independent lineage.

Because BPP implements the Jukes-Cantor substitution model, it performs best when samples are separated by less than 10% sequence divergence (Flouri et al., 2018). Therefore, we performed barcoding distance threshold and bGMYC on the entire dataset (Fig. 3i, 3ii), as well independently on each of three major clades recovered in phylogenetic analyses (Fig. 3iii,3iv; Table 3; see results below)

Table 3
Results of the Bayesian Phylogenetics and Phylogeography (BPP) analyses across all samples and for each clade analyzed separately. Each analysis was run on the complete genetic dataset, excluding *ND2*, which was used in lineage discovery, and on the nuDNA genetic dataset only.

Taxonomic Sampling	Lineage Identification Method	No. Putative Species	Genes Tested in BPP	No. BPP Species (pp)
All	barcoding distance thresholds	12	nuDNA, ND1, 16S	12 (1.00)
			nuDNA	12 (0.97)
	bGMYC	11	nuDNA, ND1, 16S	11 (1.00)
			nuDNA	11 (0.99)
Clade I	barcoding distance thresholds	6	nuDNA, ND1, 16S	6 (0.99)
			nuDNA	6 (0.99)
	bGMYC	3	nuDNA, ND1, 16S	3 (1.00)
			nuDNA	3 (1.00)
Clade II	barcoding distance thresholds bGMYC	3	nuDNA, ND1, 16S	3 (1.00)
			nuDNA	3 (1.00)
Clade III	barcoding distance thresholds	4	nuDNA, ND1, 16S	4 (0.52)
			nuDNA	4 (0.98)
	bGMYC	2	nuDNA, ND1, 16S	2 (1.00)
			nuDNA	2 (0.99)

2.4. Species delimitation

To investigate the number of cryptic species within Myanmar *Riopa,* we ran Bayesian species delimitation analyses on our dataset using the program Bayesian Phylogenetics and Phylogeography (BPP) v4.0 (Rannala and Yang, 2003; Yang and Rannala, 2010; Yang, 2015). The program uses rjMCMC to analyze multiple loci under the multispecies coalescent (MSC), and it estimates relative species divergence times and ancestral population sizes. The MSC model implemented in BPP assumes free recombination between loci, no recombination within a given locus, and an absence of gene flow between taxa (Yang, 2015). In a recent simulation study, BPP was shown to outperform other species delimitation methods across different speciation scenarios, generally producing fewer false positives (overestimates of numbers of species) than the other methods (Luo et al., 2018).

We ran the A10 analysis in BPP (species delimitation with a fixed guide tree) to validate the lineages recovered by barcoding threshold distance and bGMYC, basing our guide species tree off the results of our concatenated phylogenetic analysis (above). To avoid pseudoreplication, we removed *ND2* from our genetic dataset, and we concatenated *ND1* and *16S* so that the mtDNA was treated as a single locus. Therefore, the analysis was run on four loci: *BDNF*, *R35*, *RAG1*, and mtDNA, as well as on the nuDNA dataset only (Table 3). We did not phase our nuDNA for the analysis. We set the parameter locusrate=1 so that there was rate heterogeneity across loci, and in the combined nuDNA + mtDNA analyses, we used a heredity scaler so that the heredity of nuDNA = 1 and the heredity of mtDNA = 0.25. All other parameters were kept at default values, including the inverse gamma priors θ and τ_0, with θ = (3, 0.002) and τ_0 = (3,0.03). Each BPP analysis was run twice to check consistence of the performance of the rjMCMC algorithm for 20,000 generations sampled every 10 generations with a burnin of 8,000 generations.

2.5. Population structure

We used the NeighborNet algorithm (Bryant and Moulton, 2004) as implemented in the program SplitsTree v4.14.8 (Huson and Bryant, 2006) to visualize clade-level diversification and possible reticulating relationships within Myanmar *Riopa*. SplitsTree generates a phylogenetic network, which allows for visualization of all possible evolutionary histories of the samples, including all discordant splits (Houson and Bryant, 2006), giving us a clearer picture of monophyly and genetic differentiation between populations and species. We ran the program on the concatenated mtDNA dataset and on each individual nuDNA gene alignment, using HKY-corrected p-distances to generate networks. Support for inferred network splits was assessed with 1,000 bootstrap replicates; splits with bootstrap (bs) values of 70 or higher were considered

highly supported (Hillis and Bull, 1993). Lineage assignment was determined based on the results of the BPP analysis of the concatenated nuDNA + mtDNA dataset for 12 putative species.

2.6. Species tree analysis

We conducted species tree analyses on the ingroup taxa using *BEAST2 v0.15.2 (Ogilvie et al., 2017) in BEAST2. Taxa were designated as a member of a species based on the results of the BPP analysis of the concatenated nuDNA + mtDNA dataset for 12 putative species (Table 3). The results of the previous concatenated bModelTest indicated that several of the nuDNA codon position partitions were uninformative. Therefore, we changed our partitioning strategy for this analysis and partitioned nuDNA by gene instead of by codon position. *ND1* and *ND2* remained partitioned by codon position due to the higher information content of these partitions. We ran bModelTest on the ingroup taxa three times each for 100,000,000 generations, sampling every 10,000 generations to obtain estimates for the substitution model for each partition. The analysis was run with a random local clock because lineages are all closely related and so we assumed similarity of clock rates with random change across branches (Drummond and Suchard, 2010), and a Yule Speciation model. As in the first bModelTest run, the nuDNA and mtDNA were linked separately so that two trees and two clocks, one each for nuDNA and mtDNA, were estimated. Alpha and beta values on the gamma prior for each clockrate.c parameter were changed to 2.0 and 0.5, respectively, as preliminary runs under default priors produced infinitesimally low values for these parameters and caused the likelihood to approach infinity. All other priors were kept at default values. Substitution model results from this analysis for each partition are shown in Table S5.

We plugged in the substitution models obtained from bModelTest into StarBEAST2 and ran a species tree analysis twice for 100,000,000 generations each, sampling every 10,000 generations. We used a random local clock, and again changed the gamma prior on the clockrates.c parameter to an alpha and beta of 2.0 and 0.5, respectively. We viewed the output in Tracer and RWTY to determine convergence and stationarity, and discarded the first 10% of runs as burnin, leaving 18,002 trees in the posterior distribution.

2.7. Morphological analyses

We examined fluid-preserved specimens of *Riopa* from Myanmar for variation in mensural and meristic characters, selecting characters that have been used in previous skink phylogenetic studies to delimit species (Siler et al., 2010). Our final morphological dataset comprised 86 individuals and contained 14 mensural characters: snout–vent length (SVL), axilla–groin distance (AGD), midbody width (MBW), tail width (TW), tail depth (TD), head length (HL), head width (HW), head depth (HD), eye diameter (ED), eye–nares distance (END), snout length (SNL), internares distance (IND); fore limb length (FLL), and hindlimb length (HLL), and five meristic characters: midbody scale row count (MBSRC), axilla–groin scale row count (AGSRC), paravertebral scale row count (PVSRC), Finger III lamellae (FinIIILam), and Toe IV lamellae (ToeIVLam). Additionally, we counted the number of supralabial, infralabial, supraocular, superciliary, loreal, and preocular scales and examined the degree of contact between head scales; however, following the observation that these characters show little to no variation across ingroup samples, they were excluded from subsequent morphological analyses. Measurements were taken by ESF and AHM with digital calipers accurate to 0.01mm with the exception of SVL and AGD—because older specimens were often fixed with curved bodies, SVL and AGD

were measured with a string which was then measured with digital calipers accurate to the 0.01mm. All scale counts were taken on the right side of the body when possible.

We conducted principal component analyses (PCA) on our mensural and meristic character datasets separately to visualize the distribution of the putative species recovered by BPP in morphospace. We removed individuals with missing data so that the mensural character dataset contained 73 individuals, with 38 of those also included in our phylogenetic analyses, and the meristic character dataset contained 81 individuals, with 45 of those also included in our phylogenetic analyses. Before conducting PCA on the mensural data, we size-corrected individuals to account for the disproportionately large effect of SVL on variance and to address any potential changes in body shape that occur with changes in body size, using the allometric equation: $X_{adj}=\log_{10}(X)-\beta[\log_{10}(SVL)-\log_{10}(SVL_{mean})]$, where X is the original value of the mensural character, X_{adj} is the size-corrected value of the mensural character, SVL_{mean} is the average SVL across all individuals, and β is the linear regression coefficient calculated from $\log_{10}(X)$ against $\log_{10}(SVL)$ (Thorpe, 1975; Lleonart, 2000). Ideally, we would calculate β for each putative species; however, several hypothesized lineages were represented by a single individual only, making the calculation of β impossible in these instances. Therefore, we calculated one β for each measurement across our dataset; because all individuals in our dataset are members of the same radiation across Myanmar, we feel confident that this did not have a large effect on the results. Prior to conducting the PCAs, we calculated the Z scores for each variable in both the mensural and meristic datasets using the scale function in R to standardize the variance for each variable. We ran each PCA using the command prcomp in R.

3. Results

3.1. DNA sequencing and phylogenetic results

Our molecular dataset comprised 4,776 base pairs for 49 individuals—41 ingroup and eight outgroup samples with a total of 11.2% missing data across the entire concatenated alignment. The majority of missing data was confined to outgroup taxa, with only a few (n=7) ingroup taxa missing locus-specific coverage (Table S3). Our concatenated analyses in bModelTest inferred a well-supported topology (Fig. 3). Similar to the recent higher-level study of *Lygosoma* group skinks (Freitas et al., 2019), we recover a clade of *Riopa* from Myanmar with high support (posterior probability [pp] = 1.0; Fig. 3). Within Myanmar *Riopa*, three major clades are recovered (pp = 1.0 for each; Fig. 3, Clades I–III), each displaying significant intraspecific and well-supported genetic structure. These clades do not correspond to known species—individuals identified to species are not recovered as monophyletic groups (Table S3).

3.2. Cryptic lineage identification and species delimitation

Calculation of the uncorrected p-distances for the *ND2* gene used in barcoding threshold values reveals high levels of genetic diversity between samples, with observed divergences between individuals of up to 15.7% (mean=10.4 ± 3.8%; Tables 2, S4). Within each of the three major clades (Figs. 1, 3, 6; Clades I–III), the pairwise genetic distances range from 9.2–13.0% (Tables 2, S4). These *ND2* distances were used as input for the lineage barcoding threshold method and resulted in four potential thresholds at 1.7%, 5.0%, 6.8%, and 10.1%, with 6.8% corresponding to the lowest minimum threshold (Fig. 4). Based on this threshold value, we recovered 12 putative lineages, each comprising 1–14 sampled individuals (Fig. 3; Table 3). Clades I and II each were supported as comprising three lineages and Clade III supported as

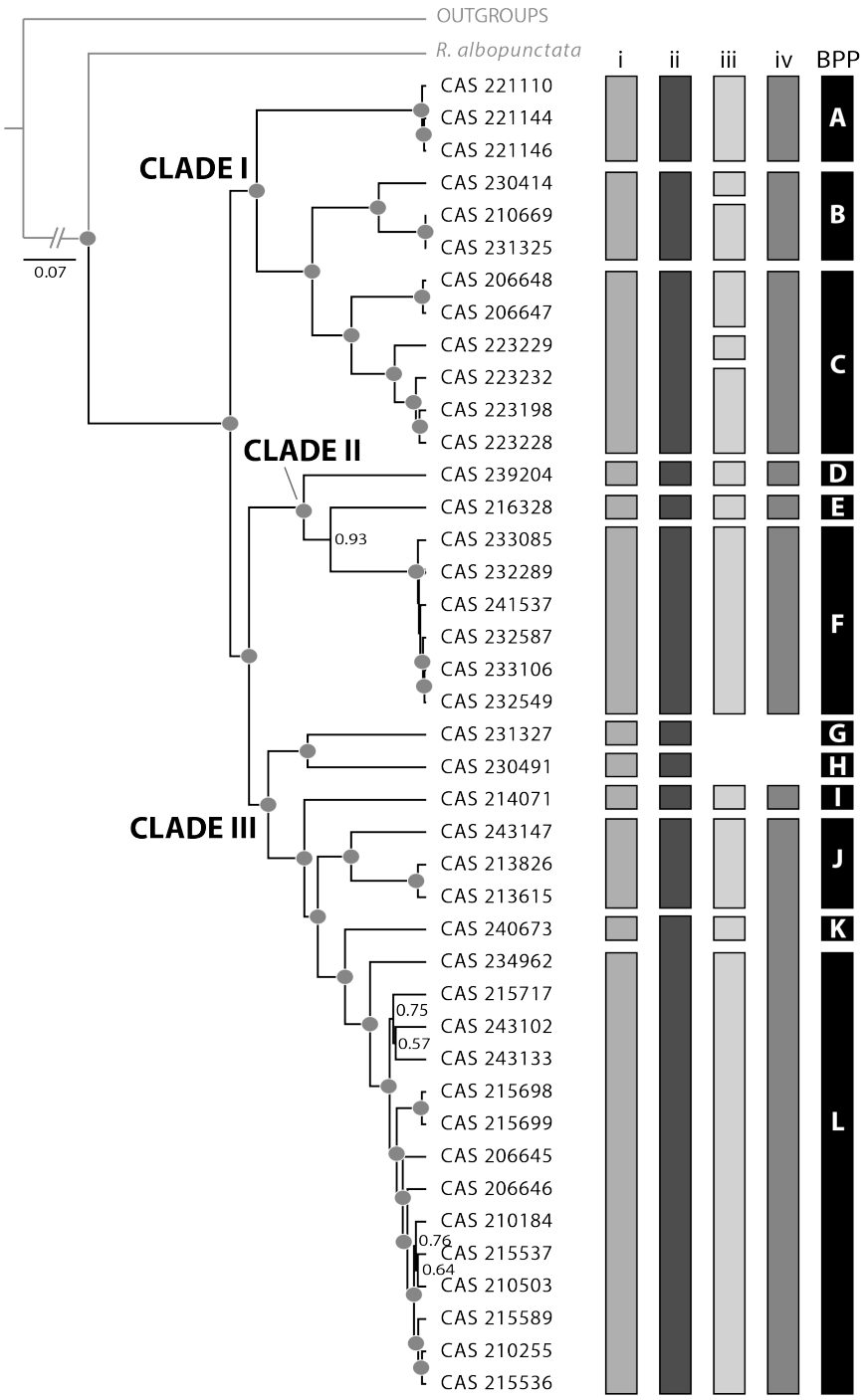

Fig. 3. Phylogeny showing the results of the concatenated bModelTest analysis performed in BEAST2. Gray circles indicate nodes that are highly supported (pp ≥ 0.95). The scale bar indicates branch lengths in average substitutions over time. The columns to the right of the topology indicate the putative lineages supported by each lineage discovery method: i—barcoding threshold values on the entire dataset; ii—bGMYC on the entire dataset; iii—barcode threshold values on each clade individually; and iv—bGMYC on each clade individually. The final column in black shows lineages supported by the BPP analysis with 12 putative lineages as input.

comprising six lineages. Comparatively, bGMYC supported 11 putative lineages, with Clades I and II again comprising three lineages, but Clade III instead comprising five lineages (Fig. 3; Table 3). Clade-specific lineage barcoding distance thresholds and bGMYC lineage identification analyses identified six and three putative lineages, respectively, for Clade I, three for Clade II, and four and two, respectively for Clade III (Fig. 3; Table 3). These intra-clade analyses excluded lineages G and H from Clade III because these samples were greater than 10% divergent from all other lineages recovered, and as a result, were not included in clade-specific BPP analyses. For within clade barcoding distance thresholds analyses, the threshold values were 2.8% for Clade I, 5.4% for Clade II, and 6.4% for Clade III.

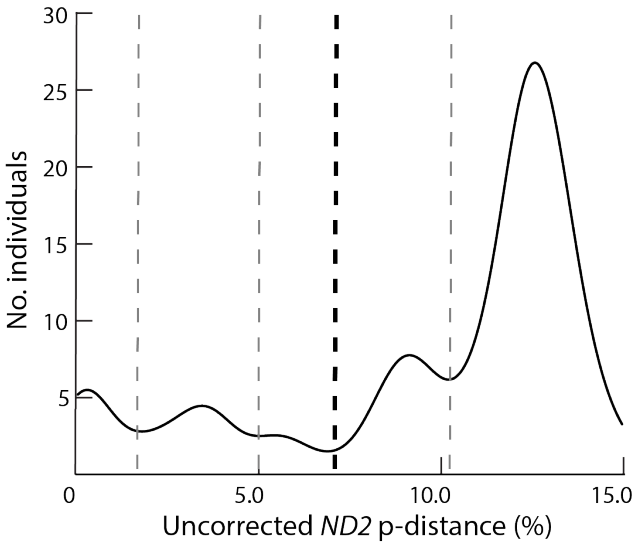

Fig. 4. Graph of the resulting barcoding threshold values for *ND2*. The gray and black dashed lines correspond to minimum values, with the bolded black dashed line at 6.8%, which represents the lowest minimum value. This value (6.8%) was used as the input value for lineage discovery using the barcode threshold method.

In most cases, BPP analyses identified all input lineages as species with high support (considered to be posterior probabilities of above 0.95; Huelsenbeck and Rannala, 2004; Yang and Rannala, 2010) for both concatenated (nuDNA + mtDNA) and nuDNA only datasets. The exception was poor support (pp=0.52) observed for four putative lineages within Clade III in analyses of the concatenated dataset however, each of the same four lineages was highly supported (pp=0.98) in analyses of the nuDNA only dataset (Fig. 3; Table 3).

3.3. Phylogenetic networks

Analysis of genetic structure using SplitsTree revealed that individual lineages were, for the most part, well defined with mtDNA but not with nuDNA (Fig. 5). In the mtDNA SplitsTree network, all individual lineages were well supported (bs=95–100) with the exception of lineage J, which was moderately supported (bs=69; Fig. 5). A split that grouped one individual of lineage L with lineage K also was recovered as highly supported (bs=89; Fig. 5). Additionally, Clades I and II were both recovered as highly supported (Clade I bs=70, Clade II bs = 91), whereas Clade III was only moderately supported (bs=67, Fig. 5). However, a subclade within Clade III comprising lineages I, J, K, and L, to the exclusion of lineages G and H, was recovered as highly supported (bs=100), and the subclade comprising lineages G and H was also recovered as highly supported (bs=91; Fig. 5). The nuDNA SplitsTree networks were less resolved than mtDNA. Both the *R35* network and the *RAG1* network had some support for individual lineages but clades were not supported, with the exception of Clade I in the *RAG1* SplitsTree network (bs=95; Fig. 5). *BDNF* was least resolved out of all four networks, with the only instance of high support found for the separation of lineage G from all other lineages (bs=86; Fig. 5). Lineage G is also well supported in the *R35* SplitsTree network (bs=100), but not in the *RAG1* SplitsTree network (bs=61). Lineages that are well supported in both the *R35* SplitsTree network and the *RAG1* SplitsTree network include A (bs=80 [*R35*] and 100 [*RAG1*]), B (bs=84 [*R35*] and 83 [*RAG1*]), and E (bs=96 [*R35*] and 90 [*RAG1*]). Two lineages were highly supported only in a single nuDNA SplitsTree network: C (bs=90 [*RAG1*]) and D (bs=94 [*R35*]). Lineages that were not highly supported across any nuDNA SplitsTree network were lineages F, H, I, J, K, and L. Several of these lineages were represented by a single sample and did not amplify for every nuDNA gene (Table S3).

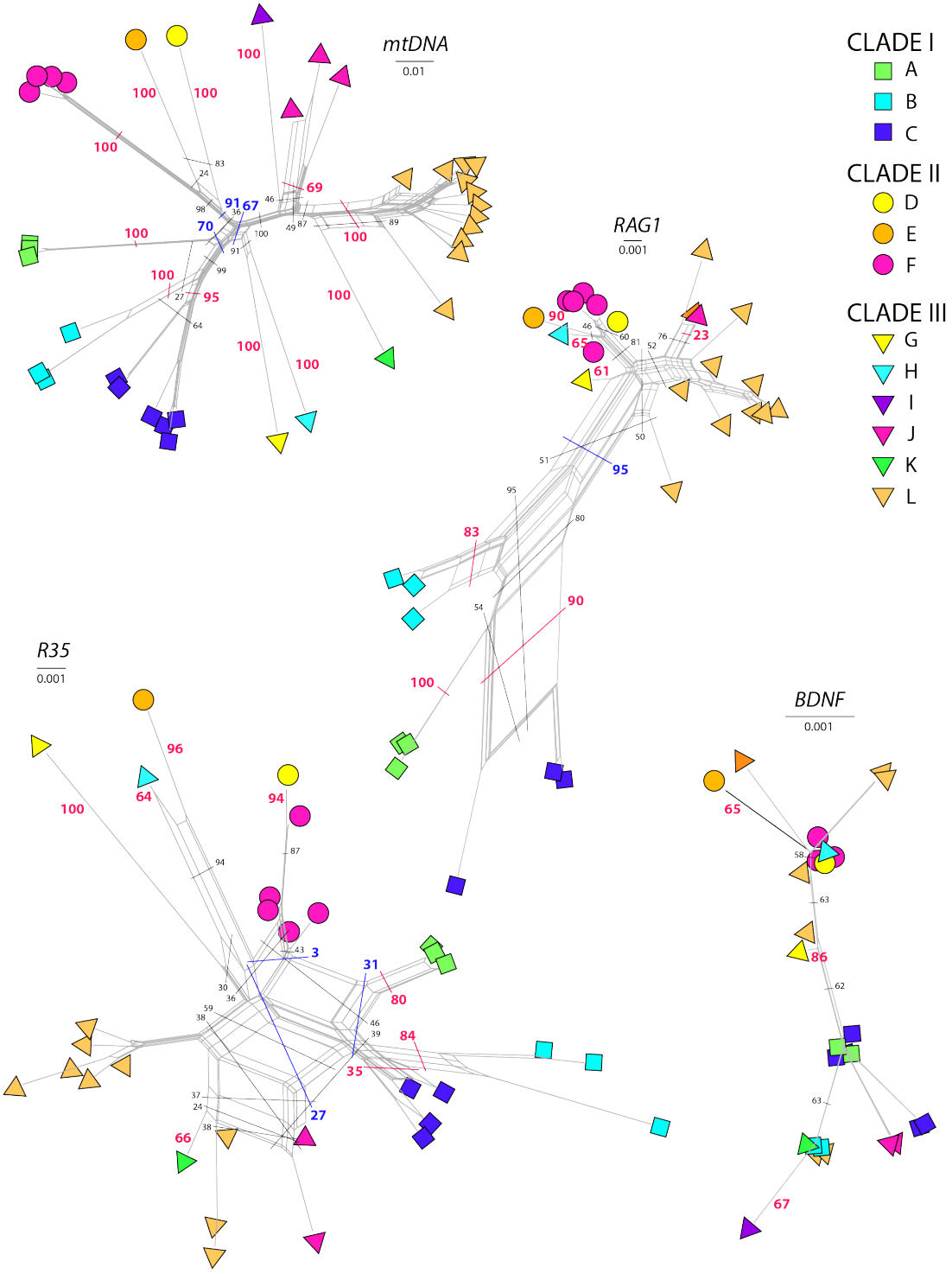

Fig. 5. SplitsTree network graphs illustrating genetic splits for four loci: mitochondrial DNA (*mtDNA*) and the nuclear genes *BDNF*, *RAG1*, and *R35*. Gray lines represent the topology of each network, and blue, pink, and black lines crossing over the gray lines indicate major splits between taxa on either side of the line, with blue representing splits between clades, pink representing splits between lineages, and black representing other major splits. The color-coded number next to each colored line show the bootstrap support value for the split. Bootstrap support was assessed via 1000 bootstrap replicates and splits with values ≥ 70 are considered to be highly supported.

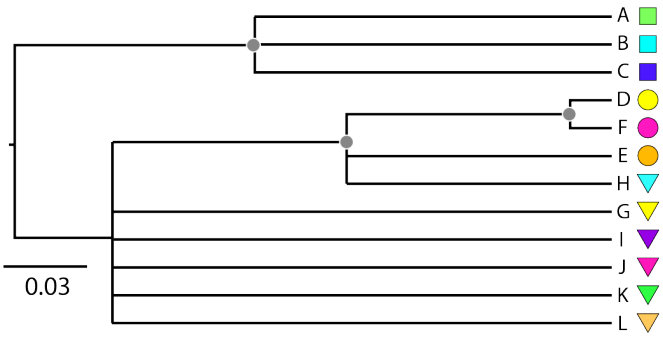

Fig. 6. Maximum clade credibility topology showing the results of the species tree analysis. Gray circles indicate nodes that are highly supported ($p \geq 0.95$). The scale bar indicates branch lengths in coalescent units.

3.4. Species tree

Species tree analysis of the 12 putative species obtained from BPP resulted in a topology with poorly supported structure (Fig. 6). Clade I is recovered with high support, although the relationships of lineage A, B, and C within Clade I are not resolved (Fig. 6). Clade II is also recovered with high support; however, lineage H is supported as part of Clade II, although its placement within the clade is not resolved (Fig. 6). Additionally, within Clade II, we recover lineages D and F as sister lineages (Fig. 6), which differs from the concatenated bModelTest analysis in which E and F are recovered as sister lineages, although this result is only moderately supported (pp=0.93, Fig. 3). A monophyletic Clade III is not recovered, with lineages G, I, J, K and L instead forming a polytomy along the backbone of the tree (Fig. 6).

3.5. Multivariate analyses of morphology

Results of the principal components analysis indicate that lineages and clades are not separated in morphospace (Fig. 7). In the mensural PCA analysis (Fig. 7), the first principal component (PC1) accounted for 36.5% of the variation and was loaded most heavily by TD, HW, HD, and FLL, suggesting that individuals are separated by body robustness, and the second principal component (PC2) accounted for 13.6% percent of the variation and loaded most heavily on AGD, MBW, TW, TD, END, and SNL, with AGD, MBW,TW, and TD negatively correlated with END and SNL, suggesting that individuals snout lengths are negatively correlated with

body size (Table S6). Similarly, in the meristic PCA analysis (Fig. 7), PC1 accounted for 45.0% of the variation and loaded most heavily on MBSRC, PVSRC, FinIIILam, and ToeIVLam, with FINIIILam and ToeIVLam negatively correlated with MBSRC and PVSRC, suggesting that body size is negatively correlated with digit length , and PC2 accounted for 21.1% percent of the variation and loaded most heavily on MBSRC and AGSRC, with MBSRC negatively correlated with AGSRC, suggesting that as the body elongates, body robustness decreases, and indicating that the degree of body elongation is important in distinguishing individuals in morphospace (Table S6). In the results of the meristic PCA, there does appear to be some separation of individuals along PC1 (Fig. 7); however, this separation does not correspond to phylogenetic placement and may be an artifact of the low samples size for some lineages. Clades or lineages do not form distinct clusters in morphospace in either the mensural or the meristic analysis. Lineage H, represented by a single sample, was excluded from both mensural and meristic analyses because the specimen was damaged. Lineage I was excluded from the mensural analysis because of its small size and damage, but it was included in the meristic analysis.

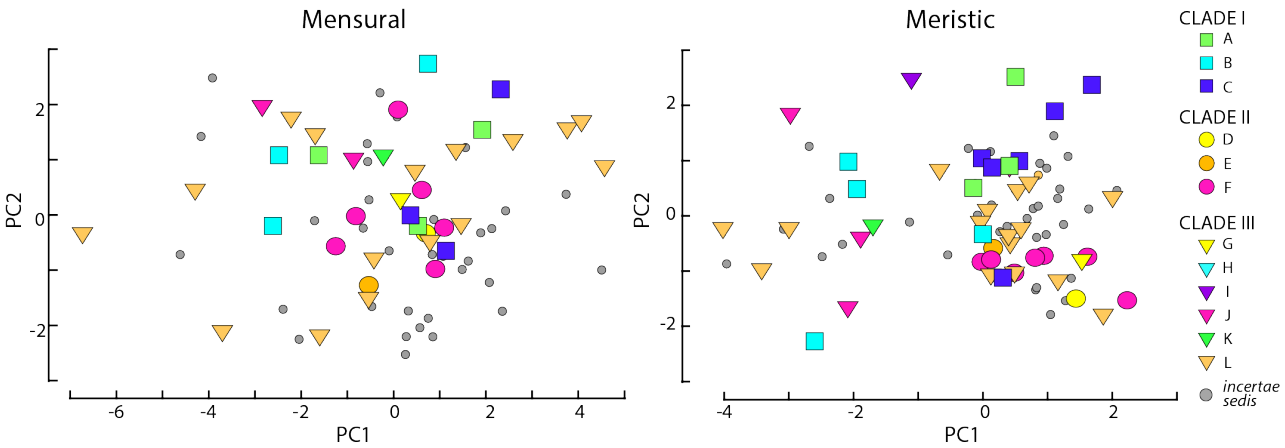

Fig. 7. Graphs of the mensural (left) and meristic (right) PCAs. Lineage H is not shown in the figure because the specimen was damaged and excluded from analyses.

4. Discussion

4.1. Genetic and morphological diversity within Myanmar Riopa

Overall, we find high levels of genetic diversity within Myanmar *Riopa* that are not consistent with previously recognized morphological species boundaries. Currently, four species in the genus are recognized to occur in the country based on morphology: *R. albopunctata*, *R. anguina*, *R. lineolata*, and *R. popae*. However, results from our species delimitation analyses suggest that Myanmar harbors as many as 13 unique evolutionary lineages—the morphologically distinct *R. albopunctata*, plus 12 putative lineages recovered in species delimitation analyses that comprise the *R. anguina-lineolata-popae* species complex. Our concatenated and coalescent phylogenetic results indicate that these 12 lineages form a clade, sister to *R. albopunctata* (Fig. 3), which suggests that Myanmar *Riopa* has diversified *in situ* within the country. These 12 lineages of the *R. anguina-lineolata-popae* species complex are separated by *ND2* mitochondrial distances of 7.2–15.7% (Table 2) and are well supported by the mtDNA SplitsTree network analysis (Fig. 5). However, their support among nuDNA SplitsTree network analyses varies, with several lineages (A, B, E, G) supported by two out of three nuDNA SplitsTree networks, two lineages (C, D) supported by one nuDNA SplitsTree network, and the remaining six lineages (F, H, I, J, K, L) not supported by any of the nuDNA SplitsTree networks (Fig. 5). These results are not surprising given that mtDNA evolves at a faster rate than nuDNA (Vawter and Brown, 1986). The species delimitation program BPP is known to delimit population-level structure in addition to species-level structure (Sukumaran and Knowles, 2017; Barley et al., 2018; Luo et al., 2018; Leaché et al., 2019), and therefore, the lack of resolution among our nuDNA networks may indicate that some of the recovered lineages are genetically structured populations or incipient species instead of full species. Additionally, the species tree analysis does not fully

resolve inter-lineage relationships (Fig. 5), which may be an artifact of low genetic sampling, or again, indicate that the lineages are insipient species.

Riopa species are small, cryptically colored, and semi-fossorial (Das, 2010), making them hard to detect during field surveys. As a result, one-half of the lineages recovered in species delimitation analyses (D, G, E, H, I, K) are represented in the dataset by a single individual, which prevents us from being able to characterize intra-lineage genetic diversity at this time. Furthermore, geographic sampling gaps exist across much of Myanmar, including in low–mid elevation regions in the eastern and southern portions of the country, and it is likely that additional unsampled genetic lineages exist within these regions. Species delimitation methods are affected by taxonomic and geographic scope of sampling, and many do not accommodate low intra-specific sampling (Lim et al., 2012), which affects their accuracy. As a result, the small sample size of many of our lineages (average $n = 3.4 \pm 3.8$) combined with the possibility of unsampled lineages in Myanmar may distort the signal of population- versus species-level diversity. Understanding the distributions of Myanmar *Riopa* is crucial to appreciating the evolutionary history of the group, therefore additional surveys targeting *Riopa* across the country are needed to better resolve population- and species-level diversity within this clade.

Despite the high amount of genetic diversity within Myanmar *Riopa*, we do not find that lineages or clades are separated in morphospace (Fig. 6). Instead, both the mensural and meristic PCAs show that there are no consistent morphological trends across lineages or clades. In the PC1 loadings for the mensural PCA and PC2 loadings for the meristic PCA, we do find the expected trend that body robustness is negatively correlated with body elongation across individuals (Gans, 1975; Wiens and Slingluff, 2001), but the other PC loadings are more difficult to interpret (Table S6) . Additionally, no lineages are separated by qualitative head scalation

patterns, with the exception of lineage F, in which all examined members have a scaly lower eyelid instead of a lower eyelid with a transparent disc. However, the taxonomic value of the lower eyelid state is a matter of debate due to its variability within clades (e.g. Broadley, 1966; Linkem et al., 2011; Freitas et al., 2019), with the state reportedly varying even between eyelids on the same individual (Hora, 1927). These morphological results suggest that intra-lineage morphology varies at least as much as inter-lineage morphology and indicates that body morphology is conservative across *Riopa* lineages in Myanmar, highlighting the limitations to employing diagnostic characters traditionally used in species delimitations studies in skinks.

Our qualitative head scalation patterns are coded in a binary fashion (e.g. presence verses absence); however, geometric morphometric analyses on skull characteristics have been shown to be a useful tool in separating species that appear qualitatively similar (Ruane, 2015; Rej and Mead, 2017; Gabelaia et al., 2018) and may help to differentiate lineages of Myanmar *Riopa* in future studies. Furthermore, we did not examine internal osteological characters or hemipenes morphology, character sets that have helped to distinguish species in other squamate systematic studies (Welton et al., 2010; Prötzel et al., 2018), and researchers undertaking future studies on *Riopa* may wish to include these additional morphological elements.

4.2. Biogeographic patterns within Myanmar Riopa

Myanmar is both geographically and geologically complex, comprising multiple regions of tectonic uplift resulting from the collision of the Indian subcontinent with the Laurasian subcontinent beginning approximately 52 million years ago (van Hinsbergen et al., 2012; Khin et al., 2017), with some eastern topographical features such as the Shan Plateau (Fig. 1) dating to the Late Cretaceous (reviewed in Licht, 2013). This complex landscape has contributed to high levels of endemism in other groups of

squamate reptiles, including two genera of geckos in Myanmar: *Cyrtodactylus* (e.g. Grismer et al., 2018a) and *Hemiphyllodactylus* (e.g. Grismer et al., 2018b), and may have driven diversification of Myanmar *Riopa* in the western and central parts of the country. Based on the localities of sampled specimens (Fig. 1), it appears that most putative Myanmar *Riopa* species are allopatric, with the possible exceptions of lineages J and L on the western side of the Irrawaddy (Ayeyarwady) River and lineages B, G, and I at Mount Popa (Fig. 1). Despite their close proximity, lineages J and L are separated by *ND2* genetic distances of 7.2–9.3%, and lineages B, G, and I separated by *ND2* genetic distances of 11.1–14.0% and may represent instances of secondary contact between lineages that diverged in allopatry.

Lineages A and C are separated from the rest of Myanmar *Riopa* by the Arakan Yoma and Chin Hills, mountains that, along with the Naga Hills to the north, form the Indo-Myanmar (Indo-Burma) Range (Fig. 1). Uplift of the Indo-Myanmar Range began approximately 37 million years ago, resulting from the collision of the Indian subcontinent with the Laurasian subcontinent (Mitchell, 1993; Licht et al., 2013). These mountains separate the western coast of Myanmar (the Assam Basin) from the country's interior Central Myanmar (Central Burma) Basin. Although the timing of the complete separation of the Central Myanmar Basin from the Assam Basin remains unknown (Licht et al., 2013), it is likely that biotic exchange could have occurred between the two regions until as recently as the early Oligocene, approximately 33 million years ago (Licht et al., 2013). This separation most likely predates the divergence of lineages A and C from the rest of Myanmar *Riopa*, suggesting that there was an instance of trans-mountain dispersal early in the diversification of the clade. The mountains in the southern Indo-Myanmar Range reach an elevation of over 3,000 m at Nat Ma Taung (Mount Victoria). Elevation data taken in the field for a subset of *Riopa* specimens indicates that individuals were

found predominately at mid-elevations, with some individuals found at higher elevations (77–2,065 m above sea level; Table S3), suggesting that parts, but not all, of the Arakan Yoma and Chin Hills may be a barrier to dispersal between eastern and western lineages. Additionally, orographic lift of monsoon winds on the western side of the mountains results in the rain shadow effect in which the Assam Basin in the west is wetter than the Central Myanmar Basin in the east, potentially exposing lineages A and C to a different set of ecological conditions than what is experienced by other members of Myanmar *Riopa*, although detailed ecological data on this group are not available.

Lineage B in Clade I and all lineages within Clades II and III are located in the central and southern portions of the Central Myanmar Basin, east of the Indo-Myanmar Range (Fig. 1). Within the southern and central portion of the Central Myanmar Basin, lineages B, E, G, H, J, and L are separated from each other by the Irrawaddy River, with B, E, G, and H found on the eastern side of the river and J and L found on the western side of the river. Lineages D, F, and K are located in the northern Central Myanmar Basin between the Chindwin and Irrawaddy Rivers. Although rivers have been implicated as barriers to dispersal of skinks in other parts of the world (Jackson and Austin, 2010; Miralles and Carranza, 2010; but see Vences et al., 2014), this is the first study recognizing the Irrawaddy River as a potential barrier to dispersal. Future studies focusing on gene flow between lineages on eastern and western sides of the river are needed to elucidate the role of the Irrawaddy River as a biogeographic barrier in Myanmar *Riopa*.

In addition to geographical boundaries, Myanmar has experienced changes in climate throughout the Miocene, Pliocene and Pleistocene, resulting from the uplift of the Himalayas and the subsequent strengthening of the South and East Asian monsoon systems (Clift et al., 2008; Zhang et al., 2015). Simulation studies suggest that the Chin Hills and the Arakan Yoma affect

the climates of the Assam and Central Myanmar Basins by playing a critical role in the strengthening and seasonality of the annual South Asian Monsoon across the Indian subcontinent (Wu et al., 2014; Wu and Hsu, 2016). These climate changes caused a transition from C3- to C4-dominated grasslands (Quade et al., 1989) and gave rise to mosaic savannah forest habitat across the Indian Subcontinent and Southeast Asia (Sun and Wang, 2005; Patnaik and Nanda, 2010; Louys and Meijaard, 2010; Ratnam et al., 2016). Fossil ungulates and hominids from Pliocene and Pleistocene deposits in South and Southeast Asia provide additional evidence for the expansion of grassland habitats in the region during this time (Takai et al., 2006; Suraprasit et al., 2014; Patnaik, 2016). Species of *Riopa* are typically found in dry to semi-dry forests and grasslands (Das, 2010; Vyas, 2014; Bhattarai et al., 2018; Prasad et al., 2018), and populations may have been isolated by patches of forest habitats as vegetation shifts occurred throughout the Tertiary, thus promoting speciation under a scenario of reduced or suspended gene flow.

Across portions of the Central Myanmar Basin, precipitation falls below 1000 mm per year (Fig. 2C; Matsuda, 2013), forming a region of semi-arid habitat known as the Central Dry Zone (Figs. 1, 2; Wu et al., 2014). This region has unique arid-adapted forest and grassland habitats and high levels of endemicity within terrestrial vertebrates (Smith, 1943; Slowinski and Wüster, 2000; Platt et al., 2003; Zug et al., 2006; Shimada et al., 2010; Grismer et al., 2018c; Poyarkov et al., 2019) and has been hypothesized as a major center of speciation (Zug et al., 2006); however, the mechanisms behind the high levels of diversification in this region remain unknown. Our results supporting multiple cryptic lineages of *Riopa* concentrated within the boundaries of the Central Dry Zone (lineages B, G, H, I, J, L; Figs. 1, 2C) provide further evidence for the important role this biogeographic region may have played in vertebrate diversification.

4.3. Are Myanmar Riopa *an example of non-ecological diversification?*

The pattern of high genetic diversity with no accompanying morphological differentiation suggests that Myanmar *Riopa* have undergone non-ecological diversification, in which genetic divergence between lineages has not been driven by adaptation to divergent environmental conditions. Non-ecological diversification results from allopatric separation of populations into isolated ecologically similar regions followed by non-ecologically mediated genetic evolution over time (Pyron et al., 2015; Czekanski-Moir and Rundell, 2019). Given the lack of morphological separation between lineages of Myanmar *Riopa*, it does not appear that lineages have been subjected to divergent natural selection or have undergone disparification (increase in morphospace area occupied over time by a clade [Czekanski-Moir and Rundell, 2019]) despite genetic diversification (Table 2). However, the lack of ecological data for Myanmar *Riopa* preclude the possibility of statistical tests of ecological differentiation within the clade, and we also lack knowledge on which morphological characters are ecologically relevant in this clade. It is possible that ecologically relevant variation exists between individuals but was not examined in this study. Additionally, we lack fossil data that could provide concrete evidence of ancestral morphology, an important consideration of whether diversification has been driven by ecological or non-ecological processes, although given the morphological uniformity of lineages within the clade, we hypothesize that the current morphology is pleisiomorphic.

Signatures of non-ecological speciation have been documented in other groups of skinks including *Eutropis* in the Philippines (Barley et al., 2013), *Carlia* and *Lampropholis* in Australia (Singhal et al., 2018), and *Cryptoblepharus* in Australia (Blom et al., 2016). Similar to our observations, these studies reveal high levels of genetic diversification not accompanied by morphological disparification, although only Blom et al. (2016) conducted explicit statistical

tests linking the morphology examined in the study with species' ecologies. In addition to these studies, the numerous instances of cryptic radiations across the Family Scincidae (see Table S1 for a list of all cryptic species described between 2014–2019) allude to non-ecological speciation as a common occurrence within scincid lizards, but this has not been tested explicitly in a statistical framework. Therefore, although it is clear that Myanmar *Riopa* constitutes a cryptic radiation, the processes contributing to diversification in the clade cannot be determined based on our current data.

4.4. Taxonomic implications

In discussing distribution patterns of *Riopa* species in Myanmar, Jayaram (1949:407) remarked, "it is likely that these are mere races of a single species." Our genetic results dispute this hypothesis and instead suggest that there is significant cryptic diversity present within the *R. anguina-lineolata-popae* species complex. However, because the species delimitation program BPP delimits both population- and species-level structure (Sukumaran and Knowles, 2017; Barley et al., 2018; Luo et al., 2018; Leaché et al., 2019), it is likely that some of the 12 lineages represent genetically divergent populations and not full species. Furthermore, using genetic data alone to diagnose species remains controversial (Bauer et al., 2011; Singhal et al., 2018; Hillis, 2019) despite the widespread adoption of the General Lineage Concept definition of species (deQueiroz, 1998; 1999), which states only that species are independently evolving lineages.

Therefore, determination of which of our Myanmar *Riopa* lineages represent new species is complicated by the lack of distinguishing morphological features and the current paucity of other pertinent natural history information, such as behavior, ecology, microhabitat preferences, and geographic distributions. The type specimens of *R. anguina*, *R. lineolata*, and *R. popae* are

housed at the Zoological Survey of India, the British Museum of Natural History, and the Museum of Comparative Zoology, respectively, and, except for *R. popae*, were not available for examination. Additionally, three sampled lineages were found at Mount Popa, the type locality of *R. popae* (lineages B, G, and I) and one sampled lineage (lineage B) was found around the approximate type locality of *R. anguina*, but no genetic samples exist from the type locality of *R. lineolata* (Fig. 1), making it difficult to assign lineages to recognized species based on their geographical distributions.

Additional studies are needed to determine what proportion of lineages identified within the *R. anguina-lineolata-popae* species warrant recognition as separate species. Because several lineages are found in close proximity with large genetic differentiation (J and L; B, G, and I; Fig. 1, Table 2), it is likely that they represent distinct species along separate evolutionary trajectories, according to the General Lineage Concept (de Queiroz, 1998, 1999). However, at this time, we decline to advance the taxonomy of this group until more data are available that will allow for improved resolution of species-level diversity within the *R. anguina-lineolata-popae* species complex. Recognizing the high levels of cryptic diversity with Myanmar *Riopa* is a critical first step in understanding the evolutionary dynamics that generate biodiversity in the region.

Acknowledgements

This research was made possible by a joint collaboration between the California Academy of Sciences (CAS), the National Museum of Natural History (NMNH) and the Smithsonian Institute, and the Myanmar Forestry Department, Ministry of Forestry. For tissue and specimen loans (Table S3), we thank J. Vindum and L. Scheinberg at CAS, L. Grismer at the La Sierra

University Herpetology Collection (LSUHC), C. Spencer at the Museum of Vertebrate Zoology (MVZ), A. Datta-Roy at the National Institute of Science Education and Research (NISER), and A. Bauer at Villanova University. We thank L. Scheinberg at CAS, A. Resetar at the Field Museum of Natural History (FMNH), and J. Rosado at the Museum of Comparative Zoology (MCZ) for facilitating collection visits for AHM. We are grateful to T. Yuri, M. Labonte and M. Penrod at the Sam Noble Oklahoma Museum of Natural History (SNOMNH) for help with molecular data collection. We thank J. Oaks for discussion of methods and help with *BEAST2 and bModelTest analyses and appreciate additional help provided by the Taming the BEAST 2018 workshop in Oberägeri, Switzerland. We also appreciate D. Mulcahy and G. Zug for helpful discussions on skinks in Myanmar. Fieldwork in Myanmar was funded by NSF grant DEB 9971861 to J. Slowinski and G. Zug. This research was supported by University of Oklahoma Alumni Funds, Graduate Student Senate Award, and Department of Herpetology Loren G. Hill Fund to ESF; funds from The University of North Carolina Asheville to AHM and RGR; and NSF grants (IOS 1353683 and DEB 1657648) to CDS. Finally, we are very grateful to the two anonymous reviewers who gave us feedback, which greatly improved our manuscript.

References

Aljanabi, S.M., Martinez, I., 1997. Universal and rapid salt-extraction of high quality genomic DNA for PCR-based techniques. Nucleic Acids Res. 25, 4692–4693. https://doi.org/10.1093/nar/25.22.4692.

Barley, A.J., White, J., Diesmos, A.C., Brown, R.M., 2013. The challenge of species delimitation at the extremes: diversification without morphological change in Philippine sun skinks. Evolution. 67, 3556–3572. https://doi.org/10.1111/evo.12219.

Barley, A.J., Brown, J.M., Thomson, R.C., 2018. Impact of model violations on the inference of species boundaries under the multispecies coalescent. Syst. Biol. 67, 269–284. https://doi.org/10.1093/sysbio/syx073.

Bauer, A.M., Parham, J.F., Brown, R.M., Stuart, B.L., Grismer, L.L., Papenfuss, T.J., Böhme, W., Savage, J.M., Carranza, S., Grismer, J.L., Wagner, P., Schmitz, A., Ananjeva, N.B., Inger, R.F., 2011. Availability of new Bayesian-delimited gecko names and the importance of character-based species descriptions. Proc. R. Soc. B. 278, 490–492. https://doi.org/10.1098/rspb.2010.1330.

Bhattarai, S., Pokheral, C.P., Lamichhane, B.R., Regmi, U.R., Ram, A.K., Subedi, N., 2018. Amphibians and reptiles of Parsa National Park, Nepal. Amphib. Reptile Conserv. 12, 35–48.

Bickford, D., Lohman, D.J., Sodhi, N.S., Ng, P.K.L., Meier, R., Winker, K., Ingram, K.K., Das, I., 2007. Cryptic species as a window on diversity and conservation. Trends Ecol. Evol. 22, 148–155. https://doi.org/10.1016/j.tree.2006.11.004.

Blom, M.P.K. Horner, P., Moritz, C., 2016. Convergence across a continent: adaptive diversification in a recent radiation of Australian lizards. Proc. R. Soc. B. 283, 20160181. https://doi.org/10.1098/rspb.2016.0181.

Bortolus, A., 2008. Error cascades in the biological sciences: the unwanted consequences of using bad taxonomy in ecology. Ambio. 37, 114–118. https://doi.org/10.1579/0044-7447(2008)37[114:ECITBS]2.0.CO;2.

Bouckaert, R., Heled, J., Kühnert, D., Vaughan, T., Wu, C.H., Xie, D., Suchard, M.A., Rambaut, A., Drummond, A.J., 2014. BEAST 2: a software platform for Bayesian evolutionary analysis. PLOS Comput. Biol. 10, e1003537. https://doi.org/10.1371/journal.pcbi.1003537.

Bouckaert, R.R., Drummond, A.J., 2017. bModelTest: Bayesian phylogenetic site model averaging and model comparison. BMC Evol. Biol. 17, 42. https://doi.org/10.1186/s12862-017-0890-6.

Brandley, M.C., Ota, H., Hikida, T., de Oca, A.N.M., Fería-Ortiz, M., Guo, X., Wang, Y., 2012. The phylogenetic systematics of blue-tailed skinks (*Plestiodon*) and the family Scincidae. Zool. J. Linn. Soc. 165, 163–189. https://doi.org/10.1111/j.1096-3642.2011.00801.x.

Broadley, D.G., 1966. A review of the *Riopa sundevalli* group (Sauria: Scincidae) in southern Africa. Arnoldia (Rhodesia) Series of Miscellaneous Publications National Museums of Southern Rhodesia. 2(34), 1–7.

Brown, S.D.J., Collins, R.A., Boyer, S., Lefort, M.C., Malumbres-Olarte, J., Vink, C.J., Cruickshank, R.H,. 2012. SPIDER: an R package for the analysis of species identity and evolution, with particular reference to DNA barcoding. Mol. Ecol. Resour. 12, 562–565. https://doi.org/10.1111/j.1755-0998.2011.03108.x.

Bryant, D., Moulton, V., 2004. Neighbor-Net: an agglomerative method for the construction of phylogenetic networks. Mol. Biol. Evol. 21, 255–265. https://doi.org/10.1093/molbev/msh018.

Ceríaco, L.M.P., Gutiérrez, E.E., Dubois, A., 2016. Photography-based taxonomy is inadequate, unnecessary, and potentially harmful for biological sciences. Zootaxa 4196, 435–445. https://doi.org/10.11646/zootaxa.4196.3.9.

Chan-ard, T., Parr, J.W.K., Nabhitabhata, J., 2015. A Field Guide to the Reptiles of Thailand. Oxford University Press, New York.

Clift, P.D., Hodges, K.V., Heslop, D., Hannigan, R., van Long, H., Calves, G., 2008. Correlation of Himalayan exhumation rates and Asian monsoon intensity. Nat. Geosci. 1, 875–880. https://doi.org/10.1038/ngeo351.

Czekanski-Moir, J.E., Rundell, R.J., 2019. The ecology of nonecological speciation and nonadaptive radiations. Trends Ecol. Evol. 34, 400–415. https://doi.org/10.1016/j.tree.2019.01.012.

Das, I., 2010. A Field Guide to the Reptiles of Southeast Asia. New Holland, London.

Datta-Roy, A., Singh, M., Karanth, K.P., 2014. Phylogeny of endemic skinks of the genus *Lygosoma* (Squamata: Scincidae) from India suggests an in situ radiation. J. Genet. 93, 163–167.

de Queiroz, K., 1998. The general lineage concept of species, species criteria, and the process of speciation. A conceptual unification and terminological recommendations, in: Howard, D.J., Berlocher, S.H. (Eds.), Endless Forms: Species and Speciation. Oxford University Press, New York, pp 57–75.

de Queiroz, K., 1999. The general lineage concept of species and the defining properties of the species category, in: Wilson, R.A. (Ed.), Species: New Interdisciplinary Essays. MIT Press, Cambridge, pp 49–89.

de Queiroz, K., 2005. Ernst Mayr and the modern concept of species. Proc. Natl. Acad. Sci. 102, 6600–6607. https://doi.org/10.1073/pnas.0502030102.

Denham, S.S., Brignone, N.F., Johnson, L.A., Pozner, R.E., 2019. Using integrative taxonomy and multispecies coalescent models for phylogeny reconstruction and species delimitation with the "*Nastanthus-Gamocarpha*" clade (Calyceraceae). Mol. Phylogenet. Evol. 130, 211–226. https://doi.org/10.1016/j.ympev.2018.10.015.

Drummond, A.J., Suchard, M.Z., 2010. Bayesian random local clocks, or one rate to rule them all. BMC Biol. 8, 114. https://doi.org/10.1186/1741-7007-8-114.

Dubois, A., 2003. The relationships between taxonomy and conservation biology in the century of extinctions. C. R. Biol. 326, s9–s21. https://doi.org/10.1016/S1631-0691(03)00022-2.

Duran, D.P., Herrmann, D.P., Roman, S.J., Gwiazdowski, R.A., Drummond, J.A., Hood, G.R., Egan, S.P., 2019. Cryptic diversity in the North American *Dromochorus* tiger beetles (Coleoptera: Carabidae: Cicindelinae): a congruence-based method for species discovery. Zool. J. Linn. Soc. 186, 250–285. https://doi.org/10.1093/zoolinnean/zly035.

Edgar, R.C., 2004. MUSCLE: multiple sequence alignment with high accuracy and high throughput. Nucleic Acids Res. 32, 1792–1797. https://doi.org/10.1093/nar/gkh340.

Erens, J., Miralles, A., Glaw, F., Chatrou, L.X., Vences, M., 2017. Extended molecular phylogenetics and revised systematics of Malagasy scincine lizards. Mol. Phylogenet. Evol. 107, 466–472. https://doi.org/10.1016/j.ympev.2016.12.008.

Flouri, T., Jiao, X., Rannala, B., Yang, Z., 2018. Species tree inference with BPP using genomic sequences and the multispecies coalescent. Mol. Biol. Evol. 35, 2585–2593. https://doi.org/10.1093/molbev/msy147.

Frankham, R., Ballou, J.D., Dudash, M.R., Eldridge, M.D.B., Fenster, C.B., Lacy, R.C., Mendelson, J.R. III, Porton, I.J., Ralls, K., Ryder, O.A., 2012. Implications of different species concepts for conserving biodiversity. Biol. Conserv. 153, 25–31. https://doi.org/10.1016/j.biocon.2012.04.034.

Freitas, E.S., Datta-Roy, A., Karanth, P., Grismer, L.L., Siler, C.D., 2019. Multilocus phylogeny and a new classification for African, Asian, and Indian supple and writhing skinks

(Scincidae: Lygosominae). Zool. J. Linn. Soc. 186, 1067–1096. https://doi.org/10.1093/zoolinnean/zlz001.

Gabelaia, M. Tarkhnishvili, D., Adriaens, D., 2018. Use of three-dimensional geometric morphometrics for the identification of closely related species of rock lizards (Lacertidae: *Darevskia*). Biol. J. Linn. Soc. 125, 709–717. https://doi.org/10.1093/biolinnean/bly143.

Gans, C., 1975. Tetrapod limblessness: evolution and functional corollaries. Amer. Zool. 15, 455–467. https://doi.org/10.1093/icb/15.2.455.

Garnett, S.T., Christidis, L., 2017. Taxonomy anarchy hampers conservation. Nat. 546, 25–27. https://doi.org/10.1038/546025a.

Geissler, P., Hartmann, T., Neang, T., 2012. A new species of the genus *Lygosoma* Hardwicke & Gray, 1827 (Squamata: Scincidae) from northeastern Cambodia, with an updated identification key to the genus *Lygosoma* in mainland Southeast Asia. Zootaxa. 3190: 56–68. http://dx.doi.org/10.11646/zootaxa.3190.1.

Grimer, L.L., Wood Jr., P.L., Thura, M.K., Zin, T., Quah, E.S.H., Murdoch, M.L., Grismer, M.S., Lin, A., Kyaw, H., Lwin, N., 2018a. Twelve new species of *Cyrtodactylus* Gray (Squamata: Gekkonidae) from isolated limestone habitats in east-central and southern Myanmar demonstrate high localized diversity and unprecedented microendemism. Zool. J. Linn. Soc. 182, 862–959. https://doi.org/10.1093/zoolinnean/zlx057.

Grismer, L.L., Wood Jr., P.L., Thura, M.K., Zin, T., Quah, E.S.H, Murdoch, M.L., Grismer, M.S., Li, Aung, Kyaw, H., Lwin, N., 2018b. Phylogenetic taxonomy of *Hemiphyllodactylus* Bleeker, 1860 (Squamata: Gekkonidae) with descriptions of three new species from Myanmar. J. Nat. Hist. 52, 881–915. https://doi.org/10.1080/00222933.2017.1367045.

Grismer, L.L., Wood Jr, P.L., Quah, E.S., Murdoch, M.L., Grismer, M.S., Herr, M.W., Espinoza, R.E., Brown, R.M., Lin, A., 2018c. A phylogenetic taxonomy of the *Cyrtodactylus peguensis* group (Reptilia: Squamata: Gekkonidae) with descriptions of two new species from Myanmar. PeerJ, 6, e5575. https://doi.org/10.7717/peerj.5575.

Hillis, D.M., Bull, J.J., 1993. An empirical test of bootstrapping as a method for assessing confidence in phylogenetic analysis. Syst. Biol. 42, 182–192. https://doi.org/10.1093/sysbio/42.2.182.

Hillis, D.M., 2019. Species delimitation in herpetology. J. Herpetol. 53, 3–12. https://doi.org/10.1670/18-123.

Hora, S.L., 1927. Notes on lizards in the Indian museum. III. On the unnamed collection of lizards of the family Scincidae. Rec. Indian Mus. 29, 1–6.

Huelsenbeck, J.P., Rannala, B., 2004. Frequentist properties of Bayesian posterior probabilities of phylogenetic trees under simple and complex substitution models. Syst. Biol. 53, 904–913. https://doi.org/10.1080/10635150490522629.

Huson, D.H., Bryant, D., 2006. Application of phylogenetic networks in evolutionary studies. Mol. Biol. Evol. 23, 254–267. https://doi.org/10.1093/molbev/msj030.

IUCN-SSC Species Conservation Planning Sub-Committee, 2017. Guidelines for Species Conservation Planning. Version 1.0. IUCN, Gland. https://doi.org/10.2305/IUCN.CH.2017.18.en.

Jackson, N.D., Austin, C.C., 2010.The combined effects of rivers and refugia generate extreme cryptic fragmentation within the common ground skink (*Scincella lateralis*). Evolution. 64, 409–428. https://doi.org/10.1111/j.1558-5646.2009.00840.x.

Jayaram. K.C., 1949. Distribution of lizards of peninsular India with Malayan affinities. Proc. Nat. Inst. Sci. India. 15, 403–408, pl XV.

Jones, G., 2017. Algorithmic improvements to species delimitation and phylogeny estimation under the multispecies coalescent. J. Math. Biol. 74, 447–467. https://doi.org/10.1007/s00285-016-1034-0.

Khin, K., Zaw, K., Aung, L.T., 2017. Geological and tectonic evolution of the Indo-Myanmar Ranges (IMR) in the Myanmar region, in: Barbar, A.J., Zaw, K., Crow, M.J. (Eds.), Myanmar: Geology, Resources, and Tectonics. Geol. Soc. London Mem. 48, 65–79. https://doi.org/10.1144/M48.4.

Knowlton, N., Jackson J.B.C., 1994. New taxonomy and niche partitioning on coral reefs: jack of all trades or master of some? Trends Ecol. Evol. 9, 7–9. https://doi.org/10.1016/0169-5347(94)90224-0.

Leaché, A.D., Zhu, T., Rannala, B., Yang, Z., 2019. The spectre of too many species. Syst. Biol. 68, 168–181. https://doi.org/10.1093/sysbio/syy051.

Licht, A., France-Lanord, C., Reisberg, L., Fontaine, C., Soe, A.N., Jaeger, J.J., 2013. A palaeo Tibet-Myanmar connection? Reconstructing the Late Eocene drainage system of central Myanmar using a multi-proxy approach. J. Geol. Soc. London. 170, 929–939. https://doi.org/10.1144/jgs2012-126.

Lim, G.S., Balke, M., Meier, R., 2012. Determining species boundaries in a world full of rarity: singletons, species delimitation methods. Syst. Biol. 61, 165–169. https://doi.org/ 10.1093/sysbio/syr030.

Linnaeus, C., 1758. Systema naturæ per regna tria naturæ, secundum classes, ordines, genera, species, cum characteribus, differentiis, synonymis, locis. Tomus I. Edito decima, reformata. L. Salvius, Stockholm.

Linkem, C.W., Diesmos, A.C., Brown, R.M., 2011. Molecular systematics of Philippine forest skinks (Squamata: Scincidae: *Sphenomorphus*): testing morphological hypotheses of interspecific relationships. Zool. J. Linn. Soc. 163, 1217–1243. https://doi.org/10.1111/j.1096-3642.2011.00747.x.

Lleonart, J., Salat, J., Torres, G.J., 2000. Removing allometric effects of body size in morphological analysis. J. Theor. Biol. 205, 85–93. https://doi.org/10.1006/jtbi.2000.2043.

Louys, J., Meijaard, E., 2010. Palaeoecology of Southeast Asian megafauna-bearing sites from the Pleistocene and a review of environmental changes in the region. J. Biogeog. 37, 1432–1449. https://doi.org/10.1111/j.1365-2699.2010.02297.x.

Luo, A., Ling, C., Ho, S.Y.W., Zhu, C.D., 2018. Comparison of methods for molecular species delimitation across a range of speciation scenarios. Syst. Biol. 67, 830–846. https://doi.org/10.1093/sysbio/syy011.

Manthey, U., Grossman, W., 1997. Amphibien & Reptilien Südostasiens. Natur und Tier—Verlag, Münster.

Matsuda, M., 2013. Upland farming systems coping with uncertain rainfall in the Central Dry Zone of Myanmar: how stable is indigenous multiple cropping under semi-arid conditions? Hum. Ecol. 41, 927–936. https://doi.org/10.1007/s10745-013-9604-x.

Meyer, C.P., Paulay, G., 2005. DNA barcoding: error rates based on comprehensive sampling. Plos Biol. 3, e422. https://doi.org/10.1371/journal.pbio.0030422.

Miller, M.A., Pfeiffer, W., Schwartz, T., 2010. Creating the CIPRES Science Gateway for inference of large phylogenetic trees. In: Gateway Computing Environments Workshop 2010. New Orleans: IEEE. https://doi.org/10.1109/GCE.2010.5676129.

Miralles, A., Carranza, S., 2010. Systematics and biogeography of the Neotropical genus *Mabuya*, with species emphasis on the Amazonian skink *Mabuya nigropunctata* (Reptilia, Scincidae). Mol. Phylogenet. Evol. 54, 857–869. https://doi.org/10.1016/j.ympev.2009.10.016.

Mitchell, A.H.G., 1993. Cretaceous–Cenozoic tectonic events in the western Myanmar (Burma)–Assam region. J. Geol. Soc. London. 150, 1089–1102. https://doi.org/10.1144/gsjgs.150.6.1089.

Mittermeier, R.A., Myers, N., Mittermeier, C.G., (Eds.). 1999. Hotspots: Earth's Biologically Richest and Most Endangered Terrestrial Ecoregions. CEMAX, Mexico City.

Myers, N., 1988. Threatened biotas: "hot spots" in tropical forests. Environmentalist. 8, 187–208. https://doi.org/10.1007/BF02240252.

Myers, N., 1990. The biodiversity challenge: expanded hot-spots analysis. Environmentalist. 10, 243–256. https://doi.org/10.1007/BF02239720.

Myers, N., Mittermeier, R.A., Mittermeier, C.G., da Fonseca, G.A.B., Kent, J., 2000. Biodiversity hotspots for conservation priorities. Nat. 853–858. https://doi.org/10.1038/35002501.

Nabhitabhata, J., Chan-ard, T., Chuaynkern, Y., 2000. Checklist of amphibians and reptiles in Thailand. Office of Environmental Policy and Planning, Bangkok, pp 80–92.

Ogilvie, H.A., Bouckaert, R.R., Drummond, A.J., 2017. StarBEAT2 brings faster species tree inference and accurate estimates of substitution rates. Mol. Biol. Evol. 34, 2101–2114. https://doi.org/10.1093/molbev/msx126.

Paradis, E., Schliep, K., 2018. ape 5.0: an environment for modern phylogenetics and evolutionary analyses in R. Bioinformatics. 35, 526–528. https://doi.org/10.1093/bioinformatics/bty633.

Patnaik, R., Nanda, A.C., 2010. Early Pleistocene mammalian faunas of India and evidence of connections with other parts of the world, in: Fleagle, J.G., Shea, J.J., Grine, F.E., Baden, A.L., Leakey, R.E. (Eds.), Out of Africa I: the first hominin colonization of Eurasia. Vertebrate Paleobiology and Paleoanthropology Series. Springer, Dordrecht. 129–143. https://doi.org/10.1007/978-90-481-9036-2.

Patnaik, R., 2016. Neogene–Quaternary mammalian paleobiogeography of the Indian subcontinent: an appraisal. C. R. Palevol. 15, 889–902. https://doi.org/10.1016/j.crpv.2015.11.004.

Platt, S.G., Ko, W.K., Khaing, L.L., Myo, K.M., Swe, T., Lwin, T., Rainwater, T.R., 2003. Population status and conservation of the critically endangered Burmese star tortoise *Geochelone platynota* in central Myanmar. Oryx. 37, 464–471. https://doi.org/10.1017/S0030605303000838.

Pons, J., Barraclough, T.G., Gomez-Zurita, J., Cardoso, A., Duran, D.P., Hazell, S., Kamoun, S., Sumlin, W.D., Vogler, A.P., 2006. Sequences-based species delimitation for the DNA taxonomy of undescribed insects. Syst. Biol. 55, 595–609. https://doi.org/10.1080/10635150600852011.

Poyarkov, J.N., Gorin, V.A., Zaw, T., Kretova, V.D., Gogoleva, S.S., Pawangkhanant, P., Che, J., 2019. On the road to Mandalay: contribution to the *Microhyla* Tschudi, 1838 (Amphibia: Anura: Microhylidae) fauna of Myanmar with description of two new species. Zool. Res. 40, 244–276. https://doi.org/10.24272/j.issn.2095-8137.2019.044.

Prasad W.K., Verma, A., Shahabuddin, G., 2018. An annotated checklist of the herpetofauna of the Rashtrapati Bhawan Estates, New Delhi, India. J. Threatened Taxa. 10, 11295–11302. https://doi.org/10.11609/jott.3235.10.2.11295-11302.

Prötzel, D., Heß, M., Scherz, M.D., Schwager, M. van't Padje, A., Glaw, F. 2018. Widespread bone-based fluorescence in chameleons. Sci. Rep. 8, 698. https://doi.org/10.1038/s41598-017-19070-7.

Pyron, R.A., Costa, G.C., Patten, M.A., Burbrink, F.T., 2015. Phylogenetic niche conservatism and the evolutionary basis of ecological speciation. Biol. Rev. 90, 1248–1262. https://doi.org/10.1111/brv.12154.

Quade, J., Cerling, T.E., Bowman, J.R., 1989. Development of Asian monsoon revealed by marked ecological shift during the latest Miocene in northern Pakistan. Nat. 342, 163–166. https://doi.org/10.1038/342163a0.

R Core Team., 2018. R: a language and environment for statistical computing. R Foundation for Statistical Computing. https://www.R-project.org/.

Rambaut, A., Drummond, A.J., Xie, D., Baele, G., Suchard, M.A., 2018. Posterior summarization in Bayesian phylogenetics using Tracer 1.7. Syst. Biol. 67, 901–904. https://doi.org/10.1093/sysbio/syy032.

Rannala, B., Yang, Z., 2003. Bayes estimation of species divergence times and ancestral population sizes using DNA sequences from multiple loci. Genetics. 164, 1645–1656.

Ratnam, J., Tomlinson, K.W., Rasquinha, D.N., Sankaran, M., 2016. Savannahs of Asia: antiquity, biogeography, and an uncertain future. Phil. Trans. R. Soc. B. 371, 20150305. http://dx.doi.org/10.1098/rstb.2015.0305.

Reid, N.M., Carstens, B.C., 2012. Phylogenetic estimation error can decrease the accuracy of species delimitation: a Bayesian implementation of the general mixed Yule-coalescent model. BMC Evol. Biol. 12, 196. https://doi.org/10.1186/1471-2148-12-196.

Reid, N.M., 2014. bGMYC: A Bayesian MCMC implementation of the general mixed Yule-coalescent model for species delimitation. R package version 1.0.2.

Rej, J.E., Mead, J.I., 2017. Geometric morphometric differentiation of two western USA lizards (Phrynosomatidae: Squamata): *Uta stansburiana* and *Urosaurus ornatus*, with implications for fossil identification. Bull. Southern California Acad. Sci. 116, 153–161. https://doi.org/10.3160/soca-116-03-153-161.1.

Ruane, S., 2015. Using geometric morphometrics for integrative taxonomy: an examination of head shapes of milksnakes (genus *Lampropeltis*). Zool. J. Linn. Soc. 174, 394–413. https://doi.org/10.1111/zoj.12245.

Sabaj, M.H., 2016. Standard symbolic codes for institutional resource collections in herpetology and ichthyology: an online reference. Version 6.5. American Society of Ichthyologists and Herpetologists. http://www.asih.org. (Accessed 2 November, 2019).

Seetharamaraju, M., Sreeker, R, Srinivasulu, C., Srinivasulu, B., Kaur, H., Venkateshwarlu, P., 2009. Rediscovery of Vosemer's Writhing Skink *Lygosoma vosmaerii* (Gray, 1839) (Reptilia: Scincidae) with a note on its taxonomy. J. Threatened Taxa. 12, 624–626. https://doi.org/10.11609/JoTT.o2160.624-6.

Seifan, M., Zohar, Y., Werner, Y.L., 2016. Reptile distribution may identify terrestrial islands for conservation: the Levant's Arava Valley as a model. J. Nat. Hist. 50, 2783–2801. https://doi.org/10.1080/00222933.2016.1205154.

Shimada, T., Aplin, K.P., Suzuki, H., 2010. *Mus lepidoides* (Muridae, Odentia) of Central Burma is a distinct species of potentially great evolutionary and biogeographic significance. Zool. Sci. 27, 449–459. https://doi.org/10.2108/zsj.27.449.

Shreve, B., 1940., Reptiles and amphibians from Burma with descriptions of three new skincs [sic]. Proc. New Engl. Zool. Club. 18, 17–26.

Siler, C.D., Diesmos, A.C., Brown, R.M., 2010. New loam-swimming skink, genus *Brachymeles* (Reptilia: Squamata: Scincidae) from Luzon and Catanduanes Islands, Philippines. J. Herpetol. 44, 49–60. https://doi.org/10.1670/08-318.1.

Singhal, S., Hoskin, C.J., Couper, P., Potter, S., Moritz, C., 2018. A framework for resolving cryptic species: a case study from the lizards of the Australian wet tropics. Syst. Biol. 67, 1061–1075. https://doi.org/10.1093/sysbio/syy026.

Skinner, A., Hutchinson, M.N., Lee, M.S.Y., 2013. Phylogeny and divergence times of Australian *Sphenomorphus* group skinks (Scincidae, Squamata). Mol. Phylogenet. Evol. 69, 906–918. https://doi.org/10.1016/j.ympev.2013.06.014.

Slowinski, J.B., Wüster, W., 2000. A new cobra (Elapidae: *Naja*) from Myanmar (Burma). Herpetologica. 56, 257–270.

Smith, M.A., 1943. The fauna of British India, Cey-lon and Burma, including the whole of the Indo-Chinese sub-region. Reptilia and Amphibia, Vol. III-Serpentes. Taylor and Francis, London.

Srinivasulu, C., Seetharamaraju, M., 2010. Reply to 'further comments on the systematic status of *Lygosoma vosmaerii* (Gray 1839)' by Raju Vyas. J. Threatened Taxa. 2, 675. https://doi.org/10.11609/JoTT.o2390.675.

Stamatakis, A., 2014. RAxML v.8: a tool for phylogenetic analysis and post-analysis of large phylogenies. Bioinform. 30, 1312–1313. https://doi.org/10.1093/bioinformatics/btu033.

Stoliczka, F., 1870. Observations on some Indian and Malayan Amphibia and Reptilia. J. Asiatic Soc. Bengal. 39, 134–228, pl. x–xii.

Sukumaran, J., Knowles, L.L., 2017. Multispecies coalescent delimits structure, not species. Proc. Natl. Acad. Sci. 114, 1607–1612. https://doi.org/10.1073/pnas.1607921114.

Sun, X., Wang, P., 2005. How old is the Asian monsoon system? Palaeobotanical records from China. Palaeogeog. Palaeoclim. Palaeoecol. 222, 181–222. https://doi.org/10.1016/j.palaeo.2005.03.005.

Suraprasit, K., Chaimanee, Y., Bocherens, H., Chavasseau, O., Jaeger, J.J., 2014. Systematics and phylogeny of middle Miocene Cervidae (Mammalia) from Mae Moh Basin (Thailand) and a paleoenvironmental estimate using enamel isotopy of sympatric herbivore species. J. Vertebr. Paleontol. 34, 179–194. https://doi.org/10.1080/02724634.2013.789038.

Takai, M., Saegusa, H., Htike, T., Thein, Z.M.M., 2006. Neogene mammalian fauna in Myanmar. Asian Paleoprim. 4, 143–172.

Tantipisanuh, N., Gale, G.A., 2018. Identification of biodiversity hotspot in national level—importance of unpublished data. Global Ecol. Conserv. 13, e00377. https://doi.org/10.1016/j.gecco.2018.e00377.

Theobald, W., 1876. Descriptive catalogue of the reptiles of British India. Thacker, Spink and Co., Calcutta.

Thorpe, R.S., 1975. Quantitative handling of characters useful in snake systematics with particular reference to intraspecific variation in the ringed snake *Natrix natrix* (L.). Biol. J. Linn. Soc. 7, 27–43. https://doi.org/10.1111/j.1095-8312.1975.tb00732.x.

Uetz, P. Freed, P., Hošek, J., (Eds.). 2019. The Reptile Database. http:// http://www.reptile-database.org/ (accessed 2 November, 2019)

van Hinsenbergen, D.J.J., Lippert, P.C., Dupont-Nivet, G., McQuarrie, N., Doubrovine, P.V., Spakman, W., Torsvik, T.H., 2012. Greater Indian Basin hypothesis and a two-stage Cenozoic collision between India and Asia. Proc. Natl. Acad. Sci. 109, 7659–7664. https://doi.org/10.1073/pnas.1117262109.

Vawter, L., Brown, W.M., 1986. Nuclear and mitochondrial DNA comparisons reveal extreme rate variation in the molecular clock. Science. 234, 194–196. https://doi.org/10.1126/science.3018931.

Vences, M., Lima, A., Mitalles, A., Glaw, F., 2014. DNA barcoding assessment of genetic variation in two widespread skinks from Madagascar, *Trachylepis elegans* and *T. gravenhorstii* (Squamata: Scincidae). Zootaxa. 3755, 477–484. http://dx.doi.org/10.11646/zootaxa.3755.5.7.

Vitt, L., Caldwell, J., 2013. Herpetology: an Introductory Biology of Amphibians and Reptiles. Academic Press, London.

Vyas, R., 2001. Notes on the distribution of *Lygosoma lineata* (Gray, 1839) and comments on the systematic status of *L. vosmaerii*. Hamadryad. 26, 360–361.

Vyas, R., 2010. Further comments on the systematic status of *Lygosoma vosmaerii* (Gray, 1839). J. Threatened Taxa. 2, 674. https://doi.org/10.11609/JoTT.o2377.674.

Vyas, R., 2014. Notes and comments on the distribution of two endemic *Lygosoma* skinks (Squamata: Scincidae: Lygosominae) from India. J. Threatened Taxa. 6, 6726–6732. https://doi.org/10.11609/JoTT.o3906.6726-32.

Warren, D., Geneva, A., Lanfear, R., 2017. RWTY (R We There Yet): an R package for examining convergence of Bayesian phylogenetic analyses. Mol. Biol. Evol. 34, 1016–1020. https://doi.org/10.1093/molbev/msw279.

Welton, L.J., Siler, C.D., Bennett, D., Diesmos, A., Duya, M.R., Dugay, R., Rico, E.L.B., Van Weerd, M., Brown, R.M., 2010. A spectacular new Philippine monitor lizard reveals a hidden biogeographic boundary and a novel flagship species for conservation. Biol. Letters. 6, 654–658. https://doi.org/10.1098/rsbl.2010.0119.

Wiens, J.J., Slingluff, J.L., 2001. How lizards turn into snakes: a phylogenetic analysis of body-form evolution in anguid lizards. Evolution. 55, 2303–2318. https://doi.org/10.1111/j.0014-3820.2001.tb00744.x.

Wu, C.H., Hsu, H.H., Chou, M.D., 2014. Effect of the Arakan Mountains in the northwestern Indochina Peninsula on the late May Asian monsoon transition. J. Geophys. Res. Atmos. 10, 769–779. https://doi.org/10.1002/2014JD022024.

Wu, C.H., Hsu, H.H., 2016. Role of the Indochina Peninsula narrow mountains in modulating the East Asia-Western North Pacific summer monsoon. J. Clim. 29, 4445–4459. https://doi.org/10.1175/JCLI-D-15-0594.1.

Yang, Z., 2015. The BPP program for species tree estimation and species delimitation. Curr. Zool. 61, 854–865. https://doi.org/10.1093/czoolo/61.5.854.

Yang, Z., Rannala, B., 2010. Bayesian species delimitation using multilocus sequence data. Proc. Natl. Acad. Sci. 107, 9264–9269. https://doi.org/10.1073/pnas.0913022107.

Zhang, R., Jiang, D., Zhang, Z., Yu, E., 2015. The impact of regional uplift of the Tibetan Plateau on the Asian monsoon climate. Palaeogeog. Palaeoclim. Palaeoecol. 417, 137–150. https://doi.org/10.1016/j.palaeo.2014.10.030.

Zug, G.R., Brown, H.H.K., Schulte II, J.A., Vindum, J.V., 2006. Systematics of the garden lizards, *Calotes versicolor* group (Reptilia, Squamata, Agamidae), in Myanmar: Central Dry Zone populations. Proc. California Acad. Sci. 57, 35–68.

SUPPLEMENTARY MATERIAL

Table S1
A list of all skink species described between 2014–2019 from Uetz et al. (2019) with their taxonomic authorities. To be considered cryptic for the purposes of this list, the species must previously have been recognized in the literature as a member of a different species, and subsequently was described as a new species based on genetic and morphological data (and not morphological data alone). Species considered cryptic are highlighted in blue.

Year	Species	Taxonomic Authority	Cryptic?
2014	*Brachymeles isangdaliri*	Davis, Feller, Brown & Siler	Yes
2014	*Brachymeles mapalanggaon*	Davis, Feller, Brown & Siler	Yes
2014	*Caledoniscincus pelletieri*	Sadlier, Whitaker, Wood Jr. & Bauer	No
2014	*Carlia sukur*	Zug & Kaiser	No
2014	*Carlia wundalthini*	Hoskin	No
2014	*Ctenotus superciliaris*	Rabosky, Hutchinson, Donnellan, Talaba & Lovette	Yes
2014	*Glaphyromorphus nyanchupinta*	Hoskin & Couper	No
2014	*Glaphyromorphus othelarrni*	Hoskin & Couper	No
2014	*Lipinia sekayuensis*	Grismer, Ismail, Awang, Rizal & Ahmad	No
2014	*Nannoscincus koniambo*	Sadlier, Bauer, Whitaker & Wood Jr.	No
2014	*Parvoscincus duwendorum*	Siler, Linkem, Cobb, Watters, Cummings, Diesmos & Brown	Yes
2014	*Parvoscincus manananggalae*	Siler, Linkem, Cobb, Watters, Cummings, Diesmos & Brown	Yes
2014	*Parvoscincus tikbalangi*	Siler, Linkem, Cobb, Watters, Cummings, Diesmos & Brown	Yes
2014	*Phaeoscincus ouinensis*	Sadlier, Shea & Bauer	No
2014	*Phaeoscincus taomensis*	Whitaker, Smith & Bauer	No
2014	*Plestiodon kuchinoshimensis*	Kurita & Hikida	Yes
2014	*Sigaloseps balios*	Sadlier, Bauer & Wood Jr.	No
2014	*Sigaloseps conditus*	Sadlier, Bauer & Wood Jr.	No
2014	*Sigaloseps ferrugicauda*	Sadlier, Smith, Shea & Bauer	No
2014	*Sigaloseps pisinnus*	Sadlier, Shea, Whitaker, Bauer & Wood Jr.	No
2015	*Liburnascincus artemis*	Hoskin & Couper	No
2015	*Sphenomorphus senja*	Grismer & Quah	No
2015	*Trachylepis adamastor*	Ceríaco	No
2016	*Brachymeles dalawangdaliri*	Davis, Geheber, Watters, Penrod, Feller, Ashford, Kouri, Nguyen, Shauberger, Sheatsley, Winfrey, Wong, Sanguila, Brown & Siler	Yes

2016	*Brachymeles ilocandia*	Siler, Davis, Freitas, Huron, Geheber, Watters, Penrod, Papeş, Amrein, Anwar, Cooper Hein, Manning, Patel, Pinaroc, Diesmos, Diesmos, Oliveros & Brown	Yes
2016	*Brachymeles ligtas*	Geheber, Davis, Watters, Penrod, Feller, Davey, Ellsworth, Flanagan, Heitz, Moore, Nguyen, Roberts, Sutton, Sanguila, Linkem, Brown & Siler	Yes
2016	*Eutropis austini*	Batuwita	No
2016	*Eutropis greeri*	Batuwita	No
2016	*Lerista hobsoni*	Couper, Amey & Worthington-Wilmer	No
2016	*Lerista vanderduysi*	Couper, Amey & Worthington-Wilmer	No
2016	*Lygosoma tabonorum*	Heitz, Diesmos, Freitas, Ellsworth & Grismer	Yes
2016	*Mabuya parviterrae*	Hedges, Lorvelec, Barré, Berchel, Combot, Vidal & Pavis	Yes
2016	*Madascincus miafina*	Miralles, Köhler, Glaw & Vences	Yes
2016	*Madascincus pyrurus*	Miralles, Köhler, Glaw & Vences	Yes
2016	*Paracontias ampijoroensis*	Miralles, Jono, Mori, Gandola, Erens, Köhler, Glaw & Vences	No
f2016	*Paracontias mahamavo*	Miralles, Jono, Mori, Gandola, Erens, Köhler, Glaw & Vences	No
2016	*Sphenomorphus sungaicolus*	Sumarli, Grismer, Wood Jr., Ahmad, Rizal, Ismail, Izam, Ahmad & Linkem	No
2016	*Trachylepis principensis*	Ceríaco, Marques & Bauer	Yes
2016	*Trachylepis thomensis*	Ceríaco, Marques & Bauer	Yes
2016	*Tytthoscincus batupanggah*	Karin, Das & Bauer	No
2016	*Tytthoscincus leproauricularis*	Karin, Das & Bauer	No
2016	*Tytthoscincus panchorensis*	Grismer, Muin, Wood Jr., Anuar & Linkem	No
2017	*Carlia insularis*	Afonso Silva, Santos, Ogilvie & Moritz	Yes
2017	*Carlia isostriacantha*	Afonso Silva, Santos, Ogilvie & Moritz	Yes
2017	*Ctenotus pallasotus*	Rabosky & Doughty	Yes
2017	*Ctenotus rhabdotus*	Rabosky & Doughty	Yes
2017	*Eumeces persicus*	Faizi, Rastegar-Pouyani, Rastegar-Pouyani, Nazarov, Heidari, Zangi, Orlova & Poyarkov	No
2017	*Nessia gansi*	Batuwita & Edirisinghe	No
2017	*Oligosoma awakopaka*	Jewell	No
2017	*Oligosoma elium*	Melzer, Bell & Patterson	Yes
2017	*Oligosoma kokowai*	Melzer, Bell & Patterson	Yes
2017	*Oligosoma prasinum*	Melzer, Bell & Patterson	Yes
2017	*Plestiodon lotus*	Pavón-Vázquez, Nieto-Montes de Oca, Mendoza-Hernández, Centenero-Alcalá, Santa Cruz-Padilla & Jiménez-Arcos	No
2017	*Plestiodon takarai*	Kurita, Ota & Hikida	Yes

2017	*Sphenomorphus dekkerae*	Shea	No
2017	*Trachylepis gonwouoi*	Allen, Tapondjou, Welton & Bauer	No
2017	*Tribolonotus choiseulensis*	Rittmeyer & Austin	Yes
2017	*Tribolonotus parkeri*	Rittmeyer & Austin	Yes
2017	*Tropidophorus sebi*	Pui, Karin, Bauer & Das	No
2017	*Tytthoscincus jaripendek*	Grismer, Wood Jr., Quah, Anuar, Ngadi, Mohd-Izam & Ahmad	No
2017	*Tytthoscincus kakikecil*	Grismer, Wood Jr., Quah, Anuar, Ngadi, Mohd-Izam & Ahmad	No
2017	*Tytthoscincus martae*	Grismer, Wood Jr., Quah, Anuar, Ngadi, Mohd-Izam & Ahmad	No
2017	*Tytthoscincus temasekensis*	Grismer, Wood Jr., Lim & Liang	No
2018	*Acontias albigularis*	Conradie, Busschau & Edwards	Yes
2018	*Acontias wakkerstroomensis*	Conradie, Busschau & Edwards	Yes
2018	*Carlia crypta*	Singhal, Hoskin, Couper, Potter & Moritz	Yes
2018	*Emoia beryllion*	Kraus	No
2018	*Eremiascincus rubiginosus*	Mecke & Doughty	No
2018	*Lampropholis bellendenkerensis*	Singhal, Hoskin, Couper, Potter & Moritz	Yes
2018	*Lampropholis elliotensis*	Singhal, Hoskin, Couper, Potter & Moritz	Yes
2018	*Lampropholis similis*	Singhal, Hoskin, Couper, Potter & Moritz	Yes
2018	*Lygosoma kinabatanganensis*	Grismer, Quah, Duzulkafly & Yambun	No
2018	*Lygosoma peninsulare*	Grismer, Quah, Duzulkafly & Yambun	No
2018	*Lygosoma samajaya*	Karin, Freitas, Shonleben, Grismer, Bauer & Das	No
2018	*Lygosoma siamensis*	Siler, Heitz, Davis, Freitas, Aowphol, Termprayoon & Grismer	Yes
2018	*Oligosoma hoparatea*	Whitaker, Chapple, Hitchmough, Lettink & Patterson	No
2018	*Ophiomorus kardesi*	Kornilios, Kumlutaş, Lymberakis & Ilgaz	Yes
2018	*Panaspis namibiana*	Ceríaco, Branch & Bauer	Yes
2018	*Panaspis thomensis*	Ceríaco, Soares, Marques, Bastos-Silveira, Scheinberg, Harris, Brehm & Jesus	Yes
2018	*Scincella nigrofasciata*	Neang, Chan & Poyarkov	No
2018	*Scolecoseps broadleyi*	Verburgt, Verburgt & Branch	No
2018	*Sphenomorphus yersini*	Nguyen, Nguyen, Nguyen, Orlov & Murphy	No
2018	*Tytthoscincus keciktuek*	Grismer, Wood Jr., Ahmad, Baizul-Hafsyam, Afiq-Shuhaimi, Rizal & Quah	No
2018	*Tytthoscincus monticolus*	Grismer, Wood Jr., Ahmad, Baizul-Hafsyam, Afiq-Shuhaimi, Rizal & Quah	No
2019	*Epibator insularis*	Sadlier, Debar, Chavis, Bauer, Jourdan & Jackman	No

2019	*Kuniesaurus albiauris*	Sadlier, Deuss, Bauer & Jourdan	No
2019	*Lerista alia*	Amey, Couper & Worthington-Wilmer	Yes
2019	*Lerista anyara*	Amey, Couper & Worthington-Wilmer	No
2019	*Lerista parameles*	Amey, Couper & Worthington-Wilmer	Yes
2019	*Oligosoma albornense*	Melzer, Hitchmough, Bell, Chapple & Patterson	No
2019	*Oligosoma auroraensis*	Melzer, Hitchmough, Bell, Chapple & Patterson	No
2019	*Oligosoma salmo*	Melzer, Hitchmough, Bell, Chapple & Patterson	No
2019	*Subdoluseps malayana*	Grismer, Dzukafly, Muin, Quah, Karin, Anuar & Freitas	No
2019	*Trachylepis raymondlaurenti*	Marques, Ceríaco, Bandeira, Pauwels & Bauer	Yes

Table S2
List of all new vertebrate species described from Myanmar between 2014–2019.

Group	Year	Species	Taxonomic Authority
Amphibian	2014	*Ichthyophis multicolor*	Wilkinson, Presswell, Sherratt, Papadopoulou & Gower
Amphibian	2014	*Tylototriton shanorum*	Nishikawa, Matsui & Rao
Amphibian	2016	*Limnonectes longchuanensis*	Suwannapoom, Yuan, Chen, Sulliva, & McLeod
Amphibian	2017	*Theloderma pyaukkya*	Dever
Amphibian	2018	*Tylototriton ngarsuensis*	Grismer, Wood Jr., Quah, Thura, Espinoza, Grismer, Murdoch & Lin
Amphibian	2019	*Ansonia kyaiktiyoensis*	Quah, Grismer, Wood Jr., Thura, Oaks & Lin
Amphibian	2019	*Microhyla fodiens*	Poyarkov, Gorin, Zaw, Kretova, Gogoleva, Pawangkhanant & Che
Amphibian	2019	*Microhyla irrawaddy*	Poyarkov, Gorin, Zaw, Kretova, Gogoleva, Pawangkhanant & Che
Amphibian	2019	*Tylototriton kachinorum*	Zaw, Lay, Pawangkhanant, Gorin & Poyarkov
Amphibian	2019	*Tylototriton panwaensis*	Grismer, Wood Jr., Quah, Thura, Espinoza & Murdoch
Fish	2014	*Schistura hypsiura*	Bohlen, Šlechtová & Udomritthiruj
Fish	2016	*Danio htamanthinus*	Kullander & Norén
Fish	2017	*Devario fangae*	Kullander
Fish	2017	*Devario myitkyinae*	Kullander
Fish	2017	*Lepidocephalichthys eleios*	Kottelat
Fish	2017	*Malihkaia aligera*	Kottelat
Fish	2017	*Oreoglanis hponkanensis*	Chen, Qin & Chen

Fish	2017	*Schistura indawgyiana*	Kottelat
Fish	2017	*Schistura nubigena*	Kottelat
Fish	2017	*Schistura wanlainensis*	Kottelat
Fish	2018	*Altigena malihkaia*	Zheng, Qin & Chen
Fish	2018	*Amblyceps improcerum*	Ng & Kottelat
Fish	2018	*Exostoma chaudhurii*	Ng & Kottelat
Fish	2018	*Laubuka tenella*	Kullander, Rahman, Norén & Mollah
Fish	2018	*Mustura celata*	Kottelat
Fish	2019	*Opsarius putaoensis*	Qin, Maung & Chen
Fish	2019	*Rhyacoschistura larreci*	Kottelat
Mammal	2017	*Hoolock tianxing*	Fan, He, Chen, Ortiz, Zhang, Zhao, Li, Zhang, Kimock, Wang, Groves, Turvey, Roos, Helgen & Jiang
Mammal	2017	*Murina hkakaboraziensis*	Soisook, Thaw, Kyaw, Oo, Pimsai, Suarez-Rubio & Renner
Reptile	2015	*Pareas vindumi*	Vogel
Reptile	2017	*Cyrtodactylus lenya*	Mulcahy, Thura & Zug (in Connette et al., 2017)
Reptile	2017	*Cyrtodactylus payarhtanensis*	Mulcahy, Thura & Zug (in Connette et al., 2017)
Reptile	2017	*Gyiophis salweenensis*	Quah, Grismer, Wood Jr., Thura, Zin, Kyaw, Lwin, Grismer & Murdoch
Reptile	2018	*Cyrtodactylus aunglini*	Grismer, Wood Jr., Thura, Win, Grismer, Trueblood & Quah
Reptile	2018	*Cyrtodactylus bayinnyiensis*	Grismer, Wood Jr., Thura, Quah, Murdoch, Grismer, Herr, Lin & Kyaw
Reptile	2018	*Cyrtodactylus chaunghanakwaensis*	Grismer, Wood Jr., Thura, Quah, Murdoch, Grismer, Herr, Lin & Kyaw
Reptile	2018	*Cyrtodactylus dammathetensis*	Grismer, Wood Jr., Thura, Zin, Quah, Murdoch, Grismer, Lin, Kyaw & Lwin
Reptile	2018	*Cyrtodactylus linnoensis*	Grismer, Wood Jr., Thura, Zin, Quah, Murdoch, Grismer, Lin, Kyaw & Lwin
Reptile	2018	*Cyrtodactylus linnwayensis*	Grismer, Wood Jr., Thura, Zin, Quah, Murdoch, Grismer, Lin, Kyaw & Lwin
Reptile	2018	*Cyrtodactylus meersi*	Grismer, Wood Jr., Quah, Murdoch, Grismer, Herr, Espinoza, Brown & Lin
Reptile	2018	*Cyrtodactylus myaleiktaung*	Grismer, Wood Jr., Thura, Win, Grismer, Trueblood & Quah
Reptile	2018	*Cyrtodactylus myintkyawthurai*	Grismer, Wood Jr., Quah, Murdoch, Grismer, Herr, Espinoza, Brown & Lin
Reptile	2018	*Cyrtodactylus naungkayaingensis*	Grismer, Wood Jr., Thura, Quah, Murdoch, Grismer, Herr, Lin & Kyaw
Reptile	2018	*Cyrtodactylus pharbaungensis*	Grismer, Wood Jr., Thura, Zin, Quah, Murdoch, Grismer, Lin, Kyaw & Lwin
Reptile	2018	*Cyrtodactylus pyinyaungensis*	Grismer, Wood Jr., Thura, Zin, Quah, Murdoch, Grismer, Lin, Kyaw & Lwin
Reptile	2018	*Cyrtodactylus sadanensis*	Grismer, Wood Jr., Thura, Zin, Quah, Murdoch, Grismer, Lin, Kyaw & Lwin
Reptile	2018	*Cyrtodactylus sadansinensis*	Grismer, Wood Jr., Thura, Zin, Quah, Murdoch, Grismer, Lin, Kyaw & Lwin
Reptile	2018	*Cyrtodactylus sanpelensis*	Grismer, Wood Jr., Thura, Zin, Quah, Murdoch, Grismer, Lin, Kyaw & Lwin

Reptile	2018	*Cyrtodactylus shwetaungorum*	Grismer, Wood Jr., Thura, Zin, Quah, Murdoch, Grismer, Lin, Kyaw & Lwin
Reptile	2018	*Cyrtodactlylus sinyineensis*	Grismer, Wood Jr., Thura, Zin, Quah, Murdoch, Grismer, Lin, Kyaw & Lwin
Reptile	2018	*Cyrtodactylus welpyanensis*	Grismer, Wood Jr., Thura, Zin, Quah, Murdoch, Grismer, Lin, Kyaw & Lwin
Reptile	2018	*Cyrtodactylus yathepyanensis*	Grismer, Wood Jr., Thura, Zin, Quah, Murdoch, Grismer, Lin, Kyaw & Lwin
Reptile	2018	*Cyrtodactylus ywanganensis*	Grismer, Wood Jr., Thura, Quah, Grismer, Murdoch, Espinoza & Lin
Reptile	2018	*Hemiphyllodactylus linnwayensis*	Grismer, Wood Jr., Thura, Zin, Quah, Murdoch, Grismer, Lin, Kyaw & Lwin
Reptile	2018	*Hemiphyllodactylus montawaensis*	Grismer, Wood Jr., Thura, Zin, Quah, Murdoch, Grismer, Lin, Kyaw & Lwin
Reptile	2018	*Hemiphyllodactylus tonywhitteni*	Grismer, Wood Jr., Thura, Zin, Quah, Murdoch, Grismer, Lin, Kyaw & Lwin
Reptile	2018	*Hemiphyllodactylus uga*	Grismer, Wood Jr., Zug, Thura, Grismer, Murdoch, Quah & Lin
Reptile	2018	*Hemiphyllodactylus ywanganensis*	Grismer, Wood Jr., Zug, Thura, Grismer, Murdoch, Quah & Lin
Reptile	2018	*Ptychozoon popaense*	Grismer, Wood Jr., Thura, Grismer, Brown & Stuart
Reptile	2019	*Cnemaspis thayawthadangyi*	Lee, Miller, Zug & Mulcahy
Reptile	2019	*Cnemaspis tanintharyi*	Lee, Miller, Zug & Mulcahy
Reptile	2019	*Cyrtodactylus mombergi*	Grismer, Wood Jr, Quah, Thura, Herr & Lin
Reptile	2019	*Cyrtodactylus nyinyikyawi*	Grismer, Wood Jr., Thura, Win & Quah
Reptile	2019	*Cyrtodactylus pinlaungensis*	Grismer, Wood Jr., Quah, Thura, Oaks & Lin
Reptile	2019	*Cyrtodactylus pyadalinensis*	Grismer, Wood Jr., Thura, Win & Quah

Table S3

List of samples used in this study with their associated GenBank numbers. The Clade column refers to the Bayesian Phylogenetics and Phylogeography (BPP) putative species identification for the specimen based on molecular data, and the Original Species Epithet column refers to the species that the specimen was identified as when accessioned. Museum abbreviations follow Sabaj (2016).

Species	Museum No.	Clade	Original Species Epithet	Decimal Latitude	Decimal Longitude	Elevation (m)	*BDNF*	*R35*	*RAG1*	*ND1*	*ND2*	*16S*
Lygosoma quadrupes	ENS 13639	---	---	---	---	---	---	KX774339	MK409543	KX774344	---	MG367368
Mochlus brevicaudis	MVZ 249721	---	---	8.3484	0.6011	893	HM160590	HM161064	HM161159	HM160781	---	MK414546
Mochlus guineensis	MVZ 252551	---	---	6.3672	-1.0330	---	---	MK409501	MK409528	MK409590	---	MK414548
Mochlus sundevallii	WC-DNA 1077	---	---	14.9000	37.9500	---	---	MK409516	MH130041	MK409605	MH142365	MK414562
Subdoluseps bowringii	LSUHC 6998	---	---	---	---	---	HQ907230	HQ907637	HQ907230	HQ907328	HQ907430	MN841798
Subdoluseps herberti	LSUHC 11803	---	---	6.6300	100.1800	---	---	MF981874	MN850172	MF981877	---	MN841799

Subdoluseps samajaya	CAS 259777	---	---	1.5235	110.3882	---	---	MF981876	MK409542	MF981879	---	MG020475
Riopa albopunctata	CES 14/823	---	---	---	---	---	---	---	MK409544	MK409620	---	MK414540
Riopa sp.	CAS 221110	A	*anguina*	21.0261	93.0268	---	MN850099	MN850140	MN850173	MN850204	MN850239	MN841800
Riopa sp.	CAS 221144	A	*anguina*	20.9437	92.9500	---	MN850100	MN850141	MN850174	MN850205	MN850240	MN841801
Riopa sp.	CAS 221146	A	*anguina*	20.8732	92.9296	---	MN850101	MN850142	MN850175	MN850206	MN850241	MN841802
Riopa sp.	CAS 210669	B	*lineolata*	20.9046	95.2337	---	MN850102	MN850143	MN850176	MN850207	MN850242	MN841803
Riopa sp.	CAS 230414	B	*bowringii*	17.0489	96.0939	23	MN850103	MK409505	MK409532	MK409594	MN850243	MK414552
Riopa sp.	CAS 231325	B	*lineolata*	20.8979	95.2344	710	MN850104	MN850144	MN850177	MN850208	MN850244	MN841804
Riopa sp.	CAS 206647	C	*anguina*	17.7199	94.5404	---	MN850105	MN850145	MN850178	MN850209	MN850245	MN841805
Riopa sp.	CAS 206648	C	*anguina*	17.7177	94.5321	---	MN850106	MN850146	MN850179	MN850210	MN850246	MN841806
Riopa sp.	CAS 223198	C	*anguina*	19.3099	94.1501	---	MN850107	MN850147	---	MN850211	MN850247	MN841807
Riopa sp.	CAS 223228	C	*anguina*	19.3136	94.1461	---	MN850108	MK409503	MK409530	MK409592	MN850248	MK414550
Riopa sp.	CAS 223229	C	*anguina*	19.3136	94.1461	---	MN850109	---	---	MN850212	MN850249	MN841808
Riopa sp.	CAS 223232	C	*anguina*	19.3144	94.1490	---	MN850110	---	---	MN850213	MN850250	MN841809
Riopa sp.	CAS 239204	D	*anguina*	25.6738	95.5906	160	MN850111	MN850148	MN850180	MN850214	MN850251	MN841810
Riopa sp.	CAS 216328	E	*popae*	23.0682	96.2243	---	MN850112	MN850149	MN850181	MN850215	MN850252	MN841811
Riopa sp.	CAS 232289	F	popae	25.4761	95.6183	226	MN850113	MN850150	MN850182	MN850216	MN850253	MN841812
Riopa sp.	CAS 232549	F	*lineolata*	25.1893	96.2936	221	MN850114	MN850151	MN850183	MN850217	MN850254	MN841813
Riopa sp.	CAS 232587	F	*bowringii*	25.1861	96.2899	222	MN850115	MN850152	MN850184	MN850218	MN850255	MN841814
Riopa sp.	CAS 233085	F	*bowringii*	25.2834	96.2899	224	MN850116	MN850153	MN850185	MN850219	MN850256	MN841815
Riopa sp.	CAS 233106	F	*popae*	24.9805	96.3543	235	MN850117	MN850154	MN850186	MN850220	MN850257	MN841816
Riopa sp.	CAS 241537	F	sp.	25.1831	96.2902	199	MN850118	MN850155	MN850187	MN850221	MN850258	MN841817
Riopa sp.	CAS 231327	G	*popae*	20.8979	95.2344	710	MN850119	MF981875	MK409534	MF981878	MN850259	MK414554
Riopa sp.	CAS 230491	H	sp.	21.0819	96.3626	264	MN850120	MN850156	MN850188	MN850222	MN850260	MN841818
Riopa sp.	CAS 214071	I	*lineolata*	20.8861	95.2263	---	MN850121	---	---	MN850223	MN850261	MN841819
Riopa sp.	CAS 213615	J	*lineolata*	20.0654	94.6242	---	MN850122	MK409506	MK409533	MK409595	---	MK414553
Riopa sp.	CAS 213826	J	*lineolata*	20.1917	94.4599	---	MN850123	MN850157	MN850189	MN850224	MN850262	MN841820
Riopa sp.	CAS 243147	J	sp.	21.9300	94.2021	332	MN850124	---	---	MN850225	MN850263	MN841821
Riopa sp.	CAS 240673	K	sp.	24.7544	96.3481	219	MN850125	MK409508	MK409535	MK409597	MN850264	MK414556
Riopa sp.	CAS 206645	L	*anguina*	22.3052	94.4794	---	MN850126	MN850158	MN850190	MN850226	MN850265	MN841822
Riopa sp.	CAS 206646	L	*anguina*	22.3053	94.4794	---	MN850127	MN850159	MN850191	MN850227	MN850266	MN841823

Riopa sp.	CAS 210184	L	*anguina*	22.3094	94.4208	---	MN850128	MN850160	MN850192	---	MN850267	MN841824
Riopa sp.	CAS 210255	L	*anguina*	22.3223	94.4865	---	MN850129	MN850161	MN850193	MN850228	MN850268	MN841825
Riopa sp.	CAS 210503	L	*popae*	22.3170	94.4701	---	MN850130	MN850162	MN850194	MN850229	MN850269	MN841826
Riopa sp.	CAS 215536	L	*lineolata*	22.3181	94.4573	---	MN850131	MN850163	MN850195	MN850230	MN850270	MN841827
Riopa sp.	CAS 215537	L	*lineolata*	22.3181	94.4573	---	MN850132	MN850164	MN850196	MN850231	MN850271	MN841828
Riopa sp.	CAS 215589	L	*anguina*	22.3082	94.5030	---	MN850133	MN850165	MN850197	MN850232	MN850272	MN841829
Riopa sp.	CAS 215698	L	*anguina*	22.3064	94.5503	---	MN850134	MN850166	MN850198	MN850233	MN850273	MN841830
Riopa sp.	CAS 215699	L	*anguina*	22.3064	94.5503	---	MN850135	MN850167	MN850199	MN850234	MN850274	MN841831
Riopa sp.	CAS 215717	L	*lineolata*	22.2662	94.6176	---	MN850136	MN850168	MN850200	MN850235	MN850275	MN841832
Riopa sp.	CAS 234962	L	*anguina*	21.1925	94.0497	1722	MN850137	MN850169	MN850201	MN850236	MN850276	MN841833
Riopa sp.	CAS 243102	L	sp.	22.2112	94.1718	225	MN850138	MN850170	MN850202	MN850237	MN850277	MN841834
Riopa sp.	CAS 243133	L	sp.	21.9186	94.2321	361	MN850139	MN850171	MN850203	MN850238	MN850278	MN841835

Table S4
Uncorrected ND2 p-distance between each individual.

Individual	CAS 223229	CAS 223232	CAS 206647	CAS 206648	CAS 215699	CAS 223228	CAS 232289	CAS 241537	CAS 233106	CAS 232549	CAS 233085	CAS 232587	CAS 215589	CAS 206645	CAS 234962	CAS 215536	CAS 215537
CAS 223229	---																
CAS 223232	0.030	---															
CAS 206647	0.056	0.058	---														
CAS 206648	0.056	0.058	0.005	---													
CAS 215699	0.034	0.006	0.061	0.061	---												
CAS 223228	0.034	0.006	0.061	0.061	0.006	---											
CAS 232289	0.116	0.122	0.098	0.096	0.122	0.122	---										
CAS 241537	0.116	0.122	0.098	0.096	0.122	0.122	0.005	---									
CAS 233106	0.116	0.122	0.098	0.096	0.122	0.122	0.003	0.003	---								
CAS 232549	0.116	0.122	0.098	0.096	0.122	0.122	0.003	0.003	0.000	---							
CAS 233085	0.117	0.123	0.099	0.098	0.123	0.123	0.005	0.005	0.002	0.002	---						
CAS 232587	0.117	0.123	0.099	0.098	0.123	0.123	0.005	0.005	0.002	0.002	0.003	---					
CAS 215589	0.128	0.125	0.123	0.122	0.122	0.123	0.134	0.134	0.134	0.134	0.133	0.136	---				

CAS 206645	0.127	0.123	0.123	0.122	0.120	0.122	0.134	0.134	0.134	0.134	0.133	0.136	0.026	---	[redacted]			
CAS 234962	0.136	0.133	0.125	0.127	0.130	0.131	0.137	0.137	0.137	0.137	0.136	0.139	0.058	0.038	---			
CAS 215536	0.131	0.125	0.127	0.125	0.122	0.123	0.134	0.134	0.134	0.134	0.133	0.136	0.003	0.023	0.055	---		
CAS 215537	0.128	0.125	0.123	0.122	0.122	0.123	0.130	0.130	0.130	0.130	0.128	0.131	0.008	0.021	0.053	0.008	---	
CAS 210503	0.128	0.125	0.123	0.122	0.122	0.123	0.130	0.130	0.130	0.130	0.128	0.131	0.008	0.021	0.053	0.008	0.000	
CAS 243102	0.136	0.130	0.122	0.120	0.127	0.128	0.130	0.130	0.130	0.130	0.128	0.131	0.034	0.020	0.044	0.034	0.029	
CAS 243133	0.134	0.134	0.127	0.125	0.134	0.133	0.130	0.130	0.130	0.130	0.128	0.131	0.037	0.023	0.049	0.037	0.030	
CAS 206646	0.127	0.127	0.125	0.123	0.123	0.125	0.130	0.130	0.130	0.130	0.128	0.131	0.017	0.015	0.050	0.017	0.012	
CAS 210184	0.127	0.123	0.122	0.120	0.120	0.122	0.128	0.128	0.128	0.128	0.127	0.130	0.009	0.023	0.055	0.009	0.002	
CAS 210255	0.131	0.125	0.127	0.125	0.122	0.123	0.134	0.134	0.134	0.134	0.133	0.136	0.003	0.023	0.055	0.000	0.008	
CAS 213826	0.142	0.139	0.131	0.130	0.136	0.137	0.134	0.134	0.134	0.134	0.133	0.136	0.038	0.029	0.049	0.038	0.037	
CAS 214164	0.140	0.140	0.128	0.127	0.137	0.139	0.131	0.131	0.131	0.131	0.130	0.133	0.040	0.034	0.053	0.040	0.038	
CAS 231445	0.131	0.134	0.127	0.125	0.131	0.133	0.133	0.133	0.133	0.133	0.131	0.134	0.037	0.030	0.053	0.040	0.038	
CAS 214071	0.122	0.125	0.114	0.113	0.122	0.125	0.127	0.130	0.127	0.127	0.125	0.128	0.087	0.093	0.104	0.090	0.088	
CAS 230414	0.088	0.081	0.082	0.078	0.078	0.081	0.119	0.119	0.119	0.119	0.120	0.117	0.133	0.122	0.128	0.130	0.130	
CAS 210669	0.090	0.088	0.084	0.081	0.088	0.091	0.130	0.130	0.130	0.130	0.131	0.128	0.142	0.137	0.143	0.139	0.137	
CAS 231325	0.090	0.088	0.084	0.081	0.088	0.091	0.130	0.130	0.130	0.130	0.131	0.128	0.142	0.137	0.143	0.139	0.137	
CAS 231440	0.130	0.127	0.127	0.125	0.123	0.125	0.123	0.123	0.123	0.123	0.125	0.122	0.093	0.082	0.090	0.093	0.085	
CAS 243147	0.110	0.110	0.105	0.104	0.107	0.108	0.110	0.110	0.110	0.110	0.111	0.108	0.084	0.072	0.085	0.084	0.082	
CAS 221110	0.093	0.095	0.091	0.090	0.093	0.096	0.113	0.113	0.113	0.113	0.114	0.114	0.122	0.114	0.120	0.122	0.122	
CAS 214165	0.093	0.095	0.091	0.090	0.093	0.096	0.116	0.116	0.116	0.116	0.117	0.117	0.119	0.111	0.120	0.119	0.119	
CAS 215698	0.093	0.095	0.091	0.090	0.093	0.096	0.113	0.113	0.113	0.113	0.114	0.114	0.122	0.114	0.120	0.122	0.122	
CAS 239204	0.127	0.122	0.110	0.108	0.119	0.122	0.087	0.087	0.087	0.087	0.085	0.088	0.125	0.122	0.123	0.122	0.120	
CAS 216328	0.123	0.122	0.117	0.116	0.119	0.122	0.090	0.090	0.090	0.090	0.091	0.091	0.131	0.120	0.130	0.131	0.130	
CAS 231327	0.128	0.122	0.108	0.104	0.120	0.120	0.127	0.127	0.127	0.127	0.128	0.125	0.123	0.117	0.128	0.123	0.120	
CAS 230491	0.119	0.120	0.113	0.111	0.119	0.122	0.123	0.125	0.123	0.123	0.125	0.122	0.117	0.114	0.119	0.117	0.117	
CAS 240673	0.143	0.143	0.133	0.134	0.143	0.145	0.145	0.145	0.145	0.145	0.143	0.146	0.107	0.096	0.082	0.104	0.102	

Table S4 Continued
Uncorrected ND2 p-distance between each individual.

Individual	CAS 210503	CAS 243102	CAS 243133	CAS 206646	CAS 210184	CAS 210255	CAS 213826	CAS 214164	CAS 231445	CAS 214071	CAS 230414	CAS 210669	CAS 231325	CAS 231440	CAS 243147	CAS 221110	CAS 214165
CAS 243102	0.029	---															
CAS 243133	0.030	0.024	---														
CAS 206646	0.012	0.023	0.026	---													
CAS 210184	0.002	0.030	0.032	0.014	---												
CAS 210255	0.008	0.034	0.037	0.017	0.009	---											
CAS 213826	0.037	0.030	0.034	0.030	0.038	0.038	---										
CAS 214164	0.038	0.030	0.035	0.032	0.040	0.040	0.008	---									
CAS 231445	0.038	0.029	0.032	0.032	0.040	0.040	0.020	0.021	---								
CAS 214071	0.088	0.098	0.099	0.091	0.090	0.090	0.093	0.095	0.099	---							
CAS 230414	0.130	0.127	0.133	0.131	0.128	0.130	0.133	0.136	0.125	0.133	---						
CAS 210669	0.137	0.142	0.148	0.142	0.136	0.139	0.148	0.145	0.137	0.140	0.047	---					
CAS 231325	0.137	0.142	0.148	0.142	0.136	0.139	0.148	0.145	0.137	0.140	0.047	0.000	---				
CAS 231440	0.085	0.088	0.090	0.091	0.087	0.093	0.082	0.087	0.087	0.096	0.117	0.125	0.125	---			
CAS 243147	0.082	0.082	0.090	0.082	0.084	0.084	0.085	0.090	0.084	0.095	0.104	0.113	0.113	0.056	---		
CAS 221110	0.122	0.122	0.125	0.123	0.123	0.122	0.128	0.123	0.120	0.125	0.104	0.111	0.111	0.120	0.108	---	
CAS 214165	0.119	0.119	0.122	0.120	0.120	0.119	0.125	0.120	0.117	0.122	0.104	0.111	0.111	0.117	0.105	0.003	---
CAS 215698	0.122	0.122	0.125	0.123	0.123	0.122	0.128	0.123	0.120	0.125	0.104	0.111	0.111	0.120	0.108	0.000	0.003
CAS 239204	0.120	0.128	0.128	0.120	0.119	0.122	0.136	0.134	0.134	0.134	0.123	0.134	0.134	0.136	0.116	0.111	0.114
CAS 216328	0.130	0.120	0.125	0.123	0.128	0.131	0.125	0.123	0.122	0.125	0.128	0.136	0.136	0.125	0.108	0.117	0.117
CAS 231327	0.120	0.117	0.127	0.122	0.119	0.123	0.125	0.128	0.122	0.122	0.111	0.131	0.131	0.125	0.116	0.125	0.128
CAS 230491	0.117	0.116	0.119	0.119	0.116	0.117	0.122	0.119	0.114	0.127	0.125	0.134	0.134	0.130	0.107	0.127	0.127
CAS 240673	0.102	0.096	0.107	0.099	0.104	0.104	0.101	0.099	0.101	0.125	0.154	0.157	0.157	0.117	0.114	0.128	0.128

Table S5
The substitution models for each partition determined by bModelTest.

Partition	Substitution Model	Has Equal Base Frequencies	Has Rate Heterogeneity	Gamma Shape Parameter	Has Invariable sites	Proportion of Invariable Sites
BDNF	TN93	Yes	Yes	0.221	Yes	0.947
R35	TN93	Yes	Yes	0.348	Yes	0.772
RAG1	TN93	Yes	Yes	0.464	Yes	0.793
ND1_1	TN93	No	Yes	0.407	Yes	0.386
ND1_2	TN93	No	Yes	0.211	Yes	0.705
ND1_3	TN93	No	Yes	0.219	No	---
ND2_1	TN93	No	Yes	0.336	Yes	0.265
ND2_2	TN93	No	Yes	0.180	Yes	0.610
ND2_3	TN93	No	Yes	3.239	No	---
16S	TN93	No	Yes	0.150	Yes	0.635

Table S6
Percent variation and loadings of the first two principal components (PC) in the mensural and meristic principal components analyses.

MENSURAL	PC1	PC2
Percent Variation	36.5%	13.6%
AGD	0.101	-0.371
MBW	-0.297	-0.374
TW	-0.287	-0.337
TD	-0.325	-0.328
HL	-0.278	0.057
HW	-0.356	-0.061
HD	-0.346	-0.078
ED	-0.224	0.272
END	-0.194	0.366
SNL	-0.232	0.307
IND	-0.219	-0.233
FLL	-0.339	0.210
HLL	-0.292	0.296
MERISTIC	**PC1**	**PC2**
Percent Variation	45.0%	21.1%
MBSRC	0.532	-0.795
AGSRC	0.198	0.457

PVSRC	0.461	0.260
FinIIILam	-0.453	0.201
ToeIVLam	-0.510	0.226

Chapter 3: Historical Biogeography of *Lygosoma* group skinks across the Old World Tropics

Elyse S. Freitas | Nicolas Poyarkov | Aniruddha Datta-Roy | K. Praveen Karanth | Cameron D. Siler

Formatted for Journal of Biogeography

Abstract

Aim: This study investigates the historical biogeography of *Lygosoma* group skinks across the Old World tropics and seeks to understand how large-scale geological and climatic processes affected diversification of the clade. In particular, we focus on the role of the geological evolution of India and mainland Southeast Asia in facilitating dispersal and dispersion of species across large geographic areas.

Location: Africa, South Asia, Southeast Asia, and the Sunda Shelf.

Methods: We conducted Bayesian fossilized birth-death divergence dating for 40 ingroup lineages and species of the genera *Lygosoma*, *Mochlus*, *Riopa*, and *Subdoluseps* on a concatenated alignment of nuclear and mitochondrial genes. We reconstructed ancestral ranges and estimated shifts in evolutionary rates and species through time for all genera. We also investigated the effects of geographic sampling on our biogeographic results by sub-sampling our phylogenetic results and generating null distributions of the probabilities of ancestral ranges.

Results: We found that *Lygosoma* group skinks began to diversify 53.5 mya (68.7–40.6) from an ancestral range that included India and dispersed throughout the Old World tropics. Diversification continued throughout the Eocene and Miocene and was not accompanied by

shifts in evolutionary rates. Our resampling analyses indicated that biogeographic reconstruction is influenced by the geographic sampling.

Main conclusions: The collision of the Indian subcontinent with the Eurasian had profound effects on species across the Old World tropics, including *Lygosoma* group skinks. However, most the estimated diversification dates for the clade predate uplift of the Himalayas and onset of the South Asian monsoon weather pattern, suggesting that diversification was mainly facilitated by dispersion of species across wide geographic areas, along with dispersal from India to Africa. However, increased sampling across the Old World tropics is needed to confirm our hypotheses.

Keywords: dispersal, dispersion, fossilized birth-death dating, geographic sampling, India-Eurasia collision, Scincidae,

1 | INTRODUCTION

The modern distributions of higher-level taxa are influenced by geological and climatic processes that occur across large temporal and spatial scales (Morrone & Crisco, 1995; Wiens & Donoghue, 2004), including plate tectonics, emergent land area, orogeny, erosion, sea level changes, ocean currents, and climate change (Hall, 2009). These processes provide the backdrop for evolution, dispersal, and extinction of species over millions of years (Lomolino et al., 2010). By reconstructing the history of diversification of extant taxa through time in relation to geologic and climatic processes, researchers can infer the historical biogeography and evolution of global biodiversity and gain insights into the origin and diversification of major clades (e.g. Gamble et al., 2008; Karin et al., 2016; Yuan et al., 2016).

Of particular interest to historical biogeographers is the evolution and diversification of clades across the Old World tropics. Located between 30º N and 30º S across Africa, Australia, Eurasia, and parts of the Pacific (Fig. 1), the Old World tropics is a geologically complex region, composed of multiple continental plates, terranes, and oceanic islands (Hall, 2009). This region is recognized for its high biodiversity (Myers et al., 2000), and comprises six major biogeographic realms: (1) sub-Saharan Africa, (2) the Indian subcontinent, (3) the Philippines, (4) mainland Southeast Asia, (5) Sundaland, and (6) Wallacea (Fig. 1). Recently, attention has been given to the role animal and plant dispersal has played in shaping current biodiversity within biogeographic realms, focusing on the impacts of large-scale geological and climatic changes on biotic exchange between realms (Brown et al., 2013; de Bruyn et al., 2014, Klaus et al., 2016). For example, the impact of the Indian supercontinent with the Eurasian supercontinent and the resulting uplift of the Himalayas, opened up new rocky habitats for *Cyrtodactylus* geckos and facilitated eastward and westward dispersal of the clade from a proto-trans-Himalayan ancestral range into Southeast Asia and the Western Himalayas (Agarwal et al., 2014).

The modern geography of the Old World tropics formed from millions of years of continental fragmentation, amalgamation, and volcanic activity (McLoughlin, 2001; Hall, 1996, 2009, 2011; Chatterjee et al., 2017). After the collision of the Indian subcontinent with the Eurasian subcontinent approximately 59–55 million years ago (mya) in the Eocene (Zhang et al., 2012; Hu et al., 2016; Chatterjee et al., 2017) the spatial configuration of Africa, India, mainland Southeast Asia, and Sundaland, has remained mostly consistent (Hall, 2009; Potter & Szatmari, 2009). Wallacea was formed beginning 23 mya when the Australian plate collided with Sundaland near western Sulawesi causing mountain building and widespread volcanism across Wallacea and leading to the formation of oceanic islands in the region (Hall, 2009, 2011).

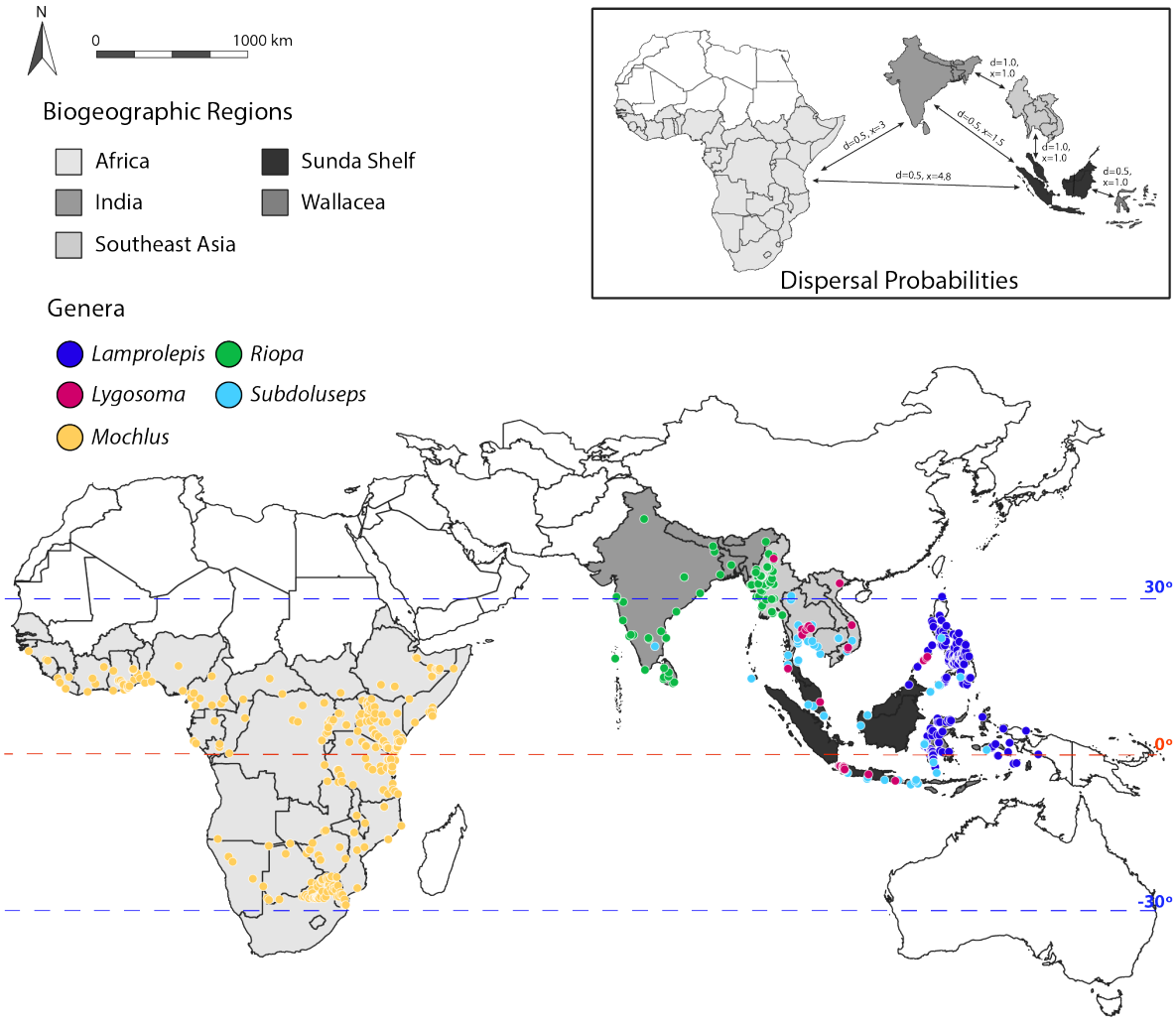

Figure 1 Map of the Old World tropics with major biogeographic regions mentioned in text shaded in gray and the localities of *Lygosoma* group skink individuals indicated by a color dot, with the color corresponding to the genus. Data on localities obtained from GBIF (accessed January, 2020). Blue dashed lines indicate the northern and southern boundaries of the Old World tropics at 30º north and south, and the red dashed line denotes the equator. The inset map shows the dispersal probabilities and distance modifiers used in our biogeographic analyses. Distances between biogeographic regions in the inset are not to scale.

In addition to spatial geographical evolution, the topography and climate of the Old World tropics has undergone major changes in the last 55 million years (Morely, 2012; Chatterjee et al., 2017). Patterns of ocean circulation changed after the break-up of Gondwana and the subsequent northward movement of Africa, Australia, and India, which resulted in global cooling and aridifying; this changing climate was later exacerbated by the uplift of major mountain belts and the by the permanent formation of the Antarctic ice sheet 14 mya (Zachos et al., 2001; Potter &

Szatmari, 2009). In the Old World tropics, the collision between India and Eurasia had profound consequences on the orography and climate of South and Southeast Asia. At the time of collision, both India and Southeast Asia had warm and humid climates with seasonal precipitation (Licht et al., 2014; Spicer et al., 2017; Shukla & Mehrotra, 2018), which may have been driven by seasonal transitions of the Intertropical Convergence Zone (Spicer et al., 2017). However, the collision initiated the uplift of the Tibetan Plateau starting 50 mya and Himalayan mountains starting 30 mya, which created inland rain shadows across central Asia (Chatterjee et al., 2013, 2017) and drove the formation of the South and East Asian monsoon systems (Sun & Wang, 2005; Clift et al., 2008; Zhang et al., 2015; Chatterjee et al., 2017). The monsoons increased total precipitation, rainfall seasonality, and humidity across South Asia, Southeast Asia, Sundaland, and eastern China (Sun &Wang, 2005; Clift et al., 2008; Morley, 2012) and the South Asian monsoon has large effect on the seasonally predominate surface currents across the Indian Ocean (Schott et al, 2009). Although the exact timing of onset of both systems remains controversial, studies have suggested that they were established by 24 mya and have experienced increases and decreases in intensity across the Miocene (Sun & Wang, 2005; Clift et al., 2008; Sanyal et al., 2010). These shifts in intensity have been attributed to orographic changes in the region (Clift et al., 2008; Sanyal et al., 2010) and external forces including the growth of the Antarctic ice sheet (Ao et al., 2016).

Despite the seasonally high rainfall that characterizes the Asian monsoon systems, increasing global aridity throughout the Miocene, Pliocene, and Pleistocene led to major shifts in tropical Asian ecosystems. Fossil evidence indicate the spread of C4 grasslands throughout South Asia starting 16 mya (Ratnam et al., 2016) and becoming dominant 9–7 mya (Quade et al., 1989; Takai et al., 2006; Ratnam et al., 2016), which may have facilitated exchange of open-grassland-

adapted fauna between Africa, South Asia, and Southeast Asia (Barry et al., 1985, 1991; Suraprasit et al., 2014; Patnaik et al., 2016). Glacial-interglacial cycles in the Pliocene and Pleistocene changed emergent land area across the Philippines, Sundaland and Wallacea, with glacial periods corresponding to low sea levels and allowing faunal exchange across formerly disjunct areas (Voris, 2000; Zhong et al., 2004; Lohmann et al., 2011; Brown et al., 2013).

Faunal exchange between biogeographic regions in the Old World tropics followed by species-level diversification within biogeographic regions has occurred repeatedly through time. Dispersal and diversification patterns have been well documented in and between the Philippines, Sundaland, and Wallacea, (e.g. Gorog et al., 2004; Esselstyn et al., 2009; Oliveros & Moyle, 2010; Siler et al., 2010, 2012; Thomas et al., 2012; Linkem et al., 2013; Barley et al., 2015; Beck et al., 2017; Tänzler et al., 2016; O'Connell et al., 2018; Rowsey et al., 2018; Reilly et al., 2018, 2019; Rowe et al., 2019; Tsang et al., 2020), in which island archipelagos and changing sea levels create a natural laboratory for such research. These island studies have suggested that *in-situ* diversification occurs following dispersal to new areas (Esselstyn et al., 2009; Oliveros & Moyle, 2010; Siler et al., 2012; Barley et al., 2015; Tänzler et al., 2017; Rowe et al., 2019), and that dispersal between biogeographic regions is common (Esselstyn et al. 2009; Linkem et al., 2013; Tänzler et al., 2017; Rowe et al., 2019; Tsang et al., 2020). Following dispersal, clades experience an increase in speciation rate that then slows over time, which is attributed to increased ecological opportunity post colonization. (Esselstyn et al., 2009; Rowe et al., 2019). Nevertheless, in their study on murid rodents across Wallacea and the Sunda Shelf, Rowe et al. (2019) found that while diversification rates increased following colonization, there were no statistically significant rate shifts from the Muridae background speciation rate. In contrast, stagnant or decreasing diversification rates, as found in *Rhacophorus* frogs when they

dispersed across islands in Sundaland, suggest that habitats have reached equilibrium (O'Connell et al., 2018).

In contrast, patterns of dispersal and diversification of species across mainland biogeographic regions in the Old World tropics (Africa, India, mainland Southeast Asia) have received less attention; however, these studies have also shown the ability of species to disperse across major biogeographic barriers (e.g. Bocxlaer et al., 2009). The role of India in facilitating faunal exchange across the Old World tropics is of particular interest to researchers studying the historical biogeography of clades in the region. Previously, it was hypothesized that India was isolated after breaking off from Gondwana—the Noah's Arc hypothesis (McKenna, 1973), but recent fossil data (Briggs, 2003; Rust et al., 2010; Chatterjee et al., 2017; Stebner et al., 2017, Thein et al., 2017) and phylogenetic metadata studies (Klaus et al., 2016) suggest that faunal exchange between the subcontinent and other areas was dynamic throughout India's northward journey (Klaus et al., 2016). Recent molecular phylogenetic studies on the historical biogeography of widespread higher-level vertebrate clades across the continental Old World tropics suggest that a majority of the clades that have been studied that diversified after the collision of India and Eurasia originated in and subsequently dispersed out of Southeast Asia, (Adenominae toads [Bocxlaer et al., 2011]; *Boiga* snakes [although the sister genus is in Africa, Weinell et al., in press]; Draconinae agamids [Grismer et al., 2016]; *Eutropis* skinks [Barley et al., 2015]; *Hylarana* group frogs [Oliver et al., 2015]; *Tersiphone* flycatchers [Fabre et al., 2012]; and *Varanus* monitor lizards [Vidal et al., 2012]), although there is also evidence that clades originated in and subsequently dispersed out of Africa (Rhacophoridae frogs [Li et al., 2013]; Campephagidae birds [Pepke et al., 2019]). In most cases (but see Li et al., 2013; Grismer et al., 2016), the geologic and climatic factors that facilitate dispersal between these mainland

biogeographic regions are not discussed, with attention instead focused on the biogeography of the focal clades among island systems. Here we investigate the historical continental and island biogeography of a widespread clade of scincid lizards across the Old World tropics, focusing on diversification patterns of continental lineages and the role of India played in the clade's modern distribution.

Lizards in the Family Scincidae (skinks) comprise more than 1,600 species (Uetz et al., 2020) distributed globally, with species found across diverse habitats on every continent except Antarctica (Vitt & Caldwell, 2013). Trans-oceanic dispersal within the Scincidae is common, allowing species to colonize oceanic islands and landmasses separated by large bodies of water (Rocha et al., 2006; Carranza et al., 2008; Linkem et al., 2013; Skinner et al., 2013; Karin et al., 2016), indicating that skinks are remarkable dispersers across inhospitable boundaries. Previous molecular phylogenetic studies have suggested that crown scincids began to diversify approximately 100 mya in the Cretaceous (Wiens et al., 2006; Skinner et al., 2011; Burbrink et al., 2019), although a study by Tałanda (2018) placed the fossil lizard *Ardeosaurus brevipes*, from the Ettling Quarry in present-day Germany, within Scincidae, which suggests that the family originated much earlier in the Jurassic approximately 157–152 mya in the Laurasia supercontinent.

Lygosoma group skinks comprise five genera of predominately small, elongate-bodied, semifossorial lizards (with the exception of *Lamprolepis*, which is larger and arboreal) distributed across the Old World tropics (Freitas et al., 2019): *Lamprolepis* found in the Philippines and across Wallacea, *Lygosoma* found in mainland Southeast Asia and the Sundaland, *Mochlus* found in sub-Saharan Africa, *Riopa* found in India and western mainland Southeast Asia, and *Subdoluseps* found in India, mainland Southeast Asia, Sundaland, and

Wallacea (Fig. 1). The broad distribution of this clade across the six major biogeographic regions in the Old World tropics allows us to investigate the effects of the geologic and climatic evolution of the region on species diversification. Divergence dating on major lineages within the Lygosominae subfamily of skinks to which *Lygosoma* group skinks belong suggests that the clade began to diversify 56.8–21.8 mya (mean=38.2 mya; Skinner et al., 2011), which indicates that diversification of this group occurred after the India-Eurasia collision. However, there are no divergence timing data for genus- and species-level diversification of *Lygosoma* group skinks, so that how orography and climate changes across the Old World tropics impacted this clade is unknown. The highest species-level diversity of *Lygosoma* group skinks are found in mainland Southeast Asia, and we hypothesize that this region represents the origin of diversity of the group (Croizat et al., 1974), in line with most previous higher level taxonomic studies of the region (e.g. Barley et al., 2015; Oliver et al., 2015). Previous phylogenetic studies of *Lygosoma* group skinks have revealed that Indian species are not monophyletic, suggesting multiple dispersals between India and mainland Southeast Asia relatively early in the diversification history of the group (Datta-Roy et al., 2014; Freitas et al., 2019). In contrast, species from Africa form a clade, which suggests a single dispersal event to Africa followed by species-level diversification. Using an updated phylogeny with increased taxonomic and genetic sampling, we investigate the timing of diversification, reconstruct the biogeographic history, and examine diversification rates of *Lygosoma* group skinks to test the following hypotheses: **(1)** *Lygosoma* group skinks initially diversified in mainland Southeast Asia and subsequently dispersed to India and Africa after the collision of the Indian subcontinent with the Asian subcontinent; **(2)** dispersal to Africa was transoceanic from India facilitated by ocean currents that established due to the onset of the South Asian Monsoon; **(3)** Miocene cooling and aridification increased species-level

diversification rates of *Mochlus* in Africa and *Riopa* in India and mainland Southeast Asia; and **(4)** sea level changes in the Pliocene and Pleistocene facilitated the dispersal of *Lygosoma* and *Subdoluseps* into the Sundaland.

2 | MATERIALS AND METHODS

2.1 | Taxonomic sampling

2.1.1 | Extant taxa

Divergence dating and biogeographic analyses are impacted by the taxonomic sampling of the phylogeny (Heath et al., 2008; Schulte II, 2013; Soares and Schrago, 2015) with low taxonomic sampling affecting the precision of the dating estimates when rate heterogeneity among lineages is high. Therefore, we used the most comprehensive sampling of *Lygosoma* group skinks to date for phylogenetic reconstruction and biogeographic analyses, including one member of each recognized species for which we had sampling (25 species included of 52 recognized species [25/52] consisting of 1/3 *Lamprolepis*, 7/15 *Lygosoma*, 5/19 *Mochlus*, 6/9 *Riopa*, and 6/6 *Subdoluseps* species). Additionally, 11 of the 12 unnamed lineages within the *Riopa anguina-lineolata-popae* species complex in Myanmar were included (Freitas et al., 2020). Although a number of recent studies have described additional species within *Lygosoma* group skinks based on molecular data (Heitz et al., 2016; Karin et al., 2018; Siler et al., 2018; Grismer et al., 2019), the taxonomy of the clade remains poorly characterized, and there are a number of distinct unnamed cryptic lineages within each genera (ESF pers. obs.). Therefore, we used the barcoding threshold method, described below, to add an additional four unnamed operational taxonomic units (OTUs) to our ingroup dataset, for a total ingroup sampling of 40 lineages (Table S1).

To determine objectively the number of unnamed OTUs to include in our ingroup sampling, we used the barcoding threshold method. This method examines pairwise genetic distances between individuals to determine the numerical cutoff value that represents the transition between intra- and interspecific genetic diversity in tested samples (Meyer & Paulay, 2005). This threshold value is contingent on the number and relatedness of samples included in the analysis and is not a biologically meaningful number. Therefore, although this method is promising for lineage discovery, it is not ideal for species delimitation (Meyer & Paulay, 2005); nevertheless, the barcode threshold method is useful as an objective tool to identify divergent genetic diversity within a set of sequences, as it is used here. Samples representing 151 individuals from the genera *Lygosoma*, *Mochlus*, *Riopa*, and *Subdoluseps* were sequenced and aligned for the mitochondrial gene (mtDNA) *ND1* (see sequencing and alignment methods below). The resulting alignment was analyzed using JModelTest v2.1.10 (Darriba et al., 2012) to determine the best method of substitution across all sites in *ND1*; the alignment was not partitioned because the current implementation of the barcoding threshold method does not accommodate data partitioning when calculating distance matrices. Pairwise *ND1* distances between individuals were calculated using the *dist.dna* function in the R v3.5.3 (R Core Team, 2019) program ape v5.3 (Paradis & Schliep, 2018), using the substitution model TN93 as determined by JModelTest. The barcoding threshold value was calculated using the *localMinima* function, and the resulting value of 5.6% genetic divergence was set as the threshold to determine the number OTUs using the function *tclust*. This analysis suggested that there were 44 OTUs represented by the 151 sampled individuals. The resulting OTUs mostly corroborated the species-level status of all named species and delimited lineages of Myanmar *Riopa*, with the following exceptions: the species *Riopa goaensis* was not considered distinct from the species *R. guentheri*; the species

Subdoluseps frontoparietale was not considered distinct from *S. bowringii*; and several species were separated into multiple OTUs. In all of these cases, we based our taxonomic assignment on previous published species accounts and considered *R. goaensis*, *R. guentheri*, *S. frontoparietale*, and *S. bowringii* as separate species and continued to treat named species with multiple recovered OTUs as single species. Finally, an additional OTU was included for a genetically divergent sample that did not have *ND1* sequence data available. The resulting taxonomic sampling included 40 ingroup *Lygosoma* group individuals and 27 outgroups, 20 of which were obtained from GenBank (Table S1).

2.1.2 | Fossil taxa

We obtained taxonomic and temporal data for the fossil scincids that were used to calibrate the fossilized birth-death model (Heath et al., 2014) from the Paleobiology Databased (accessed October 2019). Although there are multiple fossils classified as members of Scincidae, most lack or have ambiguous diagnostic characters and cannot be easily ascribed to clades within the family. Only 11 fossils, five of which were fossils of extant species, could be confidently placed with the scincid tree of life and were used in our analyses (see Table S2 for a list of all fossil taxa included in our analyses).

2.2 | Genetic sampling and sequencing

We sequenced seven nuclear genes (nuDNA)—brain-derived neurotrophic factor (*BDNF*), oocyte maturation factor (*CMOS*), prolactin receptor (*PRLR*), prostaglandin E receptor 4 (*PTGER4*), RNA fingerprint protein 35 (*R35*), recombination activating gene 1 (*RAG1*), and synuclein alpha interacting protein (*SNCAIP*); and one mitochondrial gene (mtDNA)—NADH

dehydrogenase subunit 1 (*ND1*) following standard PCR and sequencing protocols (e.g. Siler et al., 2011). Genes were chosen based on their use in previous phylogenetic studies of skinks (e.g. Brandley et al., 2011; Freitas et al., 2019), and primers and annealing temperatures are listed in Table S3. Raw sequence data were checked for quality in Geneious v10.2.4 (Biomatters Ltd) and aligned by eye. All genes sequenced for this study are protein-coding genes; therefore, each alignment was translated to amino acids in Geneious to look for erroneous internal stop codons and amino acid mismatches, which indicate errors in alignment.

2.3 | Maximum likelihood analyses and species tree analysis

Maximum likelihood phylogenetic analyses were conducted in IQ-TREE v1.6.12 (Nguyen et al., 2015) on each gene separately using the combined (ingroup + outgroup taxa) dataset to check for gene tree discordance. Each gene was partitioned by codon position, and automatic model selection (Kalyaanamoorthy et al., 2017) with the AICc selection criteria was used so that IQ-TREE calculated the best substitution model for each partition and implemented that partition in phylogenetic analysis. Support for each node was assessed using 100 non-parametric bootstrap replicates. Results revealed significant gene-tree discordance among ingroup taxa as expected based on the results of previous analyses (Freitas et al., 2019).

We conducted additional IQ-TREE analyses on ingroup taxa only using the same methods as described above and used the resulting gene trees to generate a species tree in ASTRAL-III (Zhang et al., 2018). Support for the species tree was assessed using the local posterior probability, which measures the posterior probability for the quadripartition surrounding the node, not the bipartition (Sayyari & Mirarab, 2016). The species tree indicated that the main regions of gene tree discordance regard the relationship of *Lamprolepis smaragdina* to the rest of

the *Lygosoma* group skinks and the relationships between the genera *Mochlus*, *Riopa*, and *Subdoluseps* (Fig. S1), consistent with previous studies (Freitas et al., 2019).

2.4 | Topology tests

Unfortunately, the current implementation of the fossilized birth-death method for dating analysis cannot accommodate co-estimation of the species tree, which is problematic for *Lygosoma* group skinks as the clade has gene tree discordance and unresolved nodes in the species tree. To surmount this issue, we used maximum likelihood topology testing to compare different node constraint configurations against the unconstrained topology to test hypotheses of relationships within the clade. We used the AU test (Shimodaira, 2002) implemented in IQ-TREE on the concatenated ingroup alignment to test six different topological configurations (placement of *Lamprolepis smaragdina* in relation to the rest of the *Lygosoma* group skinks + the relationship of *Mochlus*, *Riopa*, and *Subdoluseps*) against the unconstrained tree to examine if the unconstrained tree is significantly worse than the constrained trees (Fig. S2). Significance was assessed with 10,000 RELL replicates (Kishino et al., 1990). Prior to this analysis, we used PartitionFinder v2.1.1 (Lanfear et al., 2012) on the ingroup concatenated alignment to estimate jointly the best partitioning scheme and models of substitution for the data, using the greedy search algorithm to test all models and setting branchlengths = linked and model selection = aicc. The resulting best scheme was applied in phylogenetic estimation of the constrained and unconstrained trees.

2.5 | Divergence dating analyses

The AU test suggested that the unconstrained tree could not be rejected when compared to constrained trees (Figure S2) and so we used the unconstrained tree for dating analysis. To determine the best partitioning scheme and substitution models for each partition in the dating analysis, we used the program Partition Finder v2.1.1 as above on the ingroup + outgroup concatenated alignment. Divergence dating was done in MrBayes v3.2.6 (Ronquist et al., 2012) implementing the fossilized birth-death method (FBD; Heath et al., 2014), which uses date ranges from all existing fossils to estimate node ages. This method does not require the input of calibration probability densities for fossils or the exact placement of the fossil along the phylogeny (Heath et al., 2014). We set the extant sample probability prior to 0.60, which suggests that we have an estimated ingroup sampling coverage of 60% and we used previously estimated secondary calibrations for the age of the root of Scincidae (Wiens et al., 2006; Skinner et al., 2011; Burbrink et al., 2019) to set the prior for the age of the root to treeagepr = offsetexp(94.4,108.5), where 94.4 is the minimum age of the root 108.5 is the mean age of the root in millions of years. All other FBD priors were set to default values. We used the igr clock variance prior and set igrvarpr = exp(37) and the clockratepr = lognorm(-7.1,0.61) as in Zhang et al., (2016). We conducted four runs, each consisting of four chains, for 40,000,000 generations for each run. Results were examined for convergence and stationarity in Tracer v1.7.1 (Rambaut et al., 2018).

2.6 | Ancestral area reconstructions

We used the program BioGeoBEARS v1.1.2 (Matzke, 2013) in R to reconstruct geographical evolutionary history of *Lygosoma* group skinks. BioGeoBEARS calculates the maximum likelihood of model parameters and then calculates probability of ancestral ranges at each node

using the optimized parameter values (Matzke, 2014) We ran 12 different biogeographic models in BioGeoBEARS: DEC, DEC+J, DEC+x, DEC+J+x, DIVALIKE, DIVALIKE+J, DIVALIKE+x, DIVALIKE+J+x, BAYAREALIKE, BAYAREALIKE+J, BAYAREALIKE+x, and BAYAREALIKE+J+x taking into account the effects of jump dispersal (+J) and distance (+x) on range evolution across the phylogeny. We compared the resulting likelihoods of each model with AICc and considered the model with the lowest AICc value to be the best-fit model to our data (Akaike, 1974). Prior to analysis, we trimmed our FBD topology to include only extant ingroup species using the command extract.clade in the R package ape.

We included five biogeographic realms in our analysis, which were chosen based on each region's unique geological history: sub-Saharan Africa (hereafter, Africa), the Indian subcontinent (India), mainland Southeast Asia (Southeast Asia), Sundaland, and Wallacea (Fig. 1). These realms have been designated as separate biogeographic regions in many previous studies (e.g. Oliver et al., 2015; Grismer et al., 2016; Wienell et al., in press). Many additional boundaries exist within these large-scale realms identified based on fine-scale analyses of climate (Wu et al., 2014), vegetation (van Welzen et al., 2011; Ratnam et al., 2016) or animal distributions (Inger, 1999), but these are hard to incorporate in macroevolutionary analyses and may not be relevant at large spatial and temporal scales. We did not include the Philippines biogeographic realm in our analyses despite the occurrence of the species *Lamprolepis smaragdina* across most islands in the archipelago because the oceanic archipelago is not a focal area of this study and including additional regions increases the state space of BioGeoBEARS analyses, affecting the computation time. Previous studies have shown that *L. smaragdina* dispersed to the Philippines from Wallacea in the Miocene (Linkem et al., 2013). The Philippine island of Palawan is considered part of the Sundaland biogeographic realm in line with previous

studies (e.g. Barley et al., 2015) despite its mainland Southeast Asia origin approximately 30 mya (Hall, 1996). Biogeographic studies of the island suggest that it is home to both Sundaic and Philippine taxa, suggesting that it plays an important role in the dispersal of species between Sundaland and the Philippine archipelago (Esselstyn et al., 2010).

We allowed dispersal of species between Africa-India, Africa-Sundaland, India-Southeast Asia, India-Sundaland, Southeast Asia-Sundaland, and Sundaland-Wallacea (Fig. 1). We did not allow dispersals between Africa-Southeast Asia, Africa-Wallacea, India-Wallacea, and Southeast Asia-Wallacea because there is no direct straight-line dispersal route between these regions. Overland dispersals and transoceanic dispersals were given dispersal probabilities of 1.0 and 0.5, respectively. In the six models with the +x free parameter, the dispersal probabilities were multiplied by a distance matrix in which the distance between adjacent areas (i.e. India-Southeast Asia and Southeast Asia-Sundaland) was set to 1.0 and transoceanic dispersals were given a numeric value that reflected the relative Euclidian distance between the regions (Fig. 1). The maximum number of areas a single species was allowed to inhabit was three, in line with the observation that the most widespread species, *Subdoluseps bowringii*, is found across Southeast Asia, Sundaland, and Wallacea (ESF pers. obs.). Therefore, we allowed ancestors to inhabit all combinations of two or three biogeographic regions except for those requiring the aforementioned disallowed dispersal routes. The disallowed area combinations were Africa-India-Wallacea, Africa-Southeast Asia-Wallacea, and India-Indochina-Wallacea, but we kept the states of Africa-Southeast Asia, Africa-Wallacea, and India-Wallacea, because these could occur if a widespread taxon across three regions went extinct in one portion of its range. Therefore, 22 ancestral states were allowed, including the null range (no areas inhabited). We ran a time-stratified analysis in which dispersal between Sundaland-Wallacea was allowed only more

recently than 25 mya, consistent with the geological history of the region. States were considered likely if they were reconstructed with a greater than 10% probability.

Because different biogeographic regions have been sampled at different proportions, we investigated the effects of geographic sampling on biogeographic reconstruction. Specifically, because we only include approximately 60% of all *Lygosoma* group skink lineages in our analyses we were wanted to understand how changes in the proportion of geographic sampling (i.e. changes in the number of species from different geographic regions included in the phylogeny) would affect our inferences. Africa has the lowest proportion of sampled species of all biogeographic regions included in the analysis (5/19 versus 7/8 from India, 19/23 from mainland Southeast Asia, 9/16 from Sundaland, and 2/2 from Wallacea; this list includes the unnamed lineages and species in our phylogeny). Therefore, we rarefied the geographic taxa used in biogeographic analysis by randomly resampling ingroup species in our FBD phylogeny using the sample_n command in the R package dplyr v0.8.3 (Wickham et al., 2019) so that each region had the same proportion of species sampled as in Africa, rounding up to the nearest whole number (Africa=5 species, India = 3 species, Southeast Asia=7 species, Sundaland=5 species, Wallacea =1 species). We reran BioGeoBEARS as above on the reduced topology. This analysis was repeated 200 times to get a distribution of ancestral states across the root and genus nodes in the phylogeny (nodes 1 & 5–8 in Figs. 2, 3; Table 1). The resulting null distribution of ancestral state probabilities were tested for significant bimodality with Hartigan's dip test (Hartigan & Hartigan, 1985) using the command dip.test in the R package diptest v0.75-7 (Maechler, 2016), with distributions considered to be bimodal if they had a significance level of $p \leq 0.05$. We then compared the null distribution to the results from the original (complete taxonomic sampling) BioGeoBEARS analysis. An ancestral state was considered significantly different from the null

if it had a z-score ≥ 2.0 (fell outside of two standard deviations of the mean). We interpreted a significant bimodality p-value or a significantly different probability as an indication that taxonomic sampling affected the node's ancestral state reconstructions.

2.7 | Diversification rate shifts analysis

We investigated whether there are shifts in diversification rate over time in *Lygosoma* group skinks using the program Bayesian Analysis of Evolutionary Mixtures (BAMM) v2.5.0 (Rabosky, 2014). BAMM uses reversible jump MCMC analysis to sample different models of lineage diversification and detect shifts in the evolutionary rate across a phylogeny. We used the speciation-extinction model and specified the approximate sampling proportion separately for each genus to avoid bias that is caused when assuming a single sampling proportion across tree. We set the expected number of rate shifts to 1.0. Prior to analysis, we used the setBAMMpriors command in the R package BAMMtools v2.1.7 (Rabosky et al., 2014) to calculate starting values for the MCMC chain. The analysis was run twice, each for 12,000,000 generations, and we discarded the first 10% of generations of each run as burnin. We analyzed the output in BAMMtools using the commands getEventData to obtain the posterior distribution of the number of rate shifts across the topology and computeBayesFactors to compare different models using Bayes Factors. A Bayes Factor higher than 20 was considered support for the alternative model of rate shifts over the null model of no rate shifts (Rabosky, 2014).

3 | RESULTS

3.1 | Phylogenetic reconstructions, topology tests, and divergence dating

The phylogeny showed that *Lygosoma* group skinks are monophyletic within Scincidae. However, despite increased genetic and taxonomic sampling over previous molecular phylogenetic studies (Datta-Roy et al., 2014; Freitas et al., 2019), the relationships of *Lamprolepis smaragdina* to the rest of the *Lygosoma* group skinks and of the genera *Mochlus*, *Riopa*, and *Subdoluseps* remain unresolved (Figs. 2, S1, S3). All other nodes within *Lyogosma* group skinks are well-supported in the concatenated analysis as in Freitas et al. (2019) although the relationships between Southeast Asian *Riopa* clades are resolved with high support as more similar to what is depicted in the Southeast Asian *Riopa* species tree topology than the concatenated topology in Freitas et al. (2020). In addition to indicating poor resolution at the *Lamprolepis* + *Lygosoma* and *Mochlus* + *Riopa* + *Subdoluseps* nodes, the species tree indicates that some sub-generic- and pecies-level relationships are not well resolved (Fig. S1).

Our analyses also show additional novel phylogenetic results. We recover the species *Lygosoma veunsaiense* (Geissler et al., 2012) as part of the genus *Larutia* (Fig. S3), and therefore, we formally reclassify it here as *Larutia veunsaiense*. We note that with this reclassification, the *Lygosoma* group skinks comprise 51 recognized species instead of 52. Furthermore, we confirm that the species *Lygosoma koratense* is a member of the genus *Lygosoma* (Fig. 2), a classification that had been questioned by Freitas et al. (2019) based on the more robust morphology of this species compared with other members of *Lygosoma*. Additionally, we reidentify the sample of *Lygosoma isodactylum* included in Freitas et al. (2019) as a member of the species *Lygosoma angeli*, based on identical sequence data to multiple individuals identified as of *L. angeli* (ESF pers. obs.). Finally, we find that *Lygosoma siamense* as described by Siler et al. (2018) is not monophyletic and instead comprises three distinct lineages in mainland Southeast Asia and Sundaland (Figs. 2, 3).

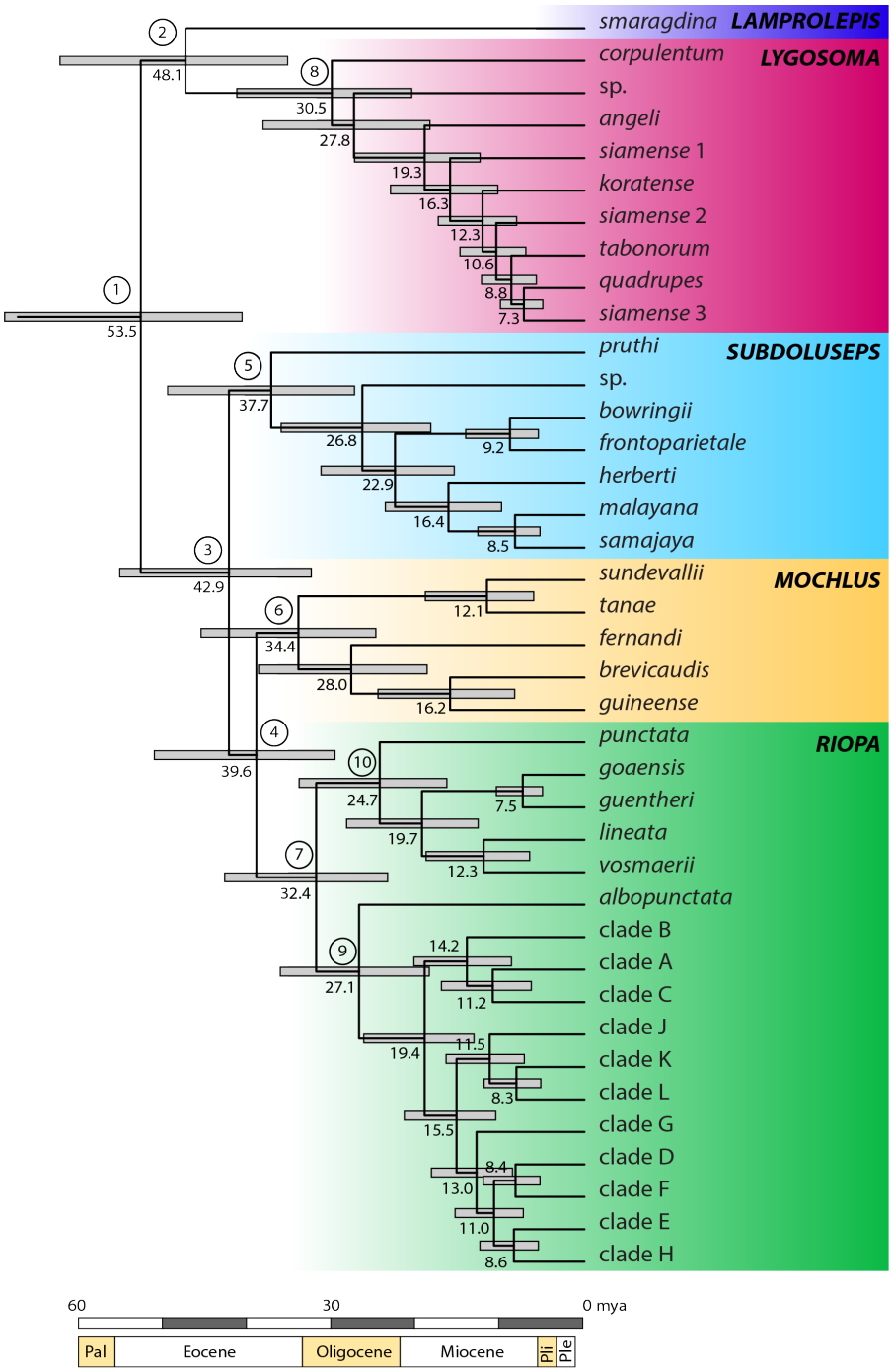

Figure 2 Bayesian concatenated topology of *Lygosoma* group skinks (outgroups and fossil calibrations have been removed). Each genus is bounded in a different color box, which corresponds to the colors in Figure 1. Numbers below each node represent the mean divergence date for that node, and the gray bars indicate the 95% hpd interval for each node. Numbers in circles above select nodes are used for descriptor purposes and correspond to node numbers in Figures 3, 4 and Table 1.

Topology tests comparing the likelihood of the unconstrained topology to six different constrained topologies indicate that the unconstrained tree is not significantly worse than any constrained tree (Fig. S2; Table S4). Furthermore, we find that trees with a constrained sister relationship between *Mochlus* and *Subdoluseps* are significantly worse than all other topological configurations (Table S4). Therefore, we conducted Bayesian fossilized birth-death divergence dating on the unconstrained concatenated topology.

Results from divergence dating indicate that *Lygosoma* group skinks began to diversify approximately 53.5 mya (95% highest posterior density = 68.7–40.6 mya) in the Eocene. *Lamprolepis* split from *Lygosoma* 48.1 mya (62.1–35.1), *Subdoluseps* split from *Mochlus* + *Riopa* 42.9 mya (55.1–32.4), and *Mochlus* and *Riopa* split 39.6 mya (51.0–29.6; Fig. 2, Table 1). Most major within-genera diversification events occurred 35–25 mya, and species-level diversification peaked 13–8 mya (Fig. 2).

3.2 | Ancestral area reconstruction and diversification rates

The best-fit model to our data was DEC+J (Table 2), which suggests that jump-dispersal across large distances occurs within the group, and relative distance between regions (+x) does not have an effect on the model. The most probable root ancestral range for *Lygosoma* group skinks was reconstructed as widespread across India, Southeast Asia, and Sundaland (probability [p]=28%), although a number of other ranges were considered likely (Fig. 3, node 1; Table 1), all of which included India and were widespread across multiple biogeographic regions. The large number of ranges considered possible is likely a result of the large number of states and maximum range size allowed in our biogeographic analyses. The BioGeoBEARS resampling analysis suggested that the ancestral state probability of India-Southeast Asia-Sundaland was significantly different

from the null distribution, which indicates that root node reconstruction depends on geographic sampling, although none of the other possible ancestral ranges were significantly different from the null distribution (Table 3).

Table 1 Results of fossilized birth-death divergence dating and biogeographic reconstruction for *Lygosoma* group skinks. The node number matches the node numbers in Figures 2–4. All ages are in millions of years.

Node	Split	Mean	Median	95% highest posterior density	Reconstructed ancestral range probabilities
1	*Lygosoma* group skinks	53.5	52.6	68.7–40.6	28% I-SA-SS, 15% I-SS, 13% A-I-SA, 12% A-I-SS, 32% Other
2	*Lamprolepis-Lygosoma*	48.1	47.3	62.1–35.1	54% Sunda Shelf, 26% SA-SS, 20% Southeast Asia
3	*Subdoluseps-Mochlus + Riopa*	42.9	42.1	55.1–32.4	37% India, 19% A-I-SA, 15% A-I, 11% I-SA, 18% Other
4	*Mochlus-Riopa*	39.6	38.9	51.0–29.6	32% India, 24% Africa, 21% A-I, 14% A-I-SA, 8% Other
5	*Subdoluseps*	37.7	37.1	49.4–27.2	34% India, 31% Southeast Asia, 12% I-SA, 23% Other
6	*Mochlus*	34.4	33.9	45.4–24.7	100% Africa
7	*Riopa*	32.4	31.8	42.6–23.3	79% India, 20% I-SA, 1% Other
8	*Lygosoma*	30.5	29.9	41.2–20.5	88% SA, 10% SA-SS, 2% Other
9	*Riopa* Southeast Asian subgenus	27.1	26.7	36.0–18.4	89% Southeast Asia, 11% Other
10	*Riopa* Indian subgenus	24.7	24.3	33.8–16.3	100% India

The most probable range for the ancestor of *Lamprolepis-Lygosoma* was reconstructed as Sundaland (p=54%; Fig. 3, node 2; Table 1), followed by Southeast Asia-Sundaland (p=26%) and Southeast Asia (p=20%), whereas the range for the ancestor of *Mochlus-Riopa-Subdoluseps* was India (p=37%; Fig. 4, node 3; Table 1), followed by Africa-India-Southeast Asia (p=19%) and Africa-India (p=15%). Both the ancestor of *Mochlus-Riopa* and *Subdoluseps* were reconstructed as occurring in India with high probability (p=32% and 34%, respectively, Fig. 4, nodes 4–5; Table 1), with the ancestor of *Mochlus-Riopa* also reconstructed as occurring in

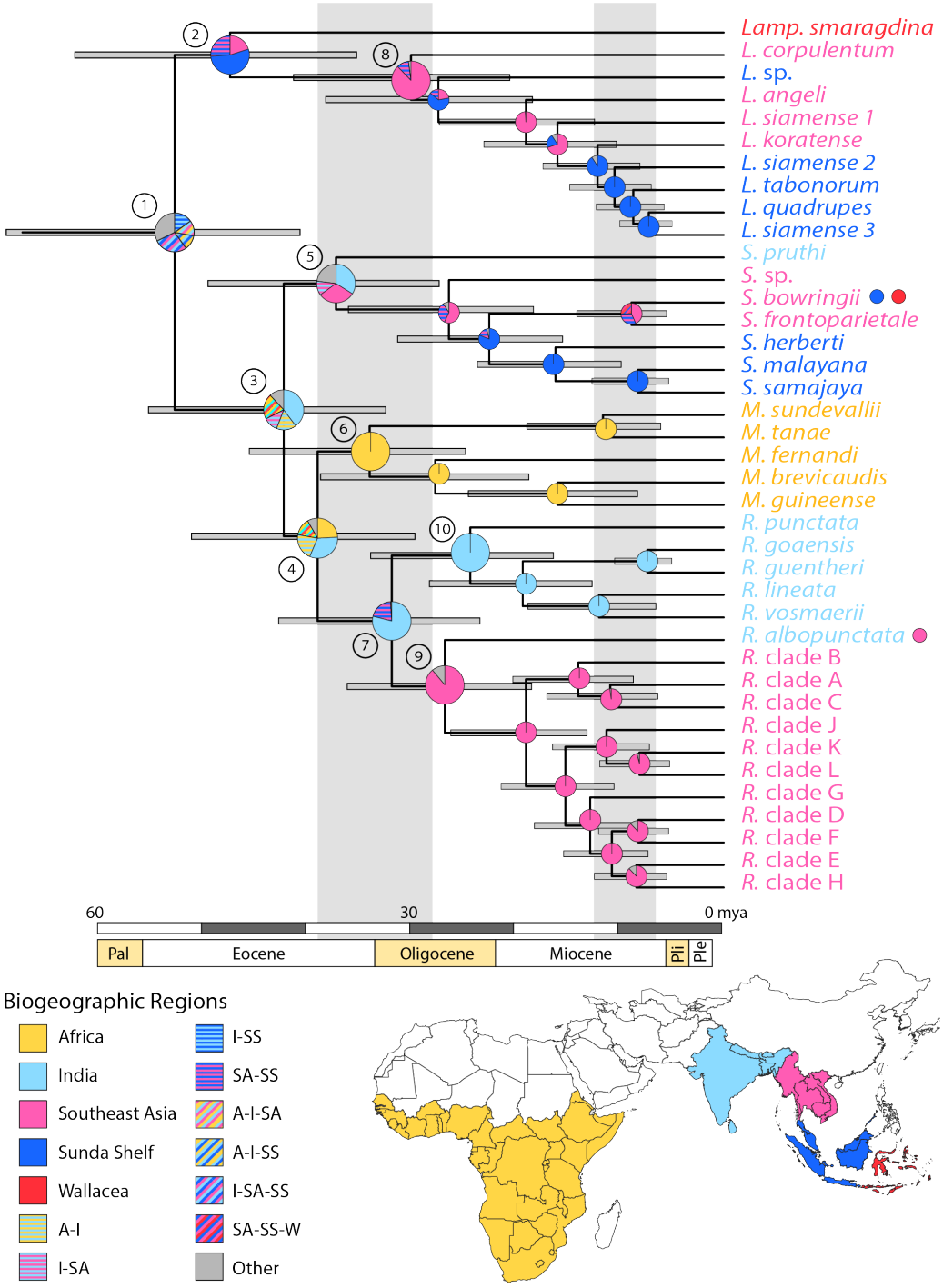

Figure 3 Bayesian concatenated topology of *Lygosoma* group skinks (outgroups and fossil calibrations have been removed). Pie graphs at each node indicate the most probable ancestral ranges at that node (states reconstructed with >10% probability), with the colors corresponding to those in the legend and the map. The gray bars indicate the 95% hpd interval for each node. The color dots next to *S. bowringii* and *R. albopunctata* indicate that those species are found across multiple biogeographic regions, with the color of the dot corresponding to the region. Numbers in circles above select nodes are used for descriptor purposes and correspond to node numbers in Figures 2, 4, and Table 1.

Table 2 Summary statistics for all models ran in BioGeoBEARS, ordered by AICc. The bolded model was the one with the best fit to the data.

Model	LnL	Num. Params	d	e	j	x	AICc	AICc weight
DEC +J	**-47.16**	**3**	**0.003**	**0.001**	**0.042**	**0.000**	**101.0**	**0.40**
DEC +J +x	-47.02	4	0.005	0.001	0.065	-1.690	103.2	0.13
DIVALIKE +J	-48.24	3	0.004	0.001	0.051	0.000	103.2	0.14
DIVALIKE +J +x	-47.02	4	0.005	0.001	0.065	-1.690	103.2	0.13
DEC +x	-48.48	3	0.007	0.002	0.000	-2.500	103.6	0.11
DEC	-50.13	2	0.005	0.002	0.000	0.000	104.6	0.07
DIVALIKE +x	-50.43	3	0.011	0.002	0.000	-2.500	107.5	0.02
DIVALIKE	-52.42	2	0.008	0.002	0.000	0.000	109.2	0.01
BAYAREALIKE +J	-52.00	3	0.003	0.002	0.070	0.000	110.7	0.00
BAYAREALIKE +J +x	-51.08	4	0.003	0.002	0.085	-1.040	111.3	0.00
BAYAREALIKE	-62.91	2	0.004	0.021	0.000	0.000	130.2	0.00
BAYAREALIKE +x	-62.53	3	0.007	0.021	0.000	-1.890	131.7	0.00

Africa (p=24%), widespread across Africa-India (p=21%) or widespread across Africa-India-Southeast Asia (p=14%), and the ancestor of *Subdoluseps* also reconstructed as occurring in Southeast Asia (p=31%) or widespread across India-Southeast Asia (p=12%). Diversification rate shifts analysis indicates that there has not been a shift in the evolutionary rate in any branch across the phylogenetic tree. Plots of speciation rates over time for each genus show that speciation rates have declined over time (Fig. 3).

Results of the BioGeoBEARS resampling analyses suggested that the majority of generated null distributions had significant bimodality, indicating that geographic sampling does affect the biogeographic reconstructions (Fig. 5, Table S5). The most probable ancestral state for the root (India-Southeast Asia-Sundaland) and for the genus *Riopa* (India) were significantly different from the null distribution of probabilities (p=0.03 and p<0.00, respectively), with the root range of India-Southeast Asia-Sundaland considered not as probable in the resampling analyses whereas the *Riopa* range of India considered more probable in the resampling analyses (Fig. 5). The other major nodes' most probable states were not significantly different from the null distribution.

4 | DISCUSSION

4.1 | India is the ancestral range of *Lygosoma* group skinks

The results of our divergence dating analysis using the fossilized birth-death method (FBD) resulted in a mean divergence time for *Lygosoma* group skinks of 53.5 mya (68.7–40.6), shortly after the collision of the Indian subcontinent with the Eurasian subcontinent 59–55 mya (Zhang et al., 2012; Hu et al., 2016; Chatterjee et al., 2017). This date is much older than 38.2 mya estimated by Skinner et al. (2011) using the traditional node dating method with two fossil

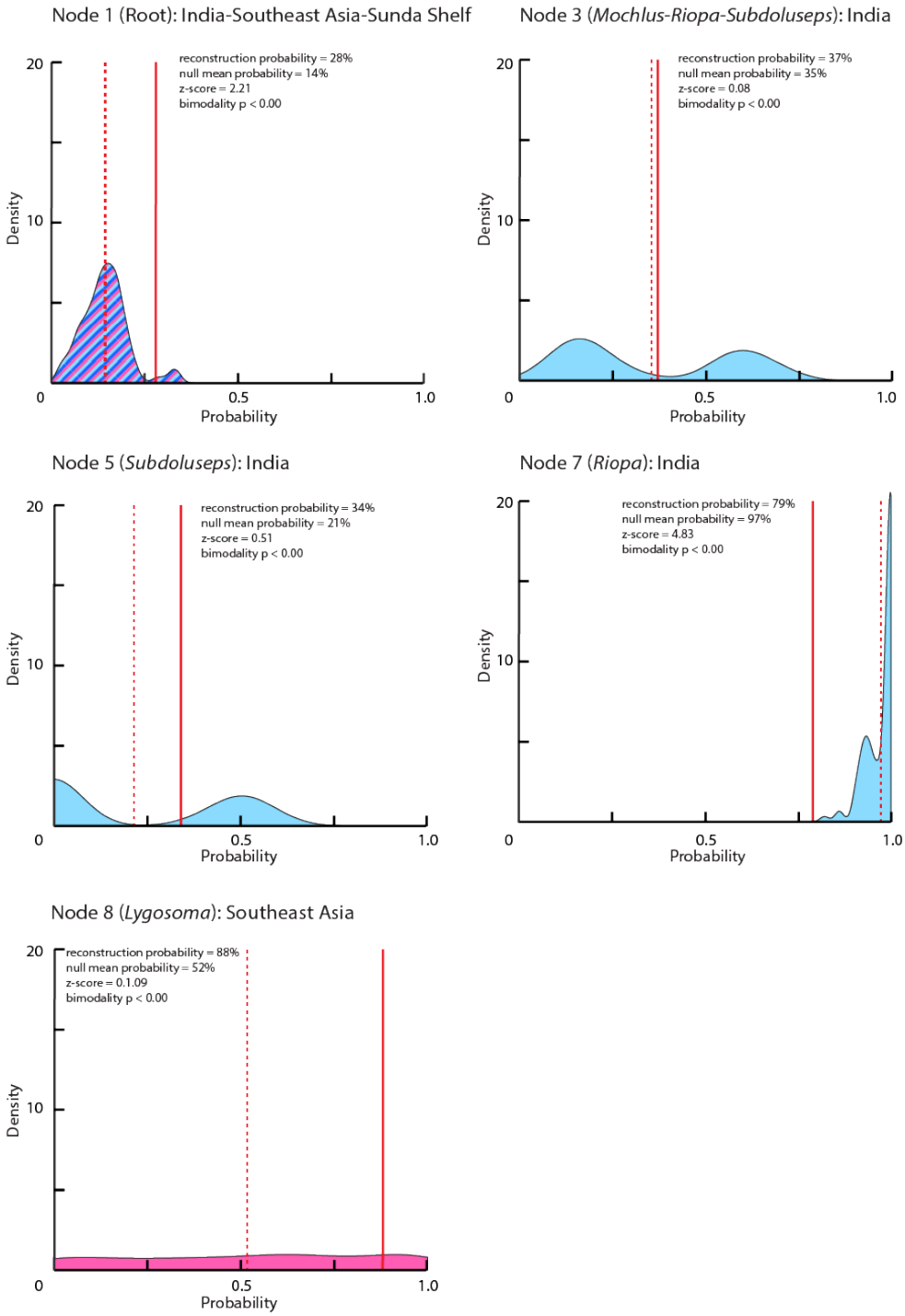

Figure 4 Null distributions for the most probable ancestral ranges at the root node and for all genera, excluding *Lamprolepis*. The solid red line indicates the probability of the range at the for the full-species topology, and the dashed red line indicates the mean probability of the null distribution. Summary statistics are given for each graph. Colors match the range colors in Figure 3.

calibrations. In comparing the FBD method with traditional node dating, Saladin et al. (2017) found that the FBD method resulted in older ages than traditional node dating, which the authors attributed to differences in how fossil calibration points are treated in the analyses (as minimum ages in traditional node dating versus anywhere in the clade in the FBD method). It was also shown that the traditional node dating method is more sensitive to extant and fossil taxonomic sampling (Saldin et al., 2017). In their broad study of lygosomine skinks, Skinner et al. (2011) only include two extant members of *Lygosoma* group skinks (*Lamprolepis smaragdina* and *Subdoluseps bowringii*), and therefore, our increased taxonomic sampling as well as use of FBD dating method resulted in an older, more robust estimate for the diversification of *Lygosoma* group skinks.

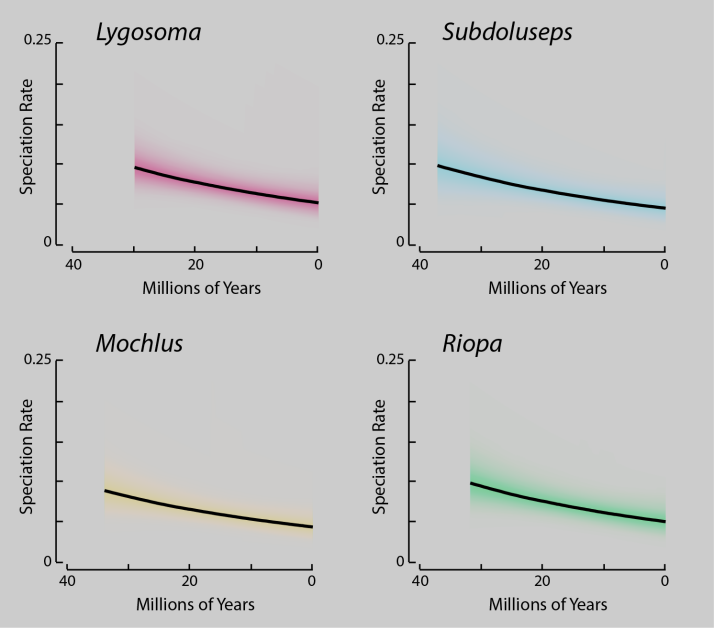

Figure 5 Plots of speciation rate through time for each genus, excluding *Lamprolepis*.

Although we hypothesized that *Lygosoma* group skinks originated in Southeast Asia because of the high genus- and species-level diversity in the region, ancestral state reconstructions suggest that the most probable range was widespread across India, Southeast Asia, and Sundaland, although the relative probability for this distribution is low (Fig. 4). Despite the large number of probable range states for the ancestor of *Lygosoma* group skinks, India is reconstructed as part of the ancestral range in all of them, suggesting that the Indian subcontinent

is the center of origin for the group (Fig. 4). However, whether the group diversified in India or across a wider area that includes Africa, Southeast Asia, and/or Sundaland is unknown.

Our BioGeoBEARS analyses using species subsets also suggested that *Lygosoma* group skinks diversified in a range that was, or included, India (Table S5), but the reconstructed ranges from this analysis was dependent on geographic sampling. In particular, the root range of India-Southeast Asia-Sundaland obtained from complete taxonomic sampling was significantly different than the null distribution of probabilities for that range using species subsets.

The timing of diversification of *Lygosoma* group skinks corresponds with the Great Indo-European Interchange (Chatterjee et al., 2017), where an increase in global temperatures (the Eocene thermal maximum) combined with a decrease in sea level and the collision of India with Eurasia led to faunal exchange of terrestrial tetrapods across Europe, South Asia, and Southeast Asia (Clementz et al., 2011; Smith et al., 2016; Chatterjee et al., 2017). Therefore, it is possible that the ancestor of *Lygosoma* group skinks participated in the Great Indo-European Interchange and was widespread across the Old World tropics. Increased ingroup species sampling along with dense sampling of the sister clade and other closely related outgroups is needed to resolve the ancestral state of the group more accurately.

4.2 | Genus-level diversification resulted from dispersion and founder-event speciation

Our results indicate that the major genus-level diversification events in *Lygosoma* group skinks occurred in the late Eocene to early Oligocene (38–30 mya), prior to the uplift of the Himalayas (Chatterjee et al., 2013, 2017) and onset of the South Asian monsoon (Clift et al., 2008; Chatterjee et al., 2017). Results of phylogenetic analyses indicate that while *Mochlus*, *Riopa*, and *Subdoluseps* form a well-supported clade to the exclusion of *Lygosoma* and *Lamprolepis,* the

order of separation of three genera are not well resolved. AU topology tests indicate that the tree resulting from concatenated analyses is not significantly worse than the constrained topologies, and so we use the concatenated topology in our biogeographic analyses, which corresponds with the species tree topology of Freitas et al. (2019). Increased taxonomic and genetic sampling is needed to determine if this lack of resolution is a result of missing data or a true hard polytomy, in which rapid diversification of these genera limits the ability to resolve the relationships (Whitfield & Lockhart, 2007).

The timing of divergence of *Lygosoma* group skink genera is similar to the timing of the diversification events estimated for Sun skinks (genus *Eutropis*) across India and Southeast Asia (Barley et al., 2015). Species in the genus *Eutropis* are found in the same habitats as the genera *Lygosoma*, *Riopa*, and *Subdoluseps*, and the contemporaneous divergence timings of these clades may indicate that diversification was driven by the same processes. The center of origin of *Eutropis* was reconstructed as Southeast Asia, which is concordant with *Lygosoma* and possibly *Subdoluseps*, but not with *Riopa* (Fig. 4). Throughout the Eocene, global temperatures cooled and aridity increased (Zachos et al., 2001), which may have initiated the spread of savannahs throughout South and Southeast Asia (Ratnam, 2016). However, fossil data suggest multiple shifts between more arid and more humid habitats across Sundaland during this time (Morley, 2012), indicating that spatially- and temporally localized shifts in climate and habitat existed within the larger global cooling trend, and most likely affected the diversification of species within major biogeographic regions. Nevertheless, in the late Eocene, continuous habitat unbroken by major orographic barriers existed between India and Southeast Asia (Chatterjee et al., 2017) and faunal exchange between India and continental Southeast Asia increased (Klaus et al., 2016). Therefore, it is possible that diversification of *Lygosoma* group skinks resulted from

dispersion from an Indian ancestral range into previously inaccessible regions across Southeast Asia. Theory suggests that species with larger range sizes are more likely to speciate as a result of the increased probability that an emergent barrier will bisect their range (Rosenzweig, 1975; Gaston, 1998). It then follows that geographic dispersion increasing range size from a smaller to larger area (Cracraft, 1994) would promote speciation and that any geological or climatic event that promotes faunal exchange also promotes diversification, even in the absence of major shifts in environmental conditions. Our results indicate that genus-level diversification of *Lygosoma* group skinks did not coincide with any major known geological or climatic event, including major orographic uplift, and we suggest that diversification occurred as a result of faunal exchange between India and Southeast Asia.

Our results also rule out the role of the onset of the seasonal South Asian monsoon weather pattern in the dispersal of the *Mochlus* ancestor from India to Africa. *Mochlus* began to diversify 34.4 mya (45.4–24.7), which likely predates the establishment of the South Asian monsoon. Although the exact timing of monsoon onset is unknown, its intensity is hypothesized to coincide with elevational changes of the Himalayas (Clift et al., 2008; Zhang et al., 2015; Chatterjee et al., 2017), which began to uplift approximately 30 mya (Chatterjee et al., 2013, 2017). Nevertheless, fossil data have suggested that seasonal monsoon-like weather patterns did exist in the region at the time (Licht et al., 2014; Spicer et al., 2017; Shukla & Mehrotra, 2018). Additionally, overland and island "stepping stone" connections between Africa and Eurasia existed intermittently both prior to and after the collision of India with Asia (Chatterjee et al., 2013, 2017), and may have facilitated dispersal of species between regions. However, given the lack of *Lygosoma* group skink fossils and sister species in the Arabian Peninsula or northern Africa, it is unlikely that overland dispersals promoted diversification in the same way as they did in

Lygosoma, *Riopa*, and *Subdoluseps*. Instead, we hypothesize that *Mochlus* diversified as a result of founder-event speciation, in which the ancestor of the genus dispersed transoceanically across the Indian Ocean, perhaps arriving in eastern central Africa, which currently harbors the highest species-level diversity of *Mochlus* and may be the center of origin of the genus.

In another potential example of founder-event speciation, the genus *Lamprolepis* split from *Lygosoma* 48.1 mya (62.1–35.1) in Southeast Asia and/or the Sunda Shelf (Fig. 3; Table 1). *Lamprolepis* subsequently went extinct from these biogeographic regions (with the exception of two *Lamprolepis* species of with small ranges on Borneo) after it dispersed to Wallacea in the early Miocene (Linkem et al., 2013). *Lamprolepis smaragdina* later dispersed into the Philippines (Linkem et al., 2013) while *Lygosoma* diversified in Southeast Asia 30.5 mya (41.2–20.5), with species' ancestral ranges subsequently transitioning between Southeast Asia and Sundaland. Although founder-event speciation is an important mechanism in island biogeography (Paulay & Meyer, 2002), its role in facilitating faunal exchange between Southeast Asia and Sundaland is less clear, given that these two regions are connected, and distribution of species could therefore result from dispersion. The Southeast Asia and Sundaland biogeographic regions are separated by an emergent barrier along the Thai-Malay peninsula, at or approximately 500 km south of the Isthmus of Kra (Hughes et al., 2003; Baltzer et al., 2008; Parnell et al., 2013). Although the Thai-Malay Peninsula was formed more than 100 mya (McLoughlin, 2001; Hall, 2009), the barrier is often attributed to more recent species- and population-level divergences from the Pliocene and Pleistocene (e.g. Patou et al., 2010; Luo et al., 2014; Beck et al., 2017). The type of barrier at the Isthmus of Kra remains unknown and has been attributed to Mio-Pliocene marine transgressions (e.g. Woodruff et al., 2003; de Bruyn et al., 2005) or to abrupt climate transitions (Baltzer et al., 2008; Hughes et al., 2009), with fossil

evidence suggesting that the barrier shifted north and south throughout the Pleistocene (Suraprasit et al., 2019). Furthermore, population-level studies of taxa distributed across the Isthmus of Kra have revealed that it is a leaky barrier for some taxa (e.g. Dejtaradol et al., 2016; Boontop et al., 2017), and, may have comprised mixed open grassland-closed canopy forest that could have facilitated faunal exchange between Southeast Asia and Sundaland in the middle Pleistocene (Suraprasit et al., 2019).

Speciation rates in *Lygosoma* group skinks following genus-level diversification have decreased (Fig. 5), similar to results found in other taxa in the Old World tropics (e.g. murid rodents, Rowe et al., 2019). This pattern is attributed to dispersal of an ancestor to a new region, followed by speciation. However, there is no change in rate configuration between the root and tips of the phylogeny, which may indicate that *Lygosoma* group skinks did not experience key innovations such as novel morphological or ecological adaptations that would have driven diversification (Rabosky, 2014). Instead, it appears that genus-level diversification of *Lygosoma* group skinks occurred as a result of stochastic dispersion and dispersal events, similar to what has been inferred for other skink groups in the Old World tropics (e.g. Linkem et al., 2013).

4.3| Species-level diversification within *Lygosoma* group skinks

Our results suggest that most species-level divergences within *Lygosoma* group skinks occurred in the middle to late Miocene (13–8 mya) and not more recently during Pliocene–Pleistocene glacial cycles as we had hypothesized. Although the Plio-Pleistocene glacial cycles and associated changes in sea level and habitat shifts are well-known as drivers of speciation across the Old World tropics, especially in island systems (e.g. Fabre et al., 2012; Reilly et al., 2019), Miocene climatic and habitat changes are also associated with diversification (e.g. O'Connell et

al., 2018). At the start of the Miocene (~23 mya), the Himalayas and the South Asian monsoon system were fully established (Clift et al., 2008; Sunyal et al., 2010 Chatterjee et al., 2017), and the Australian plate had collided with the Eurasian plate, forming Wallacea (Hall 2009, 2011). The Early and Middle Miocene climate was warm and humid (Morley, 2012; Srivastava et al., 2014) reaching a climatic optimum approximately 14 mya (Böhme, 2003; Holbourn et al., 2015), which coincided with peak faunal exchange between India and Southeast Asia (Klaus et al., 2016). Subsequent cooling throughout the late Miocene facilitated the spread of savannah habitats across South and Southeast Asia (Ratnam, 2016). Interestingly, this five million year burst of speciation within *Lygosoma* group skinks occurred regardless of biogeographic realm, with *Lygosoma* and *Subdoluseps* diversifying in Southeast Asia and Sundaland, *Riopa* diversifying in Southeast Asia, and *Mochlus* diversifying in sub-Saharan Africa (Fig. 3). This coincident diversification may indicate a common driver of diversification across genera. With the exception of species in the genus *Lamprolepis*, most species of *Lygosoma* group skinks are found in more open and arid environments (Das, 2010; Vyas, 2014; Freitas et al, 2018), which suggests that diversification may have been in response to the opening of previously closed-canopy habitats (Morley, 2012).

Additionally, although climate throughout the Micoene shifted from warm and tropical to cooler and humid, regions across South and Southeast Asia experienced climatic oscillations, that is associated with changes in exhumation rate of the Himalayas and the resulting shift in monsoon intensity (Clift et al., 2008). Chemical weathering, sedimentation, and fossil evidence suggests that throughout the late Miocene and Pliocene, both the South and Southeast Asian monsoon systems have experienced shifts in intensity, with marked decreases 16.5–15 mya and 10.5–3.5 mya (Clift et al., 2008). These shifts may be associated with the high levels of Miocene

faunal turnover in the region (Barry et al., 1985; Patnaik, 2016) and could have contributed to speciation with *Lygosoma* group skinks by facilitating dispersion and dispersal during drier periods, and then creating barriers to gene flow during more humid periods.

4.4 | Importance of geographic sampling in biogeographic reconstructions

Although taxonomic sampling is known to have an important impact on the inferred dates of divergence dating analyses (Heath et al., 2008; Schulte II, 2013; Soares and Schrago, 2015), the impact of geographic sampling on biogeographic reconstructions is not well-studied. Intuitively, it makes sense that having a greater representation of species from across the geographic distribution of the clade under study will result in more robust ancestral area reconstructions. Nevertheless, given the rarity of genetic voucher samples of *Lygosoma* group skinks in museums and the difficulty of finding most species in the wild (Das, 2010; Geissler et al., 2011, Vyas, 2014), we were interested in understanding exactly how our biogeographic reconstructions would change if we had lower geographic representation in our phylogeny. We found that across all major nodes, geographic sampling had a large impact on our results (Table S5). Most of our generated null distributions had significant bimodality, indicating that the probability of the ancestral state at that node shifted dramatically as geographic sampling changed (Fig. 5; Table S5). These results underscore the importance of continued global biodiversity surveys to detect rare or under-sampled species and the necessity of taxonomic research in biological sciences. Therefore, we admit that although the biogeographic scenario for *Lygosoma* group skinks as presented above is based on the most robust taxonomic and geographic sampling of the group to date, it should be considered a hypothesis in need of further investigation.

ACKNOWLEDGEMENTS

For tissue loans (Table S1), we thank J. Vindum and L. Scheinberg at the California Academy of Sciences (CAS), A. Resetar at the Field Museum of Natural History (FMNH), L. Grismer at the La Sierra University Herpetology Collection (LSUHC), C. Spencer at the Museum of Vertebrate Zoology (MVZ), D. Rödder at the Zoologisches Forschungsmuseum Alexander Koenig (ZFMK), A. Aowphol at the Zoological Museum of Kasetsart University (ZMKU), and A. Bauer at Villanova University. We are extremely grateful to T. Yuri, M. Labonte, and M. Penrod at the Sam Noble Oklahoma Museum of Natural History (SNOMNH) for help with molecular data collection. We thank D. Arcila at the SNOMNH for help with divergence dating analyses and A. Santaquiteria at the SMNOMNH for help with BioGeoBEARS analyses. This research was supported by University of Oklahoma (OU) Graduate Student Senate funds, an OU Department of Biology Adams Scholarship, and an OU Robberson Research Grant to ESF, National Postdoctoral fellowship (PDF/2017/000476 entry number 15225; http://dx.doi.org/10.13039/501100001843) to ADR, and NSF grants (IOS 1353683 and DEB 1657648) to CDS.

REFERENCES

Agarwal, I., Bauer, A. M., Jackman, T. R., Karanth, K. P. (2014). Insights into Himalayan biogeography from geckos: a mol;ecular phylogeny of *Cyrtodactylus* (Squamata: Gekkonidae). *Molecular Phylogenetics and Evolution*, 80, 145–155.

Akaike, H. (1974). A new look at the statistical model identification. *IEEE Transactions on Automatic Control*, 19, 716–723.

Ao, H., Roberts, A. P., Dekkers, M. J., Liu, X., Rohling, E. J.Shi, Z., … Zhao, X. (2016). Late Miocene-Pliocene Asian monsoon intensification linked to Antarctic ice-sheet growth. *Earth and Planetary Science Letters*, 444, 75–87.

Baltzer, J. L., Davies, S. J., Bunyavejchewin, S., & Noor, N. S. M. (2008). The role of desiccation tolerance in determining tree species distributions along the Malay-Thai Peninsula. *Functional Ecology*, 22, 221–231.

Barley, A. J., Datta-Roy, A., Karanth, K. P., & Brown, R. M. (2015). Sun skink diversification across Indian-Southeast Asian biogeographical interface. *Journal of Biogeography*, 42, 292–304.

Barry, J. C., Johnson, N. M., Raza, S. M., & Jacobs, L. L. (1985). Neogene mammalian faunal change in southern Asia: correlations with climatic, tectonic, and eustatic events. *Geology*, 13, 637–640.

Barry, J. C., Morgan, M. E., Winkler, A. J., Flyn, L. J., Lindsay, E. H., Jacobs, L. L, & Pilbeam, D. (1991). Faunal interchange and Miocene terrestrial vertebrates of Southern Asia. *Paleobiology*, 17, 231–245.

Beck, S. V., Carvalho, G. R., Barlow, A., Rüberm L., Tan, H. H., Nugroho, E., … de Bruyn, M. (2017). Plio-Pleistocene phylogeography of the Southeast Asian blue panchax killifish, *Aplocheilus panchax*. *PLoS ONE*, 12, e0179557.

Bocxlaer, I. V., Biju, S. D., Loader, S. P., & Bossuyt. (2009). Toad radiation reveals into-India dispersal as a source of endemism in the Western Ghats-Sri Lanka biodiversity hotspot. *BMC Evolutionary Biology*, 9, 131.

Böhme, M. (2003). The Miocene Climatic Optimum: evidence from ectothermic vertebrates of central Europe. *Palaeogeography, Palaeoclimatology, Palaeoecology*, 195, 389–401.

Boontop, Y., Kumaran, N., Schutze, M. K., Clarke, A. R., Cameron, S. L., & Krosch, M. N. (2017). Population structure in *Zeugodacus cucurbitae* (Diptera: Tephritidae) across Thailand and the Thai-Malay Peninsula: natural barriers to a great disperser.

Brandley, M. C., Wang, y., Guo, X., Montes de Oca, A. N., Fería-Ortíz, M., Hikida, T., & Ota, H. (2011). Accommodating heterogenous rates of evolution in molecular divergence dating methods: an example using intercontinental dispersal of *Plestiodon* (*Eumeces*) lizards. *Systematic Biology*, 60, 3–15.

Briggs, J. C. (2003). The biogeographic and tectonic history of India. *Journal of Biogeography*, 30, 381–388.

Brown, R. M., Siler, C. D., Oliveros, C. H., Esselstyn, J. A., Diesmos, A. C., Hosner, P. A., … Alcala, A. C. (2013). Evolutionary processes of diversification in a model island archipelago. *Annual Review of Ecology, Evolution, and Systematics*, 44, 411–435.

Burbrink, F. T., Grazziotin, F. G., Pyron, R. A., Cundall, D., Donnellan, S., Irish, F., … Zaher, H. (2019). Integrating genomic-scale data for Squamata (lizards, snakes, amphisbaenians) shows no support for key traditional morphological relationships. *Systematic Biology*, syz062.

Carranza, S. & Arnold, E. N. (2003). Investigating the origins of transoceanic distributions: mtDNA shows *Mabuya* lizards (Reptilia, Scincidae) crossed the Atlantic twice. *Systematics and Biodiversity*, 2, 275–282.

Chatterjee, S., Goswami, A., & Scotese, C. R. (2013). The longest voyage: tectonic, magmatic, and paleoclimatic evolution of the Indian plate during its northward flight from Gondwana to Asia. *Gondwana Research*, 23, 238–267.

Chatterjee, S., Scotese, C. R., & Bajpai, S. (2017). *The Restless Indian Plate and its Epic Voyage from Gondwana to Asia: its Tectonic, Paleoclimate, and Paleobiogeographic Evolution. Special Paper 529*. Boulder: Geological Society of America.

Clementz, M., Bajpai, S., Ravikant, V., Thewissen, J. G. M., Saravanan, N., Singh, I. B., & Prasad, V. (2011). Early Eocene warming events and the timing of terrestrial faunal exchange between India and Asia. *Geology*, 39, 15–18.

Clift, P. D., Hodges, K. V., Heslop, D., Hannigan, R., van Long, H., & Calves, G. (2008). Correlation of Himalayan exhumation rates and Asian monsoon intensity. *Nature Geoscience*, 1, 875–880.

Cracraft, J. (1994). Species diversity, biogeography, and the evolution of biotas. *American Zoologist*, 34, 33–47.

Croizat, L., Nelson, G., & Rosen, D. E. (1974). Centers of origin and related concepts. *Systematic Zoology*, 23, 265–287.

Darriba, D., Taboada, G. L., Doallo, R., & Posada, D. (2012). JModelTest2: more models, new heuristics and parallel computing. *Nature Methods*, 9, 772.

Das, I. (2010). *A Fieldguide to the Reptiles of Southeast Asia*. London: New Holland.

Datta-Roy, A., Singh, M., & Karanth, K. P. (2014). Phylogeny of endemic skinks of the genus *Lygosoma* (Squamata: Scincidae) from India suggests an in situ radiation. *Journal of Genetics*, 93, 163–167.

de Bruyn, M., Nugroho, E., Hossain, M. M., Wilson, J. C., & Mather, P. B. (2005) Phylogeographic evidence for the existence of an ancient biogeographic barrier: the Isthmus of Kra Seaway. *Heredity*, 94, 370–378.

de Bruyn, M., Stelbrink, B., Morley, R. J., Hall, R., Carvalho, G. R., van den Bergh, G., … von Rintelen, T. (2014). Borneo and Indochina are major evolutionary hotspots for Southeast Asian biodiversity. *Systematic Biology*, 63, 879–901.

Dejtaradol, A., Renner, S. C., Karapan, S., Bates, P. J. J., Moyle, R. G., & Päckert, M. (2016). Indochinese-Sundaic faunal transition and phylogeographical divides north of the Isthmus of Kra in Southeast Asian Bulbuls (Aves: Pycnonotidae). *Journal of Biogeography*, 43, 471–483.

Esselstyn, J. A., Timm, R. M., & Brown, R. M. (2009). Do geological or climatic processes drive speciation in dynamic archipelagos? The tempo and mode of diversification in southeast Asian shrews. *Evolution*, 63, 2595–2610.

Esselstyn, J. A., Oliveros, C. H., Moyle, R. G., Peterson, A. T., McGuire, J. A., & Brown, R. M. (2010). Integrating phylogenetic and taxonomic evidence illuminates complex biogeographic patterns along Huxley's modification of Wallace's line. *Journal of Biogeography*, 37, 2054–2066.

Fabre, P. H., Irestedt, M., Fjeldså J., Bristol, R., Groombridge, J. J., Irham, M., & Jønsson, K. A. (2012). Dynamic colonization exchanges between continents and islands drive diversification in paradise-flycatchers (*Tersiphone*, Monarchidae). *Journal of Biogeography*, 39, 1900–1918.

Freitas, E. S., Bauer, A. M., Siler, C. D., Broadley, D. G., & Jackman, T. R. (2018). Phylogenetic and morphological investigation of the *Mochlus afer-sundevallii* species complex (Squamata: Scincidae) across the arid corridor of sub-Saharan Africa. *Molecular Phylogenetics and Evolution*, 127, 280–287.

Freitas, E. S., Datta-Roy, A. Karanth, K. P., Grismer, L. L., & Siler, C. D. (2019). Multilocus phylogeny and a new classification for African, Asian, and Indian supple and writhing skinks (Scincidae: Lygosominae). *Zoological Journal of the Linnenan Society*, 186, 1067–1096.

Freitas, E. S., Miller, A. H., Reynolds, R. G., & Siler, C. D. A taxonomic conundrum: characterizing a cryptic radiation of Asian gracile skinks (Squamata: Scincidae: *Riopa*) in Myanmar. *Molecular Phylogenetics and Evolution*, 146, 106754.

Gaston, K. J. (1998). Species-range size distributions: products of speciation, extinction, and transformation. *Philosophical Transactions of the Royal Society London B*, 353, 219–230.

Geissler, P. Nguyen, T. Q., Phung, T. M., Van Devender, R. W., Hartmann, T., Farkas, B., … & Böhme, W. (2011). A review of Indochinese skinks of the genus *Lygosoma* Hardwicke & Gray, 1827 (Squamata: Scincidae), with natural history notes and an identification key. *Biologia*, 66, 1159–1176.

Geissler, P., Hartmann, T., & Neang, T. (2012). A new species of the genus *Lygosoma* Hardwicke & Gray, 1827 (Squamata: Scincidae) from northeastern Cambodia, with an updated identification key to the genus *Lygosoma* in mainland Southeast Asia. *Zootaxa*, 3190, 56–68.

Gamble, T., Bauer, A. M., Greenbaum, E., & Jackman, T. R. (2008). Evidence for Gondwanan vicariance in an ancient clade of gecko lizards. *Journal of Biogeography*, 35, 88–104.

Gorog, A. J., Sinaga, M. H., & Engstrom, M. D. (2004). Vicariance or dispersal? Historical biogeography of three Sunda Shelf murine rodents (*Maxomys surifer*, *Leopoldamys sabanus*, and *Maxomys whiteheadi*). *Biological Journal of the Linnean Society*, 81, 91–109.

Grismer, J. L., Schulte II, J. A., Alexander, A., Wagner, P., Traversl S. L., Buehler, M. D., … Brown, R. M. (2016). The Eurasian invasion: phylogenomic data reveal multiple Southeast Asian origins for Indian dragon lizards. *BMC Evolutionary Biology*, 16, 43.

Grismer, L. L., Dzukafly, Z., Muin, M. A., Quah, E. S. H., Karin, B. R., Anuar, S., & Freitas, E. S. (2019). A new skink of the genus *Subdoluseps* (Hardwicke & Gray, 1828) from Peninsular Malaysia. *Zootaxa*, 4609, 358–372.

Hartigan, J. A. & Hartigan, P. M. (1985). The dip test of unimodality. *Annals of Statistics*, 13, 70–84.

Hall, R. (1996). Reconstructing Cenozoic SE Asia. In R. Hall & D. Blundell (Eds.), *Tectonic Evolution of Southeast Asia* (106, pp 153–184). London: Geological Society of London.

Hall, R. (2009). Southeast Asia's changing palaeogeography. *Blumea*, 54, 148–161.

Hall, R. (2011). Australia–SE Asia collision: plate tectonics and crustal flow. In R. Hall, M. A. Cottam, & M. E. J. Wilson (Eds.), *The SE Asian Gateway: History and Tectonics of the Australia–Asia Collision* (355, pp 75–109). London: Geological Society of London.

Heath, T. A., Hedtke, S. M., & Hillis, D. M. (2008). Taxon sampling and the accuracy of phylogenetic analyses. *Journal of Systematics and Evolution*, 46, 239–257.

Heath, T. A., Huelsenbeck, J. P., & Stadler, T. (2014). The fossilized birth-death process for coherent calibration of divergence-time estimates. *PNAS*, E2964.

Heitz, B. B., Diesmos, A. C., Freitas, E. S., Ellsworth, E. D., Grismer, L. L., Aowphol, A., Brown, R. M., & Siler, C. D. (2016). A new supple skink, genus *Lygosoma* (Reptilia: Squamata: Scincidae), from the western Philippines. *Herpetologica*, 72, 352–361.

Holbourn, A., Kuhnt, W., Kochhann, K. G. D., Andersen, N., Meier, K. J. S. (2013). Global perturbation of the carbon cycle at the onset of the Miocene Climatic Optimum. *Geology*, 43, 123–126.

Hu, X., Garzanti, E., Wang, J., Huang, W., An, W., & Webb, A. (2016). The timing of India–Asia collision onset—facts, theories, controversies. *Earth Science Reviews*, 160, 264–299.

Hughes, J. B., Round, P. D., & Woodruff, D. S. (2003). The Indochinese-Sundaic faunal transition at the Isthmus of Kra: an analysis of resident forest bird species distributions. *Journal of Biogeography*, 30, 569–580.

Inger, R. F. (1999). Distributions of amphibians in Southern Asia and adjacent islands. In W. E. Duellman (Ed.), *Patterns of Distribution of Amphibians: a Global Perspective*. Baltimore: John Hopkins University Press.

Kalyaanamoorthy, S., Minh, B. Q., Wong, T. K. F., von Haeseler, A., & Jermiin, L. S. (2017). ModelFinder: fast model selection for accurate phylogenetic estimates. *Nature Methods*, 14, 587–589.

Karin, B. R., Metallinou, M., Weinell, J. L., Jackman, T. R., & Bauer, A. M. (2016). Resolving the higher-order phylogenetic relationships of the circumtropical *Mabuya* group (Squamata: Scincidae): an out-of-Asia diversification. *Molecular Phylogenetics and Evolution*, 102, 220–232.

Karin, B. R., Freitas, E. S., Shonlebin, S., Grismer, L. L., Bauer, A. M., & Das, I. (2018). Unrealized diversity in an urban rainforest: a new species of *Lygosom*a (Squamata: Scincidae) from western Sarawak, Malaysia (Borneo). *Zootaxa*, 4370, 345–362.

Kishino, H., Miyata, T., & Hasegawa, M. (1990). Maximum likelihood inference of protein phylogeny and the origin of chloroplasts. *Journal of Molecular Evolution*, 31, 151–160.

Klaus, S., Morley, R. J., Plath, M., Zhang, Y. P., Li, J. T. (2016). Biotic interchange between the Indian subcontinent and mainland Asia through time. *Nature Communications*, 7, 12132.

Lanfear, R., Calcott, B., Ho, S. Y. W., & Guidon, S. (2012). PartitionFinder: combined selection of partitioning schemes and substitution models for phylogenetic analyses. *Molecular Biology and Evolution*, 29, 1695–1701.

Li, J. T., Li, Y., Klaus, S., Rao, D. Q., Hillis, D. M., & Zhang, Y. P. (2013). Diversification of rhacophorid frogs provides evidence for accelerated faunal exchange between India and Eurasia during the Oligocene. *PNAS*, 110, 3441–3446.

Licht, A., Boura, A., De Franceschi, D., Ducrocq, S., Soe, A. N., & Jaeger, J. J. (2014). Fossil woods from the late middle Eocene Pondaung Formation, Myanmar. *Review of Palaeobotany and Palynology*, 202, 29–46.

Linkem, C. W., Brown, R. M., Siler, C. D., Evans, B. J., Austin, C. C., Iskandae, D. T., … McGuire, J. A. (2013). Stochastic faunal exchanges drive diversification in widespread Wallacean and Pacific island lizards (Squamta: Scincidae: *Lamprolepis smaragdina*). *Journal of Biogeography*, 40, 507–520.

Lohman, D. J., de Bruyn, M., Page, T., von Rintelen, K., Hall, R., Ng, P. K. L., … von Rintelen, T. (2011). Biogeography of the Indo-Australian Archipelago. *Annual Review of Ecology. Evolution, and Systematics*, 42, 205–226.

Lomolino, M. V., Riddle, B. R., Whittaker, R. J., & Brown, J. H. (2010). *Biogeography. Fourth Edition.* Sunderland: Sinauer Associates, Inc.

Luo, S. J., Zhang, Y., Johnson, W. E., Miao, L, Martelli, P., Antunes, A., … O'Brien, S. O. (2014) Sympatric Asian felid phylogeography reveals a major Indochinese-Sundaic divergence. *Molecular Ecology*, 23, 2072–2092.

Maechler, M. (2016). diptest: Hartigan's dip test statistic for unimodality. —Correcyed. R package 0.75-7. https://CRAN.R-project.org/package=diptest.

Matzke, N. J. (2013). Probabilistic historical biogeography: new models for founder-event speciation, imperfect detection, and fossils allow improved accuracy and model-testing. *UC Berkeley Electronic Theses and Dissertations*. http://escholarship.org/uc/item/8227p52c.

Matzke, N. J. (2014). Model selection in historical biogeography reveals that founder-event speciation is a crucial process in island clades. *Systematic Biology*, 63, 951–970.

McKenna, M. C. C. (1973). Sweepstakes, filters, corridors, Noah's Arks, and beached Viking funeral ships in paleogeography. In D. H. Tarling & S. K. Runcorn (Eds.), *Implications of Continental Drift to the Earth Sciences*. London: Academic Press.

McLoughlin, S. (2001). The breakup history of Gondwana and its impact on pre-Cenozoic floristic provincialism. *Australian Journal of Botany*, 49, 271–300.

Meyer, C. P. & Paulay, G. (2005). DNA barcoding: error rates based on comprehensive sampling. *Plos Biology*, 3, e422.

Morrone, J. J. & Crisci, J. V. (1995). Historical biogeography: introduction to methods. *Annual Review of Ecology, Evolution, and Systematics*, 26, 373–401.

Morley, R. J. (2012). A review of the Cenozoic palaeoclimate history of Southeast Asia. In D. J. Gower, K., Johnson, J. Richarson, B. Rosen, Rüber, L., & S. Williams (Eds.), *Biotic Evolution and Environmental Change in Southeast Asia*. (79–114). Cambridge: Cambridge University Press.

Myers, N., Mittermeier, R. A., Mittermeier, C. G., da Fonseca, G. A. B., & Kent, J. (2000). Biodiversity hotspots for conservation priorities. *Nature*, 403, 853–858.

Nguyen, L. T., Schmidt, H. A., von Haeseler, A., & Minh, B. Q. (2015). IQ-TREE: a fast and effective stochastic algorithm for estimating maximum likelihood phylogenis. *Molecular Biology and Evolution*, 32, 268–274.

O'Connell, K. A., Smart, U., Smith, E. N., Hamidy, A., Kurniawan, N., & Fujita, M. K. (2018). Within-island diversification underlies parachuting frog (*Rhacophorus*) species accumulation on the Sunda Shelf. *Journal of Biogeography*, 45, 929–940.

Oliver, L. A., Prendini, E., Kraus, F., & Raxworthy, C. J. (2015). Systematics and biogeography of the *Hylarana* frog (Anura: Ranidae) radiation across tropical Australasia, Southeast Asia, and Africa. *Molecular Phylogenetics and Evolution*, 90, 176–192.

Oliveros, C. H., & Moyle, R. G. (2010). Origin and diversification of Philippine bulbuls. *Molecular Phylogenetics and Evolution*, 54, 822–832.

Paradis, E. & Schliep, K. (2018). ape 5.0: an environment for modern phylogenetics and evolutionary analyses in R. *Bioinformatics*, 35, 526–528.

Parnell, J. (2013). The biogeography of the Isthmus of Kra: a review. *Nordic Journal of Botany*, 31, 1–15.

Patnaik, R. (2016). Neogene–Quaternary mammalian paleobiogeography of the Indian subcontinent: an appraisal. *Comptes Endus Palevol*, 15, 889–902.

Patou, M. L., Wilting, A., Gaubert, P., Esselstyn, J. A., Criaid, C., Jennings, A. P. … Veron, G. (2010). Evolutionary history of the *Paradoxurus* palm civiets—a new model for Asian biogeography. *Journal of Biogeography*, 37, 2077–2097.

Paulay, G. & Meyer, C. (2002). Diversification in the tropical Pacific: comparisons between marine and terrestrial systems and the importance of founder speciation. *Integrative and Comparative Biology*, 42, 922–934.

Pepke, M. L., Irestedt, M., Fjeldså, J., Rahbek, C., & Jønsson, K. A. (2019). Reconciling supertramps, great speciators, and relict species with the taxon cycle stages of a large island radiation (Aves: Campephagidae). *Journal of Biogeography*, 46, 1214–1225.

Potter, P. E. & Szatmari, P. (2009). Global Miocene tectonics and the modern world. *Earth-Science Reviews*, 96, 279–295.

Quade, J., Cerling, T. E., & Bowman, J. R. (1989). Development of Asian monsoon revealed by marked ecological shift during the latest Miocene in northern Pakistan. *Nature*, 342, 163–166.

R Core Team. (2018). R: a language and environment for statistical computing. R Foundation for Statistical Computing. https://www.R-project.org/.

Rabosky, D. L. (2014). Automatic detection of key innovations, rate shifts, and diversity-dependence on phylogenetic trees. *PLoS ONE*, 9, e89543.

Rabosky, D. L., Grundler, M. C., Anderson, C. J., Title, P. O., Shi, J. J., Brown, J. W., … Larson, J. G. (2014). BAMMtools: an R package for the analysis of evolutionary dynamics on phylogenetic trees. *Methods in Ecology and Evolution*, 5, 701–707.

Rambaut, A., Drummond, A. J., Xie, D., Baele, G., & Suchard, M.A. (2018). Posterior summarization in Bayesian phylogenetics using Tracer 1.7. *Systematic Biology*, 67, 901–904.

Ratnam, J., Tomlinson, K. W., Rasquinha, D. N., & Sankaran, M. (2016). Savannahs of Asia: antiquity, biogeography, and an uncertain future. *Philisophical Transactions B*, 57, 20150305.

Reilly, S. B., Stubbs, A. L., Karin, B. R., Bi, K., Arida, E., Iskander, D. T., & McGuire, J. A. (2018). Leap-frog dispersal and mitochondrial introgression: phylogenomics and

biogeography of *Limnonectes* fanged frogs in the Lesser Sundas Archipelago of Wallacea. *Journal of Biogeography*, 46, 757–769.

Reilly, S. B., Stubbs, A. L., Karin, B. R., Arida, E., Iskander, D. T., & McGuire, J. A. (2019). Recent colonization and expansion through the Lesser Sundas by seven amphibian and reptile species. *Zoologica Scripta*, 48, 614–626.

Rocha, S., Carretero, M. A., Vences, M., Glaw, F., & Harris, D. J. (2006). Deciphering patterns of transoceanic dispersal: the evolutionary origin and biogeography of coastal lizards (*Cryptoblepharus*) in the western Indian Ocean region. *Journal of Biogeography*, 33, 13–22.

Ronquist, F., Telsenko, M., van der Mark, P., Ayres, D. L., Darling, A., Höhna, S., … Huelsenbeck, J. P. (2012). MrBayes 3.2: efficient Bayesian phylogenetic inference and model choice across a large model space. *Systematic Biology*, 61, 539–542.

Rosenzweig, M. L. (1975). On continental steady states of species diversity. In M. L. Cody & J. M. Diamond (Eds.), *Ecology and Evolution of Communities* (121–140).

Rowe, K. C., Achmadi, A. S., Fabre, P. H., Schenk, J. J., Steppan, S. J., & Esselstyn, J. A. (2019). Oceanic islands of Wallacea as a source for dispersal and diversification of murine rodents. *Journal of Biogeography*, 46, 2752–2768.

Rowsey, D. M., Heaney, L. R., & Jansa, S. A. (2018). Diversification rates of the "old endemic" murine rodents of Luzon Island, Philippines are inconsistent with incumbency effects and ecological opportunity. *Evolution*, 72, 1420–1435.

Rust, J., Singh, H., Rana, R. S., McCann, T., Singh, L., Anderson, K., … Grimaldi, D. (2010). Biogeographic and evolutionary implications of a diverse paleobiota in amber from the early Eocene of India. *PNAS*, 17, 18360–18365.

Saladin, B., Leslie, A., Wüest, R. O, Litsios, G., Conti, E., Salamin, N., & Zimmermann, N. E. (2017). Fossils matter: improved estimates of divergence times in *Pinus* reveal older diversification. *BMC Evolutionary Biology*, 17, 95.

Sanyal, P., Sarkar, A., Bhattacharya, S. K., Kumar, R., Ghosh, S. K., & Agrawal, S. (2010). Intensification of monsoon microclimate and asynchronous C_4 appearance: isotopic evidence from the Siwalik sediments.

Sayyari, E. & Mirarab, S. Fast coalescent-based computation of local branch support from quartet frequencies. *Molecular Biology and Evolution*, 33, 1654–1668.

Schott, F. A., Xie, S. P., & McCreary Jr., J. P. (2009). Indian Ocean circulation and climate variability. *Review of Geophysics*, 47, RG1002.

Schulte II, J. A. (2013). Undersampling taxa will underestimate molecular divergence dates: an example from the South American lizard clade Liolaemini. *International Journal of Evolutionary Biology*, 2013, 628467.

Shimodaira, H. 2002. An approximately unbiased test of phylogenetic tree selection. *Systematic Biology*, 51, 492–508.

Shukla, A. & Mehrotra, R. C. (2018). Early Eocene plant megafossil assemblage of western India: paleoclimatic and paleobiogeographic implications. *Review of Palaeobotany and Palynology* 258, 123–123.

Siler, C., D., Oaks, J. R., Esselstyn, J. A., Diesmos, A., C., & Brown, R. M. (2010). Phylogeny and biogeography of Philippine bent-toed geckos, (Gekkonidae: *Cyrtodactylus*) contradict a prevailing model of Pleistocene diversification. *Molecular Phylogenetics and Evolution*, 55, 699–710.

Siler, C. D., Diesmos, A. C., Alcala, A. C., & Brown, R. M. (2011). Phylogeny of the Philippine slender skinks (Scincidae: *Brachymeles*) reveals underestimated species diversity, complex biogeographical relationships, and cryptic patterns of lineage diversification. *Molecular Phylogenetics and Evolution*, 59, 53–65.

Siler, C. D., Oaks, J. R., Welton, L. J., Linkem, C. W., Swab, J. C., Diesmos, A. C., & Brown, R. M. (2012). Did geckos ride the Palawan raft to the Philippines? *Journal of Biogeography*, 39, 1217–1234.

Siler, C. D., Heitz, B. B., Davis, D. R., Freitas, E. S., Aowphol., A., Termprayoon, K., & Grismer, L. L. (2018). New supple skink, genus *Lygosoma* (Reptilia: Squamata: Scincidae), from Indochina and redescription of *Lygosoma quadrupes*. *Journal of Herpetology*, 52, 332–347.

Skinner, A., Hugall, A. F., & Hutchinson, M. N. (2011). Lygosomine phylogeny and the origins of Australian scincid lizards. *Journal of Biogeography*, 38, 1044–1058.

Skinner, A., Hutchinson, M. N., & Lee, M. S. Y. (2013). Phylogeny and divergence times of Australian Sphenomorphus group skinks (Scincidae, Squamata). *Molecular Phylogenetics and Evolution*, 69, 906–918.

Smith, T., Kumar, K., Rana, R. S., Folie, A., Solé, F., Noiret, C., … Rose, K. D. (2016). New early Eocene vertebrate assemblage from western India reveals a mixed fauna of European and Gondwana affinities. *Geoscience Frontiers*, 7, 969–1001.

Soares, A. E. R. & Schrago, C. G. (2015). The influence of taxon sampling on Bayesian divergence time inference under scenarios of rate heterogeneity among lineages. *Journal of Theoretical Biology*, 364, 31–39.

Spicer, R., Yang, J., Herman, A., Kodrul, T., Aleksandrova, G., Maslova, N., … Jin, J. H. (2017). Paleogene monsoons across India and South China: drivers of biotic change. *Gondwana Research*, 49, 350–363.

Srivistava, G., Mehrotra, R. C., Shukla, A., & Tiwari, R. P. (2014). Miocene vegetation and climate in extra peninsular India: megafossil evidences. *Specieal Publication of the Palaeontological Society of India*, 5, 283–290.

Stebner, F., Szadziewski, R., Singh, H., Gunkel, S., & Rust, J. (2017). Biting midges (Diptera: Ceratopogonidae) from Cambay amber indicate that the Eocene fauna of the Indian subcontinent was not isolated. *PLoS ONE*, 12, e0169144.

Sun, X. & Wang, P. (2005). How old is the Asian monsoon system?—Palaeobotanical records from China. *Palaeogeography, Palaeoclimatology, Palaeoecology*, 222, 181–222.

Suraprasit, K., Chaimanee, Y., Bocherens, H., Chavasseau, O., & Jaeger, J. J. (2014). Systematics and phylogeny of Middle Miocene Cervidae (Mammalia) from Mae Moh Basin (Thailand) and a paleoenvironmental estimate using enamel isotopy of sympatric herbivore species. ˆJournal of Vertebrate Paleontologyø, 34, 179–194.

Suraprasit, K., Jongautchariyakul, S., Yamee, C., Pothichaiya, C. & Bocherens, H. (2019). New fossil and isotope evidence for the Pleistocene zoogeographic transition and hypothesized savanna corridor in peninsular Thailand. *Quaternary Science Reviews*, 221, 105861.

Takai, M., Saegusa, H., Htike, T., & Thein, Z. M. M. (2006). Neogene mammalian fauna in Myanmar. *Asian Paleoprimatology*, 4, 143–172.

Tałanda, M. (2018). An exceptionally preserved Jurassic skink suggests lizard diversification preceded fragmentation of Pangaea. *Palaeontology*, 61, 659–677.

Tänzler, R., Van Dam, M. H., Toussaint, E. F. A., Suhardjono, Y. R., Balke, M., & Riedel, A. (2016). Macroevolution of hyperdiverse flightless beetles reflects the complex geological history of the Sunda Arc. *Scientific Reportsi*, 6, 18793.

Thein, Z. M. M., Htike, T., Soe, A. N., Sein, C., Maung, M. & Takai, M. (2017). Review of the investigation of primate fossils in Myanmar. In A. J. Barber, K. Zaw, & M. J. Crow (Eds.), *Myanmar: Geology, Resources, and Tectonics*. London: The Geological Society of London.

Thomas, D. C., Hughes, M., Phutthai, T., Ardi, W. H., Rajbhandary, S., Rubite, R., … & Richardson, J. E.(2012). West to east dispersal and subsequent rapid diversification of the mega-diverse genus *Begonia* (Begoniacea) in the Malesian archipelago. *Journal of Biogeography*, 39, 98–113.

Tsang, S. M., Wiantoro, S., Veluz, M. J., Sugita, N., Nguyen, Y. L., Simmons, N. B., & Lohman, D. J. (2020). Dispersal out of Wallacea spurs diversification of *Pteropus* flying foxes, the world's largest bats (Mammalia: Chiroptera). *Journal of Biogeography*, 47, 527–537.

Uetz, P. Freed, P., Hošek, J., (Eds.). 2020. The Reptile Database. http://www.reptile-database.org/ (accessed January, 2020)

van Welzen, P. C., Parnell, J. A., & Slik, J. W. F. (2011). Wallace's line and plant distributions: two or three phytogeographical areas and where to group Java? *Biological Journal of the Linnean Society*, 103, 531–545.

Vidal, N., Marin, J., Sassi, J., Battistuzzi, F. U., Donnellan, S., Fitch, A. J., … Hedges, S. B. (2012). Molecular evidence for an Asian origin of monitor lizards followed by Tertiary dispersals to Africa and Australasia. *Biology Letters*, 8, 1–3.

Vitt, L., Caldwell, J., 2013. *Herpetology: an Introductory Biology of Amphibians and Reptiles.* London: Academic Press.

Voris, H. K. (2000). Maps of Pleistocene sea levels in Southeast Asia: shorelines, river systems, and time durations. *Journal of Biogeography*, 27, 1153–1167.

Vyas, R. (2014). Notes and comments on the distribution of two endemic Lygosoma skinks (Squamata: Scincidae: Lygosominae) from India. *Journal of Threatened Taxa*, 6, 6726–6732.

Weinell, J. L., Barley, A. J., Siler, C. D., Orlov, N. L., Ananjeva N. B., Oaks, J. R., Burbrink, F. T., Brown, R. M. (In Press). Phylogenetic relationships and biogeographic range evolution in at-eyed snakes *Boiga. Zoological Journal of Linnean Society*.

Whitfield, J. B., & Locjhart, P. J. (2007). Deciphering ancient rapid radiations. *Trends in Ecology and Evolution*, 22, 258–265.

Wickham, H., François, R., Henry, L., & Müller, K. (2019). dplyr: a grammar of data manipulation. R package version 0.8.3. https://CRAN.R-project.org/package=dplyr

Wiens J. J. & Donoghue, M. J. (2004). Historical biogeography, ecology, and species richness. *Trends in Ecology and Evolution*, 19, 639–644.

Wiens, J. J., Brandley, M. C., & Reeder, T. W. (2006). Why does a trait evolve multiple times within a clade? Repeated evolution of snakelike body form in squamate reptiles. *Evolution*, 60, 123–141.

Woodruff, D. S. (2003). Neogene marine transgressions, palaeogeography, and biogeographic transitions in the Thai-Malay Peninsula. *Journal of Biogeography*, 30, 551–567.

Wu, C. H., Hsu, H. H., & Chou, M. D. (2014). Effect of the Arakan Mountains in the northwestern Indochina Peninsula on the late May Asian monsoon transition. *Journal of Geophysical Research: Atmospheres*, 10, 769–779.

Yuan, Z. Y., Zhou, W. W., Chen, X., Poyarkov Jr., N. A., Chen, H. M., Jang-Liaw, N. H., … Che, J. (2016). Spatiotemporal diversification of the true frogs (Genus *Rana*): a historical framework for a widely studied group of model organisms. *Systematic Biology*, 65, 824–842.

Zachos, J., Pagani, M., Sloan, L., Thomas, E., Billups, K. (2001). Trends, rhythms, and aberrations in global climate 65 ma to present. *Science*, 292, 686–693.

Zhang, C., Stadler, T., Kloppstein, S., Heath, T. A., & Ronquist, F. (2016). Total-evidence dating under the fossilized birth-death process. *Systematic Biology*, 65, 228–249.

Zhang, C., Rabiee, M., Sayyari, E., & Mirarab, S. (2018). ASTRAL-III: polynomial time species tree reconstruction from partially resolved gene trees. *BMC Bioinformatics*, 19(Supp 6), 15–30.

Zhang, Q., Willems, H., Ding, L., Gräfe, K. U., & Apel, E. (2012). Initial India-Asia continental collision and foreland basin evolution in the Tethyan Himalaya of Tibet: evidence from stratigraphy and paleontology. *The Journal of Geology*, 120, 175–189.

Zhang, R., Jiang, D., Zhang, Z., & Yu, E. (2015). The impact of regional uplift of the Tibetan Plateau on the Asian monsoon climate. *Palaeogeographyu, Palaeoclimatology, Palaeoecology*, 417, 137–150.

Zhong, H., Geng, J., Wong, H. K., Ma, Z., & Wu, N. (2004). A semi-quantitative method for the reconstruction of eustatic sea level history from seismic profiles and its application to the southern South China Sea. *Earth and Planetary Science Letters*, 223, 443–459.

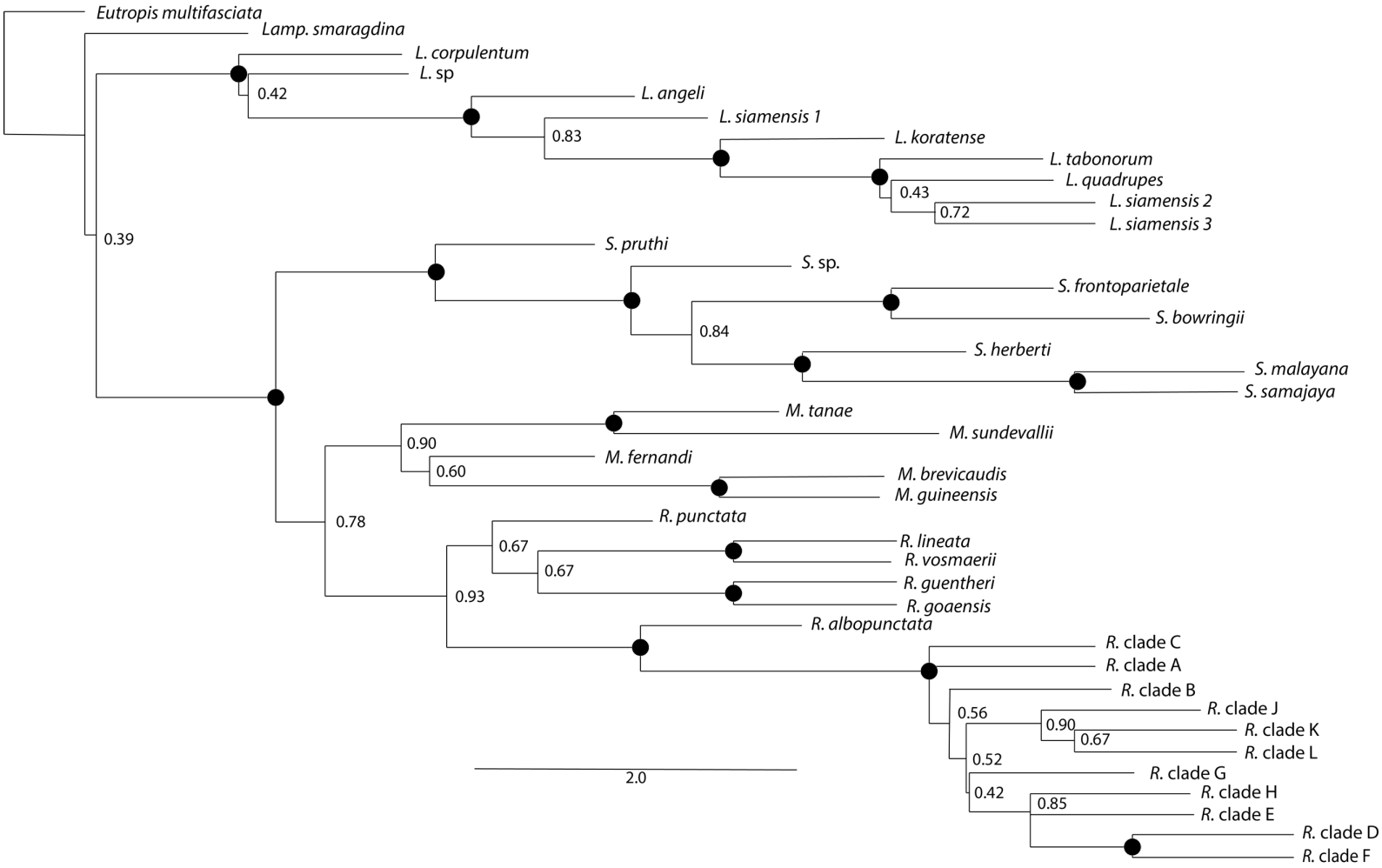

Figure S1 ASTRAL-III species tree topology for *Lygosoma* group skinks. Black circles denote nodes with local posterior probabilities ≥0.95. Probabilities <0.95 are written at each node.

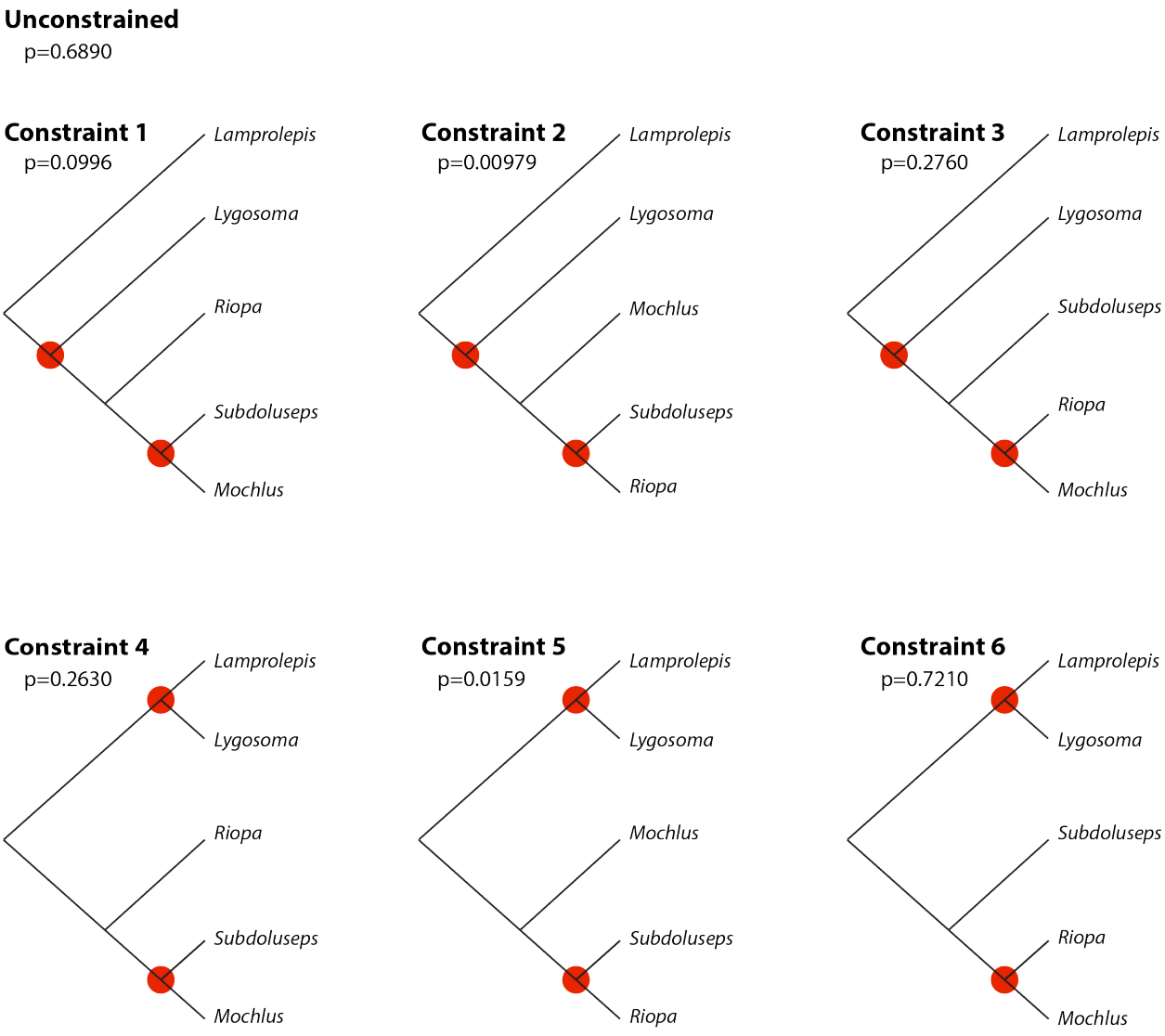

Figure S2 Constraint trees used in AU topology tests, with the red circles indicated the nodes that were constrained. The p-value for each constraint is shown. P-values of ≤0.05 were considered significantly unlikely.

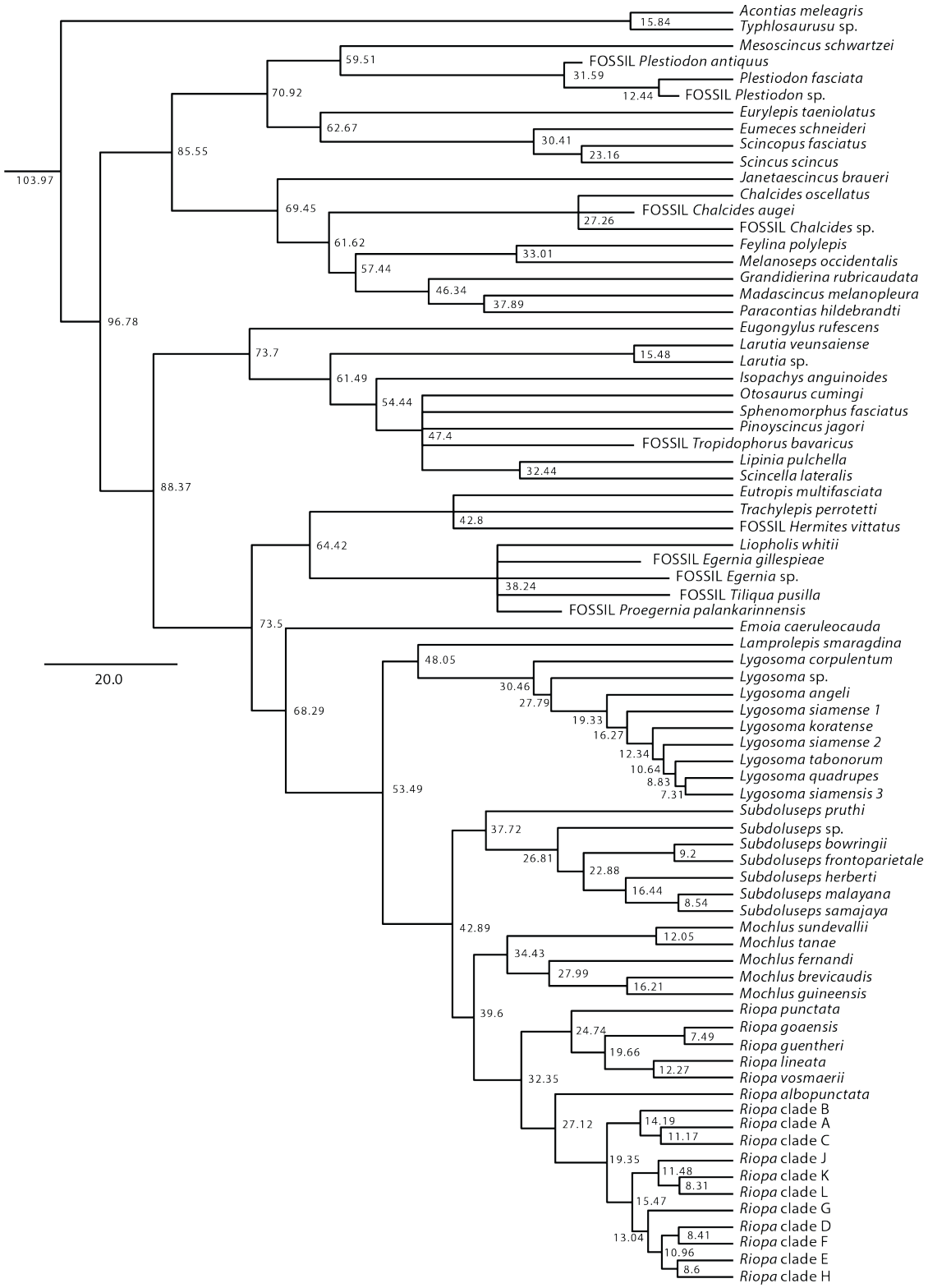

Figure S3 Bayesian concatenated topology of *Lygosoma* group skinks including all outgroups and fossil calibrations. Fossils were used to calibrate the tree and did not have any associated data, so their placement along the topology does not reflect their actual phylogenetic relationships, outside of belonging to the specific clade. The scale bar represents is in time units (millions of years).

Table S1 Ingroup and outgroup taxa used in phylogenetic analyses and their associated GenBank numbers.

Species	Museum No.	Country	BDNF	CMOS	PRLR	PTGER4	R35	RAG1	SNCAIP	ND1
Lamprolepis smaragdina	KU 337740	Philippines	X	MK409416	MK409464	MK409495	MK409524	---	MK409578	MK409613
Lygosoma angeli	---	Vietnam	X	X	X	---	X	X	X	X
Lygosoma corpulentum	LSUHC 9321	Cambodia	HQ907231	X	MK409453	HQ907531	HQ907638	MK409538	MK409565	HQ907329
Lygosoma koratense	---	Cambodia	X	X	---	X	X	partial	X	X
Lygosoma quadrupes	---	Indonesia	X	MK409409	---	MK409489	KX774339	MK409543	MK409572	KX774344
Lygosoma siamense 1	LSUHC 8002	Cambodia	KJ555045	X	---	X	X	X	X	KJ555052
Lygosoma siamense 2	LSUHC 9062	Malaysia	X	X	---	X	X	X	X	X
Lygosoma siamense 3	LSUHC 9990	Malaysia	X	X	---	X	X	X	X	X
Lygosoma sp.	ZFMK 71715	Malaysia	X	X	X	X	X	X	X	---
Lygosoma tabonorum	PNM 9821	Philippines	X	MK409400	---	MK409484	KX774338	MK409537	MK409564	KX774343
Mochlus brevicaudis	MVZ 249721	Ghana	HM160590	MK409389	HM160878	MK409474	HM161064	HM161159	HM161256	HM160781
Mochlus fernandi	PEM R5444	Gabon	X	MK409404	MK409455	MK409487	MK409513	MH129995	MK409568	MK409602
Mochlus guineensis	MVZ 252556	Ghana	X	MK409392	MK409424	MK409476	MK409502	MK409529	MK409556	MK409591
Mochlus sundevallii	UTEP 21777	Democratic Republic of Congo	X	MK409386	MK409441	X	MK409497	MH130034	MK409551	MK409586
Mochlus tanae	FMNH 255922	Tanzania	X	X	X	X	X	X	X	X
Riopa albopunctata	---	Nepal	X	X	X	X	X	X	X	X
Riopa clade A	CAS 221110	Myanmar	MN850099	X	---	X	MN850140	MN850173	X	MN850204
Riopa clade B	CAS 230414	Myanmar	MN850103	MK409395	MK409449	MK409479	MK409505	MK409532	MK409559	MK409594
Riopa clade C	CAS 239204	Myanmar	MN850108	MK409393	MK409447	MK409477	MK409503	MK409530	MK409557	MK409592
Riopa clade D	CAS 239204	Myanmar	MN850111	X	X	X	MN850148	MN850180	X	MN850214
Riopa clade E	CAS 216328	Myanmar	MN850112	X	X	X	MN850149	MN850181	X	MN850215
Riopa clade F	CAS 233106	Myanmar	MN850117	X	X	X	MN850154	MN850186	X	MN850220
Riopa clade G	CAS 231327	Myanmar	MN850119	MK409397	MK409451	MK409481	MF981875	MK409534	MK409561	MF981878
Riopa clade H	CAS 230491	Myanmar	MN850120	X	X	X	MN850156	MN850188	X	MN850222

Riopa clade J	CAS 213615	Myanmar	MN850122	MK409396	MK409450	MK409480	MK409506	MK409533	MK409560	MK409595
Riopa clade K	CAS 240673	Myanmar	MN850125	X	MK409452	MK409482	MK409508	MK409535	MK409562	MK409597
Riopa clade L	CAS 243133	Myanmar	MN850139	X	X	X	MN850171	MN850203	X	MN850238
Riopa goaensis	BMNH 1966	India	---	---	MK409467	---	---	MK409545	MK409581	MK409619
Riopa guentheri	CES 13/802	India	---	---	MK409468	---	---	MK409546	MK409582	MK409621
Riopa lineata	CES 13/805	India	---	---	MK409469	---	---	MK409547	MK409583	MK409615
Riopa punctata	CES 14/811	India	---	---	MK409471	---	---	MK409549	---	MK409616
Riopa vosmaerii	BNHM 1975	India	---	---	MK409472	---	---	MK409550	MK409585	MK409618
Subdoluseps bowringii	FMNH 261839	Cambodia	X	MK409387	MK409442	MK409473	MK409498	MK409526	MK409552	MK409587
Subdoluseps frontoparietale	ZMKUR 00705	Thailand	X	MK409401	X	MK409485	MK409509	MK409539	MK409566	MK409598
Subdoluseps herberti	LSUHC 11803	Malaysia	X	X	X	X	X	X	X	MF981877
Subdoluseps malayana	LSUHC 12098	Malaysia	X	MK409405	MK409456	---	MK409514	MK409541	MK409569	MK409603
Subdoluseps pruthi	CES 09/905	India	---	---	MK409470	---	---	MK409548	MK409584	MK409617
Subdoluseps samajaya	CAS 259777	Indonesia	X	MK409406	MK409457	MK409488	MF981876	MK409542	MK409570	MF981879
Subdoluseps sp.	CAS 231439	Myanmar	X	X	X	X	X	X	X	X
Acontias meleagris	Chimeric	---	GU457870	AY662572	JN880799	JN662868	HQ876348	HQ180119	GU432696	AY315568
Chalcides oscellatus	MVZ 242790	Somalia	HM160584	---	HM160872	HM160967	HM161058	HM161153	HM161250	HM160775
Emoia caeruleocauda	MVZ 239361	Indonesia	HM160585	---	HM160873	---	HM161059	HM161154	HM161251	HM160776
Eugongylus rufescens	Chimeric	---	HM160671	---	HM160957	HM161049	HM161144	HM161240	HM161334	HM160862
Eumeces schneiderii	MVZ 234475	Iran	HQ655168	DQ675390	JN880835	JN662870	JN568485	DQ675333	---	AY649193
Eurylepis taeniolatus	MVZ 246017	Iran	HM160586	---	HM160874	HM160968	HM161060	HM161155	HM161252	HM160777
Eutropis multifasciata	KU 337427	Philippines	X	MK409412	MK409460	MK409491	MK409520	X	MK409574	MK409609
Feylina polylepis	Chimeric	---	HM160587	---	HM160875	HM160969	HM161061	HM161156	HM161253	HM160778
Granderina rubricauda	MVZ 238841	Madagascar	GU457871	AY662571	---	JN662869	JN568493	---	GU432697	AY662556
Isopachys anguinoides	ZMKUR 00709	Thailand	---	X	X	X	X	---	X	X
Janetaescincus braueri	No voucher	Mauritius	HM160672	---	HM160958	HM161050	HM161145	HM161241	HM161335	HM160863
Larutia sp.	---	Vietnam	X	X	---	X	X	---	X	X
Larutia veunsaiense	---	Vietnam	X	X	X	X	X	---	X	X

Liopholis whitii	SAMA R34781	Australia	HM160591	---	HM160879	HM160972	HM161065	HM161160	HM161257	HM160782
Lipinia pulchella	THNC 56379	Philippines	HQ907220	---	---	X	MK409518	---	X	MK409607
Madascincus melanopleura	UMM A208656	Madagascar	HM160589	---	HM160877	HM160971	HM161063	HM161158	HM161255	HM160780
Melanoseps occidentalis	CAS 20783	Equatorial Guinea	KP843150	---	---	KP843178	---	---	---	AY649191
Mesoscincus schwartzei	UTA R50296	Guatemala	HM160578	---	HM160866	HM160961	HM161052	HM161147	HM161244	HM160769
Otosaurus cumingi	KU 338082	Philippines	X	MK409413	MK409461	MK409492	MK409521	---	MK409575	MK409610
Paracontias hildebrandti	UMM Z209166	Madagascar	HM160592	---	HM160880	HM160973	HM161066	---	---	HM160783
Pinoyscincus jagori	KU 338232	Philippines	X	MK409417	MK409465	MK409496	MK409525	---	MK409579	MK409614
Plestiodon fasciatus	KU 289463	United States	X	MK409411	---	X	MK409519	---	X	MK409608
Scincella lateralis	MVZ 246056	United States	HM160593	---	HM160881	HM16097	HM161067	HM161162	HM161258	HM160784
Scincopus fasciatus	MVZ 242724	Niger	HM160595	---	HM160882	---	HM161069	HM161164	---	HM160786
Scincus scincus	MVZ 234537	Iran	HM160667	---	HM160954	---	HM161140	HM161236	HM161331	HM160858
Sphenomorphus fasciatus	KU 338668	Philippines	X	MK409414	MK409462	MK409493	MK409522	---	MK409576	MK409611
Trachylepis perrotetti	MVZ 245351	Ghana	HM160668	---	HM160955	HM161047	HM161141	HM161237	HM161332	HM160859
Typhlosaurus sp.	MVZ 164850	---	HM160669	---	---	HM161048	HM161142	HM161238	HM161333	HM16086

Table S2 List of the fossil calibrations used in this study. Species highlighted in red are fossils of extant species. Species with stars next to their names have genetic data available and were used in our phylogenetic analysis. The taxonomic authority lists the authors who described the extinct fossils.

Fossil	Citation	Age (mya)	Clade
Chalcides augei	Čerňanský, et al., 2019	16.0–13.7	*Chalcides oscellatus** *Chalcides* sp.
Chalcides sp.	Venczel & Hír, 2013	11.1–0.0	*Chalcides oscellatus** *Chalcides augei*
Egernia gillespieae	Thorn et al., 2019	16.0–11.6	*Egernia* sp. *Liopholis whitii** *Proegernia palankarinnensis* *Tiliqua pusilla*
Egernia sp.	Myers et al., 2001	11.6–0.0	*Egernia gillespieae* *Liopholis whitii** *Proegernia palankarinnensis* *Tiliqua pusilla*

Hermites vittatus	Čerňanský & Syromyatnikova, 2019	7.2–0.0	*Eutropis multifasciata** *Trachylepis perrotetti**
Plestiodon antiquus	Holman, 1981	24.8–20.4	*Plestiodon fasciatus** *Plestiodon* sp.
*Plestiodon fasciatus**	Holman & Grady, 1989	2.6–0.0	*Plestiodon antiquus* *Plestiodon* sp.
Plestiodon sp.	Tucker et al., 2014	13.6–0.0	*Plestiodon antiquus* *Plestiodon fasciatus**
Proegernia palankarinnensis	Martin, et al., 2004	28.4–23.0	Egernia gillespieae Egernia sp. Liopholis whitii* Tiliqua pusilla
Tiliqua pusilla	Shea & Hutchinson, 1992	11.6–5.3	*Egernia gillespieae* *Egernia* sp. *Liopholis whitii** *Proegernia palankarinnensis*
Tropidophorus bavaricus	Böhme, 2010	16.0–13.6	*Isopachys anguinoides** *Larutia* sp.* *Larutia veunsaiense** *Lipinia pulchella** *Otosaurus cumingi** *Pinoyscincus jagori** *Scincella lateralis** *Sphenomophus fasciatus**

Table S3 The primers and annealing temperatures used in this study.

Gene	Primer	Sequence (5'–3')	Annealing Temp (ºC)	Reference
BDNF	BDNF.F	GACCATCCTTTTCCTKACTATGGTTATTTCATACTT	61	Leaché &McGuire, 2006
	BDNF.R	CTATCTTCCCCTTTTAATGGTCAGTGTACAAAC		
CMOS	cmosG73.1	GGCTRTAAARCARGTGAAGAAA	52.5	Whiting et al., 2003
	cmosG74.1	GARCWTCCAAAGTCTCCAATC		
PRLR	PRLR.F1	GACARYGARGACCAGCAACTRATGCC	55	Townsend et al., 2008
	PRLR.R3	GACYTTGTGRACTTCYACRTAATCCAT		
PTGER4	PTGER4.F1	GACCATCCCGGCCGTMATGTTCATCTT	55	Townsend et al., 2008
	PTGER4.R5	AGGAAGGARCTGAAGCCCGCATACA		
R35	R35.F	GACTGTGGAYGAYCTGATCAGTGTGG	55	Fry et al., 2006
	R35.R	GCCAAAATGAGSGAGAARCGCTTCTG		
RAG1	RAG1.R13	TCTGCTGTTAATGGAAATTCAAG	53	

	RAG1.R13.rev	AAAGCAAGGATAGCGACAAGAG		Adapted from Groth & Barrowclough, 1999 by unknown
SNCAIP	SNCAIP.F10	CGCCAGYTGYTGGGRAARGAWAT	55	Townsend et al., 2008
	SNCAIP.R13	GGWGAYTTGAGDGCACTCTTRGGRCT		
ND1	16dR	CTACGTGATCTGAGTTCAGACCGGAG	53	Leaché & Reeder, 2002
	tMet	TCGGGGTATGGGCCCRARAGCTT		

Table S4 Summary statistics for the AU test. LogL = the log likelihood of the tree, deltaL = the difference between the log likelihood of the tree and the log likelihood of the tree with the highest log likelihood (constraint 6), AU test p = the p-value for the AU test. P was considered significant at a vale of ≤0.05.

Tree	LogL	deltaL	AU test p
Unconstrained	-28351.290	0.000	0.689
Constraint 1	-28361.124	9.834	0.100
Constraint 2	-28364.035	12.746	0.010
Constraint 3	-28353.333	2.043	0.276
Constraint 4	-28358.950	7.660	0.263
Constraint 5	-28361.825	10.535	0.016
Constraint 6	-28351.290	0.000	0.721

Table S5 Results of biogeographic reconstructions after reducing geographic sampling of *Lygosoma* group skinks. Cells with dashed lines indicate states that were never reconstructed as ancestral ranges for the node. Bolded cells indicate the most probable ancestral range in the full-taxa phylogeny. P-values for bimodality are considered significant if the ≥0.05. The range state Wallace and all ranges including Wallacea were never reconstructed as probable, and so are removed from this table for clarity. A = Africa, I = India, SA= Southeast Asia, SS = Sundaland.

	A	I	SA	SS	A-I	A-SA	A-SS	I-SA	I-SS	SA-SS	A-I-SA	A-I-SS	A-SA-SS	I-SA-SS
Node 1: Root														
Bimodality p-value	0.00	0.00	0.00	0.00	0.00	0.00	0.00	0.00	0.00	0.00	0.00	0.00	0.01	**0.00**
Mean null reconstruction probability	0.00	0.02	0.03	0.09	0.03	0.04	0.04	0.07	0.13	0.06	0.07	0.12	0.16	**0.14**

Mean null reconstruction standard deviation	0.00	0.02	0.04	0.07	0.01	0.01	0.02	0.08	0.11	0.02	0.05	0.06	0.07	**0.06**
Original reconstruction probability	0.00	0.02	0.02	0.02	0.01	0.04	0.01	0.08	0.15	0.05	0.13	0.12	0.07	**0.28**
Z-score	-0.52	-0.21	-0.39	-0.99	-1.25	0.21	-1.33	0.09	0.22	-0.28	1.31	0.04	-1.30	**2.21**
Node 3: *Mochlus-Riopa-Subdoluseps*														
Bimodality p-value	0.88	**0.00**	0.14	0.04	0.17	0.06	0.06	0.13	0.05	0.05	0.21	0.14	0.81	0.31
Mean null reconstruction probability	0.09	**0.35**	0.05	0.06	0.16	0.10	0.05	0.06	0.04	0.00	0.01	0.01	0.01	0.00
Mean null reconstruction standard deviation	0.05	**0.22**	0.05	0.05	0.06	0.07	0.06	0.06	0.05	0.00	0.02	0.02	0.02	0.00
Original reconstruction probability	0.01	**0.37**	0.01	0.00	0.15	0.06	0.00	0.11	0.03	0.00	0.19	0.00	0.02	0.01
Z-score	-1.76	**0.08**	-0.78	-1.14	-0.19	-0.53	-0.84	0.93	-0.30	-0.62	11.36	-0.61	0.83	1.63
Node 5: *Subdoluseps*														
Bimodality p-value	---	**0.00**	0.00	0.00	---	---	---	0.07	0.21	0.00	---	---	---	0.00
Mean null reconstruction probability	---	**0.21**	0.27	0.47	---	---	---	0.00	0.00	0.04	---	---	---	0.00
Mean null reconstruction standard deviation	---	**0.25**	0.23	0.30	---	---	---	0.01	0.01	0.07	---	---	---	0.00
Original reconstruction probability	---	**0.34**	0.31	0.08	---	---	---	0.12	0.04	0.03	---	---	---	0.09
Z-score	---	**0.51**	0.16	-1.29	---	---	---	9.22	3.21	-0.08	---	---	---	Infinity
Node 7: *Riopa*														
Bimodality p-value	0.41	**0.00**	0.31	0.18	0.02	0.35	0.29	0.00	0.08	0.31	0.23	0.01	0.20	0.34
Mean null reconstruction probability	0.00	**0.97**	0.00	0.00	0.00	0.00	0.00	0.02	0.00	0.00	0.00	0.00	0.00	0.00
Mean null reconstruction standard deviation	0.00	**0.04**	0.00	0.00	0.00	0.00	0.00	0.04	0.00	0.00	0.00	0.00	0.00	0.00
Original reconstruction probability	0.00	**0.79**	0.01	0.00	0.00	0.00	0.00	0.20	0.00	0.00	0.00	0.00	0.00	0.00

Z-score	-0.40	**-4.83**	4.02	-0.65	-0.70	-0.65	-0.53	4.89	-0.72	-0.66	-0.63	-0.55	-0.52	-0.64
Node 8: *Lygosoma*														
Bimodality p-value	---	---	**0.00**	0.00	---	---	---	---	---	0.00	---	---	---	---
Mean null reconstruction probability	---	---	**0.52**	0.38	---	---	---	---	---	0.10	---	---	---	---
Mean null reconstruction standard deviation	---	---	**0.33**	0.35	---	---	---	---	---	0.10	---	---	---	---
Original reconstruction probability	---	---	**0.88**	0.01	---	---	---	---	---	0.10	---	---	---	---
Z-score	---	---	**1.09**	-1.08	---	---	---	---	---	0.00	---	---	---	---

Chapter 4: Locomotion and kinematics in three species of co-distributed skinks from Southeast Asia (Family Scincidae: *Eutropis macularia*, *Sphenomorphus maculatus*, *Subdoluseps bowringii-frontoparietale*)

ELYSE S. FREITAS, PHILIP J. BERGMANN, ANCHALEE AOWPHOL, and CAMERON D. SILER

Formatted for Biological Journal of the Linnean Society

ABSTRACT

Locomotion is an essential function in the life of vertebrates and higher locomotor performance is correlated with increased survival. Although numerous studies over the past three decades have made substantial progress in understanding the locomotion and locomotor kinematics in squamate reptiles, we still lack an understanding of how locomotion occurs across the diversity of body forms in squamate reptiles. In this study, we investigate the locomotion and kinematics of three co-distributed skink species from Southeast Asia: *Eutropis macularia*, *Sphenomorphus maculatus*, and *Subdoluseps bowringii-frontoparietale*. We find that more elongate species, *Subdoluseps bowringii-frontoparietale*, the more elongate species, has greater axial bending whereas *Sphenomorphus maculatus*, the species with the relatively longest hind limb length, has a higher maximum velocity. We also find correlations between stride mechanics (stride duration, stride length, and duty factor) and maximum velocity across all three species and correlations between stride mechanics and morphology in *Eutropis macularia* and *Sphenomorphus maculatus*. Finally, statistical analyses suggest that the two robust-limbed species, *Eutropis*

macularia and *Sphenomorphus maculatus* have higher reliance on limbed propulsion during locomotion than *Subdoluseps bowringii -frontoparietale*.

KEYWORDS: analysis of covariance (ANCOVA) — biomechanics — body elongation — canonical correlation analysis (CCA) — hind limb stride cycle — locomotor performance — principal components analysis (PCA) — undulatory locomotion —velocity

INTRODUCTION

Locomotion in vertebrates is essential for predator escape (Martin & López, 1995; Husak, 2006; Domenici et al., 2008), food acquisition (Higham, 2007), and dispersal (Medina et al., 2018), and may also have important indirect effects on sexual selection (Husak & Fox, 2008). In squamate reptiles, locomotor performance has been directly tied to survival, with studies showing that juveniles that run faster are more likely to reach adulthood (Jayne & Bennett, 1990; Garland Jr. & Losos, 1994; Miles, 2004; Husak, 2006). Therefore, selection on locomotor performance will result in species evolving morphological and behavioral strategies that maximize locomotor performance in a given environment (e.g. Arnold, 1983; Garland Jr. and Losos, 1994; Wainwright et al., 2005; Bergmann & Irschick, 2010). For example, Calsbeek & Irschick (2007) investigated morphology, habitat use, locomotor performance, and survival of *Anolis sagrei* lizards and found that males with longer limbs ran better on broad surfaces, whereas males with shorter limbs ran better on narrow surfaces. The authors compared this experimental result to the perches that the lizards were found on in their natural habitat and found that the males that favored perches that matched the diameter on which they performed best had a higher survival rate, showing that optimal locomotor performance in a given situation is a function of a species'

morphology, ecology, and behavior. However, although numerous studies have investigated locomotion in relation to morphology in squamate lizards (e.g. Huey & Hertz, 1984; Garland Jr., 1985; Losos, 1990a, 1990b; Gans & Fusari, 1994; Bauwens et al., 1995; Reilly & Delancy, 1997; Fieler& Jayne, 1998; Irschick & Losos, 1998; Vanhooydonck et al., 2006; Bergmann & Irschick, 2010; Zamora-Camacho et al., 2014; Morinaga & Bergmann, 2019), we still lack an understanding of the kinematics of locomotion across most species. Understanding how an organism's morphology correlates with its locomotor performance is important to recognizing broader patterns of organismal diversity and ecomorphology. Therefore, this lack of data affects our understanding of the evolution of morphology and ecology of squamates.

Reptiles in the order Squamata (lizards and snakes), are ideal model organisms for investigating the influence of morphology on locomotor performance given the high numbers of species and morphological and ecological diversity of the group (e.g. Vitt & Caldwell, 2013). Squamate reptiles comprise more than 10,750 recognized species (Uetz et al., 2020) and are found in most aquatic and terrestrial ecosystems (excluding the Arctic and Antarctic), with species exhibiting arboreal, fossorial, rupicolous, and/or terrestrial habits (Vitt & Caldwell, 2013). Previous studies have provided essential detail on morphology and locomotion in squamates, and from these data, we have put together a general picture of locomotion and the kinematics of locomotion (i.e. how species locomote) in squamate reptiles (Sukhanov, 1974; Russel & Bauer, 2008). There are two kinematic models of locomotion in limbed squamates. The first model suggests that velocity is a function of stride length (total distance traveled during swing and stance phases), stride duration (total time of swing and stance phases), and duty factor (the proportion of the stride that is the stance phase), with increased stride length, decreased stride duration, and decreased duty factor correlating with increased velocity during locomotion

(Sukhanov, 1974). This model has been corroborated by studies of lizard locomotion, which have shown that as speed increases, an individual's stride duration decreases and its stride length increases (Reilly & Delancy, 1997; Fieler & Jayne, 1998; Bergmann and Irschick, 2010). Additionally, the proportion of time that the foot is in contact with the ground also decreases at increased speeds (Relliy & Delancy, 1997; Fieler & Jayne, 1998; but see Bergmann & Irschick, 2010). In limbed squamates, hind limbs are the source of propulsion during locomotion (Losos, 1990a; Russel & Bauer, 2008) and larger species or species with longer limbs relative to body size reach higher velocities than their congeners with smaller hind limbs (Losos, 1990a, 1990b; Bauwens et al., 1995; Calsbeek & Irschick, 2007; Bergman & Irschick, 2010). These results indicate that the relative hind limb length compared to body size is advantageous for the evolution of higher sprint speeds in lizards.

However, numerous morphological studies of elongate-bodied squamates show that as the body lengthens the relative limb lengths decrease (Lande, 1978; Greer & Wadsworth, 2003; Wiens et al., 2006; Bergmann & Irschick, 2010; Siler & Brown, 2011). This fact then raises the question of if and how limb-reduced elongate-bodied species maintain the same level of locomotor performance as sympatric fully limbed stocky-bodied species that may be subject to similar predation pressures and resource limitations. The second kinematic model of locomotion in limbed squamates suggest that increased trunk length leads to increased axial bending during locomotion (Sukhanov, 1974). Furthermore, it has been observed that at higher speeds, lizards increase axial bending, with more elongate-bodied species bending their bodies more than stocky-bodied species (Sukhanov, 1974) as their locomotion transitions from limbed- to undulatory locomotion (Gans, 1986; Gans & Fusari, 1994; Morinaga & Bergmann, 2019). Ritter (1992) found that stocky-bodied species bent their bodies laterally via standing (discreet) waves

of lateral flexion at lower forward velocities and switched to travelling (continuous) waves of lateral flexion at higher forward velocities, whereas species with more elongate bodies and relatively shorter limbs always locomoted with traveling waves of lateral flexion regardless of the forward velocity. However, although elongate-bodied species bend their bodies more than stocky bodied species, they do not attain higher maximum velocities than stocky-bodied species (Bergmann & Irschick, 2010) nor is the energetic cost of locomotion decreased (Walton et al., 1990). This then suggests that undulation has evolved to maintain locomotor performance in elongate-bodied species instead of facilitating the evolution of an elongate body. In limbed species, undulation of the body increases stride length (Russel & Bauer, 2008) by contributing to pelvic rotation (Fieler & Jayne, 1998), and may therefore provide a mechanism by which elongate-bodied species can maintain locomotor performance at levels similar to less elongate species. Therefore, the general picture that has emerged over the last three decades of research into the mechanics of locomotion in lizards is a trade-off between relative hind limb length and relative body elongation in which species rely on either hind limb propulsion or axial bending to locomote.

Here we further investigate this biomechanics trade-off in three terrestrial co-distributed skink species found in Southeast Asia, with the goal of contributing to a broader understanding of locomotion squamates. These three species have similar maximum body sizes (max SVL) but exhibit different degrees of relative hind limb lengths and body elongation, reported here as the average ratios of hind limb length to body size (HLL/SVL), trunk length to body size (AGD/SVL), and midbody width to body size (MW/SVL): *Eutropis macularia* is a stocky-bodied species (max SVL = 62–65 mm, HLL/SVL = 0.2, AGD/SVL = 0.5, MW/SVL = 0.2; Fig. 1A) found in mixed deciduous and dry dipterocarp habitats; *Sphenomorphus maculatus* is a

relatively longer-limbed species (max SVL = 67 mm, HLL/SVL = 0.3, AGD/SVL = 0.5, MW/SVL = 0.1; Fig. 1B) found in forested areas, most often in rocky habitats at the edge of streams; and *Subdoluseps bowringii* and *Sub. frontoparietale* are elongate-bodied short-limbed semi-fossorial sister species (max SVL = 57 mm, HLL/SVL = 0.1, AGD/SVL = 0.6, MW/SVL = 0.1; Fig. 1C) found in leaf litter in mixed deciduous and dry dipterocarp habitats, with *Sub. bowringii* widespread throughout Southeast Asia and *Sub. frontoparietale* restricted to a single region in central Thailand (Das, 2010; Grismer, 2011; Chan-ard et al., 2015). Given their status as sister species (Freitas et al., 2019) and their almost identical morphologies, we treat *Subdoluseps bowringii* and *Subdoluseps frontoparietale* as a single species. These three species are diurnal ecological generalists, found across multiple pristine and disturbed habitat types and presumably feeding on a wide variety of invertebrates (Das, 2010; Grismer, 2011; Chan-ard et al., 2015), and were seen being active most often in the mornings and afternoons (ESF pers. observation). The differences in body shape and relative limb sizes across these sympatric species makes them an ideal group to study diversity in locomotor kinematics and performance relative to diversity in morphology. Therefore, we examine inter- and intraspecific locomotor performance and kinematics of these species to answer the following questions: (1) How do these species differ across morphospace? (2) Do differences in morphology between species result in differences in locomotor performance? (3) Do species with different morphologies differ in their locomotor kinematics? And (4) do intraspecific differences in performance and locomotion correspond with body size? In our interspecific comparisons, we expect *Sph. macuatus* to reach higher velocities than *E. macularia*, and *Sub. bowringii-frontoparietale* due to its relatively longer hind limbs We expect that the more elongate species, *Sub. bowringii-frontoparietale* will rely more on axial bending than limb propulsion during locomotion whereas

E. macularia and *Sph. maculatus* rely more on their limbs during locomotion, as exhibited through significant correlations between their limb biomechanics and performance. In our intraspecific comparisons, we expect that larger individuals will reach higher velocities than smaller individuals, but kinematics will not differ significantly across body sizes.

MATERIALS AND METHODS

SPECIMEN COLLECTION

Field work was conducted in central and southern Thailand from July–November by ESF and AA under Thailand National Research Council permit to ESF (NRC) 54/60 and University of Oklahoma IACUC protocol R17-019 (see Table S1 for locality and voucher information). A total of 101 juvenile and adult skinks representing four species, *Eutropis macularia* (n=32), *Sphenomorphus maculatus* (n=32), *Subdoluseps bowringii* (n=32), and *Sub. frontoparietale* (n=5) were caught using pitfall traps or by hand. Locomotion trials were conducted at Sakaerat Environmental Research Station (SERS) in Nakhon Ratchasima Province, Thailand, and individuals not collected at SERS were transported to the field station within three days of capture. During the course of the trials, individuals were stored outside on a covered patio in plastic containers with leaves and substrate to allow them to hide, and they were fed a selection of wild-caught termites and ants every other day. Individuals used in the locomotion trials were kept a maximum of seven days before either being vouchered (n=43) or released at the point of capture (n=58). Individuals that were vouchered were euthanized by being submerged in a jar with aqueous chloretone (Simmons, 2015), fixed in 10% formalin, and are accessioned and

stored in 70% ethanol at the Sam Noble Oklahoma Museum of Natural History (SNOMNH) or Zoological Museum of Kasetsart University (ZMKU).

BODY MEASUREMENTS

To compare kinematics and performance across species we took the following ten body measurements with digital calipers accurate to 0.1 mm: snout–vent length (SVL), axilla–groin distance (AGD), midbody width (MW), head length (HL), head width (HW), fore-limb length (FLL), thigh length (ThighL), shin length (ShinL), Finger III length (Fin3L), and Toe IV length (Toe4L) (Fig. 1; Bergmann & Irschick, 2010; see Freitas et al., 2019 for detailed definitions of SVL, MW, HL, and HW). We also examined lizards' tails to determine if the tail was original, regenerated (regrown fully or partially), or autotomized (stubby). Whenever possible, all handed measurements were taken on the right side of the individual. Individuals that were not vouchered (n=58) were measured by ESF before being released, and they were released at least 12 hours post-measuring to allow them to recuperate from the stress of being handled. For live individuals, each morphological character was measured in triplicate, and the average value of all three measurements was used in subsequent analyses. For vouchered specimens, measurements were taken at the SNOMNH or ZMKU by ESF. Several vouchered individuals were not able to be measured (n=11 [10 *Sph. maculatus*, 1 *Sub. bowringii*, all adults]), and so these were included in our locomotor analyses but excluded from analyses that included morphological variables.

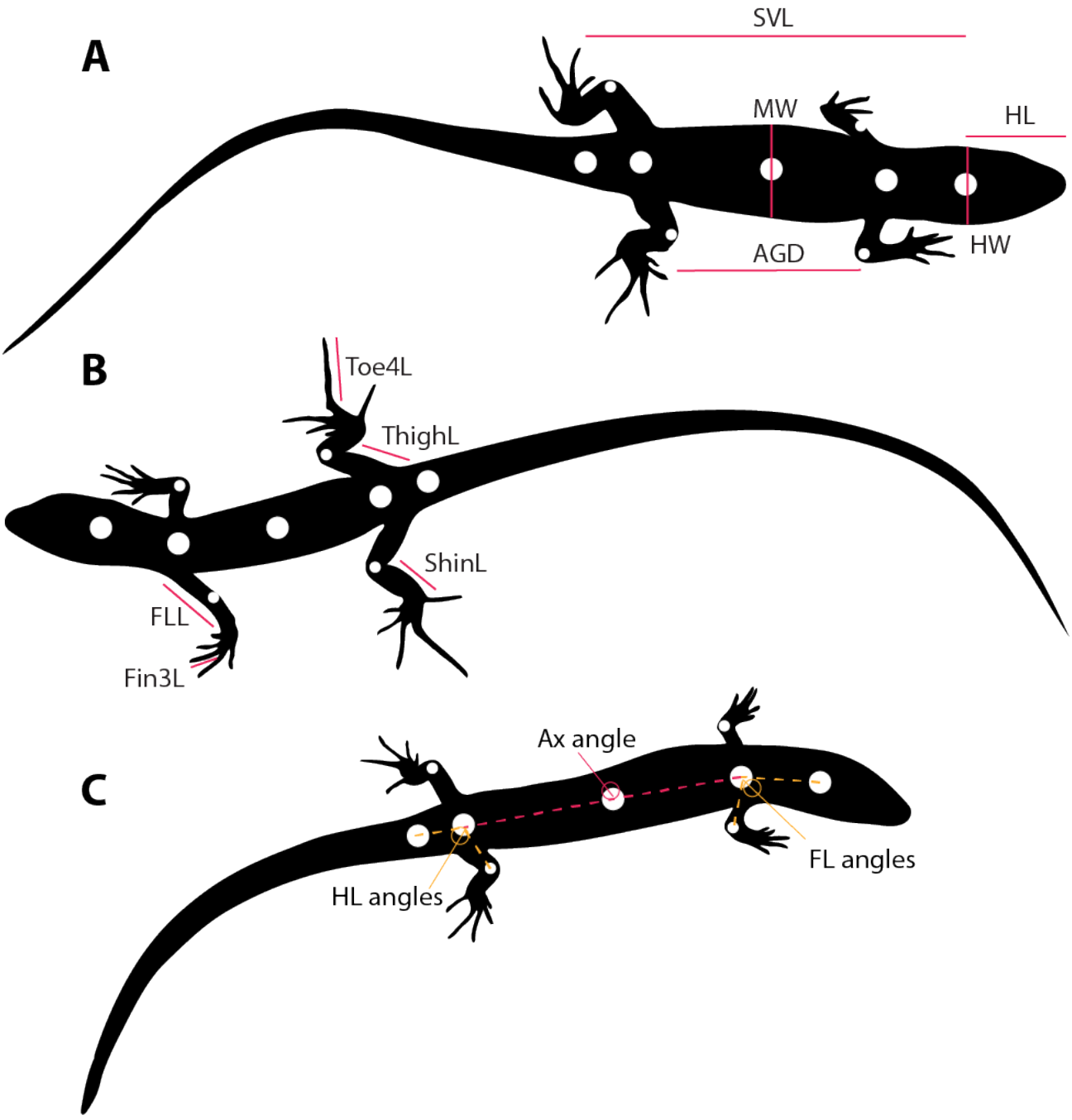

Figure 1. Illustrations of the three species of skink and all morphological and biomechanics measurements used in this study. White circles indicate where the painted points were located on the body. A) *Eutropis macularia*: AGD = axilla–groin distance, HL = head length, HW = head width, MW = midbody width, SVL = snout–vent length. B) *Sphenomorphus maculatus*: Fin3L = finger 3 length, FLL = fore-limb length, ShinL = shin length, ThighL = thigh length, Toe4L = toe 4 length. C) *Subdoluseps bowringii-frontoparietale*: AX angle = axial angle, FL angles = fore-limb protraction and retraction angles, HL angles = hind limb protraction and retraction angles.

LOCOMOTION TRIALS

All locomotion trials were conducted between 1100 and 1700 hr outdoors on a covered patio at SERS from July–November 2017. White dots were painted on the dorsal side of each individual along the midline of the body at the occiput, pectoral and pelvic girdles, midbody (halfway between the pectoral and pelvic girdles), opposite the cloaca, and on each elbow and knee (Fig. 1) using a washable non-toxic paint pen to track the xy coordinates of these landmarks during the trials (Bergman & Irschick, 2010). The instantaneous temperature and relative humidity were measured immediately after each trial using a Kestrel 3500 meter. Prior to November, trials were conducted only after ambient temperature reached 27ºC following the protocol of Bergmann & Irschick (2010). In November, the temperature decreased, and trials were performed at ambient temperatures of 20–24ºC; however, all three species were still active in the forest around SERS at this time (ESF pers. obs.), and so temperatures never fell below the thermal threshold of the lizards. Therefore, we felt justified in conducting experiments *in situ* rather than transferring individuals to a more controlled environment for locomotor data collection. Correlation analyses of ambient temperature and relative humidity against maximum velocity and maximum acceleration (see methods below) indicated that the decrease in temperature did not affect the results of the trials (temperature-maximum velocity $r^2 = -0.15$; temperature-maximum acceleration $r^2 = -0.06$; relative humidity-maximum velocity $r^2 = 0.13$, relative humidity-maximum acceleration $r^2 = 0.13$).

Locomotion trials were conducted on a one meter long portable track built by PJB that was 15 cm wide with 15 cm tall clear plexiglass sides. The soil substrate used in the trials was collected from SERS, air dried for three days, and sifted using a #60 sieve from the Student 6-Screen Sieve Set (Forestry Suppliers) to a particle size of 0.423 mm so that the substrate was

standardized across trials. When not in use, the substrate was stored in an airtight plastic fish bag to prevent it from humidifying. The track was filled with substrate to a depth of approximately 5 mm.

Each individual was filmed running on the track with a Casio Exilim 12-megapixel high-speed digital camera at a frame rate of 240 frames per second (Bergmann & Irschick, 2010). Lizards were motivated to run by a tap on the tail or by drumming our fingers on the edge of the track to startle them. Three trials were taken of each individual to account for differences in behavior and performance (Losos et al., 2002; Bergmann & Irschick, 2010). The order of individuals was randomized for each trial and all individuals received a minimum of ten minutes rest between trials. Because most trials included multiple runs by the lizard, videos were trimmed to include only a single run. An ideal run was one in which the lizard accelerated from a stopped position and ran in a straight line for at least two fore-limb and hind limb stride cycles.

It should be noted that an individual's locomotor performance on the track is not identical with their performance in nature given the homogenous conditions on the track versus the heterogenous conditions in the wild (Irschick & Losos, 1998). Furthermore, most individuals did not appear to demonstrate the same maximum velocity on the track as they did in the wild (ESF pers. obs.; Garland Jr. & Losos, 1994; Losos et al., 2002), and videos were not eliminated from analyses if the individual appeared to perform at a suboptimal speed because removal of these videos would have decreased our sample size. Therefore, the measurements of maximum velocity and acceleration obtained in this study should not be considered as the maximum performance ability for each species either in a laboratory or natural setting. However, we are confident that the data we present are true representations of the results of the trials and therefore

point to accurate, albeit simplified, similarities and differences between species (Irschick & Losos, 1998).

VIDEO DIGITIZATION AND MEASUREMENTS OF LOCOMOTOR VARIABLES

The painted points on each individual were digitized in MatLab 2019b (MathWorks, Inc.) using the environment DLTdv5 designed by Tyson Hedrick (2010; see Hedrick, 2008) to get the xy coordinates of each point over the course of the run. The resulting coordinate data were smoothed using a sixth-level smoothing spline in the MatLab Curve Fitting Toolbox on the second derivative (acceleration) of the xy coordinates (Bergmann & Irschick, 2010) to remove noise associated with stochastic error in the digitization process. We calculated the run maximum velocity from the occiput point and selected the run with the highest maximum velocity for subsequent analyses to avoid pseudoreplication from using all three runs for each individual in analyses.

For the best run, we collected the following 18 performance and kinematic measurements for a single hind limb stride following Bergmann & Irschick (2010). A hind limb stride includes both the hind limb swing and stance (step) and is defined as beginning at the video frame in which the entire foot (including toes) lifted off the substrate until the following frame that the foot lifted off the substrate: maximum velocity of the midbody point (in meters per second, MaxV), maximum acceleration of the midbody point (in meters per second squared, MaxAcc), minimum acceleration of the midbody point (which is the maximum negative acceleration, in meters per second squared, MinAcc), stride length (distance the midbody point traveled in meters, StrideL), stride duration (time stride lasted in seconds, StrideDur), step duration (time that foot was in contact with the substrate in seconds, StepDur), duty factor (the proportion of the

stride that was the step, DutyF), maximum velocity axial angle (measured as the angle formed from the pectoral, midbody, and pelvic points at the instantaneous MaxV, MaxVAx), maximum acceleration axial angle (measured as the angle formed from the pectoral, midbody, and pelvic points at the instantaneous MaxAcc, MaxAccAx), minimum axial angle (measured as the smallest angle formed from the pectoral, midbody, and pelvic points, MinAx), hind limb protraction angle (measured as the angle formed from the vent, pelvic, and knee points when hind limb reached its maximum forward extension, HLPro), hind limb protraction velocity (instantaneous velocity in meters per second at point of maximum hind limb protraction, HLProV), hind limb protraction acceleration (instantaneous acceleration in meters per second squared at point of maximum hind limb protraction, HLProAcc), hind limb retraction angle (measured as the angle formed from the vent, pelvic, and knee points when hind limb reached its maximum backwards extension, HLRetr), hind limb retraction velocity (instantaneous velocity in meters per second at point of maximum hind limb retraction (HLRetrV), hind limb retraction acceleration (instantaneous acceleration in meters per second squared, HLRetrAcc), fore-limb protraction angle (measured as the angle formed from the occiput, pectoral, and elbow points when fore-limb reached its maximum forward extension, FLPro), and fore-limb retraction (measured as the angle formed from the occiput, pectoral, and elbow points when fore-limb reached its maximum backwards extension, FLRetr; Fig. 1). Whenever possible, the hind limb stride cycle involved the animal's right hind limb, and all protraction and retraction angles were measured using the limbs on the right side of the body; however, in the videos in which the stride cycle of the left hind limb was analyzed due to visibility issues (n=3), protraction and retraction angles were measured for the left limbs. All velocities and accelerations were measured in MatLab by calculating the first and second derivative of the xy coordinates, respectively, and all

angles were measured using ImageJ. StrideL, StrideDur, and StepDur were calculated by manually determining the relevant start and end frames in ImageJ and then using time and distance measurements calculated from xy coordinates in MatLab. DutyF was calculated by dividing StepDur by StrideDur. As a note: because of the way limb angles were measured, higher HLPro and FLRetr angles indicate the limb was closer to the body whereas higher HLRetr and FLPro angles indicate the limb was farther from the body. We define the following groups of locomotor characters: performance comprises all maximum velocity and acceleration locomotor variables (n=7 variables), stride mechanics comprises all locomotor characters involving the description of the stride (n=4), and biomechanics comprises all body angle locomotor characters (n=7).

JUSTIFICATION FOR NOT APPLYING PHYLOGENETIC CORRECTIONS TO OUR DATA

Phylogenetic corrections are used to correct for the process of evolution when comparing species' traits and can be explained as follows: one of the assumptions of all univariate and multivariate statistical analyses is that the residual errors of data from different treatments are independent (Tabachnik & Fidel, 2014), meaning that data for one observation is not dependent on or influenced by data from another observation. This assumption does not always hold true for trait data from separate species because species are descended from a common ancestor and therefore are not independent (Felsenstein, 1985). For example, the evolution of a snake-like morphology in two sister species of the skink genus *Brachymeles* (Siler et al., 2011) is likely to have occurred in the common ancestor of those species, and not independently in the two terminal branches leading from the ancestor to the species. For species that are more distantly related, such as a snake-like skink in the genus *Brachymeles* and a snake-like skink in the genus

Scelotes (Whiting et al., 2003), the evolution of a snake-like morphology may still be dependent on the starting point that existed in the common ancestor of the genera. A number of methods have been proposed to correct for the non-independence of species' traits including phylogenetic independent contrasts (Felsenstein, 1985) and phylogenetic least squares (Grafen, 1989), and these techniques are used widely in the literature when comparing locomotion and morphological data across multiple species (e.g. Garland Jr. & Losos, 1994; Bauwens et al., 1995; Bergmann & Irshick, 2010).

However, implementing phylogenetic corrections is not without its own statistical and assumptive shortfalls (e.g. Westoby et al., 1995; Losos, 2011; Cooper et al., 2016; Uyeda et al., 2018). These shortfalls include the assumption that trait evolution is constant across clades and that we know the underlying evolutionary model of the characters in question (Losos, 2011). These assumptions are unlikely to hold for the species used in our analyses given the large amount of time that they have been evolving independently. In a time-calibrated phylogeny of lygosomine skinks, Skinner et al. (2011) recovered the ancestor of *Eutropis* and *Subdoluseps* as occurring 68.2 million years ago (mya) and the ancestor of *Sphenomorphus* and *Eutropis-Subdoluseps* as occurring 81.5 mya (and see Freitas et al., prev. chapter for an explanation of why these dates may be underestimates). This suggests that species in these clades have been evolving independently from each other since before the extinction of the dinosaurs, making assumptions of evolutionary rate constancy unlikely to hold true.

Furthermore, our primary goal in this study was to understand how body elongation and limb reduction, on the path towards becoming "snake-like", affects locomotor performance in scincid lizards. Therefore, we are not addressing questions on how morphology and locomotion are

correlated across the skink phylogeny (Garland Jr. et al., 1992), and so correcting for phylogenetic signal in these morphological and locomotor traits is not necessary.

PRINCIPAL COMPONENTS ANALYSIS OF MORPHOLOGY AND LOCOMOTOR VARIABLES

Phylogenetic analyses reveal that *Subdoluseps bowringii* and *Sub. frontoparietale* are not reciprocally monophyletic and may form a species complex (Freitas et al., 2019), and preliminary principal components analysis (PCA) of these species suggest that they do not differ in morphospace. Therefore, we conducted all subsequent statistical analyses of morphological and locomotor variables on these two species combined as a single "species." Prior to statistical analyses, we examined Pearson correlation matrices of the locomotor characters for multicollinearity, combining data from all species together, using the corrplot.mixed graphing function in the R v3.6.2 (R Core Team, 2019) package corrplot v0.84 (Wei and Simko, 2017). We considered characters with $r^2 \geq 0.7$ as multicollinear. For the locomotor characters, the velocity values MaxV, HLProV, and HLRetrV were highly correlated (MaxV-HLProV $r^2 = 0.89$; MaxV-HLRetrV $r^2 = 0.88$; HLProV-HLRetrV $r^2 = 0.77$), and the stride value StepDur was highly correlated with StrideDur and DutyF (StrideDur-StepDur $r^2 = 0.95$; StepDur-DutyF $r^2 = 0.74$), and so we removed HLProV, HLRetrV, and StepDur from all subsequent statistical analyses. Morphological variables are generally highly colinear, and so we removed SVL from all statistical analyses.

To investigate morphological and locomotor similarities and differences between species, we used PCA to explore intra- and interspecific distribution of species in multivariate space for morphology, locomotion (all locomotor variables combined), performance (MaxV, MaxAcc, MinAcc, HLProAcc, HLRetrAcc), stride mechanics (StideL, StrideDur, DutyF), and

biomechanics (MaxVAx, MaxAccAx, MinAx, HLPro, HLRetr, FLPro, FLRetr). PCA is a dimension-reduction technique that returns a set of independent components that describe the strength and direction of correlation between raw variables and is therefore a useful tool in which to evaluate which variables in a multivariate dataset are the most important to the process under study. We ran the PCAs in R using the command prcomp in the stats v3.6.2 package (R Core Team, 2019). For the morphology PCA, we size-size corrected all individuals within each species to remove the disproportionately large effect of body size on the variance, so that we could include juveniles and adults in the same analysis. Therefore, we size-corrected each measurement against the species-specific mean SVL and applied a character-specific regression coefficient to transform the value using the equation:

$$X_{adj}=\log_{10}(X)-\beta[\log_{10}(SVL)-\log_{10}(SVL_{mean})]$$

where X is the original value of the character, X_{adj} is the size-corrected value of the character, SVL_{mean} is the average SVL across all individuals, and β is the species-specific linear regression coefficient calculated from $\log_{10}(X)$ against $\log_{10}(SVL)$ (Thorpe, 1975; Lleonart, 2000) using the command lm in the stats package in R. We also ran PCAs of each species individually using $\log_{10}$-transformed measurements without a size correction to examine if juveniles and adults cluster differently in morphospace. The results of the species-specific morphology PCAs suggested that the majority of variation between adults and juveniles is in body size, and so we broke species into three separate age classes—hatchlings (<31 mm), juveniles (31–45 mm and adults (>45 mm) to facilitate data exploration in the locomotor PCAs. Although both *E. macularia* and *Sph. maculatus* reach larger adult sizes than *Sub.bowringii-frontoparietale* (62–65 mm, 67 mm, and 57 mm, respectively; Grismer, 2011), their minimum adult sizes are not recorded, and so we designated the size bins equally for exploratory analyses, based on personal

observations of live animals by ESF. We used these age class bins as well as bins for the tail status of the individuals (whole, regenerated, or autotomized) to examine if size or tail status had different distributions in locomotor space, and we also used bins for MaxV to explore the effect of speed on the distribution of stride mechanics and biomechanics in multivariate space. All PCAs on morphological and locomotor variables were conducted on the correlation matrix, implemented by setting scale=T. In the results (below), we report any principal components loadings with values ≥ 0.3.

ANALYSIS OF COVARIANCE OF LOCOMOTOR VARIABLES BY SPECIES AND AXILLA–GROIN DISTANCE

To determine if *E. macularia*, *Sph. maculatus*, and *Sub. bowringii-frontoparietale* differ significantly across each locomotor variable, we conducted analysis of covariance (ANCOVA) for each locomotor variable, grouping by species. We included AGD as a covariate to examine if body size (proxy for age, see above) affects locomotion. We first set orthogonal contrasts in R from the default contr.treatment to contr.sum using the options command from the base R package. We then used the command lm in the stats package in R to generate linear models of each response variable against the predictor variables species and AGD, including a species-by-AGD interaction term with the following model in R:

locomotor variable ~ species + AGD + species:AGD

After running each model, we checked the residuals for normality and homoscedasticity using plots of the residuals versus fitted values, quantile-quantile plots, histograms, and density plots; residuals did not deviate significantly from assumptions except for FLRetr, so we reran the model using $\log_{10}$-transformed FLRetr values. A p value of $p \leq 0.05$ was considered significant. For variables that were significantly different across species, we conducted a Tukey's post-hoc

test on the model results using the command glht in the R package multcomp v1.4-12 (Hothorn et al., 2008).

CANONICAL CORRELATIONS OF MORPHOLOGY AND LOCOMOTOR VARIABLES

To investigate if the degree of body elongation affects locomotion, we ran combined species canonical correlation analyses (CCAs) of size-corrected morphological variables (see above) against locomotor variables. Because we are primarily interested in the correlation of limb and body measurements with locomotion, we removed HW and HL from this analysis. Given the large number of morphological and locomotor characters measured and our low sample size for each species, we were not able to conduct analyses on the complete morphological dataset against the complete locomotor dataset. Therefore, we ran CCAs on the following data subsets: morphology (AGD, FLL, Fin3L, ThighL, ShinL, Toe4L, MW, excluding head size) against kinematics (MaxV, MaxAcc, MinAcc, HLProAcc, HLRetrAcc), morphology against stride mechanics (StrideL, StrideDur, DutyF), morphology against axial biomechanics (MaxVAx, MaxAccAx, MinAx), and morphology against limb biomechanics (HLPro, HLRetr, FLPro, FLRetr).

Additionally, we were interested in investigating if species were using their morphologies differently when locomoting, and so we ran species-specific CCAs on the same above data subsets without size-correcting the morphological variables. We were also interested in investigating how performance and stride mechanics are correlated within species and if either or both were also correlated with biomechanics, and so we conducted species-specific CCAs testing performance against stride mechanics, performance against axial biomechanics, performance against limb biomechanics, stride mechanics against axial biomechanics, stride mechanics

against limb biomechanics, and axial biomechanics against limb biomechanics. Previous studies have indicated that individuals perform differently before and after tail autotomization (reviewed in McElroy & Bergmann, 2013). Although the direction of performance change is not consistent across taxonomic groups, all studies investigating tail autonomy and performance in skinks suggested that performance declined after tails were lost. Therefore, to avoid any confounding effects of tail status, we excluded individuals with autotomized tails from the CCA analyses (n=17), including only individuals with whole or regenerated tails (n=84).

Prior to running the CCA analyses, we examined histogram, density, and Q-Q plots of each locomotor character for the combined species dataset and for each morphological and locomotor character for each species-specific dataset to check for deviations from a normal distribution. Characters that were not normally distributed were $\log_{10}$-transformed before analyses. Because all acceleration characters had negative values, we added 10 to each value before $\log_{10}$-transforming.

We ran CCA using the cc command in the R package CCA v1.2 (González & Déjean, 2012). To check if the first canonical variate was significant, we calculated Wilk's Lambda, which was then used to calculate the X^2 statistic (as in Tabachnik & Fidel, 2014). The X^2 statistic was used to determine p, with a $p \leq 0.05$ considered significant. For all significant CCAs, we analyzed how much variance from the raw or log-transformed variables was captured by the first canonical variate, and we performed a redundancy analysis (Rotenberry et al., 1996) to analyze how much variance the first canonical variate captured from its opposite raw or log-transformed variables. Loadings for significant CCAs were considered important if they had a value ≥0.3 (Tabachnik & Fidel, 2014).

RESULTS

MORPHOLOGICAL PRINCIPAL COMPONENTS ANALYSIS

Results from the combined-species, size-corrected morphological PCA indicate that all three species are separated in morphospace by body size and body elongation (Fig. 2; Table 1). The first principal component (PC1) accounts for 79.5% of the variance and loads most heavily on all characters excluding MW, but with AGD negatively correlated with all other body measurements. This PC1 loading pattern suggests that as relative AGD (body elongation) increases, other measurements of body size decrease. The second principal component (PC2) accounts for 9.2% of the variance and loads most heavily on negative MW and positive Toe4L.

Table 1. Results of the combined species morphological PCA. Loadings used in interpretation are bolded. Character definitions are in the text.

Morphology	PC1	PC2
Variance (%)	79.5	9.2
Cumulative Variance (%)	79.5	88.7
AGD	**-0.312**	0.251
HL	**0.328**	-0.173
HW	**0.351**	-0.085
FLL	**0.363**	0.015
Fin3L	**0.354**	0.177
ThighL	**0.350**	0.244
ShinL	**0.358**	0.173
Toe4L	**0.331**	**0.399**
MW	0.232	**-0.787**

Altogether, the results suggest that *Subdoluseps bowringii-frontoparietale* is more elongate than *Eutropis macularia* and *Sphenomorphus maculatus* whereas *E. macularia* and *Sph. maculatus* are similar in body size but differ in midbody width and the length of Toe IV (Fig. 2). Species-specific PCAs were not size-corrected and, as expected, body size has a disproportionately large effect on the variance, with PC1 representing size (as in Losos, 1990b). For *E. macularia*, PC1

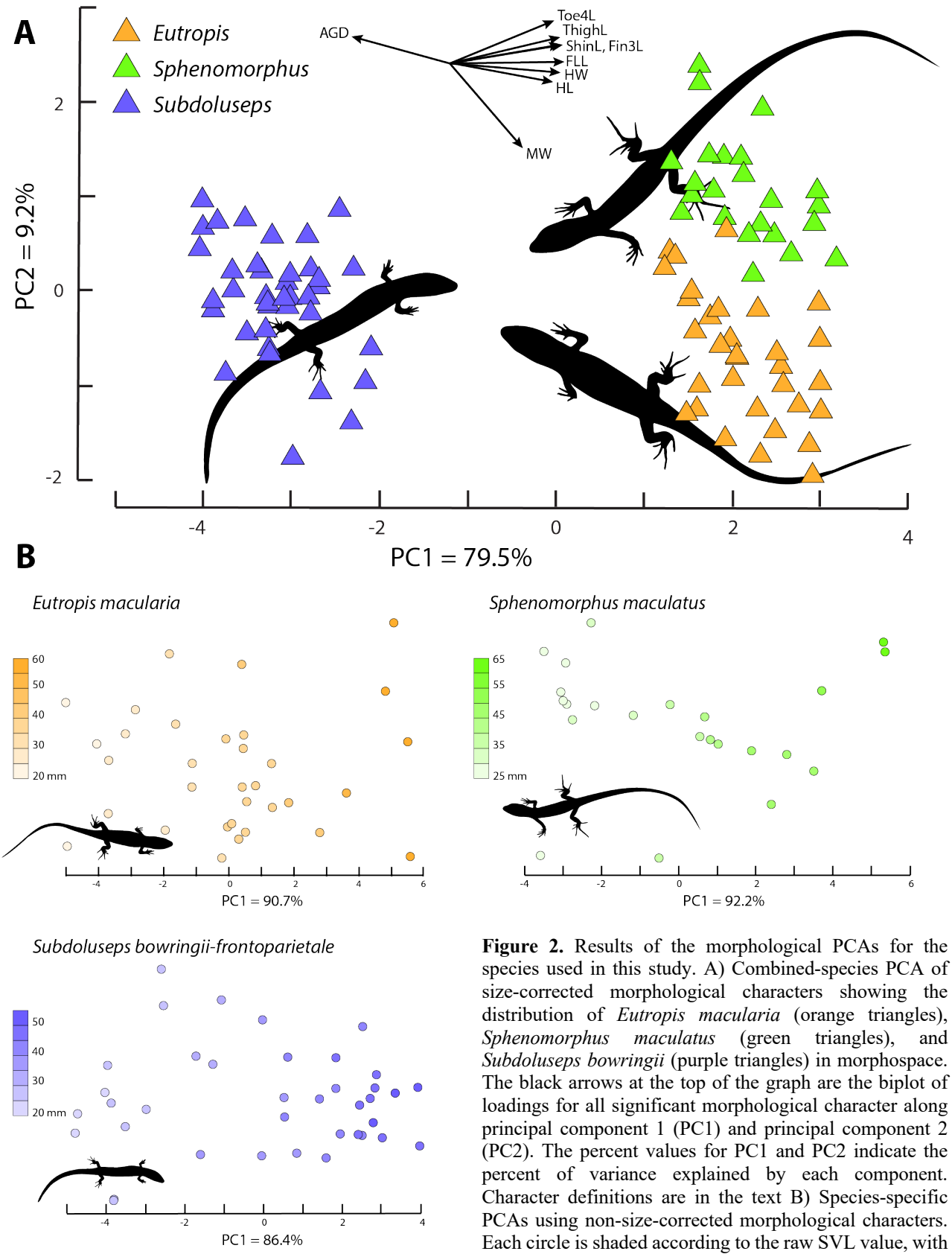

Figure 2. Results of the morphological PCAs for the species used in this study. A) Combined-species PCA of size-corrected morphological characters showing the distribution of *Eutropis macularia* (orange triangles), *Sphenomorphus maculatus* (green triangles), and *Subdoluseps bowringii* (purple triangles) in morphospace. The black arrows at the top of the graph are the biplot of loadings for all significant morphological character along principal component 1 (PC1) and principal component 2 (PC2). The percent values for PC1 and PC2 indicate the percent of variance explained by each component. Character definitions are in the text B) Species-specific PCAs using non-size-corrected morphological characters. Each circle is shaded according to the raw SVL value, with more shading indicating a larger individual. The percent values for PC1 indicate the percent of variance explained by the component.

accounts for 90.7% of the variance, for *Sph. maculatus*, PC1 accounts for 92.2% of the variance, and for *Sub. bowringii-frontoparietale*, PC1 accounts for 86.4% of the variance. Across all species-specific PCAs, juveniles differ from adults along PC1 but not PC2, indicating that there is not a large effect of allometric growth on the characters that were included in the analyses (Fig. 2).

LOCOMOTOR PRINCIPAL COMPONENTS ANALYSIS

Species-specific locomotor PCAs indicate that neither age nor tail status affected the distribution of locomotor variables in multivariate space. Additionally, species-specific PCAs on stride mechanics and biomechanics (excluding performance) indicate that neither age class, tail status, nor maximum velocity clustered individuals in multivariate stride mechanics + biomechanics space. Therefore, we conducted the remaining locomotor PCAs on all species combined, including individuals of all age classes, speeds, and tail statuses.

The combined-species locomotor PCA indicates that locomotor variables are much less correlated than they are for morphological PCAs (Fig. 3A). PC1 accounts for 20.5% of the variance and loads most heavily on negative MaxV, negative MaxAcc, negative HLProAcc, negative HLRetrAcc, and StrideDur, whereas PC2 accounts for 14.7% of the variance and loads most heavily on negative HLRetrAcc, negative DutyF, negative HLPro, and negative FLRetr (Fig. 3A; Table 2). Therefore, species are primarily separated by performance and secondarily separated by stride mechanics and biomechanics. Additionally, it appears that *Sub. bowringii-frontoparietale* has a smaller distribution in locomotor space than both *E. macularia* and *Sph. maculatus* with the majority of *Sub. bowringii-frontoparietale* individuals clustered in the middle

Table 2. Results of the combined-species locomotor PCAs. Loadings used in interpretation are bolded. Character definitions are in the text.

All Locomotor Characters	**PC1**	**PC2**
Variance (%)	20.5	14.7
Cumulative Variance (%)	20.5	35.2
MaxV	**-0.341**	-0.040
MaxAcc	**-0.430**	-0.240
MinAcc	-0.237	-0.269
HLProAcc	**-0.399**	-0.273
HLRetrAcc	**-0.325**	**-0.318**
StrideL	0.104	-0.133
StrideDur	**0.414**	-0.222
DutyF	0.254	**-0.419**
MaxVAx	0.174	-0.186
MaxAccAx	0.064	-0.199
MinAx	0.253	-0.221
HLPro	0.150	**-0.399**
HLRetr	0.067	-0.082
FLPro	0.073	-0.257
FLRetr	-0.016	**-0.310**
Performance	**PC1**	**PC2**
Variance (%)	49.9	26.5
Cumulative Variance (%)	49.9	76.4
MaxV	**0.356**	**0.558**
MaxAcc	**0.543**	0.192
MinAcc	0.294	**-0.670**
HLProAcc	**0.534**	0.161
HLRetrAcc	**0.455**	**-0.422**
Stride Mechanics	**PC1**	**PC2**
Variance (%)	50.6	33.4
Cumulative Variance (%)	50.6	84.0
StrideL	**0.304**	**0.901**
StrideDur	**0.708**	0.004
DutyF	**0.638**	**-0.433**
Biomechanics	**PC1**	**PC2**
Variance (%)	24.1	19.3
Cumulative Variance (%)	24.1	43.4
MaxVAx	**0.390**	-0.173
MaxAccAx	**0.370**	**0.389**
MinAx	**0.539**	0.167
HLPro	**0.363**	**0.341**
HLRetr	0.155	**0.392**
FLPro	**0.414**	**-0.414**
FLRetr	**0.305**	**-0.590**

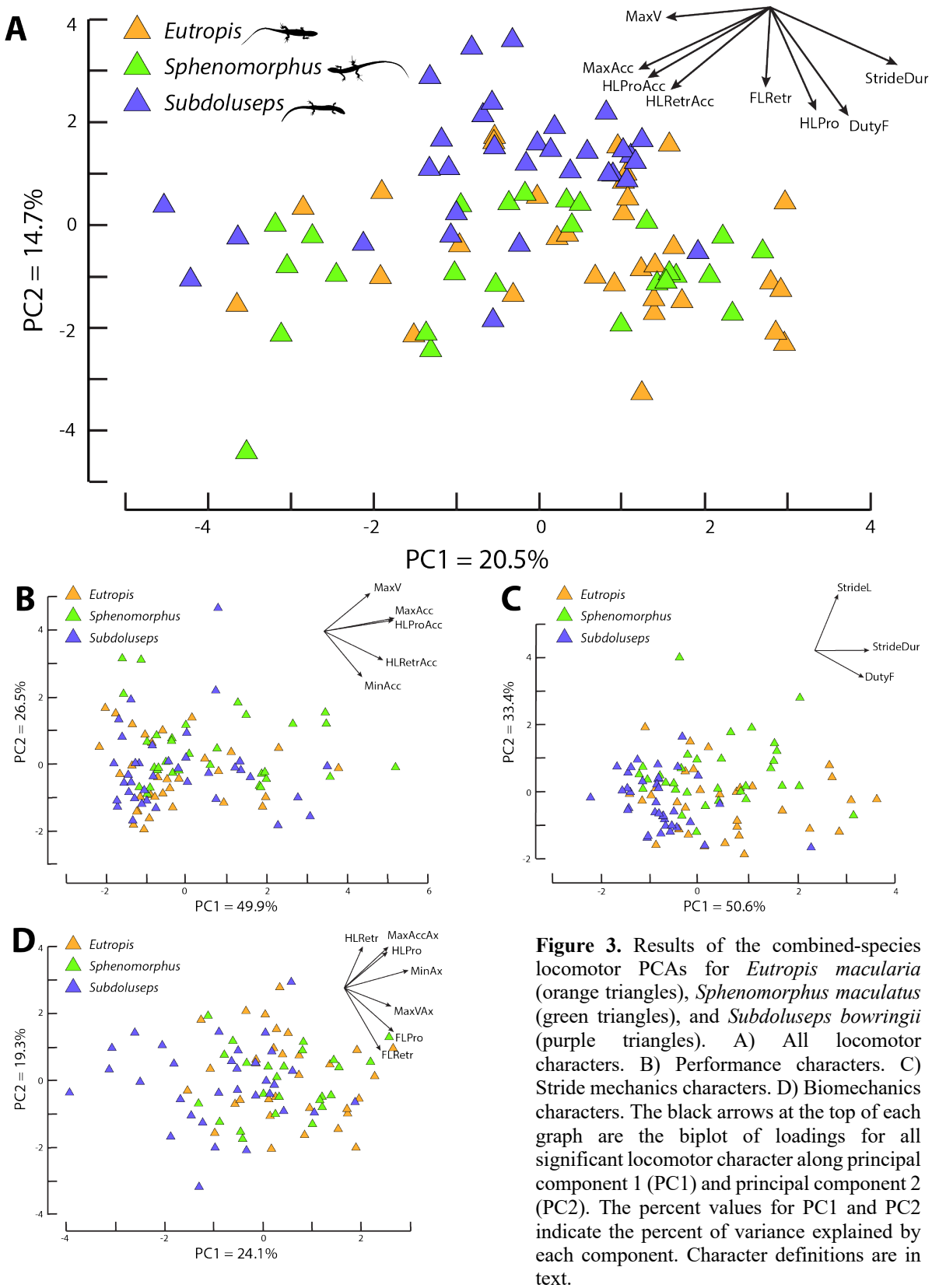

Figure 3. Results of the combined-species locomotor PCAs for *Eutropis macularia* (orange triangles), *Sphenomorphus maculatus* (green triangles), and *Subdoluseps bowringii* (purple triangles). A) All locomotor characters. B) Performance characters. C) Stride mechanics characters. D) Biomechanics characters. The black arrows at the top of each graph are the biplot of loadings for all significant locomotor character along principal component 1 (PC1) and principal component 2 (PC2). The percent values for PC1 and PC2 indicate the percent of variance explained by each component. Character definitions are in text.

of PC1 and near the top of PC2. In contrast, the other two species overlap considerably and are distributed more evenly across multivariate space.

As expected from the results of the locomotor PCA (all variables together), the performance PCA (on the variables MaxV, MaxAcc, MinAcc, HLProAcc, HLRetrAcc; Fig. 3B; Table 2), the stride mechanics PCA (on the variables StideL, StrideDur, DutyF; Fig. 3C; Table 2), and the biomechanics PCA (on the variables MaxVAx, MaxAccAx, MinAx, HLPro, HLRetr, FLPro, FLRetr; Fig. 3D; Table 2) show that *E. macularia and Sph. maculatus* overlap highly in multivariate space but that *Sub. bowringii-frontoparietale* appears to occupy more confined and distinct clusters in multivariate space. This differential distribution of species across multivariate space suggests that there are differences in locomotion between the elongate- and stocky-bodied species. For the performance PCA, PC1 accounts for 49.9% of the variance and loads most heavily on all characters excluding MinAcc whereas PC2 accounts for 26.5% of the variance and loads most heavily on MaxV, negative MinAcc, and negative HLRetrAcc (Fig. 3B; Table 2). For the stride mechanics PCA, PC1 accounts for 50.6% of the variation and loads most heavily on all characters whereas PC2 account for 33.4% of the variance and loads most heavily on StrideL and negative DutyF (Fig. 3C; Table 2). For the biomechanics PCA, PC1 accounts for 24.1% of the variance and loads most heavily on all characters excluding HLRetr, and PC2 accounts for 19.3% of the variance and loads most heavily on MaxAccAx, HLPro, HLRetr, negative FLPro, and negative FLRetr (Fig. 3D; Table 2).

ANALYSIS OF COVARIANCE

Results of the analyses of covariance (ANCOVAs; Table 3) indicate that the only locomotor response variable that was significantly different across species was MaxV (p=0.049), with the Tukey test indicating that *Sub. bowringii-frontoparietale* differs significantly from *Sph. macularia* (p=0.042; Fig. 4A; Table 3). However, there was not a significant effect of AGD on MaxV (p=0.30; Table 3) nor was there a significant interaction between species and AGD (p=0.127; Table 3). Although only MaxV was significant different between species, the response variable StrideDur had a significant interaction term of species and AGD (p=0.024; Fig. 4B; Table 1). Additionally, several response variables were significantly affected by AGD, with all showing a positive correlation. These response variables were StrideL (p<0.000), DutyF (p=0.002), HLPro (p=0.023), and MinAx (p=0.017; Fig. 4C–F; Table 3). All other locomotor response variables showed no significant differences between species and across AGD.

CANONICAL CORRELATION ANALYSIS

Results from the combined-species canonical correlations analyses (CCA) indicated that there was no significant correlation between morphology against axial angles, but that morphology against performance, morphology against stride mechanics, and morphology against hind limb angles was significant (Table 4). For morphology (AGD, FLL, Fin3L, ThighL, ShinL, Toe4L, MW) against performance (MaxV, MaxAcc, MinAcc, HLProAcc, HLRetrAcc) (Wilks' Λ=0.465, X^2=50.150, p<0.05; Table 5), the morphology variate loaded on Fin3L and ThighL and explained 5.7% of morphological variance, whereas the performance variate loaded on MaxV and MaxAcc

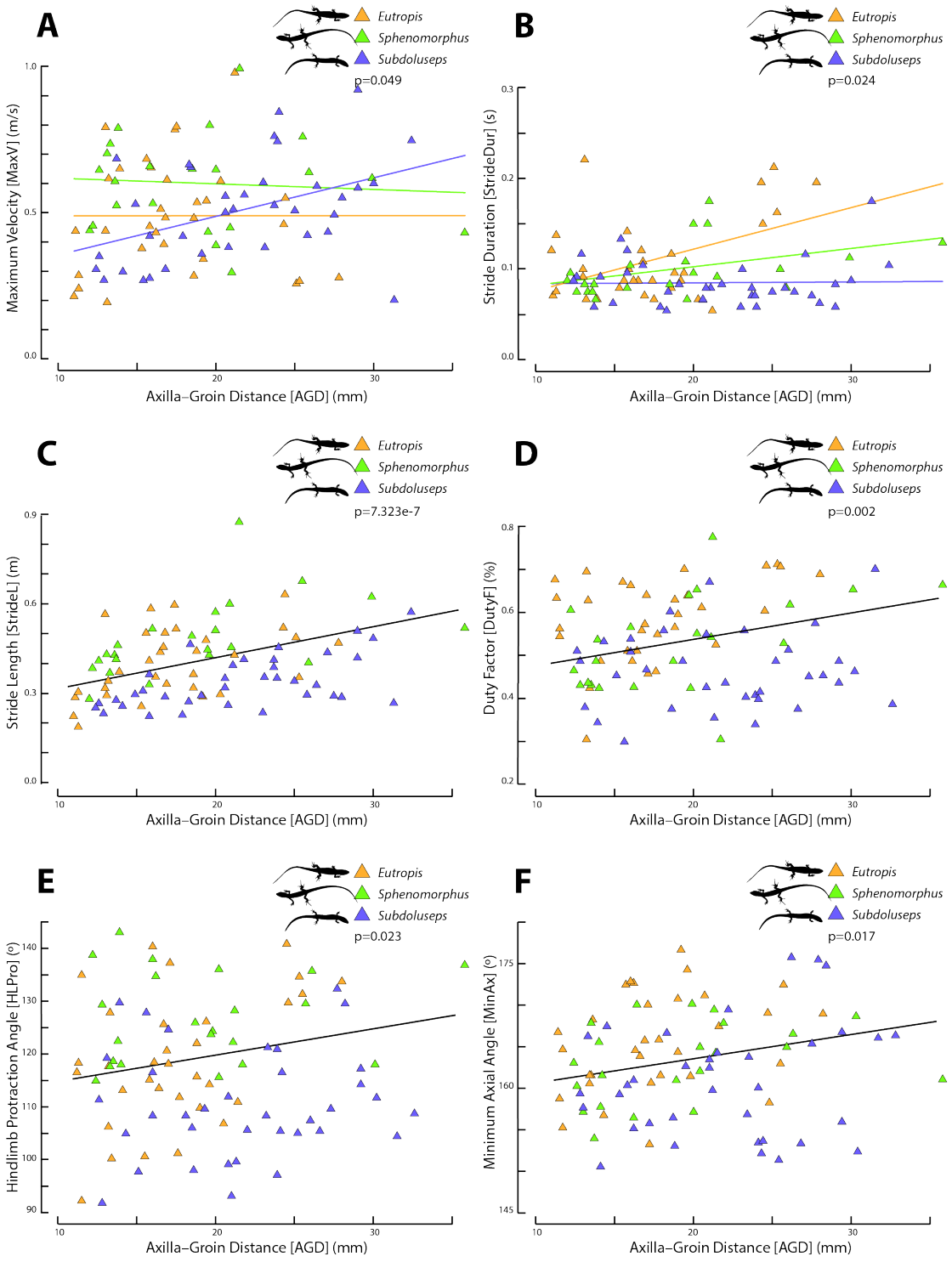

Figure 4. Graphs of the ANCOVA results for all significant tests showing values *Eutropis macularia* (orange triangles), *Sphenomorphus maculatus* (green triangles), and *Subdoluseps bowringii* (purple triangles), and fitted regression lines. Color lines in A and B indicate that significant differences were found for each species (A) and that the interaction term was significant (B). Black lines in C–G indicate that significant differences were found for across AGD but not for species. P-values for each test are shown below the legend.

and explained 14.3% of the performance variance (Table 5). Variance in morphology explained 3.6% of the variance in performance (Table 5). For morphology against stride mechanics (StrideL, StrideDur, DutyF) Wilks' Λ=0.391, X^2=62.426, p<0.001; Table 5), the morphology variate loaded on all morphological characters with AGD negatively correlated with the other characters and explained 75.7% of the variance, whereas the stride mechanics variate loaded on all stride mechanics characters and explained 44.0% of the variance (Table 5). Variance in morphology explained 20.6% of the variance in stride mechanics (Table 5).

Table 3. Results of the ANCOVA of species and body size (AGD) for all locomotor characters. Significant p-values are bolded.

	Species:AGD p-value	Species p-value	AGD p-value
Performance			
MaxV	0.127	**0.049**	0.295
MaxAcc	0.252	0.077	0.630
MinAcc	0.556	0.610	0.722
HLProAcc	0.598	0.162	0.600
HLRetrAcc	0.123	0.104	0.292
Stride Mechanics			
StrideL	0.828	0.348	**0.000**
StrideDur	**0.024**	---	---
DutyF	0.139	0.688	**0.002**
Biomechanics			
MaxVAx	0.508	0.232	0.200
MaxAccAx	0.643	0.244	0.860
MinAx	0.868	0.809	**0.017**
HLPro	0.106	0.051	**0.023**
HLRetr	0.281	0.227	0.276
FLPro	0.621	0.394	0.191
FLRetr	0.388	0.230	0.429

For morphology against limb angles (HLPro, HLRetr, FLPro, FLRetr) (Wilks' Λ=0.363, X^2=58.822, p<0.001; Table 5), the morphology variate again loaded on all morphological characters with AGD negatively correlated with the other characters and explained 55.3% of the

variance, whereas the limb angle variate loaded on HLPro and explained 21.5% of the variance (Table 4). Variance in morphology explained 11.5% of the variance in hind limb angles (Table 4).

Results of the species-specific CCAs indicated that there was no significant correlation between morphology and performance, morphology versus axial angles, performance against axial angles, performance against limb angles, and axial angles against limb angles for all three species (Table 4). Morphology against stride mechanics was significant for *E. macularia* (Λ=0.062, X^2=57.149, p<0.001; Table 4) and *Sph. maculatus* (Λ=0.033, X^2=35.921, p<0.025; Table 4), but not for *Sub. bowringii-frontoparietale* (Table 4). For *E. macularia*, the morphology variate loaded most heavily on all morphological characters and explained 62.1% of the variance whereas the stride mechanics variate loaded on all stride mechanics characters and explained 41.1% of the variance (Table 6). Variance in *E. macularia* morphology explained 31.7% of the variance in their stride mechanics. For *Sph. maculatus*, the morphological variate loaded on all morphological characters and explained 82.1% of the variance, whereas the stride mechanics variate loaded on all stride mechanics characters and explained 28.7% of the variance (Table 6). Variance in *Sph. maculatus* morphology explained 27.0% of the variance in stride mechanics (Table 6). Morphology against limb angles was only significant for *E. macularia* (Λ=0.046, X^2=61.780, p<0.001; Table 4). In this result, the morphological variate loaded on all morphological characters excluding MW and explained 22.6% of the variance, whereas the limb angles variate loaded on all limb angle characters and explained 24.8% of the variance (Table 7). Variance in morphology explained 20.5% of the variance in limb angles (Table 7). Performance against stride mechanics was significant for all three species (*E. macularia* Λ=0.033, X^2=73.020,

Table 4. Summary statistics for the CCA analyses. Significant tests are bolded. N = number of individuals, df = degrees of freedom. P-values were obtained from Chi-squared tables and thus represent the upper limit of the true p-value. Sample sizes vary across tests due to missing data for some individuals. Character definitions are in the text.

Species-combined	**N**	**Wilks' Λ**	X^2	**df**	**p (<)**
Morphology-Performance	**73**	**0.465**	**50.150**	**35**	**0.050**
Morphology-Stride Mechanics	**73**	**0.391**	**62.426**	**21**	**0.001**
Morphology-Axial Biomechanics	72	0.634	29.815	21	0.100
Morphology-Limb Biomechanics	**65**	**0.363**	**58.822**	**28**	**0.010**
Eutropis macularia	**N**	**Wilks' Λ**	X^2	**df**	**p**
Morphology-Performance	27	0.095	45.830	35	0.250
Morphology-Stride Mechanics	**27**	**0.062**	**57.159**	**21**	**0.001**
Morphology-Axial Biomechanics	27	0.248	28.559	21	0.250
Morphology-Limb Biomechanics	**27**	**0.046**	**61.780**	**28**	**0.001**
Performance-Stride Mechanics	**27**	**0.033**	**73.020**	**15**	**0.001**
Performance-Axial Biomechanics	27	0.383	20.613	15	0.250
Performance-Limb Biomechanics	27	0.276	27.030	20	0.250
Stride Mechanics-Axial Biomechanics	27	0.621	10.704	9	0.500
Stride Mechanics-Limb Biomechanics	**27**	**0.383**	**21.087**	**12**	**0.050**
Limb Biomechanics-Axial Biomechanics	27	0.763	5.951	12	0.950
Sphenomorphus maculatus	**N**	**Wilks' Λ**	X^2	**df**	**p**
Morphology-Performance	17	0.115	20.509	35	0.990
Morphology-Stride Mechanics	**17**	**0.033**	**35.921**	**21**	**0.025**
Morphology-Axial Biomechanics	16	0.066	25.777	21	0.250
Morphology-Limb Biomechanics	13	0.004	33.746	28	0.250
Performance-Stride Mechanics	**27**	**0.029**	**75.801**	**15**	**0.001**
Performance-Axial Biomechanics	26	0.400	18.759	15	0.250
Performance-Limb Biomechanics	22	0.205	25.346	20	0.250
Stride Mechanics-Axial Biomechanics	**26**	**0.387**	**20.398**	**9**	**0.025**
Stride Mechanics-Limb Biomechanics	22	0.297	20.661	12	0.100
Limb Biomechanics-Axial Biomechanics	22	0.634	7.743	12	0.900
Subdoluseps bowringii-frontoparietale	**N**	**Wilks' Λ**	X^2	**df**	**p**
Morphology-Performance	29	0.324	24.227	35	0.950
Morphology-Stride Mechanics	29	0.267	29.682	21	0.250
Morphology-Axial Biomechanics	29	0.492	15.966	21	0.900
Morphology-Limb Biomechanics	25	0.335	19.681	28	0.900
Performance-Stride Mechanics	**30**	**0.046**	**75.541**	**15**	**0.001**
Performance-Axial Biomechanics	30	0.490	17.470	15	0.500
Performance-Limb Biomechanics	26	0.343	21.380	20	0.500
Stride Mechanics-Axial Biomechanics	30	0.692	9.402	9	0.500
Stride Mechanics-Limb Biomechanics	26	0.427	17.849	12	0.250
Limb Biomechanics-Axial Biomechanics	26	0.483	15.581	12	0.250

p<0.001; *Sph. maculatus* Λ=0.029, X^2=75.800, p<0.001; *Sub. bowringii-frontoparietale* Λ=0.046, X^2=75.541, p<0.001; Table 4). For *E. macularia*, the performance variate loaded on negative MaxV, MinAcc, and HLRetrAcc and explained 24.1% of the variance whereas the stride mechanics variate loaded on all stride mechanics characters with StrideL negatively correlated with the other characters and explained 43.2% of the variance (Table 8). Variance in *E. macularia* performance explained 40.8% of the variance in stride mechanics whereas stride mechanics explained 22.7% of the variance in performance (Table 8). For *Sph. maculatus*, the performance variate loaded on negative MaxV and positive MinAcc and explained 23.6% of the variance, whereas the stride mechanics variate loaded on negative StrideL and DutyF and explained 24.8% of the variance (Table 8). Variance in *Sph. maculatus* performance explained 23.2% of the variance in stride mechanics and variance in stride mechanics explained 22.1% of the variance in performance (Table 8). For *Sub. bowringii-frontoparietale*, the performance variate loaded on MaxV, MaxAcc, and HLProAcc and accounted for 25.8% of the variance whereas the stride mechanics variate loaded on all stride mechanics characters with StrideL negatively correlated with the other characters and explained 44.7% of the variance (Table 8). Variance in *Sub. bowringii-frontoparietale* performance explained 40.5% of the variance in stride mechanics and variance in stride mechanics explained 23.3% of the variance in performance (Table 8). Stride mechanics against axial angles was only significant for *Sph. maculatus* (Λ=0.387, X^2=20.398, p<0.025; Table 4). The stride mechanics variate loaded on negative DutyF and explained 24.0% of the variance, whereas the axial angles variate loaded on negative MaxAccAx and explained 19.2% of the variance (Table 9). Variance in stride mechanics explained 8.0% of the variance in axial angles and variance in axial angles explained

Table 5. Detailed results of the significant combined-species CCA analyses. All morphological variables were size-corrected before analyses. Redundancy refers to the amount of variance in the variate that is explained by the variance in the opposite variate. Loadings used in interpretation are bolded. Character definitions are in the text.

Morphology-Performance, significant			
Morphology variate		*Performance variate*	
Variance (%)	5.7	Variance (%)	14.3
Redundancy (%)	---	Redundancy (%)	3.6
AGD	0.002	MaxV	**-0.554**
FLL	0.221	MaxAcc	**-0.603**
Fin3L	**0.352**	MinAcc	0.173
ThighL	**0.382**	HLProAcc	0.130
ShinL	0.196	HLRetrAcc	0.014
Toe4L	0.046		
MW	0.206		
Morphology-Stride Mechanics, significant			
Morphology variate		*Stride Mechanics variate*	
Variance (%)	75.7	Variance (%)	44.0
Redundancy (%)	---	Redundancy (%)	20.6
AGD	**-0.834**	StrideL	**0.581**
FLL	**0.934**	StrideDur	**0.690**
Fin3L	**0.963**	DutyF	**0.711**
ThighL	**0.922**		
ShinL	**0.937**		
Toe4L	**0.800**		
MW	**0.660**		
Morphology-Axial Biomechanics, not significant			
Morphology variate		*Limb Biomechanics variate*	
Variance (%)	50.1	Variance (%)	49.3
Redundancy (%)	---	Redundancy (%)	11.8
AGD	**-0.919**	MaxVAx	**0.726**
FLL	**0.767**	MaxAccAx	**0.850**
0Fin3L	**0.633**	MinAx	**0.479**
ThighL	**0.703**		
ShinL	**0.678**		
Toe4L	**0.449**		
MW	**0.721**		
Morphology-Limb Biomechanics, significant			
Morphology variate		*Limb Biomechanics variate*	
Variance (%)	55.3	Variance (%)	21.5
Redundancy (%)	---	Redundancy (%)	11.5
AGD	**-0.533**	HLPro	**0.911**
FLL	**0.839**	HLRetr	-0.134

Fin3L	**0.777**	FLPro	0.103
ThighL	**0.911**	FLRetr	0.029
ShinL	**0.782**		
Toe4L	**0.833**		
MW	**0.376**		

Table 6. Detailed results of the CCA analyses of morphology against stride mechanics for each species. Redundancy refers to the amount of variance in the variate that is explained by the variance in the opposite variate. Loadings used in interpretation are bolded. Character definitions are in the text.

***Eutropis macularia*, significant**			
Morphology variate		*Stride Mechanics variate*	
Variance (%)	62.1	Variance (%)	41.1
Redundancy (%)	---	Redundancy (%)	31.7
AGD	**0.759**	StrideL	**0.560**
FLL	**0.877**	StrideDur	**0.781**
Fin3L	**0.733**	DutyF	**0.556**
ThighL	**0.882**		
ShinL	**0.788**		
Toe4L	**0.661**		
MW	**0.789**		
***Sphenomorphus maculatus*, significant**			
Morphology variate		*Stride Mechanics variate*	
Variance (%)	82.1	Variance (%)	28.7
Redundancy (%)	---	Redundancy (%)	27.0
AGD	**0.849**	StrideL	**0.715**
FLL	**0.917**	StrideDur	**0.495**
Fin3L	**0.946**	DutyF	**0.325**
ThighL	**0.912**		
ShinL	**0.933**		
Toe4L	**0.905**		
MW	**0.874**		
Subdoluseps bowringii-frontoparietale, not significant			
Morphology variate		*Stride Mechanics variate*	
Variance (%)	51.7	Variance (%)	24.9
Redundancy (%)	---	Redundancy (%)	13.8
AGD	**-0.838**	StrideL	**-0.814**
FLL	**-0.595**	StrideDur	-0.282
Fin3L	**-0.563**	DutyF	-0.066
ThighL	**-0.700**		
ShinL	**-0.784**		
Toe4L	**-0.656**		
MW	**-0.842**		

Table 7. Detailed results of the CCA analyses of morphology against limb biomechanics for each species. Redundancy refers to the amount of variance in the variate that is explained by the variance in the opposite variate. Loadings used in interpretation are bolded. Character definitions are in the text.

***Eutropis macularia*, significant**			
Morphology variate		*Limb Biomechanics variate*	
Variance (%)	22.6	Variance (%)	24.8
Redundancy (%)	---	Redundancy (%)	20.5
AGD	**0.568**	HLPro	**0.581**
FLL	**0.412**	HLRetr	**0.395**
Fin3L	**0.568**	FLPro	**0.504**
ThighL	**0.617**	FLRetr	**0.495**
ShinL	**0.430**		
Toe4L	**0.381**		
MW	0.231		
Sphenomorphus maculatus, not significant			
Morphology variate		*Limb Biomechanics variate*	
Variance (%)	1.6	Variance (%)	43.6
Redundancy (%)	---	Redundancy (%)	41.6
AGD	0.014	HLPro	**-0.477**
FLL	-0.025	HLRetr	**0.591**
Fin3L	0.188	FLPro	**0.944**
ThighL	0.001	FLRetr	**0.526**
ShinL	0.198		
Toe4L	0.117		
MW	0.145		
Subdoluseps bowringii-frontoparietale, not significant			
Morphology variate		*Limb Biomechanics variate*	
Variance (%)	2.5	Variance (%)	24.7
Redundancy (%)	---	Redundancy (%)	9.6
AGD	-0.067	HLPro	**0.437**
FLL	0.045	HLRetr	**0.557**
Fin3L	-0.267	FLPro	**-0.362**
ThighL	-0.247	FLRetr	**0.594**
ShinL	0.033		
Toe4L	-0.105		
MW	-0.152		

Table 8. Detailed results of the CCA analyses of performance against stride mechanics for each species. Redundancy refers to the amount of variance in the variate that is explained by the variance in the opposite variate. Loadings used in interpretation are bolded. Character definitions are in the text

***Eutropis macularia*, significant**			
Performance variate		*Stride Mechanics variate*	
Variance (%)	24.1	Variance (%)	43.2
Redundancy (%)	22.7	Redundancy (%)	40.8
MaxV	**-0.980**	StrideL	**-0.552**
MaxAcc	-0.142	StrideDur	**0.666**
MinAcc	**0.309**	DutyF	**0.740**
HLProAcc	0.037		
HLRetrAcc	**0.354**		
***Sphenomorphus maculatus*, significant**			
Performance variate		*Stride Mechanics variate*	
Variance (%)	23.6	Variance (%)	24.8
Redundancy (%)	22.1	Redundancy (%)	23.2
MaxV	**-0.947**	StrideL	**-0.717**
MaxAcc	-0.227	StrideDur	0.262
MinAcc	**0.399**	DutyF	**0.400**
HLProAcc	-0.177		
HLRetrAcc	0.202		
***Subdoluseps bowringii-frontoparietale*, significant**			
Performance variate		*Stride Mechanics variate*	
Variance (%)	25.8	Variance (%)	44.7
Redundancy (%)	23.3	Redundancy (%)	40.5
MaxV	**-0.973**	StrideL	**-0.810**
MaxAcc	**-0.354**	StrideDur	**0.667**
MinAcc	0.200	DutyF	**0.490**
HLProAcc	**-0.344**		
HLRetrAcc	0.243		

Table 9. Detailed results of the CCA analyses of axial biomechanics against stride mechanics for each species. Redundancy refers to the amount of variance in the variate that is explained by the variance in the opposite variate. Loadings used in interpretation are bolded. Character definitions are in the text.

Eutropis macularia, not significant			
Axial Biomechanics variate		*Stride Mechanics variate*	
Variance (%)	33.3	Variance (%)	35.2
Redundancy (%)	10.0	Redundancy (%)	10.5
MaxVAx	**0.524**	StrideL	**-0.931**
MaxAccAx	**0.788**	StrideDur	**-0.434**
MinAx	**0.324**	DutyF	-0.021
***Sphenomorphus maculatus*, significant**			
Axial Biomechanics variate		*Stride Mechanics variate*	
Variance (%)	19.2	Variance (%)	24.0
Redundancy (%)	8.0	Redundancy (%)	10.0
MaxVAx	0.164	StrideL	0.289
MaxAccAx	**-0.708**	StrideDur	0.269
MinAx	0.214	DutyF	**-0.750**
Subdoluseps bowringii-frontoparietale, not significant			
Axial Biomechanics variate		*Stride Mechanics variate*	
Variance (%)	28.4	Variance (%)	31.0
Redundancy (%)	6.4	Redundancy (%)	7.0
MaxVAx	**-0.921**	StrideL	**-0.775**
MaxAccAx	0.059	StrideDur	**-0.542**
MinAx	0.023	DutyF	0.190

Table 10. Detailed results of the CCA analyses of limb biomechanics against stride mechanics for each species. Redundancy refers to the amount of variance in the variate that is explained by the variance in the opposite variate. Loadings used in interpretation are bolded. Character definitions are in the text.

***Eutropis macularia*, significant**			
Limb Biomechanics variate		*Stride Mechanics variate*	
Variance (%)	24.1	Variance (%)	40.7
Redundancy (%)	12.3	Redundancy (%)	20.8
HLPro	**0.930**	StrideL	0.135
HLRetr	0.274	StrideDur	**0.991**
FLPro	-0.153	DutyF	**0.468**
FLRetr	0.024		
Sphenomorphus maculatus, not significant			
Limb Biomechanics variate		*Stride Mechanics variate*	
Variance (%)	63.8	Variance (%)	50.6
Redundancy (%)	11.2	Redundancy (%)	23.5
HLPro	-0.131	StrideL	**0.858**
HLRetr	-0.084	StrideDur	**0.870**
FLPro	**0.712**	DutyF	0.148
FLRetr	**-0.325**		
Subdoluseps bowringii-frontoparietale, not significant			
Limb Biomechanics variate		*Stride Mechanics variate*	
Variance (%)	24.2	Variance (%)	41.8
Redundancy (%)	12.8	Redundancy (%)	22.0
HLPro	0.274	StrideL	**0.379**
HLRetr	**0.851**	StrideDur	**-0.372**
FLPro	0.231	DutyF	**-0.985**
FLRetr	**-0.341**		

10.0% of the variance in stride mechanics (Table 9). Stride mechanics against limb angles was only significant for *E. macularia* (Λ=0.383, X^2=21.087, p<0.05; Table 4). The stride mechanics variate loaded on StrideDur and DutyF and explained 40.7% of the variance whereas the limb angles variate loaded on HLPro and explained 24.1% of the variance (Table 10). Variance in stride mechanics explained 12.3% of the variance in limb angles, and variance in limb angles explained 20.8% of the variance in stride mechanics (Table 10).

DISCUSSION

Locomotor performance (defined in this study as maximum velocity and stride cycle acceleration characters; see methods) is a critical part of survival in squamate reptiles (Huey & Hertz, 1984; Jayne & Bennett, 1990; Garland Jr. & Losos, 1994; Miles, 2004; Husak, 2006). Although we have a general picture of locomotion in squamate reptiles, we still lack data on performance and kinematics across all body forms. In this paper, we examine the morphology and locomotion of three co-distributed lizards in the Family Scincidae (skinks), with the goal of understanding how differences in morphology result in differences in performance and kinematics. *Eutropis macularia* has a robust body, *Sphenomorphus maculatus* is slightly more gracile but with relatively longer hind limbs, and *Subdoluseps bowringii-frontoparietale* is elongate with relatively shorter hind limbs.

SPECIES OCCUPY DIFFERENT REGIONS OF MORPHOSPACE

The results of our size-corrected combined-species PCA indicates that the species in this study exhibit a trade-off between relative body size and relative body elongation along PC1 (Fig. 2; Table 1), showing that as body elongation increases, the size of the head and length of the limbs decreases. This trade-off between relative body size and relative body elongation in squamates has been widely documented (e.g. Greer & Wadsworth, 2003; Wiens et al., 2006; Bergmann & Irschick, 2010; Siler et al., 2011). Along PC2, species are separated by midbody width and length of the fourth toe, and it appears that these variables are most important in distinguishing *E. macularia* and *Sph. maculatus* in morphospace. This shows that these three species inhabit different regions of morphospace.

MAXIMUM VELOCITY CORRELATES WITH RELATIVE HIND LIMB LENGTH BUT NOT ABSOLUTE HIND LIMB LENGTH

Biomechanical models indicate that velocity while locomoting is determined by stride length and stride frequency (Sukhanov, 1974; Losos, 1990a). Because stride length is determined in part by limb length, this model entails two hypotheses: in interspecific comparisons, the species with the largest hind limb length relative to body size (i.e. SVL) should reach the highest velocities (Losos, 1990a; Bauwens et al., 1995) and in intraspecific comparisons, larger individuals should reach the highest velocities (Garland Jr., 1985). In line with the first hypothesis, we find that the species with longer hind limbs relative to their body size reach a higher maximum velocity (Fig. 4A; Table 5). The results of our combined-species CCA of size-corrected morphological variables against performance indicates that differences in body shape, specifically relative thigh length and relative finger length, is significantly correlated with performance. However, variation in morphology explained only 3.6% of the variation in performance (Table 5), suggesting that there are additional factors that influenced species' velocities during the trials. These factors may include differences in individuals' behavior (Garland Jr. & Losos, 1994) and unmeasured morphological variables such as muscle mass (Garland Jr., 1985; Reilly & Delancy, 1997; Vanhooydonck et al., 2006) and body condition (Garland Jr. & Losos, 1994). Nevertheless, the result of our ANCOVA reveals that *Sph. maculatus*, the species with the longest relative hind limb length, locomoted at significantly higher speeds than *Sub. bowringii-frontoparietale*, the species with the shortest relative hind limb length (Figure 4A) as seen in previous studies (Losos, 1990a; Bauwens et al., 1995; Vanhooydonck et al., 2006; Goodman, 2009; Bergmann & Irschick, 2010). This result suggests that increasing relative hind limb length is a mechanism behind higher locomotor performance in lizards.

However, we do not take these differences in performance in the track as indicating that *Sph. maculatus* are better performers in nature. Our study provides data on species' performance capacities under homogenous conditions but do not replicate conditions encountered by individuals in their environment. Performance in the wild is the target of natural selection (Arnold, 1983; Emerson & Arnold, 1989), and numerous abiotic and biotic factors affect when and how species locomote (Garland Jr. & Losos, 1994). Species may therefore use a variety of morphological and behavioral strategies to maximize locomotor performance in different situations, for example by choosing escape routes or changing the distance an individual allows a threat to approach before fleeing (Martin & Lòpez, 1995), by using different sized perches (Calsbeek & Irschick, 2007), or changing their biomechanics in response to heterogenous terrain (Kohlsdorf & Biewener, 2006). Therefore, although these results corroborate the hypothesis that the species with the longest relative hind limb length reach the fastest speeds, more data are needed to understand how this result is translates to performance in nature.

Given the importance of hind limb length in performance (Russell & Bauer, 2008), we also expected that maximum velocity would increase intraspecifically with increasing body size (i.e. adults would be faster than juveniles). Previous studies have found a correlation between body size and maximum velocity within species (Garland Jr., 1985; Calsbeek & Irschick, 2007; Zamora-Camacho et al., 2014) and between species (Losos, 1990a, 1990b), although overall support for this hypothesis has been ambiguous (Bauwens et al., 1995; Garland Jr. & Losos, 1994). In our ANCOVA, we find that intraspecific differences in maximum velocity is not significantly associated with body size for any of the species (Fig. 4A), which suggests that larger individuals, who therefore have longer hind limbs, did not reach significantly higher velocities than their smaller conspecifics. This point is also reflected in our species-specific

CCAs in which there was no correlation between raw (not size-corrected) morphology and performance (Table 4), indicating that intraspecific changes in velocity and acceleration were not correlated with morphology (i.e. larger individuals did not run faster than smaller individuals).

The fact that intraspecific differences in body size did not result in significant intraspecific differences in maximum velocity may be an artifact of individuals performing suboptimally during the trials and our small sample size (see comments in methods). However, there is a growing body of literature suggesting that the ontogeny of locomotor performance across vertebrates is more complex than may be expected from pure size and speed correlations (Carrier, 1996). Although we expect that larger individuals are faster simply as a function of their larger size, locomotor performance is a critical function for vertebrates regardless of age (Carrier, 1996). Studies of locomotion have shown that maximum velocity in juvenile squamates is significantly correlated with survival but that maximum velocity in adults is not (Jayne & Bennett, 1990; Miles, 2004; Husak, 2006). Therefore, our result that maximum velocity does not change intraspecifically across different body sizes may instead reflect the hypothesis that selection on performance is higher for juveniles than for adults (Carrier, 1996; Herrel et al., 2016).

There are two hypotheses for why selection for performance may be greater in juveniles than adults. First, the age-class difference may simply be a byproduct of the fact that poor-performing juveniles are eliminated from the population prior to adulthood, so that only high-performing adults remain (Herrel et al., 2016). This hypothesis suggests that selection on performance for adults is nonexistent because all adults perform at the same capacities. The second hypothesis suggests that selection differences on performance between adults and juveniles may result from differential pressures acting on individuals over the course of their lifetimes. Increased selection

on juveniles may result from increased predation pressure, in that smaller individuals are more at risk from a wider variety of predators than larger individuals (Stamps, 1983; Husak, 2006). Therefore, performing optimally during locomotion may be more important to survival for juveniles than it is for adults. Although the underlying mechanism differs between these two hypotheses, the ultimate result is the same: juveniles and adults have similar maximum velocities regardless of size.

MAXIMUM ACCELERATION DOES NOT DIFFER SIGNIFICANTLY BETWEEN SPECIES OR BODY SIZE

Acceleration during locomotion is important not only for determining maximum velocity, but also in determining how quickly the individual reaches maximum velocity. Therefore, some researchers have suggested that acceleration performance is more important than velocity performance in an individual's survival (Huey & Hertz, 1984). Despite biomechanical models suggesting that larger individuals should be worse performers during acceleration given the scaling of size and muscular force (Vanhooydonck et al., 2006), studies have shown that maximum velocity and maximum acceleration have coevolved (Huey & Hertz, 1984; Vanhooydonck et al., 2006). As a result, larger lizards, which locomote at higher velocities, also achieve higher maximum accelerations than smaller lizards in both intraspecific and interspecific studies of acceleration performance (Huey & Hertz, 1984; Vanhooydonck et al., 2006). However, the result of our ANCOVA analysis for all acceleration variables do not show any significant differences in acceleration variables within or between species. This result may reflect the lack of significant differences in maximum velocity within species in this study and may be due to the same cause. In the trials, the timing of maximum acceleration during the hind limb cycle differed between individuals. While maximum acceleration occurred most often

immediately after the hindlimb left the substrate, this timing varied across individuals, suggesting that individuals were behaving differently while locomoting (i.e. speeding up, maintaining speed, or slowing down; ESF pers. obs.). Alternatively, *E. macularia*, *Sph. maculatus*, and *Sub. bowringii-frontoparietale* may not exhibit inter- and intraspecific differences in their acceleration performance. These species are similar-sized generalist terrestrial skinks found in similar habitats (Das, 2010; Grismer, 2011; Chan-ard, 2015, ESF pers. obs.) and therefore, are likely preying on the same sources and under similar predation threats, so that their locomotor performances are similar. Future studies should take care to standardize acceleration performance across trials to better understand the relationship between body size and acceleration performance.

Evidence for coevolution of maximum acceleration and maximum velocity is seen in the morphological characters that are important in determining maximum velocity and maximum acceleration—Vanhooydonck et al. (2006) found that both variables were determined in part by the mass of the knee extensor muscle. However, maximum velocity was also determined by the length of the hind limb elements (Vanhooydonck et al., 2006). This suggests that evolutionary changes of increased limb length relative to body size of the lizard facilitates higher maximum velocity in lizards, but acceleration capacity depends on whether there have been parallel changes in the limb muscles. We find that maximum velocity is positively correlated with maximum acceleration in all PCAs and most CCAs (Tables 2, 4, 7), suggesting that these two variables have coevolved in the species in this study. However, maximum velocity is not correlated with acceleration during hind limb protraction and retraction in all PCA and most CCA analyses (Tables 2, 4, 7), indicating that acceleration throughout the hind limb stride cycle is decoupled from maximum velocity.

According to the biomechanics models of locomotion, at higher velocities, lizards are expected to increase their stride length, decrease their stride duration, and decrease their duty factor (Sukhanov, 1974). Previous studies have found a relationship between increased stride length, decreased stride duration, higher maximum velocity, and higher relative hind limb length (Bergmann & Irschick, 2010), corroborating biomechanical models that suggest that longer limbs increase stride length, which, along with stride frequency, results in higher maximum velocity (Losos, 1990a). In this study, we find that stride mechanics were significantly correlated with performance and with size-corrected and absolute body size (Figs. 2, 4C, 4D; Tables 2, 4, 5). The results of our species-specific performance-stride mechanics CCAs suggest that as maximum velocity and maximum acceleration increase, the distance traveled (stride length) increases while stride duration and duty factor decrease (although the correlation between stride duration and other stride mechanics characters was not significant for *Sph. maculatus*; Table 8). This result corroborates previous studies that found positive correlations between stride length and maximum velocity and negative correlations between stride duration, duty factor, and maximum velocity (Reilly & Delancy, 1997; Fieler & Jayne, 1998; Bergmann & Irschick, 2010). All together, these results indicate that as lizards move faster, they also move farther and decrease the proportion of time their foot is in contact with the substrate.

However, results of the stride mechanics PCA and the both the combined-species and species-specific CCAs of morphology against stride mechanics suggests that the relationship between stride length, stride duration, and duty factor is more complex (Fig. 3C; Tables 2, 5). In these analyses, stride duration, and duty factor are positively correlated with stride length instead of being negatively correlated with stride length. Intuitively this result makes sense: if

performance is equal across individuals, then the distance traveled for each stride will increase with increased stride duration and increased proportion of time that the foot remains in contact with the substrate. Therefore, these results suggest that the kinematics of locomotion change with changes in maximum velocity, a result that has been previously documented in lizards (Farley & Ko, 1997; Fieler & Jayne, 1998; Russell & Bauer, 2008).

We also find that stride mechanics are dependent on the relative and absolute size of an individual. Our combined-species CCA indicates that increases in relative body size and decreases in relative body elongation correlate with increases in all three stride mechanics characters. This result suggests that individuals with larger relative body sizes increase the frequency and length of their strides and maintain contact with the ground for a longer proportion of time during the hind limb cycle. Species-specific CCAs suggest that absolute body size is also important in stride mechanics. These analyses indicate that increased body size is correlated with increases in all three stride mechanics characters (Table 6), suggesting that absolutely larger individuals also increase the frequency and length of each stride and the proportion of time that the foot remains in contact with the ground. However, this result is significant only for *E. macularia* and *Sph. maculatus* (Tables 4, 5). The lack of significance for this relationship in the *Sub. bowringii-frontoparietale* CCA may suggest that stride mechanics in *Sub. bowringii-frontoparietale* is decoupled from limb morphology. Studies have shown that axial bending increases in elongate-bodied species (Gans, 1976; Ritter, 1992; Bergmann & Irschick, 2010) and undulation increases stride length by rotating the pelvis forward (Russel & Bauer, 2008). Therefore, *Sub. bowringii-frontoparietale* may use axial bending to compensate for or enhance the action of the limbs during locomotion (but see below for a discussion regarding the lack of significant morphology-axial bending correlations for this species). As a

result, correlations between stride mechanics and morphology in elongate-bodied reduced-limbed species may differ from those seen in species with relatively longer limbs.

Our ANCOVA results also reveal a significant positive relationship between absolute body size and stride length and duty factor (Fig. 4C, 4D) but not for stride duration. Instead, our ANCOVA for stride duration across species and body size indicates that there is a significant interaction between species and AGD (Fig. 4B). However, this analysis does not take velocity into account, and so whether this result is due to a velocity-body size relationship, behavioral differences, or a species-body size-stride mechanics relationship is unknown. To our knowledge, there have been no studies comparing limb velocities in relation to forward body velocities across species. Both Reilly & Delancy (1997) and Fieler & Jayne (1998) found that timing variables associated with hind limb stride mechanics increased as individuals' velocities increased, but these studies investigated intraspecific changes in limb velocities across velocities, not interspecific changes. Given the biomechanical relationship between stride length, stride frequency, and velocity, we note that individuals with longer hind limbs traveling at a fixed forward velocity will need to move their limbs faster than individuals with relatively smaller hind limbs that are traveling at the same velocity, indicating that the larger individuals will have shorter stride durations. However, different species may use their morphologies differently when locomoting (e.g. by compensating for shorter limbs via lateral undulation), and so the relationship between stride duration and body size may differ across species. However, we were not able to detect significant differences in morphology and biomechanics across species in this study (see below), and so additional interspecific studies controlling for velocity and acceleration should be conducted to better understand the relationship between body size and stride duration across species.

MORPHOLOGY AND BIOMECHANICS

The species in this study, *E. macularia*, *Sph. maculatus*, and *Sub. bowringii-frontoparietale* exhibit different degrees of body elongation and relative limb lengths (Fig. 2). Therefore, we hypothesized that these species would exhibit differences in their biomechanics when locomoting. Previous studies comparing locomotion in non-elongate- and elongate-bodied lizards have indicated that the morphological trade-off between body elongation and relative limb lengths has led to changes in the amount and degree of axial bending during locomotion, with elongate-bodied species bending their trunks more when locomoting (Sukhanov, 1974; Ritter, 1992; Bergmann & Irschick, 2010; Morinaga & Bergmann, 2019). In squamate reptiles, elongation of the trunk occurs through addition of the number of presacral vertebrae (Greer & Wadsworth, 2003; Bergmann & Irschick, 2012). This increase in the number of vertebrae leads to greater flexibility of the vertebral column in snakes (Jayne, 1982) and in both elongate-bodied, limbed and limbless lizards (Morinaga & Bergmann, 2019), and therefore facilitates increased amplitudes of axial bending (Morinaga & Bergmann, 2019). The results of our biomechanics PCA indicate that *Sub. bowringii-frontoparietale* has a more negative distribution along PC1 than *E. macularia* and *Sph. maculatus* (Fig. 3D), which suggests that *Sub. bowringii-frontoparietale* is able to attain smaller axial angles (i.e. more axial bending) than the other two species in our study. However, our combined-species and species-specific CCAs do not reveal a significant correlation between morphology and the degree of axial bending (Table 4). Similarly, the results from our ANCOVA do not indicate that species differ significantly in the amount of axial bending (Fig. 4F). However, the ANCOVA does suggest that there is a significant

relationship between AGD and axial bending, but in the opposite expected direction: larger individuals have larger axial angles, indicating that they bend their bodies less (Fig. 4F).

We hypothesize that this lack of significant correlation between morphology and axial bending is an artifact of the way this character was measured in our analyses. Measurements of axial angles were taken at three discreet points only during the hind limb cycle (at the point of maximum velocity, at the point of maximum acceleration, and at the point of minimum axial angle), and calculated bending data using three points spaced widely along the dorsum (Fig. 1). However, studies of undulatory locomotion have suggested that undulation occurs continuously along the body in elongate species (Ritter, 1992; Morinaga & Bergmann, 2019). Furthermore, these studies have used more than three points to quantify axial bending. Therefore, our measurements may not actually capture the totality of axial bending during locomotion but instead capture it at specific points, for which we found no significant differences between species, despite an observed trend for increased bending in *Sub. bowringii-frontoparietale*.

Interestingly, there was a significant correlation between stride mechanics and axial bending in *Sph. maculatus* (Table 4), which shows that duty factor is correlated with the axial angle at maximum acceleration (Table 9). Across all species, maximum acceleration most often occurred at the first frame in the hind limb cycle immediately after the foot has pushed off of the substrate, although this varied across trials depending on the behavior of the individual (ESF pers. obs.). Therefore, there may be a correlation between axial bending and propulsive force during locomotion, although whether this is only specific to *Sph. maculatus* or is also seen in *E. macularia* and *Sub. bowringii-frontoparietale* requires additional analyses that includes a factor describing when maximum acceleration occurred during the trial. Alternatively, the correlation between axial bending and duty factor may exist only in species with certain morphologies: *Sph.*

maculatus has a narrower body than *E. macularia* and larger relative hind limb length than both *E. macularia* and *Sub. bowringii-frontoparietale* (Fig. 2), and therefore, the morphological combination of a gracile body with relatively large hind limbs may facilitate both hind limb propulsion and axial bending during locomotion.

Unlike axial bending, which has been shown to increase with increases in body elongation (e.g. Bergmann & Irschick, 2010), there is not a clear understanding on how morphology correlates with limb biomechanics. Our biomechanics PCA suggests that greater axial angles (i.e. less axial bending) is associated with greater hind limb protraction angles (planting the foot closer to the body when stepping forward with the hind limb), greater fore-limb protraction angles (planting the hand farther from the body when stepping forward with the fore-limb), and greater fore-limb retraction angles (fore-limb is closer to the body when it is lifted off the ground; Fig. 3D). This result suggests that limb use increases as axial bending decreases and may point to a trade-off between elongation and limb use during locomotion. Although this trade-off makes sense intuitively, our CCA of limb biomechanics against axial biomechanics was not significant (Table 4), indicating that the apparent trade-off between axial bending and limb bending is not strong. Bergmann & Irschick (2010) also observed a trade-off between hind limb protraction and axial bending but the correlation between these characters was found along their kinematics PC4 indicating that it is only recovered after accounting for other correlations between locomotor variables.

However, we do find a significant correlation between relative morphology and limb biomechanics in the combined-species CCA analyses (Table 4). This analysis indicates that increases in relative body size are associated with higher hind limb protraction angles (Table 5), which suggests that species with relative longer hind limbs are able to have greater forward

extension of the hind limbs when stepping forward. Absolute hind limb length is also important in increasing fore-limb retraction, as shown by the significant increase in hind limb protraction angle with increases in body size in our ANCOVA analysis (Fig. 4G) and may be the mechanism behind the increase stride length (distance traveled) with increases in body size. The correlation between body size and hind limb protraction angle is also seen in our species-specific CCA analysis of morphology against limb biomechanics in *E. macularia* in which increases in body size result in increases in all limb protraction and retraction angles (Table 7). However, this result is not completely intuitive because, whereas greater hind limb protraction and fore limb retraction angles indicate that the limb is closer to the body, greater hind limb retraction and greater fore-limb retraction angles indicate that the limb is farther from the body (Fig. 1). Therefore, to have increases across all limb angles, there would need to be significant axial bending, which was not found in *E. macularia*. CCAs of morphology against limb biomechanics for *Sph. maculatus* and *Sub. bowringii-frontoparietale* were not significant.

Previous studies have revealed conflicting results about the relationship between performance, stride mechanics and limb biomechanics during locomotor performance. At different walking and trotting speeds, Reilly and Delancy (1997) found that the phrynosomatid species *Sceloporus clarkii* increased its velocity by retracting the femur more quickly, but maintained the same hind limb protraction angle across speeds, whereas Fieler & Jayne (1998) found that at higher trotting and sprinting speeds, the iguanid species *Dipsosaurus dorsalis* increased femur retraction speeds and changed the hind limb protraction angle. Results of our species-specific CCA analysis of stride mechanics against limb biomechanics for *E. macularia* suggest that higher stride duration and duty factor is correlated with greater hind limb protraction angle but not with other limb angles. Because increases in stride duration and duty factor are

associated with slower velocities, the result of a correlation between the increase in hind limb protraction angles with step duration and duty factor may reflect "choosiness" on the part of the individual, in which slower individuals take more time in planting their foot as they locomote and therefore are able to extend their limb farther than they might at higher velocities. However, CCAs for stride mechanics and limb biomechanics were not significant for *Sph. maculatus* and *Sub bowringii-frontoparietale*, suggesting that this result may be species-specific. Furthermore, CCAs of performance against limb biomechanics was not significant for any species, suggesting that velocity and acceleration are not tightly linked to limb biomechanics. However, species exhibit different gaits at different speeds (Farley & Ko, 1997; Reilly & Delancy, 1997; Fieler & Jayne, 1998; Russell & Bauer, 2008), so to get a more robust comparison of the biomechanics across species, performance variables including velocity and acceleration need to be held constant across trials.

CONCLUSIONS

Understanding how an organism's morphology correlates with its locomotor performance is important to recognizing broader patterns of organismal diversity and ecomorphology. Biomechanical models of locomotion suggest that longer limbs increase stride length and that stride length and stride frequency together determine maximum velocity (Sukhanov, 1974). However, given the diversity of body forms within squamate reptiles, we hypothesize that species with different morphologies will exhibit differences in their locomotor performance and kinematics. Our results indicate that *Sph. maculatus*, the species with the relatively longest hind limbs, reached significantly higher velocities than *Sub. bowringii-frontoparietale*, which has the relatively shortest hind limbs. However, in intraspecific comparisons, we do not find that smaller

individuals are significantly slower than larger individuals. Across all three species, larger stride lengths were correlated with higher velocities while stride duration and duty factor decreased at higher velocities; however, the relationship between stride length, strider duration, and duty factor is complex and appears to be velocity dependent. Finally, *Sub bowringii-frontopareietale* tended to have increased axial bending than *E. macularia* and S*ph. maculatus* although this was not significantly correlated with morphology or performance.

ACKNOWLEDGEMENTS

We thank the National Research Council of Thailand for granting permits for this research to ESF (permit no. 54/60). For fieldwork help and logistics, we thank A. Rujirawan, N. Ampai, P. Puanprapai, S. Yodthong, K. Termprayoon, A. Aksornneam, N, Warrit, B. Tweedy, and N. Freitas. We thank the former director, T. Artchawakom, current director, S. Wangsothorn, and staff of Sakaerat Environmental Research Station for permission to conduct this research, helping us set up pitfall traps, and providing us a wonderful place to stay. We are grateful to G. Morinaga for training in data collection, and M. Patten and C. Curry for help with statistical analyses. S. Maguire was instrumental in data entry and video editing. This research was supported by a 2016 Fulbright Fellowship and University of Oklahoma Graduate Student Senate research funds to ESF and Kasetsart University Research and Development Institute funds (project no. 74.60) to AA.

REFERENCES

Arnold SJ. 1983. Morphology, performance and fitness. *American Zoologist* **23:** 347–361.

Bauwens D, Garland Jr. T, Castilla AM, Van Damme R. 1995. Evolution of sprint speed in lacertid lizards: morphological physiological and behavioral covariation. *Evolution* **49:** 848–863.

Bergmann PJ, Irschick, DJ. 2010. Alternate pathways of body shape evolution translate into common patterns of locomotor evolution in two clades of lizards. *Evolution* **64:** 1569–1582.

Bergmann PJ, Irschick DJ. 2012. Vertebral evolution and the diversification of squamate reptiles. *Evolution* **66:** 1044–1058.

Brandley MC, Huelsenbeck JP, Wiens JJ. 2008. Rates and patterns in the evolution of snake-like body form in squamate reptiles: evidence for repeated re-evolution of lost digits and long-term persistence of intermediate body forms. *Evolution* **62:** 2042–2064.

Calsbeek R, Irschick DJ. 2007. The quick and the dead: correlational selection on morphology, performance and habitat use in island lizards. *Evolution* **61:** 2493–2503.

Carrier DR. 1996. Ontogenetic limits on locomotor performance. *Physical Zoology* **69:** 467–488.

Chan-ard T, Parr JWK, Nabhitabhata J. 2015. *A field guide to the reptiles of Thailand*. New York: Oxford University Press.

Cooper N, Thomas GH, FitzJohn RG. 2016. Shedding light on the 'dark side' of phylogenetic comparative methods. *Methods in Ecology and Evolution* **7:** 693–699.

Das, I. 2010. *A fieldguide to the reptiles of Southeast Asia.* London: New Holland.

Domenici P, Turesson H, Brodersen J, Brönmark C. 2008. Predator-induced orphology enhances escape locomotion in crucian carp. *Proceedings of the Royal Society B* **275:** 195–201.

Emerson SB, Arnold SJ. 1989. Intra- and interspecific relationships between morphology, performance, and fitness. In: Wake DB, Roth G, eds. *Complex organismal functions: Integration and Evolution in Vertebrates*. New York: John Wiley & Sons Ltd., 295–314.

Farley CT, Ko TC. 1997. Mechanics of locomotion in lizards. *Journal of Experimental Biology* **200:** 2177–2188.

Felsenstein J. 1985. Phylogenies and the comparative method. *The American Naturalist* **125:** 1–15.

Fieler CL, Jayne BC. 1998. Effects of speed on the hind limb kinematics of the lizard *Dipsosaurus dorsalis*. *Journal of Experimental Biology* **201:** 609–622.

Freitas ES, Datta-Roy A, Karanth P, Grismer LL, Siler CD. 2019. Multilocus phylogeny and a new classification for African, Asian and Indian supple and writhing skinks (Scincidae: Lygosominae). *Zoological Journal of the Linnean Society* **186:** 1067–1096.

Gans C. 1986. Locomotion of limbless vertebrates: pattern and evolution. *Herpetologica* **42:** 33–46.

Gans C, Gasc JP. 1990. Tests on the locomotion of the elongate and limbless reptile *Ophisaurus apodus* (Sauria: Anguidae). *Journal of Zoology (London)* **220:** 517–536.

Gans C, Morgan WK, Allen ES. 1992. Surface locomotion of the elongate and limbless lizard *Anniella pulchra* (Anguidae). *Herpetologica* **48:** 246–262.

Gans C, Fusari M. 1994. Locomotor analysis of surface propulsion by three species of reduced-limbed fossorial lizards (*Lerista*: Scincidae) from western Australia. *Journal of Morphology* **222:** 309–326.

Garland Jr. T. 1985. Ontogenetic and individual variation in size, shape and speed in the Australian agamid lizard *Amphibolurus nuchalis*. *Journal of Zoology (London)* **207:** 425–439.

Garland Jr. T, Harvey PH, Ives AR. 1992. Procedures for the analysis of comparatice data using phylogenetically independent contrasts. *Systematic Biology* **41:** 18–32.

Garland Jr. T, Losos JB. 1994. Ecological morphology of locomotor performance in squamate reptiles. In: Wainwright PC, Reilly S, eds. *Ecological morphology: integrative organismal biology*. Chicago: University of Chicago Press, 240–302.

Gónzalez I, Déjean S. 2012. CCA: canonical correlation analysis (version 1.2). Available at: https://CRAN.R-project.org/package=CCA.

Grafen A. 1989. The uniqueness of the phylogenetic regression. *Journal of Theoretical Biology* **156:** 405–423.

Grismer LL. 2011. *Lizards of peninsular Malaysia, Singapore, and their adjacent archipelagos*. Frankfurt: Chimaira

Greer AE, Wadsworth L. 2003. Body shape in skinks: the relationship between relative hind limb length and relative snout–vent length. *Journal of Herpetology* **37:** 554–559.

Goodman BA. 2009. Nowhere to run: the role of habitat openness and refuge use in defining patterns of morphological and performance evolution in tropical lizards. *Journal of Evolutionary Biology* **22,** 1535–1544.

Hedrick TL. 2008. Software techniques for two- and three-dimensional kinematic measurements of biological and biomimetic systems. *Bioinspiration and Biomimetics* **3:** 034001.

Herrel A, Lopez-Darias M, Vanhooydonck B, Cornette R, Kohlsdorf T, Brandt R. 2016. Do adult phenotypes reflect selection on juvenile performance? A comparative study on performance and morphology in lizards. *Integrative and Comparative Biology* **56:** 469–478.

Higham TE. 2007. The integration of locomotion and prey capture in vertebrates: morphology, behavior and performance. *Integrative and Comparative Biology* **47:** 82–95.

Hothorn T, Bretz F, Westfall, P. 2008. Simultaneous inference in general parametric models. *Biometrical Journal* **50:** 346–363.

Huey RB, Hertz PE. 1984. Effects of body size and slope on acceleration of a lizard (*Stellio stellio*). *Journal of Experimental Biology* **110:**113–123.

Husak JF. 2006. Does speed help you survive? A test with collard lizards of different ages. *Functional Ecology* **20:** 174–179.

Husak JF, Fox SF. 2008. Sexual selection in locomotor performance. *Evolutionary Ecology Research* **10:** 213–228.

Irschick DJ, Losos JB. 1998. A comparative analysis of the ecological significance of maximal locomotor performance in Caribbean *Anolis* lizards. *Evolution* **52:** 219–226.

Jayne BC. 1982. Comparative morphology of the semisinalis-spinalis muscle of snakes and correlations with locomotion and constriction. *Journal of Morphology* **172:** 83–96.

Jayne BC. 1986. Kinematics of terrestrial snake locomotion. *Copeia* **1986:** 915–927.

Jayne BC. 1988. Muscular mechanisms of snake locomotion: an electromyographic study of lateral undulation of the Florida banded water snake (*Nerodia fasciata*) and the yellow rat snake (*Elaphe obsoleta*). *Journal of Morphology* **197:** 159–181.

Jayne BC, Bennett AF. 1990. Selection in locomotor performance capacity in a natural population of garter snakes. *Evolution* **44:** 1204–1209.

Kohlsdorf T, Biewener AA. 2006. Negotiating obstacles: running kinematics of the lizard *Sceloporus malachiticus*. *Journal of Zoology* **270:** 359–371.

Lande R. 1978. Mechanisms of limb loss in tetrapods. *Evolution* **32:** 73–92.

Leanard CJ. 1979. A functional morphological study of limb regression in some southern African species of Scincidae (Reptilia: Sauria). Unpublished D. Phil. Thesis, University of Cape Town.

Lleonart J, Salat, J. Torres GJ. 2000. Removing allometric effects of body size in morphological analysis, *Journal of Theoretical Biology* **205:** 85–93.

Losos JB. 1990a. The evolution of form and function: morphology and locomotor performance in West Indian *Anolis* lizards. *Evolution* **44:** 1189–1203.

Losos JB. 1990b. Ecomorphology, performance capability, and scaling of West Indina *Anolis* lizards: an evolutionary analysis. *Ecological Monographs* **60:** 369–388.

Losos JB, Creer DA, Schulte II JA. 2002. Cautionary comments on the measurement of maximum locomotor capabilities. *Journal of Zoology (London)* **258:** 57–61.

Losos JB. 2011. Seeing the forest for the trees: the limitations of phylogenies in comparative biology. *The American Naturalist* **177:** 709–727.

Martin J, López P. 1995. Influence of habitat structure on the escape tactics of the lizard *Psammodromus algirus*. *Canadian Journal of Zoology* **73:** 129–132.

McElroy EJ, Bergmann PJ. 2013. Tail autotomy, tail size and locomotor performance in lizards. *Physiological and Biochemical Zoology* **86:** 669–679.

Medina I, Cooke GM, Ord TJ. 2018. Walk, swim or fly? Locomotor mode predicts genetic differentiation in vertebrates. *Ecology Letters* **21:** 638–645.

Miles DB. 2004. The race goes to the swift: fitness consequences of variation in sprint performance in juvenile lizards. *Evolutionary Ecology Research* **6:** 63–75.

Morinaga G, Bergmann PJ. 2019. Angles and waves: intervertebral joint angles and axial kinematics of limbed lizards, limbless lizards, and snakes. *Zoology* **134:** 16–26.

R Core Team. 2019. R: a language and environment for statistical computing. R Foundation for Statistical Computing. Available at: https://www.R-project.org/.

Reilly SM, Delancy MJ. 1997. Sprawling locomotion in the lizard *Sceloporus clarkia*: the effects of speed on gait, hind limb kinematics, and axial bending during walking. *Journal of Zoology (London)* **243:** 417–433.

Ritter D. 1992. Lateral bending during lizard locomotion. *Journal of Experimental Biology* **173:** 1–10.

Rotenberry JT, Zuk M, Simmons LW, Hayes C. 1996. Phonotactic parasitoids and cricket song structure: an evaluation of alternative hypotheses. *Evolutionary Ecology* **10:** 233–243.

Russell AP, Bauer AM. 2008. The appendicular locomotor apparatus of *Sphenodon* and normal-limbed squamates. In: Gans C, Gaunt AS, Adler K, eds. *Biology of the Reptilia. Volume 21, morphology I. The skull and appendicular locomotor apparatus of Lepidosauria*. Ithaca: Society for the Study of Amphibians and Reptiles, 1–466.

Secor SM, Jayne BC, Bennett AF. 1992. Locomotor performance and energetic cost of sidewinding by the snake *Crotalus cerastes*. *Journal of Experimental Biology* **163:** 1–14.

Siler CD, Diesmos AC, Alcala AC, Brown RM. 2011. Phylogeny of the Philippine slender skinks (Scincidae: *Brachymeles*) reveals underestimated species diversity, complex biogeographical relationships, and cryptic patterns of lineage diversification. *Molecular Phylogenetics and Evolution* **59:** 53–65.

Simmons JE. 2015. Herpetological collecting and collections management, 3rd ed. *Society for the Study of Amphibians and Reptiles Herpetological Circulars* **42:** vi + 1–191.

Simon CA, Middendorf GA. 1976. Resource partitioning by an iguanid lizard: temporal and microhabitat aspects. *Ecology* **57:** 1317–1320.

Skinner A, Lee MSY, Hutchinson MN. 2008. Rapid and repeated limb loss in a clade of Scincid lizards. *BMC Evolutionary Biology* **8:** 310.

Skinner A, Lee, MSY. **2009.** Body-form evolutioni in the scincid lizard clade *Lerista* and the mode of macroevolutionary transitions. *Journal of Evolutionary Biology* **36:** 292–300.

Skinner A, Hugall AF, Hutchinson MN. 2011. Lygosomine phylogeny and the origins of Australian scincid lizards. *Journal of Biogeography* **38:** 1044–1058.

Stamps JA. 1983. The relationship between ontogenetic habitat shifts, competition and predator avoidance in a juvenile lizard (*Anolis aeneus*). *Behavioral Ecology and Sociobiology* **12:** 19–33.

Sukhanov VB. 1974. *General system of symmetrical locomotion of terrestrial vertebrates and some features of movement of lower tetrapods. Translated from Russian: 1968. Obshchaya Sistema simmetricheskoi lokomotsii nazemnykh pozvonochnykh i osobennosti peredvizheniya nizshikh tetrapod. Leningrad: Nakua Publishers.* New Delhi: Amerind Publishing Co.

Tabachnik BG, Fidell LS. 2014. *Using multivariate statistics. Sixth edition.* Essex: Pearson Education Limited.

Thorpe RS. 1975. Quantitative handling of characters useful in snake systematics with particular reference to intraspecific variation in the ringed snake *Natrix natrix* (L.). *Biological Journal of the Linnean Society* **7:** 27–43.

Uetz P, Freed P, Hošek J. 2020. The reptile database. Available at: http://www.reptile-database.org. Accessed: January 2020.

Uyeda JC, Zenil-Ferguson R, Pennell MW. 2018. Rethinking phylogenetic comparative methods. *Systematic Biology* **67:** 1091–1109.

Vanhooydonck B, Herrel A, Van Damme R, Irschick DJ. 2006. The quick and the fast: the evolution of acceleration capacity in *Anolis* lizards. *Evolution* **60:** 2137–2147.

Vitt L, Caldwell J. 2013. *Herpetology: an introductory biology of amphibians and reptiles.* London: Academic Press.

Wainwright PC, Alfaro ME, Bolnick DI, Hulsey CD. 2005. Many-to-one mapping of form to function: a general principle in organismal design? *Integrative Comparative Biology* **45:** 256–262.

Walton M, Jayne BC, Bennett AF. 1990. The energetics cost of limbless locomotion. *Science* **249:** 524–527.

Westoby M, Leishman MR, Lord JM. 1995. On misinterpreting the 'phylogenetic correction'. *Journal of Ecology* **83:** 531–534.

Wei T, Simko V. 2017. R package "corrplot": visualization of a correlation matrix (version 0.84). Available at: https://github.com/taiyun/corrplot.

Whiting AS, Bauer AM, Sites Jr. JW. 2003. Phylogenetic relationships and limb loss in sub-Saharan African scincine lizards (Squamata: Scincidae). *Molecular Phylogenetics and Evolution* **29:** 582–598.

Wiens JJ, Brandley MC, Reeder TW. 2006. Why does a trait evolve multiple times within a clade? Repeated evolution of snakelike body form in squamate reptiles. *Evolution* **60:** 123–141.

Zamora-Camacho FJ, Reguera S, Rubiño-Hispán MV, Moreno-Rueda G. 2014. Effects of limb length, body mass, gender, gravidity, and elevation on escape speed in the lizard *Psammodromus algirus. Evolutionary Biology* **41:** 509–517.

SUPPLEMENTARY MATERIAL

Table S1. Voucher, age class, tail status, and locality information for each individual used in the study. NV = Not vouchered, --- = Vouchered but not accessioned, A = Adult, H = Hatchling, J = Juvenile, R = Regenerated tail, T = Autotomized tail, W = Whole tail.

Species	Field No.	Museum No.	Age Class	Tail Status	Locality	Province	Country	Decimal Lat	Decimal Long
Eutropis macularia	ESF 428	NV	H	W	Sakaerat Environmental Research Station	Nakhon Ratchasima	Thailand	14.50409	101.92232
Eutropis macularia	ESF 429	NV	H	W	Sakaerat Environmental Research Station	Nakhon Ratchasima	Thailand	14.50449	101.92206
Eutropis macularia	ESF 433	NV	H	T	Sakaerat Environmental Research Station	Nakhon Ratchasima	Thailand	14.50536	101.92033
Eutropis macularia	ESF 437	NV	J	W	Sakaerat Environmental Research Station	Nakhon Ratchasima	Thailand	14.50153	101.92085
Eutropis macularia	ESF 456	NV	J	W	Sakaerat Environmental Research Station	Nakhon Ratchasima	Thailand	14.50400	101.93051
Eutropis macularia	ESF 457	NV	H	T	Sakaerat Environmental Research Station	Nakhon Ratchasima	Thailand	14.50250	101.92396
Eutropis macularia	ESF 461	NV	H	W	Sakaerat Environmental Research Station	Nakhon Ratchasima	Thailand	14.50398	101.92606
Eutropis macularia	ESF 462	NV	J	R	Sakaerat Environmental Research Station	Nakhon Ratchasima	Thailand	14.50430	101.92946
Eutropis macularia	ESF 472	---	A	W	Sakaerat Environmental Research Station	Nakhon Ratchasima	Thailand	14.50615	101.92722
Eutropis macularia	ESF 480	ZMKU R 00741	A	W	Boyscout Camp	Saraburi	Thailand		
Eutropis macularia	ESF 492	OMNH 46515	A	R	Sakaerat Environmental Research Station	Nakhon Ratchasima	Thailand	14.51009	101.93106
Eutropis macularia	ESF 494	OMNH 46516	A	W	Sakaerat Environmental Research Station	Nakhon Ratchasima	Thailand	14.50247	101.92410
Eutropis macularia	ESF 507	NV	A	T	Sakaerat Environmental Research Station	Nakhon Ratchasima	Thailand	14.51009	101.93106
Eutropis macularia	ESF 510	NV	J	W	Sakaerat Environmental Research Station	Nakhon Ratchasima	Thailand	14.50615	101.92722
Eutropis macularia	ESF 511	NV	A	R	Sakaerat Environmental Research Station	Nakhon Ratchasima	Thailand	14.50615	101.92722
Eutropis macularia	ESF 512	NV	J	W	Sakaerat Environmental Research Station	Nakhon Ratchasima	Thailand	14.50862	101.92943
Eutropis macularia	ESF 514	NV	J	W	Sakaerat Environmental Research Station	Nakhon Ratchasima	Thailand	14.50561	101.92759
Eutropis macularia	ESF 529	NV	J	W	Sakaerat Environmental Research Station	Nakhon Ratchasima	Thailand	14.50400	101.93051
Eutropis macularia	ESF 530	NV	H	R	Sakaerat Environmental Research Station	Nakhon Ratchasima	Thailand	14.51009	101.92759
Eutropis macularia	ESF 548	NV	J	T	Sakaerat Environmental Research Station	Nakhon Ratchasima	Thailand	14.50615	101.92722
Eutropis macularia	ESF 549	NV	J	W	Sakaerat Environmental Research Station	Nakhon Ratchasima	Thailand	14.50615	101.92722
Eutropis macularia	ESF 550	NV	J	W	Sakaerat Environmental Research Station	Nakhon Ratchasima	Thailand	14.50557	101.92746
Eutropis macularia	ESF 551	NV	J	R	Sakaerat Environmental Research Station	Nakhon Ratchasima	Thailand	14.50557	101.92746
Eutropis macularia	ESF 552	OMNH 46517	A	W	Sakaerat Environmental Research Station	Nakhon Ratchasima	Thailand	14.50285	101.92519

Eutropis macularia	ESF 555	NV	H	T	Sakaerat Environmental Research Station	Nakhon Ratchasima	Thailand	14.50826	101.92916
Eutropis macularia	ESF 562	NV	J	W	Suranaree University	Nakhon Ratchasima	Thailand		
Eutropis macularia	ESF 563	NV	J	R	Suranaree University	Nakhon Ratchasima	Thailand		
Eutropis macularia	ESF 566	NV	H	W	Sakaerat Environmental Research Station	Nakhon Ratchasima	Thailand	14.51009	101.93106
Eutropis macularia	ESF 571	NV	H	R	Sakaerat Environmental Research Station	Nakhon Ratchasima	Thailand	14.51009	101.93106
Eutropis macularia	ESF 581	OMNH 46518	J	W	Sakaerat Environmental Research Station	Nakhon Ratchasima	Thailand	14.50285	101.92519
Eutropis macularia	ESF 582	OMNH 46519	J	W	Sakaerat Environmental Research Station	Nakhon Ratchasima	Thailand	14.50285	101.92337
Eutropis macularia	ESF 584	OMNH 46520	J	W	Sakaerat Environmental Research Station	Nakhon Ratchasima	Thailand	14.50615	101.92722
Sphenomorphus maculata	ESF 426	NV	H	W	Sakaerat Environmental Research Station	Nakhon Ratchasima	Thailand	14.51009	101.93106
Sphenomorphus maculata	ESF 430	NV	H	T	Sakaerat Environmental Research Station	Nakhon Ratchasima	Thailand	14.50549	101.91934
Sphenomorphus maculata	ESF 431	NV	H	W	Sakaerat Environmental Research Station	Nakhon Ratchasima	Thailand	14.50549	101.91934
Sphenomorphus maculata	ESF 432	NV	H	T	Sakaerat Environmental Research Station	Nakhon Ratchasima	Thailand	14.50549	101.91934
Sphenomorphus maculata	ESF 449	OMNH 46526	A	R	Sakaerat Environmental Research Station	Nakhon Ratchasima	Thailand	14.51009	101.93106
Sphenomorphus maculata	ESF 458	NV	J	T	Sakaerat Environmental Research Station	Nakhon Ratchasima	Thailand	14.50576	101.91958
Sphenomorphus maculata	ESF 459	NV	H	T	Sakaerat Environmental Research Station	Nakhon Ratchasima	Thailand	14.50521	101.91899
Sphenomorphus maculata	ESF 460	NV	A	W	Sakaerat Environmental Research Station	Nakhon Ratchasima	Thailand	14.50556	101.91935
Sphenomorphus maculata	ESF 463	NV	H	W	Sakaerat Environmental Research Station	Nakhon Ratchasima	Thailand	15.51009	101.93106
Sphenomorphus maculata	ESF 464	NV	J	W	Sakaerat Environmental Research Station	Nakhon Ratchasima	Thailand	15.51009	101.93106
Sphenomorphus maculata	ESF 470	NV	J	T	Sakaerat Environmental Research Station	Nakhon Ratchasima	Thailand	15.51009	101.93106
Sphenomorphus maculata	ESF 471	OMNH 46527	A	W	Sakaerat Environmental Research Station	Nakhon Ratchasima	Thailand	15.51009	101.93106
Sphenomorphus maculata	ESF 493	NV	H	W	Sakaerat Environmental Research Station	Nakhon Ratchasima	Thailand	14.51009	101.93106
Sphenomorphus maculata	ESF 495	OMNH 46528	A	W	Sakaerat Environmental Research Station	Nakhon Ratchasima	Thailand	14.51009	101.93106
Sphenomorphus maculata	ESF 521	NV	J	W	Sakaerat Environmental Research Station	Nakhon Ratchasima	Thailand	14.51009	101.93106
Sphenomorphus maculata	ESF 522	NV	A	W	Sakaerat Environmental Research Station	Nakhon Ratchasima	Thailand	14.51009	101.93106
Sphenomorphus maculata	ESF 527	NV	J	W	Sakaerat Environmental Research Station	Nakhon Ratchasima	Thailand	14.50556	101.91935
Sphenomorphus maculata	ESF 533	---	A	W	Tambon Hat Yai	Chumphon	Thailand	9.95649	98.97788
Sphenomorphus maculata	ESF 534	---	A	W	Tambon Hat Yai	Chumphon	Thailand	9.95649	98.97788
Sphenomorphus maculata	ESF 535	---	A	W	Tambon Hat Yai	Chumphon	Thailand	9.95649	98.97788
Sphenomorphus maculata	ESF 536	---	A	W	Tambon Hat Yai	Chumphon	Thailand	9.95649	98.97788
Sphenomorphus maculata	ESF 537	---	A	R	Tambon Hat Yai	Chumphon	Thailand	9.95649	98.97788
Sphenomorphus maculata	ESF 539	---	H	R	Heo Lom Waterfall	Chumphon	Thailand	9.72946	98.68298
Sphenomorphus maculata	ESF 541	---	H	W	Heo Lom Waterfall	Chumphon	Thailand	9.72946	98.68298

Sphenomorphus maculata	ESF 543	---	A	W	On road outside of Kapo Waterfall Forest Park	Chumphon	Thailand	10.74769	99.20562
Sphenomorphus maculata	ESF 545	---	A	W	On road outside of Kapo Waterfall Forest Park	Chumphon	Thailand	10.74769	99.20562
Sphenomorphus maculata	ESF 553	NV	H	R	Sakaerat Environmental Research Station	Nakhon Ratchasima	Thailand	14.50614	101.92038
Sphenomorphus maculata	ESF 567	OMNH 46530	A	W	Sakaerat Environmental Research Station	Nakhon Ratchasima	Thailand	14.51009	101.93106
Sphenomorphus maculata	ESF 572	NV	H	W	Sakaerat Environmental Research Station	Nakhon Ratchasima	Thailand	14.50557	101.92746
Sphenomorphus maculata	ESF 573	NV	J	W	Sakaerat Environmental Research Station	Nakhon Ratchasima	Thailand	14.50482	101.91830
Sphenomorphus maculata	ESF 577	OMNH 46531	J	R	Sakaerat Environmental Research Station	Nakhon Ratchasima	Thailand	14.49745	101.91607
Sphenomorphus maculata	ESF 585	OMNH 46532	A	W	Sakaerat Environmental Research Station	Nakhon Ratchasima	Thailand	14.51009	101.93106
Subdoluseps bowringii	ESF 425	NV	H	R	Sakaerat Environmental Research Station	Nakhon Ratchasima	Thailand	14.50245	101.92447
Subdoluseps bowringii	ESF 434	NV	H	T	Sakaerat Environmental Research Station	Nakhon Ratchasima	Thailand	14.50399	101.92241
Subdoluseps bowringii	ESF 435	NV	H	W	Sakaerat Environmental Research Station	Nakhon Ratchasima	Thailand	14.50270	101.92375
Subdoluseps bowringii	ESF 438	NV	H	W	Sakaerat Environmental Research Station	Nakhon Ratchasima	Thailand	14.50524	101.92782
Subdoluseps bowringii	ESF 442	OMNH 46522	A	W	Sakaerat Environmental Research Station	Nakhon Ratchasima	Thailand	14.50963	101.93057
Subdoluseps bowringii	ESF 455	NV	H	W	Sakaerat Environmental Research Station	Nakhon Ratchasima	Thailand	14.50514	101.92711
Subdoluseps bowringii	ESF 465	OMNH 46523	J	R	Sakaerat Environmental Research Station	Nakhon Ratchasima	Thailand	14.50285	101.92337
Subdoluseps bowringii	ESF 466	OMNH	J	W	Sakaerat Environmental Research Station	Nakhon Ratchasima	Thailand	14.50285	101.92337
Subdoluseps bowringii	ESF 467	NV	H	W	Sakaerat Environmental Research Station	Nakhon Ratchasima	Thailand	14.50615	101.92722
Subdoluseps bowringii	ESF 468	NV	H	W	Sakaerat Environmental Research Station	Nakhon Ratchasima	Thailand	14.50601	101.92780
Subdoluseps bowringii	ESF 479	OMNH 46767	J	W	Boyscout Camp	Saraburi	Thailand		
Subdoluseps bowringii	ESF 481	ZMKU R 00734	A	W	Boyscout Camp	Saraburi	Thailand		
Subdoluseps bowringii	ESF 496	NV	J	T	Kasetsart University Forestry Training Station	Prachuap Khiri Khan	Thailand		
Subdoluseps bowringii	ESF 498	NV	A	R	Kasetsart University Forestry Training Station	Prachuap Khiri Khan	Thailand		
Subdoluseps bowringii	ESF 499	NV	A	R	Kasetsart University Forestry Training Station	Prachuap Khiri Khan	Thailand		
Subdoluseps bowringii	ESF 500	NV	A	W	Kasetsart University Forestry Training Station	Prachuap Khiri Khan	Thailand		
Subdoluseps bowringii	ESF 502	NV	A	W	Kasetsart University Forestry Training Station	Prachuap Khiri Khan	Thailand		
Subdoluseps bowringii	ESF 504	NV	A	T	Kasetsart University Forestry Training Station	Prachuap Khiri Khan	Thailand		
Subdoluseps bowringii	ESF 505	NV	J	W	Kasetsart University Forestry Training Station	Prachuap Khiri Khan	Thailand		
Subdoluseps bowringii	ESF 506	NV	A	W	Kasetsart University Forestry Training Station	Prachuap Khiri Khan	Thailand		
Subdoluseps bowringii	ESF 509	NV	J	R	Sakaerat Environmental Research Station	Nakhon Ratchasima	Thailand	14.50615	101.93106

Subdoluseps bowringii	ESF 515	NV	H	T	Sakaerat Environmental Research Station	Nakhon Ratchasima	Thailand	14.50561	101.92759
Subdoluseps bowringii	ESF 517	NV	J	T	Sakaerat Environmental Research Station	Nakhon Ratchasima	Thailand	14.50400	101.93051
Subdoluseps bowringii	ESF 518	NV	J	W	Sakaerat Environmental Research Station	Nakhon Ratchasima	Thailand	14.50561	101.92759
Subdoluseps bowringii	ESF 519	OMNH 46524	A	W	Sakaerat Environmental Research Station	Nakhon Ratchasima	Thailand	14.50561	101.92759
Subdoluseps bowringii	ESF 520	NV	H	W	Sakaerat Environmental Research Station	Nakhon Ratchasima	Thailand	14.50615	101.92722
Subdoluseps bowringii	ESF 524	NV	H	T	Sakaerat Environmental Research Station	Nakhon Ratchasima	Thailand	14.50270	101.92375
Subdoluseps bowringii	ESF 538	---	A	R	Tambon Hat Yai	Chumphon	Thailand		
Subdoluseps bowringii	ESF 561	NV	J	T	Suranaree University	Nakhon Ratchasima	Thailand		
Subdoluseps bowringii	ESF 564	NV	J	R	Suranaree University	Nakhon Ratchasima	Thailand		
Subdoluseps bowringii	ESF 569	NV	J	W	Suranaree University	Nakhon Ratchasima	Thailand		
Subdoluseps bowringii	ESF 570	NV	A	W	Suranaree University	Nakhon Ratchasima	Thailand		
Subdoluseps frontoparietale	ESF 476	OMNH 46768	J	W	Boyscout Camp	Saraburi	Thailand		
Subdoluseps frontoparietale	ESF 477	ZMKU R 00735	A	W	Boyscout Camp	Saraburi	Thailand		
Subdoluseps frontoparietale	ESF 478	OMNH 46769	A	W	Boyscout Camp	Saraburi	Thailand		
Subdoluseps frontoparietale	ESF 482	ZMKU R 00736	A	R	Boyscout Camp	Saraburi	Thailand		
Subdoluseps frontoparietale	ESF 483	OMNH 46770	A	W	Boyscout Camp	Saraburi	Thailand		